



UiT

THE ARCTIC
UNIVERSITY
OF NORWAY

Faculty of Science and Technology

CFD modelling of pollutant transport

Use of ANSYS Workbench® simulating emissions to air from vessel at Port of Breivika.

Synne Karoline Madsen

Master thesis in Technology and Safety in the High North, June 2019



Preface and acknowledgement

This thesis concludes my master's degree in Technology and Safety in the High North at the Faculty of Science and Technology, UiT – The Arctic University of Norway. This master thesis was completed from January to June 2019.

A special thanks to my supervisor Hassan Abbas Khawaja, for support and assistance through the process of writing the thesis. I would also like to thank my contacts, Tina Sætrum at Port of Tromsø and Susana Lopez-Aparicino at NILU for providing information and articles about cruise vessels and air pollution. Thanks to Dr. Asier Zubiaga and his team at ZHAW - Zürcher Hochschule für Angewandte Wissenschaften for providing simulations in OpenFOAM.

I would like to thank my family at home, encouraging me to do my best. And my fellow student, Lene, for several lunch breaks and good discussions. Thanks to Anne for supporting me with proof-reading of the thesis.



Synne Karoline Madsen

Tromsø, 1st of June 2019

Abstract

Historically, the Port of Tromsø is well known as the final port before entering the Arctic Sea. Nowadays, there is a noticeable traffic consisting of cruise vessels visiting Port of Tromsø before heading against the Arctic. The vessels transport passengers expecting clean air, midnight sun, northern lights, snow and ice; - and a clean environment.

Environmental considerations and air pollution in all port areas should be expected to be given more focus in the future. The thesis presents Computational Fluid Dynamics (CFD) simulations in ANSYS® illustrating emissions of CO₂ to air. CO₂ is used as indicator because of its global climate impact. The literature review refers to CDF-simulations as a method to study pollution transport in urban environment.

The two-phase model considers typical wind strength and wind direction in Tromsø. Data collection of coordinates and managing data was a time-consuming part of the thesis.

The results from the simulations indicates a potential outcome if the weather conditions are optimal. The terrain in the model is recognizable for the port's location.

From the CFD results, it is illustrated that onshore wind with high wind strength could have effect on the environment near Port of Breivika. Mitigations to prevent pollution to air from vessels are presented. As a quality check, the model file was sent to ZHAW - Zürcher Hochschule für Angewandte Wissenschaften. The results simulated in OpenFOAM is qualitatively showing the same as visible in ANSYS®.

Abbreviation

CFD – Computational Fluid Dynamics

CH₄ – Methane

CO₂ – Carbon dioxide

CSV – Comma Separated Values

ECA – Emission Control Area

GHG – Greenhouse gas

GPS – Global Positioning System

HVSC – High-Voltage Shore Connection

IMO – International Maritime Organization

ISO – International Organization for Standardization

LF – Load Factor

LNG – Liquid Natural Gas

NAS – Norse Asset Solution

N₂O – Nitrous Oxide

NO_x – Nitrogen Oxide

OGV – Oceangoing Vessels

PM – Particular Matter

SO₂ – Sulphur Dioxide

SO_x – Sulphur Oxide

VOC – Volatile Organic Compounds

Content list:

- Preface and acknowledgement III
- AbstractIV
- Abbreviation..... V
- Table list:..... VIII
- Figure list:IX
- 1 Introduction 2
 - 1.1 Background -Cruise vessels in the high North..... 2
 - 1.2 Problem description..... 3
 - 1.3 Research questions 4
 - 1.4 Structure of the thesis 4
- 2 Literature review 6
 - 2.1 Shipping emissions in a Nordic port: Assessment of mitigations strategies..... 6
 - 2.2 Case study: CFD simulation of CO₂ dispersion from urban thermal power plant: Analysis of turbulent Schmidt number and comparison with Gaussian plume model and measurements 10
 - 2.3 Weather conditions in Tromsø 14
- 3 Methodology 20
 - 3.1 Pros, cons and limitations of the simulation 20
 - 3.2 Preliminary study 21
 - 3.2.1 Small scale modelling in ANSYS 21
 - 3.2.2 Results 22
 - 3.3 CFD in ANSYS® 27
 - 3.4 Designing a model for ANSYS® 30
 - 3.4.1 Adding geometry to the terrain 33
 - 3.4.2 Finalizing the model in ANSYS® Workbench 35
 - 3.4.3 Challenges related to the modelling 44

4	Results and discussion.....	46
4.1	Case A	48
4.2	Case B	52
4.3	Case C	56
4.4	Case D	60
4.5	Air quality	64
4.5.1	Air quality per day, any risk?	64
4.5.2	How can emissions to air be reduced from vessels at port?	65
4.5.3	IMO’s adopted mandatory measures to reduce GHG emissions from shipping 72	
4.6	Results from OpenFOAM	73
4.7	Bow-tie	77
4.8	Research questions	78
5	Conclusion and recommendation	82
6	Bibliography.....	86

Table list:

Table 1 Tabular view for temperature and precipitation per month for the final year (Norwegian Meteorological Institute, 2019).....	16
Table 2 Weather statistics for Tromsø December 2017 - December 2018 (Norwegian Meteorological Institute, 2019).	16
Table 3 Settings for simulations in ANSYS®.....	41
Table 4 Overview of model and wind strength.	46

Figure list:

- Figure 1 Cruise vessel visiting Port of Tromsø, January 2019. 3
- Figure 2 Emission contribution per sectors operating in the Port of Oslo (2013). 7
- Figure 3 Bivariate plot of SO₂ concentrations as a function of wind strength and direction (left) and the CPD at the 90th percentile (right) at Port of Oslo. 9
- Figure 4 Details of domain in simulation (Toja-Silva, Chen, Hachinger, & Hase, 2017). 11
- Figure 5 Comparison between the simulation and the Gaussian plume model on the measurement point for the open place (Toja-Silva, Chen, Hachinger, & Hase, 2017). 12
- Figure 6 Vertical map of the CO₂ concentration at the urban area (Toja-Silva, Chen, Hachinger, & Hase, 2017). 13
- Figure 7 Radiation of sunbeams (Halasz, 2019). 14
- Figure 8 Tromsø is located between islands and mainland, shielded for weather conditions by fjords. 15
- Figure 9 Wind rose location top of island. 17
- Figure 10 Wind rose location Langnes, near the airport. 18
- Figure 11 Wind directions for the simulations. 19
- Figure 12 Mesh concentrated to the plume outlet, seen from bottom of figure. 22
- Figure 13 Simulation with over-dimensioned pipe. 23
- Figure 14 Emission after 5 seconds, reduced dimension on pipe. 24
- Figure 15 Emission after 60,6 seconds. 24
- Figure 16 Simulation with building, seen from the side. 25
- Figure 17 Simulation with building, seen from above. 26
- Figure 18 Path containing coordinates near Port of Tromsø, location Breivika. 30
- Figure 19 TCX Converter updating altitude for coordinates. 31
- Figure 20 Formula to convert GPS coordinates to meters, and meters refereed to the reference point in figure 19. 32
- Figure 21 Terrain ground in Solidworks with added cylinder to create domain. 33
- Figure 22 Path demonstrating coordinates of the buildings near Port of Tromsø, Breivika. 34
- Figure 23 Script for coordinating the buildings in meters, referencing to the location. 35
- Figure 24 Menu in ANSYS® Workbench. 36
- Figure 25 Geometry added to terrain constructed out of geometric points. 37
- Figure 26 Each building has its own actual height. 38

Figure 27 Zero slip boundaries -all the sides of the buildings, including the terrain.....	38
Figure 28 Mesh seen from bottom.	39
Figure 29 Mesh concentrated around buildings in the terrain.....	40
Figure 30 Solution with one large pipe as source.	42
Figure 31 Solution with three pipes as source, reduced height and diameter.	42
Figure 32 Iterations for several simulations.	43
Figure 33 Wind strength 15 m/s illustrated from above.....	48
Figure 34 Wind strength 15 m/s seen from the side.....	48
Figure 35 Wind strength 5 m/s seen from the side.....	49
Figure 36 Wind strength 5 m/s seen from above.	50
Figure 37 Wind strength 1 m/s, emission goes up.	51
Figure 38 Wind strength 15 m/s seen from the side.....	52
Figure 39 Wind strength 15 m/s seen from above.	52
Figure 40 Illustration of the vortex-effect (Sam, 2012).	53
Figure 41 Wind strength 4,25 m/s seen from above.	54
Figure 42 Wind strength 4,25 m/s seen from the side.....	54
Figure 43 Wind strength 4,25 m/s zoomed in.	55
Figure 44 Wind strength 15 m/s seen from the side.....	56
Figure 45 Wind strength 15 m/s seen from above.	56
Figure 46 Wind strength 4.25 m/s seen from above.	57
Figure 47 Wind strength 4,25 m/s seen from the side.....	57
Figure 48 Wind strength 2,8 m/s seen from the side.....	58
Figure 49 Wind strength 2.8 seen from above.	58
Figure 50 Wind strength 15 m/s with large impact.....	60
Figure 51 Wind strength 15 m/s with large impact seen from the side.....	61
Figure 52 Wind strength below 5 m/s making an unexpected impact.	61
Figure 53 Wind strength below 5 m/s making a remarkable impact.	62
Figure 54 Wind strength below 5 m/s seen from behind	63
Figure 55 Map from luftkvalitet.miljostatus.no illustrating pollution for the area representing the simulations, 24th of April 2019 (Luftkvalitet i Norge, 2019).	64
Figure 56 Open scrubber system (Laville, 2018).	66
Figure 57 Example set-up for hybrid propulsion system	68
Figure 58 Current ECA-zones (Norwegians Shipowners Association, 2014).	69
Figure 59 General design of a high-voltage shore connection system (Port of Oslo, 2012). ..	71

Figure 60 Result case 1 from OpenFOAM wind strength	73
Figure 61 Result case 1 from OpenFOAM wind strength	74
Figure 62 Result case 2 from OpenFOAM wind strength	74
Figure 63 Result case 2 from OpenFOAM wind strength	75
Figure 64 Result case 3 from OpenFOAM wind strength	75
Figure 65 Result case 3 from OpenFOAM wind strength	76
Figure 66 Bow-tie for emissions to air vessels at Port of Breivika.....	77
Figure 67 Impact of plume in addition to wind strength and vessel height.	79

1 Introduction

1.1 Background -Cruise vessels in the high North

Historically, the Port of Tromsø is well known as the final port before entering the Arctic Sea. Previously the port traffic consisted of vessels for fishing and cargo to supply to locals and scientists for wintering. Nowadays, there is a noticeable traffic consisting of cruise vessels visiting Port of Tromsø before heading against the Arctic. The vessels transport passengers expecting clean air, midnight sun, northern lights, snow and ice; - and a clean environment.

In the future it is expected and desired from local business that there will be an increase in the cruise traffic. Recent statements from local politicians welcomes the tourist industry and the economic growth this may lead to. The debate focusing air quality and local pollution from cruise vessels at port is yet not being considered as a potential problem (Rafaelsen, et al., 2019). To visualize the traffic; - if all the cruise vessels visiting the port of Tromsø in 2018 were lined up, they would create a 25km long line (Lange & Johansen, 2018).

The existing requirements under the International Convention for the Prevention of Pollution from ships (MARPOL), aim to control greenhouse gas (GHG) emissions from ships, are mainly regulating NO_x, SO_x, VOC and Methane (IMO, 2005). And the CO₂ emissions from vessels in operation is aimed managed by use of the Ship Energy Efficiency Management plan. In addition, it is required comply with the Energy Efficiency Design Index (EEDI) for design of vessels. Increased energy efficiency will lead to reduced CO₂ emissions. Further, the vessels must be able to use eco-friendly fuel (Rafaelsen, et al., 2019) as set in the regulations by IMO.

The Norwegian Ministry of Climate and Environment have through the company Enova supported terminals and ports to provide electrical onshore power at quay side to reduce the emissions to air (Enova, 2018). In 2015 Enova supported eleven onshore power projects with 51 million NOK. Enova is working to develop new energy and technology that would be efficient and necessary to accommodate the emission limits for the future. The main concern is the time left for the changes to be implemented.



Figure 1 Cruise vessel visiting Port of Tromsø, January 2019.

1.2 Problem description

Performing Computational Fluid Dynamics (CFD) simulations visualizes the emissions released to air and is a tool to estimate the emission and its dispersion at a given location. However, only 10% of the cruise vessels arriving at port of Tromsø can connect to onshore power (Sætrum, 2018). Several cruise vessels at port operates on fuel to keep the vessel functioning while passengers are visiting town.

Environmental considerations and air pollution in all port areas should be expected to be given more focus in the future. Therefore, it is of interest to do simulations of CO₂ flowing from a potential vessel from Port of Tromsø, location Breivika.

1.3 Research questions

Following research questions will be solved:

- Is it possible to make a realistic model to simulate in ANSYS® Workbench?
- Does the dispersion of CO₂ impact the environment near the Port of Tromsø, location Breivika?
- What is the impact of wind direction/strength and ship height towards the pollutant transport?

1.4 Structure of the thesis

For this thesis, the main topic is to be able to develop the set-up for the CFD in ANSYS® to be able to visualize the plume outlet for the pollutant.

The content of the assignment will include:

- Introduction of the thesis including background, problem description and research questions.
- Literature review of cases where CFD simulations have been performed, their set-up, how they have been modelled and the results of the simulations.
- The methodology in a CFD how the model is designed from coordinates until meters and a fulfilled model arranged for simulation. The results from the preliminary thesis will be presented. Thereafter, the settings for designing a large-scale model
- Result and discussion of the simulations. The emissions will be commented; does the emissions influence the geographical environment and the local community? A delve into the air quality for Tromsø and the effect polluted air could make during different wind conditions. The research question will be answered. For final, a comparison from another software named OpenFOAM.
- A conclusion of the study and a recommendation for further work.

2 Literature review

2.1 Shipping emissions in a Nordic port: Assessment of mitigations strategies.

“We use a bottom-up approach to develop a comprehensive emissions inventory for the Port of Oslo for current and future scenarios, including compliance with environmental legislation. We estimate the emission of air pollutants (NO_x , PM_{10} , SO_2) and greenhouse gases (GHGs; CO_2 , CH_4 , N_2O) from shipping and land activities in the port. The inventory shows that oceangoing vessels are the main contributor, providing 63–78% of the total NO_x , PM_{10} , SO_2 and CO_2 emissions. The main contributors among oceangoing vessels are international ferries, cruises and container vessels, and the main contributors to emissions among harbour vessels are domestic ferries”.

Monitoring of air pollutants helps identifying risk for undesirable effects to health and climate and caters for early intervention and mitigating actions. The main sources of air pollution in the urban environment is originated from industry, agriculture, on-road traffic. The climatic influence results in heating. The last few decades several countries have introduced policies and acts to reduce air pollution and climate change.

There are strict regulations for sulphur and nitrogen dioxide emissions in the maritime sector, especially in the emission control areas (ECA). Annex VI “Regulations for the prevention of Air Pollution from ships”, given by International Maritime Organization (IMO) came into force in 2005 and gives the limits for allowed sulphur content in fuel on global basis. Until first of January 2012 it was allowed with 4,5% m/m, and thereafter 3,5% m/m, and after January the first in 2020 it will be 0,50% m/m. For ECA areas the numbers will be 1,5% m/m first of January 2010, 1,0% m/m on and after first of July 2010 and 0,1% m/m on and after first of January 2015.

The methodology in this report is first a description of the Port of Oslo, which is the biggest and busiest port in Norway. Vessels in the port transport of goods, bulk cargo, and transport of passengers, as international and domestic ferries and cruise vessels. In the report the

vessels were divided into two groups: oceangoing vessels (OGV) and harbour vessels (HV). The emission estimates are based on the methodology published by US EPA (2009) and the activity log for Port of Oslo. The information used from the log is the detailed information about the arrivals, departure and operating time. They have also done calculations and simulations for the 2020- scenario with the values of the sulphur content in fuel for the time. The estimates are a function of vessel engine in kW, and a load factor (LF) under the different operational modes.

The two scenarios are set to be as in year 2013 and in the future as 2020, within the given state limits for fuel. Also, some of the vessels use liquid natural gas (LNG) as fuel.

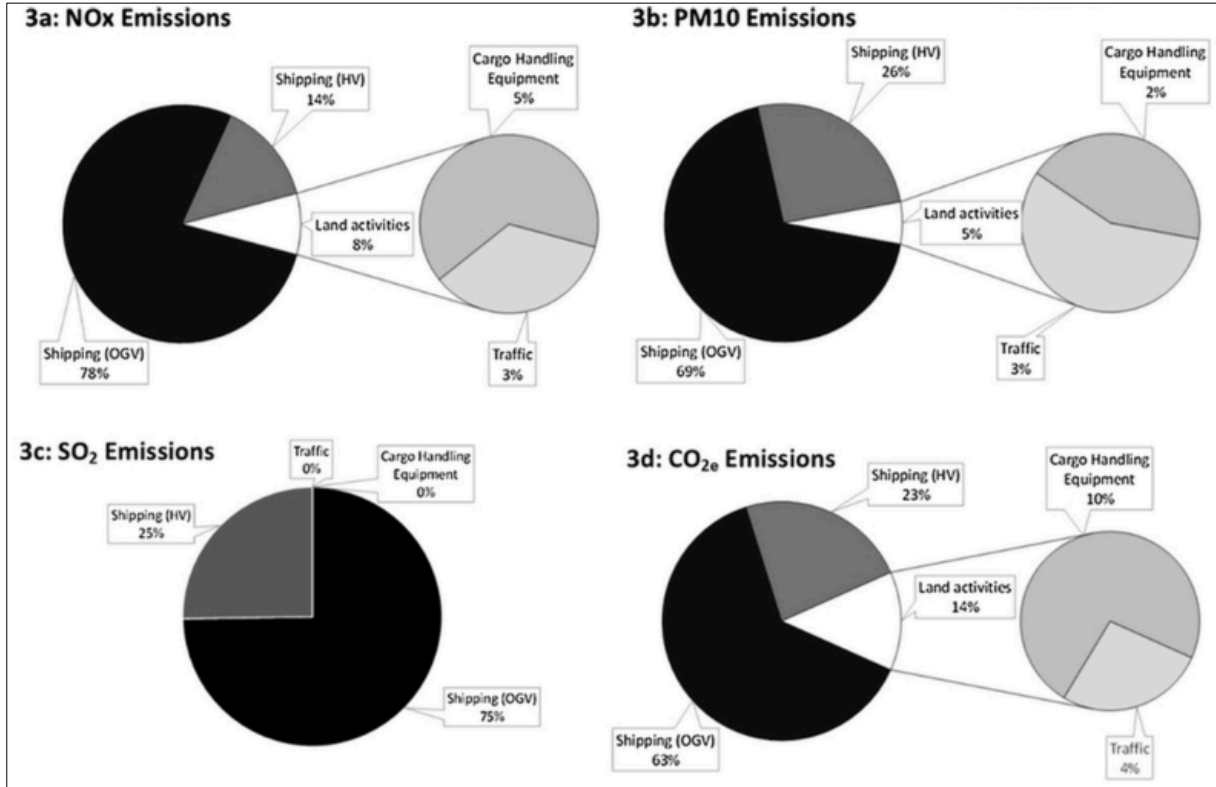


Figure 2 Emission contribution per sectors operating in the Port of Oslo (2013).

55% of the NO_x emissions occurs at port and contributes to 47% of the total emission from shipping. The emissions from cruise vessels contributes to approximately 22% of the NO_x and 19% for CO₂ of the total emissions for 2013 at Port of Oslo.

In total, the emission of pollutants is highest when vessels are manoeuvring to port.

To estimate the emissions to air at Port of Tromsø both top-down and bottom-up approach is used. The top-down approach is driven by theory, a bottom up approach is based on data collections and saved data. For this literature review, the top-down theory estimates the theory based on expected traffic and restrictions for fuel in the future.

«Based on the top-down approach, we estimate NO_x shipping emissions in Oslo region to be around 1033 tonnes in 2013, compared with around 700 tonnes estimated through a bottom-up approach. These methods differ in the geographical location of the emissions, as the fuel sale method assume that emissions occur where the fuel is sold».

The future emissions for 2020 within the fuel to content <0,1% m/m Sulphur from January 2015, besides business as usual an increase is expected without significant changes, as naturally expected:

«The evaluated 2020 scenarios are those after feasible implementation of onshore power for selected OGVs, the establishment of a strength reduction zone and the increased use of LNG by domestic ferries. To assess these scenarios, emissions are compared with the current scenario established as a baseline as it is assumed to be less uncertain».

The total emissions at the Port of Oslo is expected to be lower in 2020 than in 2013. Assuming the domestic ferries will use LNG as fuel, there would be an increase of approximately 8-15% for NO₂, CO₂, CH₄ and N₂O compared to the baseline conditions in 2013. On the positive side we could experience a decrease of >90% for SO₂ and 10% for PM₁₀ if the vessels use low Sulphur fuel would be owing to the assumption of vessels consume low levels of Sulphur in the fuel.

The possibility at Port of Oslo to provide onshore power for international ferries entails the emissions of NO_x and N₂O in 2020 to be similar to the level of the emissions in 2013, despite the increase in maritime traffic. Another measure to reduce the emissions would be a reduction in strength limit set to 12 knots. If the strength limit is reduced, and the domestic ferries would use LNG, the reduction in NO_x, PM₁₀ and CO₂ would be respectively 23, 43, and 17% at Port of Oslo.

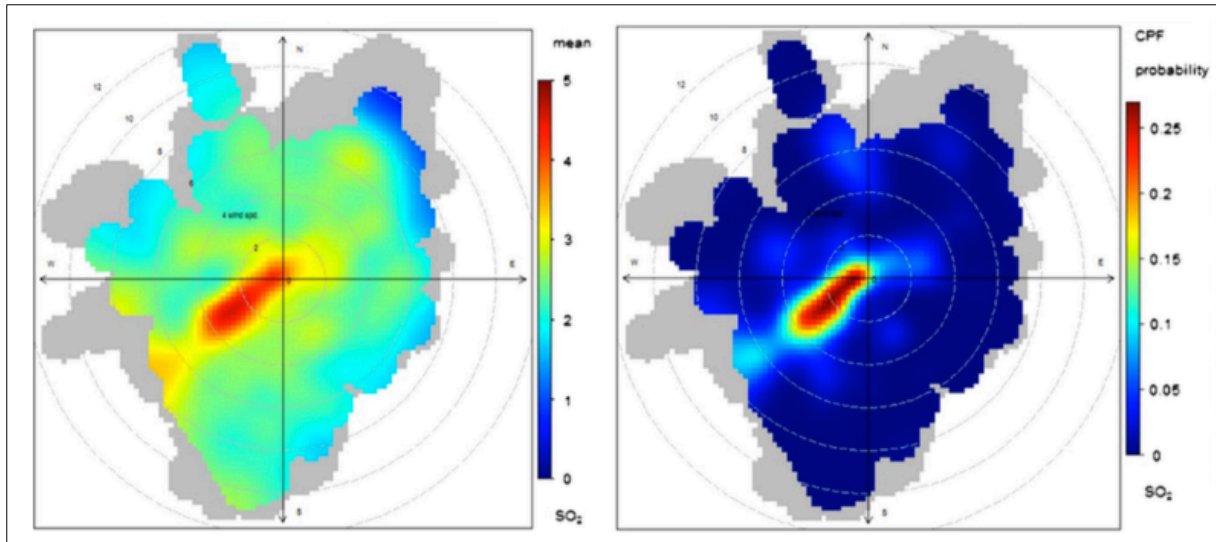


Figure 3 Bivariate plot of SO₂ concentrations as a function of wind strength and direction (left) and the CPD at the 90th percentile (right) at Port of Oslo.

Figure 2 illustrates the bivariate plot of SO₂ concentrations and its variation as a function of wind strength and direction. Bivariate plot used as a diagnostic tool to identify possible pollution sources. These plots have limitations to wind strength and direction, this to reduce the uncertainty in the calculation. Looking at this, the outcome is that the SO₂ concentration is high when the wind is from the southwest, with levels higher than the 90th percentile which is 4.5 mg m⁻³. These data show that the port may contribute to the concentration levels in the urban environment near Port of Oslo.

The report concludes that emissions from ports are contributing and influencing the air quality of the urban environment located nearby. Pollutants as NO_x, NO₂, PM and CO₂ would to be concerned for the future. The new regulations for Sulphur content in fuel would will have a positive effect on emissions of SO₂. For Port of Oslo are OGV's seen as the main contributor to the emissions at berth.

2.2 Case study: CFD simulation of CO₂ dispersion from urban thermal power plant: Analysis of turbulent Schmidt number and comparison with Gaussian plume model and measurements

“The identification and control of the greenhouse gas sources has a great relevance. Since the GHG emissions from cities and power plants are the largest human contribution to climate change.” (Toja-Silva, Chen, Hachinger, & Hase, 2017).

With use of the equations for the Gaussian plume model and simulation tools the report presents a location central in Munich (Germany) with an existing power plant containing two pipes.

The power plant is near to urban environment as well as an open field site. To secure correct data spectrometers were used to measure data for the investigation of the emission from the plant, at the same locations as the simulations was done, but therefore, the simulations where done against open field and urban environment, both with given data for wind direction and wind strength.

The real data was the reference of the simulations, according to volume of emission, wind strength and direction. When designing the model for the simulation, they know the emission

from each pipe.

Figure 4 is the measure and set up from one of the simulations:

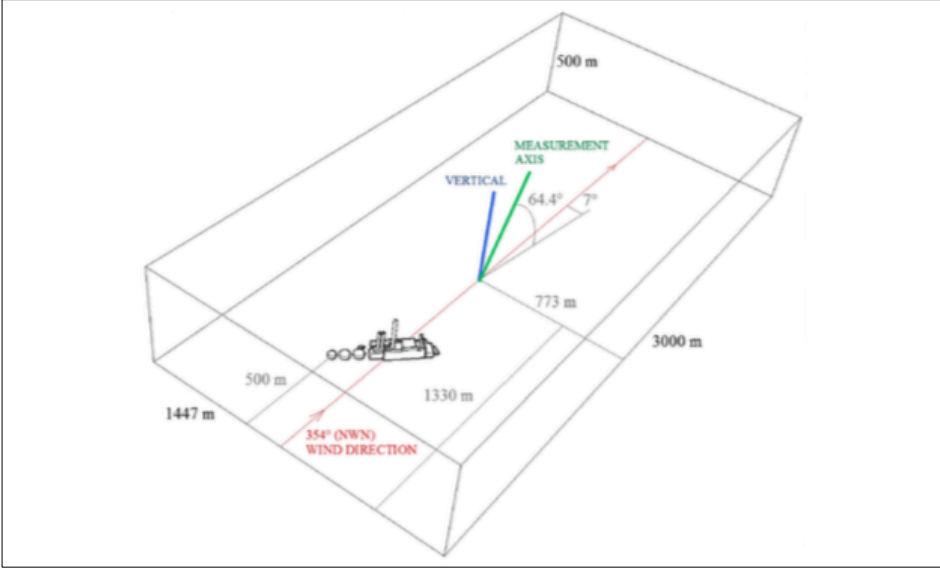


Figure 4 Details of domain in simulation (Toja-Silva, Chen, Hachinger, & Hase, 2017).

Figure 4 illustrates the distances where the power plant is located relative to the urban environment and the angle of wind and its direction.

Further, figure 5 describes the simulation compared to the calculations, consisting of two pipes, measures of distances and wind direction. When the simulations were done for the

open field, the collected data from the spectrometer and the simulation was illustrated in figure 5:

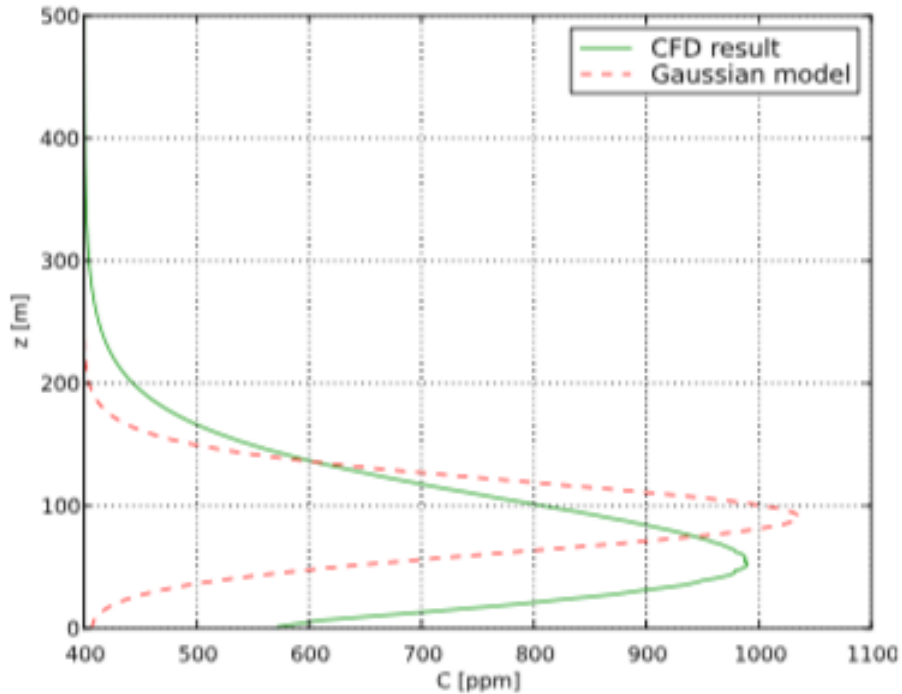


Figure 5 Comparison between the simulation and the Gaussian plume model on the measurement point for the open place (Toja-Silva, Chen, Hachinger, & Hase, 2017).

The number of cells in the mesh were increased to 8,3 million, 11,9 million, 13,8 million, 15,1 million, 17,4 million and 18,7 million cells to improve the accuracy of the simulations. By adding more cells, the simulations were more accurate at the terrain and in air, and more realistic data was collected.

The number of mesh accuracy is compensated at around 13,8 million cells, which mean that the solution would almost stabilize during the increase in mesh between 13,8 million and 18,7 million.

This report describes two different experiments; one in an open field and the second in an urban environment.

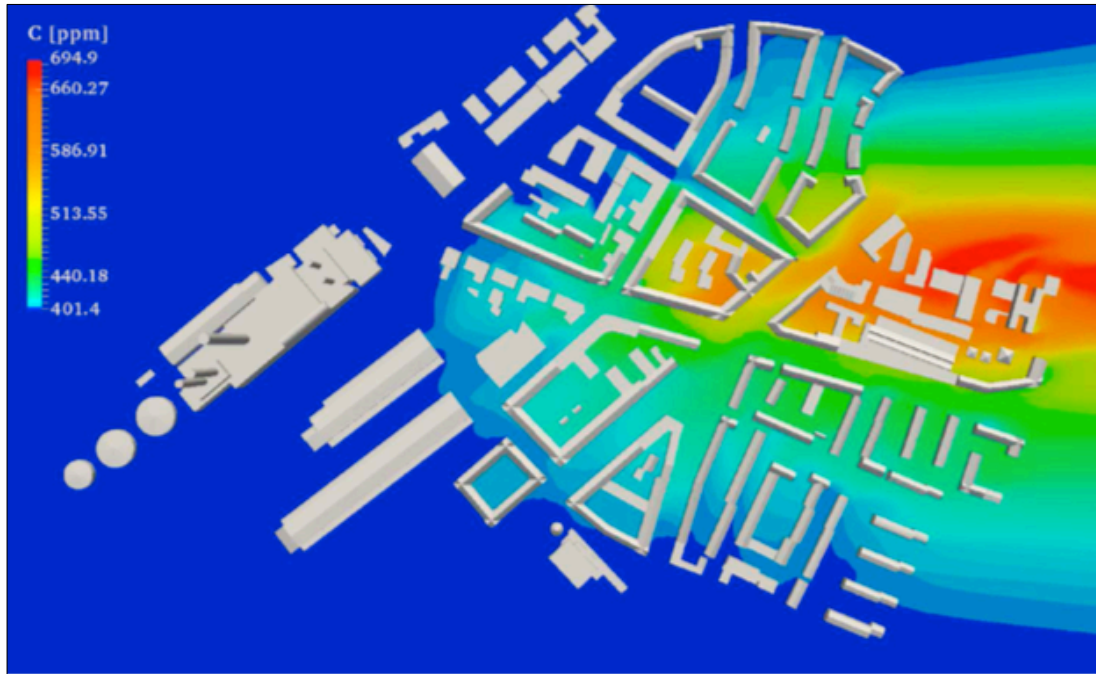


Figure 6 Vertical map of the CO₂ concentration at the urban area (Toja-Silva, Chen, Hachinger, & Hase, 2017).

Figure 6 illustrates the concentration of CO₂ at the urban area, which illustrates that the pollution captured between the streets. This because of the gas concentration is lower than air, and the downstream effect observed together with the vortex-effect.

When the experiment was performed, it was the first time that CFD simulations were compared to experimental measurements of pollution at a site. The results where compared to the Gaussian plume model, which suggested for use in an urban environment. In this study it was also demonstrated that CFD can be useful as a tool for modelling pollutant transport into air.

2.3 Weather conditions in Tromsø

The Arctic region defines areas that have their average temperature below 10 degrees Celsius for the warmest month in the year, July. Arctic defines as the area where trees has difficult to grow or does not grow at all (Barentswatch, 2015).

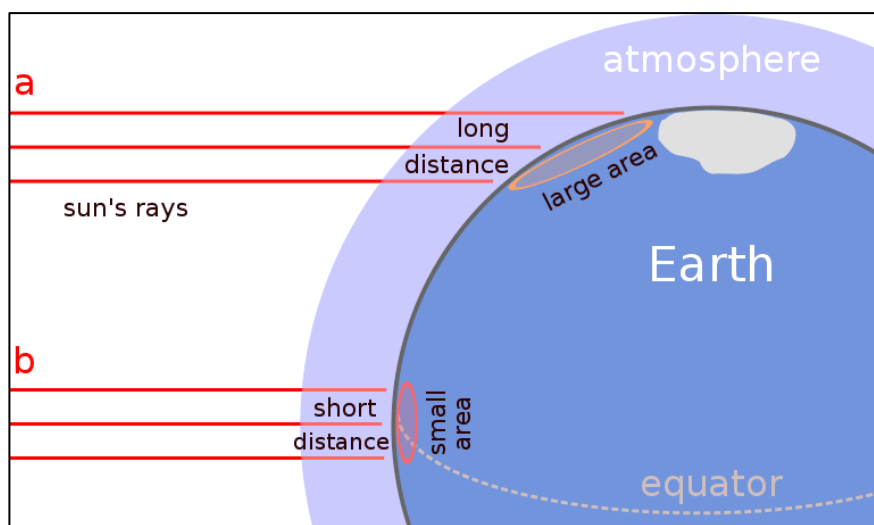


Figure 7 Radiation of sunbeams (Halasz, 2019).

The climatic conditions can be explained as the result of the inclination the earth against the sun with an inclination angle around 23,5 degrees. The temperature in the Arctic areas are colder than tropical conditions near equator since the heat radiation of the sun travels a longer distance to reach the arctic area compared to the areas along equator (Halasz, 2019).

Tromsø is located near to the Norwegian Sea at 69 degrees north, surrounded by fjords and mountains and the city is located at both on an island and on the mainland. The town is one of the largest cities by in the northern part of Norway counted by inhabitants.



Figure 8 Tromsø is located between islands and mainland, shielded for weather conditions by fjords.

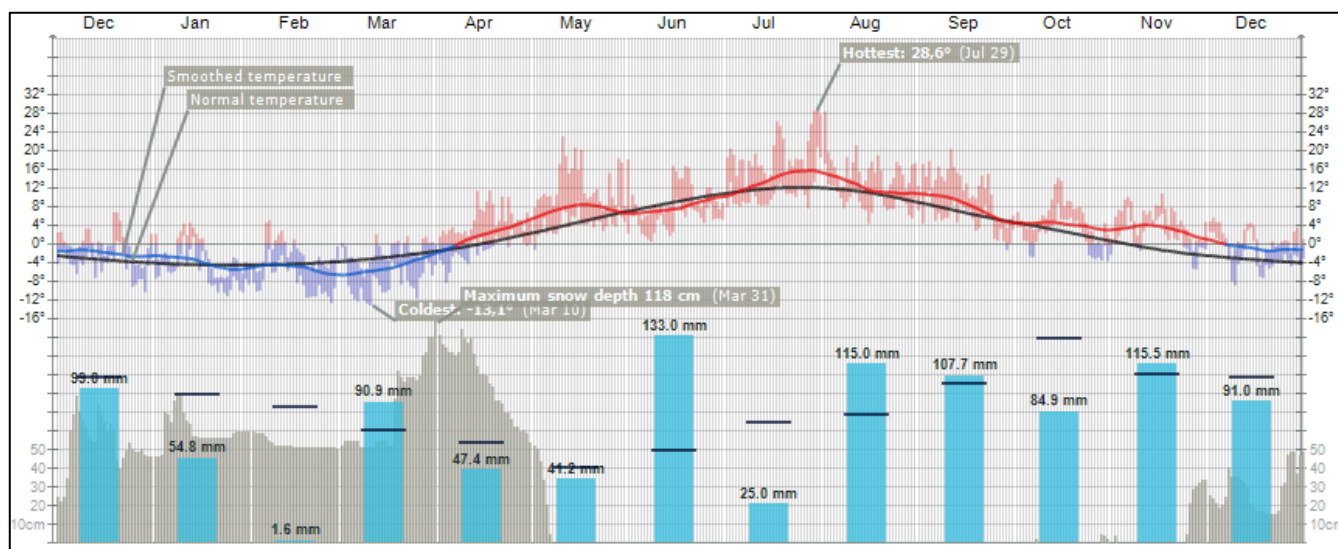
The weather conditions are relevant for executing the simulations as realistic as possible and the weather conditions are relevant. To solve this, I used the last year's data from The Norwegian Meteorological Institute for both temperature and wind will be used as input. The wind strength will be the decisive factor for the simulations.

Table 1 Tabular view for temperature and precipitation per month for the final year (Norwegian Meteorological Institute, 2019).

Months	Temperature				Precipitation			Wind	
	Average	Normal	Warmest	Coldest	Total	Normal	Highest daily value	Average	Strongest wind
Dec 2018	-0.6°C	-3.3°C	5.6°C Dec 2	-8.8°C Dec 9	91.0 mm	106.0 mm	15.1 mm Dec 7	3.9 m/s	10.4 m/s Dec 2
Nov 2018	3.5°C	-1.1°C	10.9°C Nov 16	-5.4°C Nov 27	115.5 mm	108.0 mm	18.0 mm Nov 24	3.8 m/s	12.2 m/s Nov 23
Oct 2018	3.6°C	2.7°C	14.1°C Oct 14	-3.6°C Oct 30	84.9 mm	131.0 mm	11.7 mm Oct 15	3.8 m/s	10.7 m/s Oct 21
Sep 2018	8.3°C	6.7°C	20.4°C Sep 10	-1.2°C Sep 28	107.7 mm	102.0 mm	16.1 mm Sep 26	2.9 m/s	10.3 m/s Sep 3
Aug 2018	11.8°C	10.8°C	28.4°C Aug 1	4.4°C Aug 15	115.0 mm	82.0 mm	14.0 mm Aug 22	2.5 m/s	7.8 m/s Aug 30
Jul 2018	14.6°C	11.8°C	28.6°C Jul 29	7.7°C Jul 27	25.0 mm	77.0 mm	9.5 mm Jul 20	2.2 m/s	8.7 m/s Jul 23
Jun 2018	7.3°C	9.1°C	16.8°C Jun 14	0.5°C Jun 7	133.0 mm	59.0 mm	17.5 mm Jun 24	3.3 m/s	13.0 m/s Jun 26
May 2018	8.1°C	4.8°C	23.1°C May 10	-1.2°C May 1	41.2 mm	48.0 mm	7.5 mm May 23	3.7 m/s	11.7 m/s May 20
Apr 2018	1.8°C	0.3°C	11.5°C Apr 17	-8.3°C Apr 3	47.4 mm	64.0 mm	9.8 mm Apr 8	2.4 m/s	8.7 m/s Apr 2
Mar 2018	-5.0°C	-2.7°C	2.1°C Mar 12	-13.1°C Mar 10	90.9 mm	72.0 mm	20.2 mm Mar 18	3.0 m/s	9.9 m/s Mar 17
Feb 2018	-4.9°C	-4.2°C	5.1°C Feb 6	-12.6°C Feb 26	1.6 mm	87.0 mm	0.5 mm Feb 7	3.8 m/s	11.5 m/s Feb 5
Jan 2018	-4.2°C	-4.4°C	4.6°C Jan 12	-11.1°C Jan 24	54.8 mm	95.0 mm	15.9 mm Jan 4	3.9 m/s	15.6 m/s Jan 15
Dec 2017	-1.9°C	-3.3°C	6.9°C Dec 19	-10.3°C Dec 29	99.0 mm	106.0 mm	17.8 mm Dec 5	4.1 m/s	14.3 m/s Dec 1

Based on the considered data, the typical wind direction in Tromsø is south-southwest with an average strength of 3,3 meters per second; -based on the numbers in table 1.

Table 2 Weather statistics for Tromsø December 2017 - December 2018 (Norwegian Meteorological Institute, 2019).



As shown in table 2, the mean temperature during summer term (May to October) was 9°, and the mean temperature during winter term (October to April) was -2,5°. According to the isotherm temperature the latest year, Tromsø can be defined as an Arctic area.

The wind directions for Tromsø are of most interest. By use of the webpage eklima.net provided by Norwegian Meteorological Institute it was possible to create an account and download weather data based on stored data. The wind strength and wind directions are created by choosing statistics, frequency distribution and frequency distribution with wind rose data from the operative weather stations located in Tromsø and Langnes. The data for the wind roses is set to the latest 10 years.

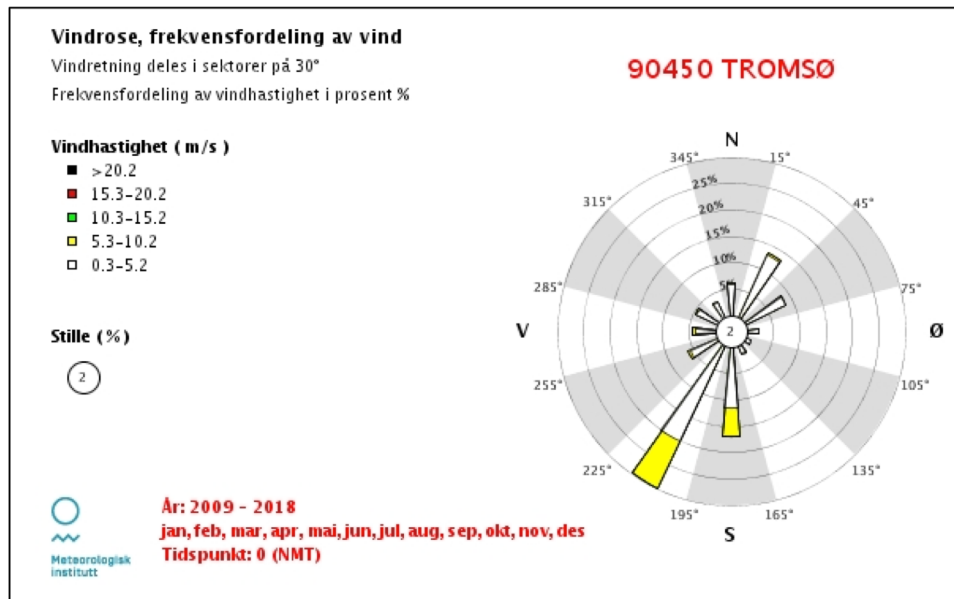


Figure 9 Wind rose location top of island.

The wind roses from eklima.net illustrates both angle and strength of the wind. The two weather stations in Tromsø are both located on the island, one on the top of the island and the other at the west side of the island, Tromsø-Langnes, near the airport. They are both illustrated and considered and presented separately in figure 9 and figure 10. The data from both wind roses are used to set estimations for wind conditions.

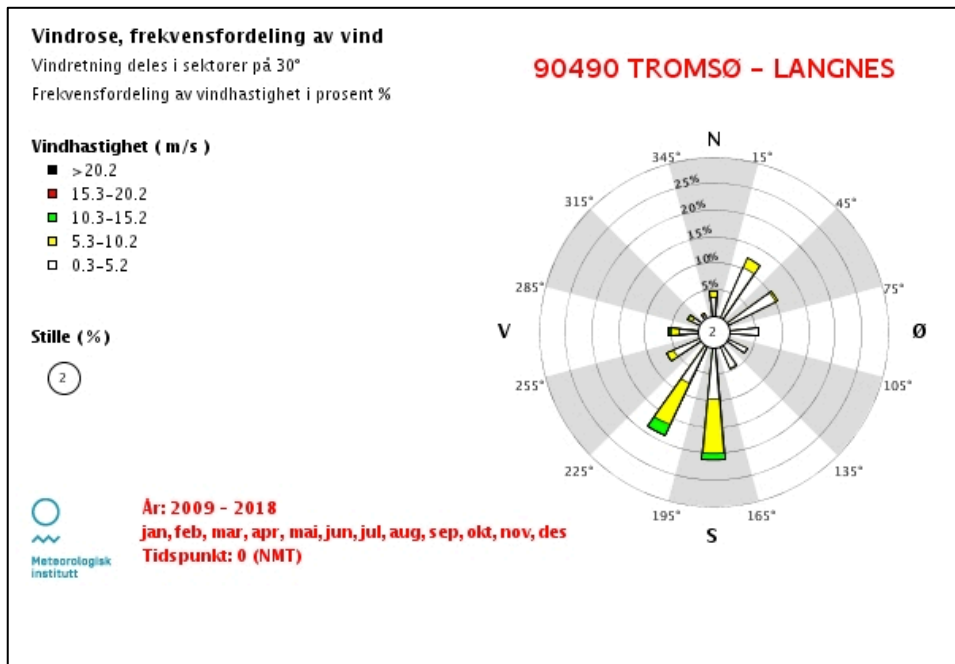


Figure 10 Wind rose location Langnes, near the airport.

As a summary of the wind roses above, figure 11 illustrates the wind directions used in the simulations.

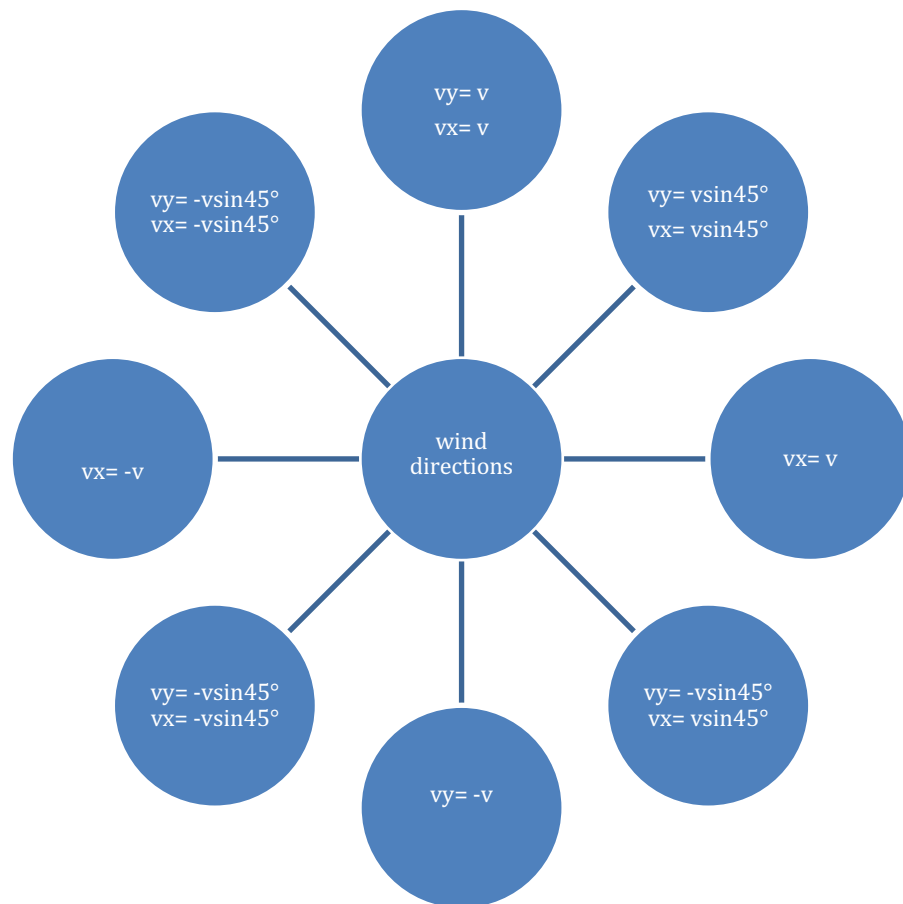


Figure 11 Wind directions for the simulations.

The value of v in the calculations are set to 3.3 m/s, 5 m/s and 12 m/s in the simulations. To calculate the strength of the wind, the model is based on the circle which gives the formula for the angle of direction: north, south, east and west.

The wind roses in figure 9 and 10 illustrates the wind strength and wind strength at every 30° in the circle. To make the simulations feasible due to the time to accomplish the report the wind strength and wind directions are set to 45° angle.

3 Methodology

Several methods have been used during the process to improve the thesis. This chapter includes pros and cons for the method be presented as well as the preliminary study from last semester. Further, this chapter contains an explanation of CFD simulation in ANSYS® and the process during the calculation process -resulting in the outcome of the simulation. Finally, it is explained how the model was made to fit into ANSYS®. This work took more time expected since the construction of the model had several obstacles.

3.1 Pros, cons and limitations of the simulation

Simulation is an effective tool to estimate released emissions to air. The results for a simulation could disprove or confirm statements related to a hypothesis. It can be used for training and learning, as well as it can be used to provoke the result, so the outcome satisfies a hypothesis. The result of the simulation could be compared to other simulations and observations to confirm the results.

The executed simulations in this thesis are only considering the dominant wind direction for Tromsø as illustrated in figure 11. The wind strength and wind direction are calculated based on figure 11. For each direction is the value v calculated. The set-up for wind strength and wind strength are available in Appendix A.

The simulations in this thesis only executes two-phase modelling; emission outlet and wind. The wind direction is the dominant force affecting the emission to air. So, the thesis doesn't take in count temperature, precipitation, fog or special weather conditions such as sudden gust of wind, blizzards and change in atmospheric pressure.

3.2 Preliminary study

The preliminary study for the master thesis had modelling of pollutant transport as theme. The study was meant to be a preface-study to get familiar with the software ANSYS® and the settings that could be used. For this, the study had four simulations, one test round and three others taken into account. The small-scale modelling will be explained in subchapter in 3.2.1, and the results will be presented subchapter in 3.2.2.

3.2.1 Small scale modelling in ANSYS

The Workbench in ANSYS® is used to design the model. The working plane in x, y, and z-direction is chosen and the sketching is done. First, a rectangle is created in the wanted dimension the emission will operate in. Thereafter implement further sketches were implemented to increase the content in the geometry, adding such as a pipe and a geometry for a building. By adding sketches into those which already in place, it is possible to give them functions later.

The construction is a rectangle with a pipe inside, this to simulate a “room” the gas is released to. This box shape allows to be controlled to be what is required; inlet or outlet of wind, or just a barrier as a wall.

One short side represents wind inlet, the second short side represents the wind outlet. The

terrain is assumed to be a flat, and the remaining walls are “closed”, so the figure is designed to have a tunnel function.

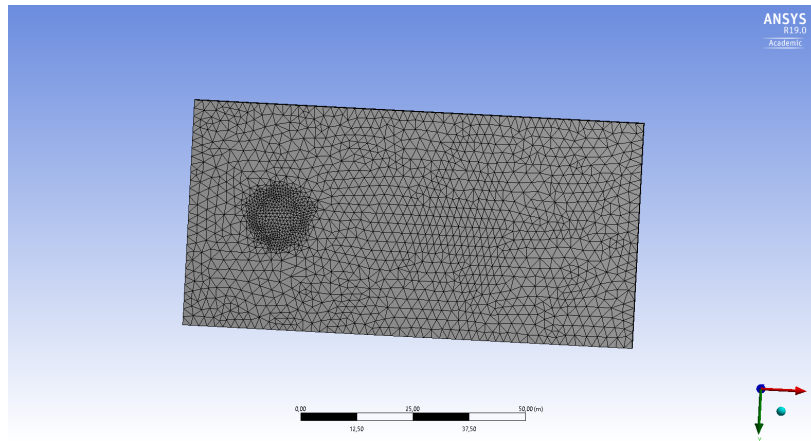


Figure 12 Mesh concentrated to the plume outlet, seen from bottom of figure.

When the sketch was finalized, the next step was to do the modelling. During modelling we introduce mesh – a process where the model is divided into several elements, which gives a wider spread of the loads for the component. Mesh is the number of elements for the figure which gives the number of cells to collect data from.

The higher number of mesh in the model, the more accuracy will there in the answer. It is also possible to concentrate the number of elements around the pipe.

The student license only allows 500.000 elements, so there where limitations for these simulations.

3.2.2 Results

3.2.2.1 Simulation 1

The first simulation was constructed like a rectangle with a stack inside, this to simulate the “room” the emission is released to. Each side of the rectangle can be set to what is desired; inlet or outlet of wind, or just a barrier as a wall. For this simulation, one short side is wind inlet, the second short side is the outlet. The terrain is flat, and the resisting walls are “closed”, so the figure is designed to have a tunnel in function.

The size of the rectangle is 50 meters *100 meters *50 meters, and the pipe inside is centred, so the pipe is located 20 meters away from the short-left hand side. The given dimensions for the pipe are; -diameter: 10 meters, height: 5 meters.

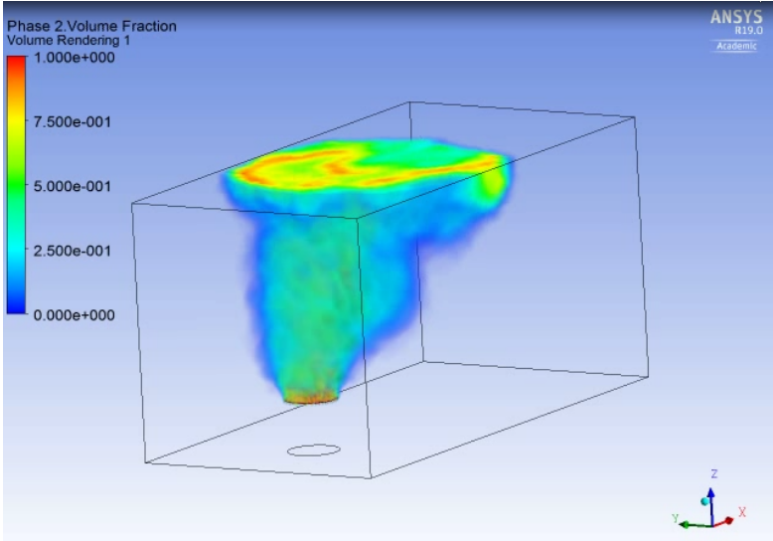


Figure 13 Simulation with over-dimensioned pipe.

For this simulation the pipe dimension was over scale according to the rest of the figure. The diameter of the pipe was over scaled and unrealistic for the emitted pollutant. The function of the walls to behave as a tunnel was seen to be as described, but the diameter of the emission was evaluated to jeopardize the expected result. Hence the pipe diameter was decreased to a realistic number.

3.2.2.2 Simulation 2

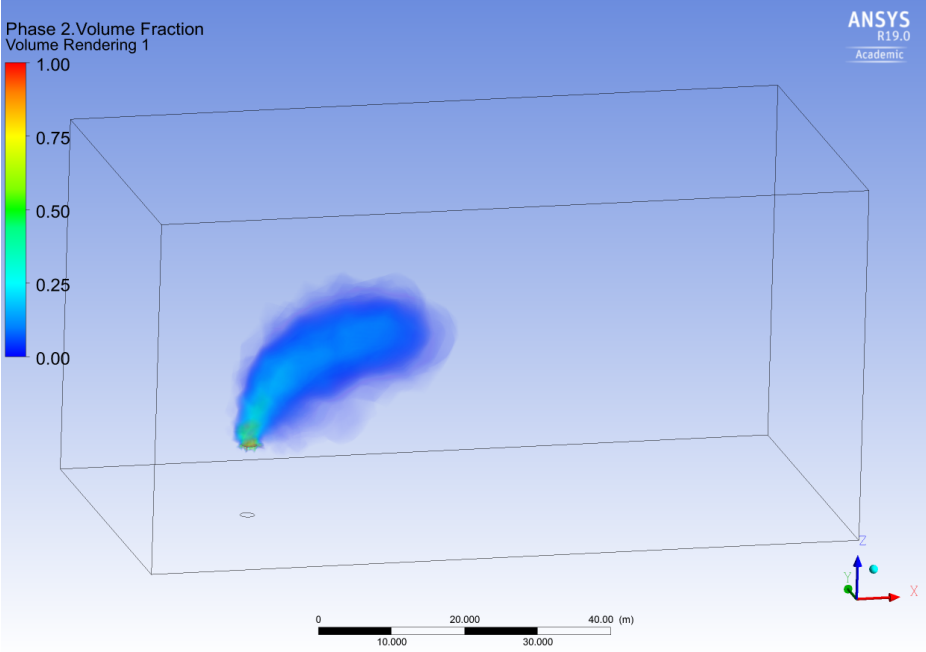


Figure 14 Emission after 5 seconds, reduced dimension on pipe.

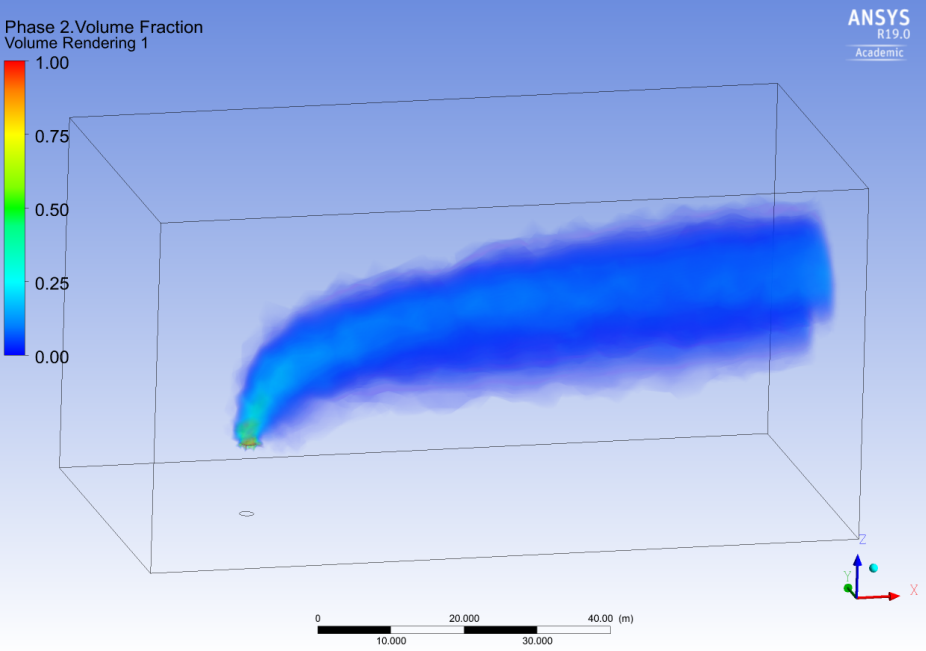


Figure 15 Emission after 60,6 seconds.

The given dimensions for the pipe: diameter 2 meters, height 5 meters.
The diameter of the pipe is set to a realistic measure and have the plume-shape as expected.

3.2.2.3 Simulation 3

This situation with a figure shaped like a tall house is placed into the simulation, to simulate the emission close to a building, for instance houses. The dimensions for the building is 12meters * 12 meters, and has the height of 35 meters and is centred due to the pipe. The original timestep was set to simulate for 15 seconds, but unfortunately the simulation where too though for the computer to calculate. The timestep was therefore set to 7,5 seconds.

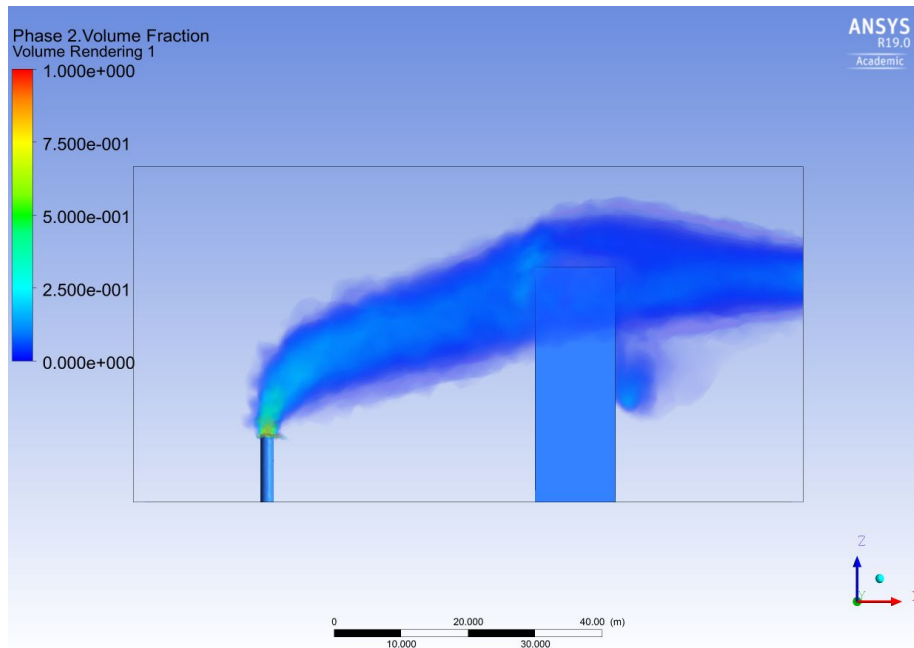


Figure 16 Simulation with building, seen from the side.

Seen from the side, there is building up a pocket of the emission from the pipe, this caused by the vortex- effect. The vortex-effect creates a pocket of pollution rear of the house, captured by the wall and kept there because of the wind at the sides. This is also happening because the gas concentration is higher than wind, and the downstream effect appears.

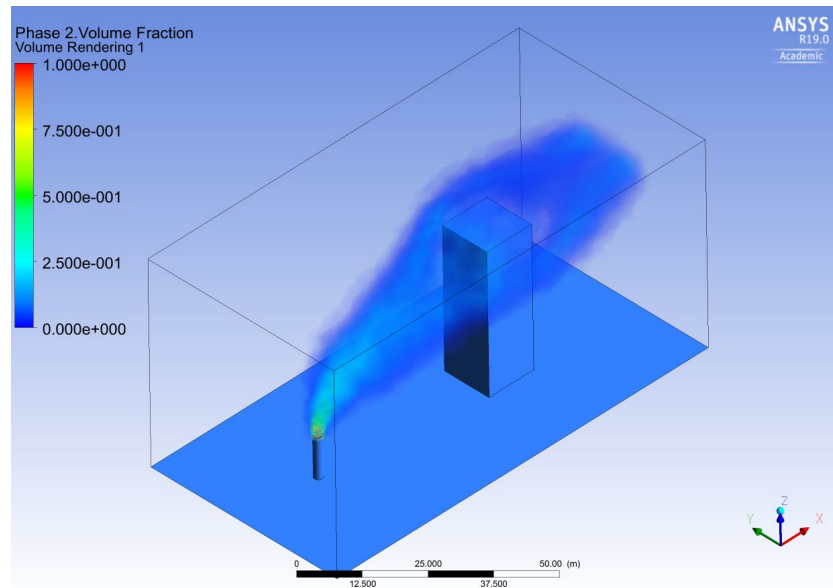


Figure 17 Simulation with building, seen from above.

When the plume is increasing in height from the ground is normal because of the pressure when the gas is emitted from the pipe. Further on, if the distance in the figure was longer, the pollution plume would be closer to the ground because of the downstream effect and the pressure difference. This result could also be expected for additional larger-scale simulations.

3.3 CFD in ANSYS®

For all flows done in ANSYS® fluent, it solves consecration equations for both mass and momentum (ANSYS, 2009). CFD stands for computational fluid dynamics which is based on three principles: conservation of momentum, energy and mass (Khawaja, CFD-DEM simulations of two phase flow in fluid beds, 2012):

Conservation of mass is presented in equation and the symbols are described in formula:

$$\frac{\partial \rho}{\partial t} + \frac{\partial(\rho u)}{\partial x} + \frac{\partial(\rho v)}{\partial y} + \frac{\partial(\rho w)}{\partial z} = 0$$

with symbol description:

ρ - fluid density

t - time

u - fluid velocity in x-direction

v – fluid velocity in y-direction

w – fluid velocity in z-direction

The formula for conservation of momentum is given by the Navier-Stokes equation in x, y and z-direction, respectively:

$$\frac{\partial(\rho u)}{\partial t} + \nabla^*(\rho u \vec{U}) = -\frac{\partial p}{\partial x} + \frac{\partial \tau_{xx}}{\partial x} + \frac{\partial \tau_{yx}}{\partial y} + \frac{\partial \tau_{zx}}{\partial z} + p f_x = 0$$

$$\frac{\partial(\rho v)}{\partial t} + \nabla^*(\rho v \vec{U}) = -\frac{\partial p}{\partial y} + \frac{\partial \tau_{xy}}{\partial x} + \frac{\partial \tau_{yy}}{\partial y} + \frac{\partial \tau_{zy}}{\partial z} + p f_y = 0$$

$$\frac{\partial(\rho w)}{\partial t} + \nabla^*(\rho w \vec{U}) = -\frac{\partial p}{\partial z} + \frac{\partial \tau_{xz}}{\partial x} + \frac{\partial \tau_{yz}}{\partial y} + \frac{\partial \tau_{zz}}{\partial z} + p f_z = 0$$

Symbol description:

p – pressure

\vec{U} – velocity vector ($u_i + v_j + w_k$)

$$\vec{f} = f_x i + f_y j + f_z k - \text{body force vector}$$

$$\tau = \begin{matrix} \tau_{xx} & \tau_{xy} & \tau_{xz} \\ \tau_{yx} & \tau_{yy} & \tau_{yz} \\ \tau_{zx} & \tau_{zy} & \tau_{zz} \end{matrix} \text{ is shear stress tensor.}$$

The formulas for momentum, energy and mass are calculated by ANSYS® in loop for a given estimated time. This because of the minimal change for each time the formula is calculated, to get the most accurate outcome of the simulations the formulas are combined in the pollutant transport equation (Khawaja, Addition of Euler Extensions in CFD Code, 2012):

$$\frac{\partial V_f}{\partial t} + \frac{\partial(V_f u)}{\partial x} + \frac{\partial(V_f v)}{\partial y} + \frac{\partial(V_f w)}{\partial z} = 0$$

Symbol description:

V_f – volume fraction of the pollutant

t - time

u - fluid velocity in x-direction

v – fluid velocity in y-direction

w – fluid velocity in z-direction

The pollutant transport equation will affect the continuity and momentum equations. Based on the given numbers in chapter 3.2.3 setup in ANSYS® would the outcome plume in the simulations be visible because of the given formula for pollutant transport.

The simulations are set to be transient, referring to the volume fraction which is monitoring over time. This is also predicting how the flow of the pollutant goes. Further, the transport equation k-epsilon model is used within the calculations:

“One of the most prominent turbulence models, the k-epsilon model has been implemented in most general purpose CFD codes and is considered the industry standard model. It has proven to be stable and numerically robust and has a well-established regime of predictive

capability. For general purpose simulations, the model offers a good compromise in terms of accuracy and robustness” (Sharcnet, 2019).

3.4 Designing a model for ANSYS®

To make the simulation as realistic as possible, the most precise location of the simulated area, including existing construction, should be used as part of the input data. The programs used for this purpose were Google Earth Pro and TCX Converter. There were some challenges while developing the simulation model. Different software and file types had to be combined and adjusted to fit together, and this work was complicated and consuming. Below is a description of how the model was built up.

The collection of data points in both distance and height are done using Google Earth Pro. By using the path-function in the software it is possible to collect points with longitude, latitude and altitude, by marking the elements, later called points, which were selected and included in the model -Illustrated the path in figure 18:

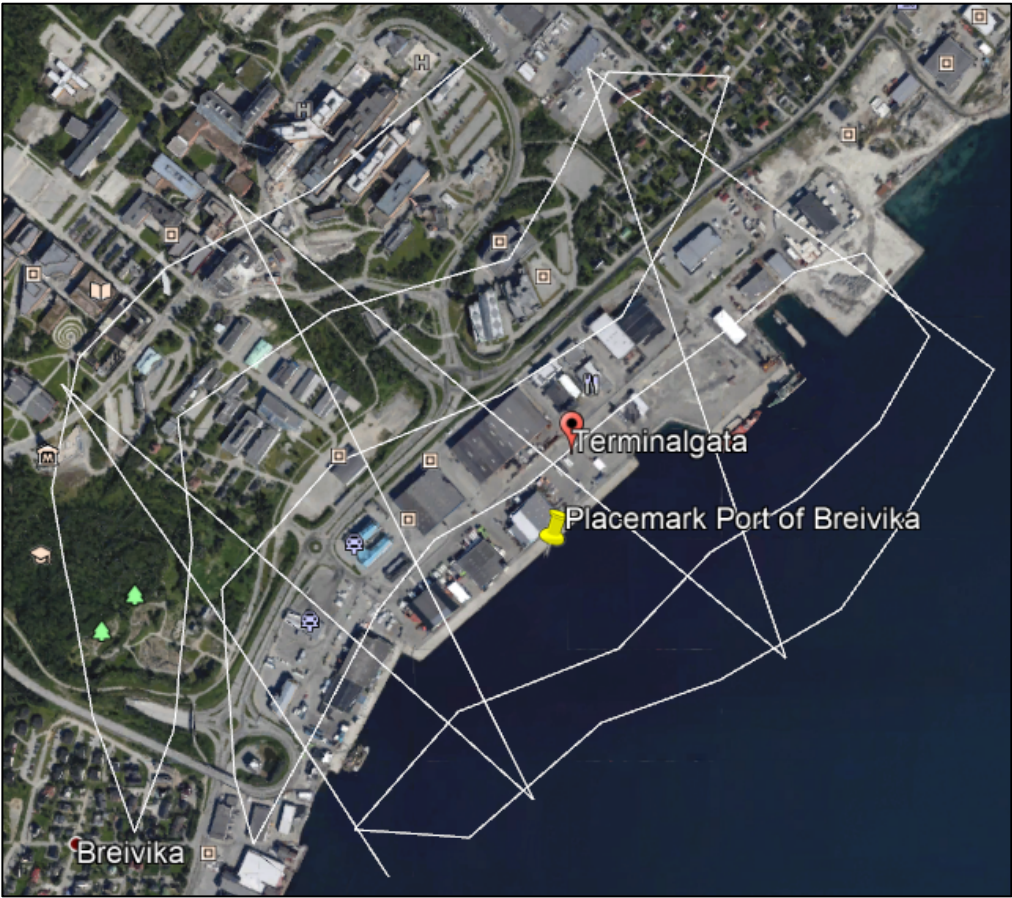


Figure 18 Path containing coordinates near Port of Tromsø, location Breivika.

When downloading coordinates from Google Earth Pro the altitude is not visible in the downloaded coordinates. By transferring the data to the TCX Converter programme it allows to add the altitude. By opening the data in TCX Converter program the altitude is updated to the coordinates and makes it possible to save a file readable in excel containing latitude, longitude and altitude. When uploading the data, the altitude is updated under “track modify”. Here is also the waypoint position error of 5 meters set, which is the lowest number available in TCX Converter. The programme is illustrated in figure 19.

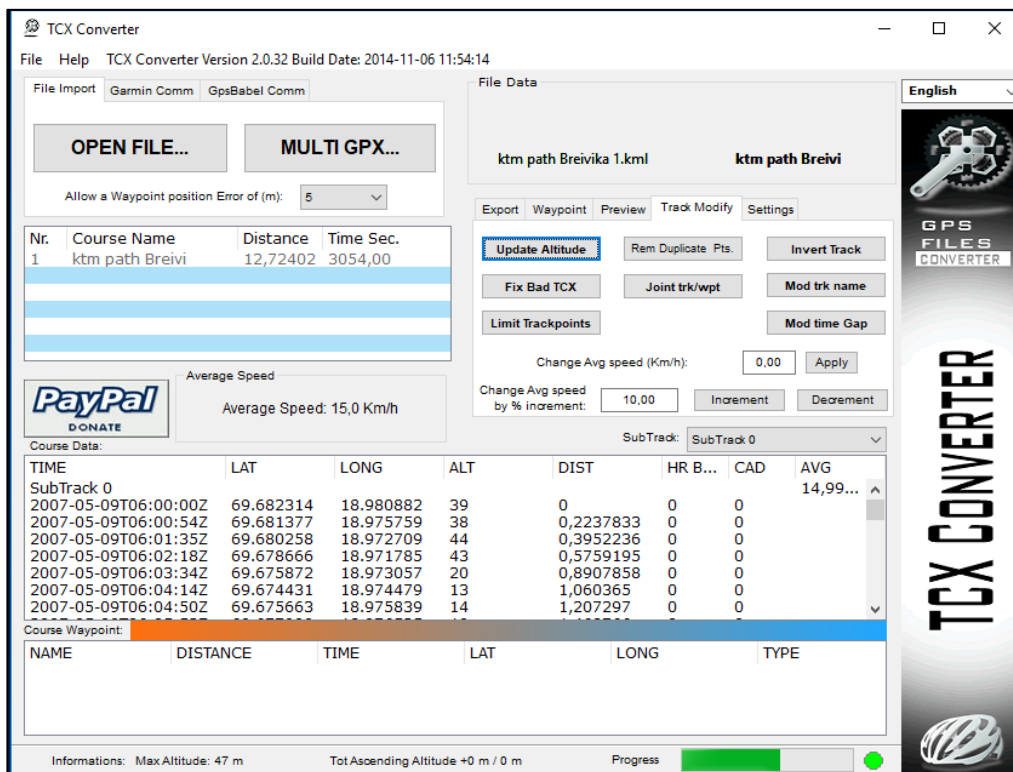


Figure 19 TCX Converter updating altitude for coordinates.

The TCX Converter uses the internet connection and the data from Google Earth Pro to calculate the altitude based on the points from the path constructed in Google Earth Pro and thereafter exported it to a CSV-file readable in Excel. CSV is an abbreviation for Comma Separated Value file and uses the comma sign as a list separator. CSV files are often used in material lists, look up tables and modelling groups. When the data is converted to Excel, there is just need for the longitude, latitude and altitude. Therefore, unnecessary information is neglected from the sheet, so the sheet only contains three parameters; x, y and z coordinates.

During the conversion of the data, longitude and latitude are in GPS-coordinates, and the altitude is in meters, therefore the longitude and latitude have to be converted to meters. This is done in Matlab. The programming in Matlab references the points to the mostly common reference system used for GPS known as World Geodetic System 84 (Palacios, 2006). The script used to change the GPS coordinates to meters can be seen in figure 20:

```

lat = data_lat_long_alt(:,1);
lon = data_lat_long_alt(:,2);
alt = data_lat_long_alt(:,3);

dczone = utmzone(mean(lat,'omitnan'),mean(lon,'omitnan'),mean(alt,'omitnan'));

utmstruct = defaultm('utm');
utmstruct.zone = dczone;
utmstruct.geoid = wgs84Ellipsoid;
utmstruct = defaultm(utmstruct);

[data_x,data_y] = mfwdtran(utmstruct,data_lat_long_alt(:,1),data_lat_long_alt(:,2),data_lat_long_alt(:,3));

data_x_2 = data_x - data_x(1,1);
data_y_2 = data_y - data_y(1,1);
data_z_2 = data_z - data_z(1,1);

```

Figure 20 Formula to convert GPS coordinates to meters, and meters refereed to the reference point in figure 19.

The final lines in the formula calculates the meters for each data point based on the first set point (centre point) in the map at Google Earth Pro. Thereafter, this data is copied into excel and the commas are edited to dots, and thereafter copied into Notepad, this because of the outcome in txt-format and the use of dots instead of commas is readable for both ANSYS® and Solidworks.

When importing the reference points for x, y and z-direction into Solidworks the coordinates are illustrated as points. The dots are being prepped in mesh to Mesh Prep Wizard function where the accuracy is adjusted and prepped to create the terrain as a plane. When the mesh is reflecting the coordinates as the given terrain, it is saved as a part for further use. The file is reopened in Solidworks, the points will appear, and a 3D sketch is created. The 3D sketch

visualises the height of the terrain. The domain for the model is created through the function “lofted surface”.

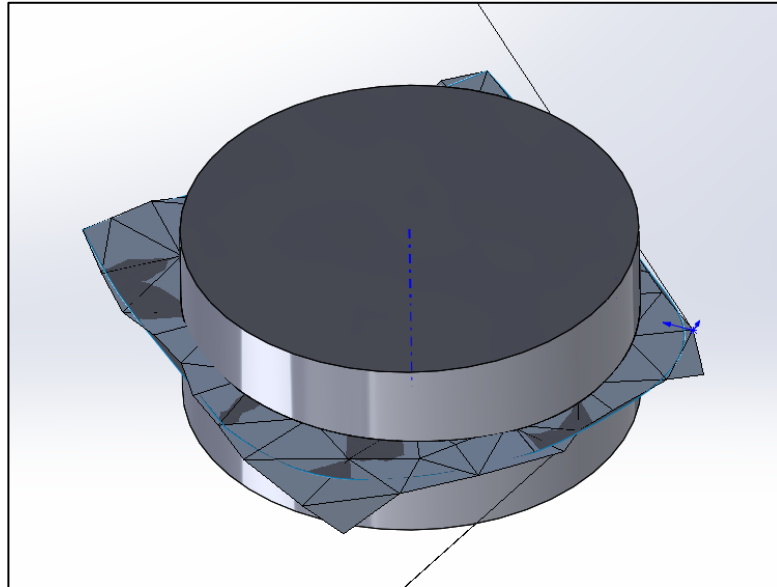


Figure 21 Terrain ground in Solidworks with added cylinder to create domain.

A cylinder is added through terrain, this to create a domain for the simulation. The figure is thereafter cut to be only the terrain in the domain of the cylinder. The circle-shape will be an advantage for further work on the simulations when adding wind conditions. The cylinder is extruded in z-direction 300 meters in both up and down from point zero in the terrain. The bottom part of the cylinder is unimportant and will be cut away and not visible at further use.

3.4.1 Adding geometry to the terrain

When the terrain is constructed, there must be some geometry in it to make the Port of Breivika geographical recognizable. Data collection for the buildings near port is done in the same way as for the geographical data was modelled. The coordinates which is the points in the path is added for each building and this task had to be done by hand, since there is no function of available for squaring buildings. In total, eight buildings, which are the largest buildings in the area, are considered. The buildings which are reconsidered and included in the model are marked with white lines in figure 22.

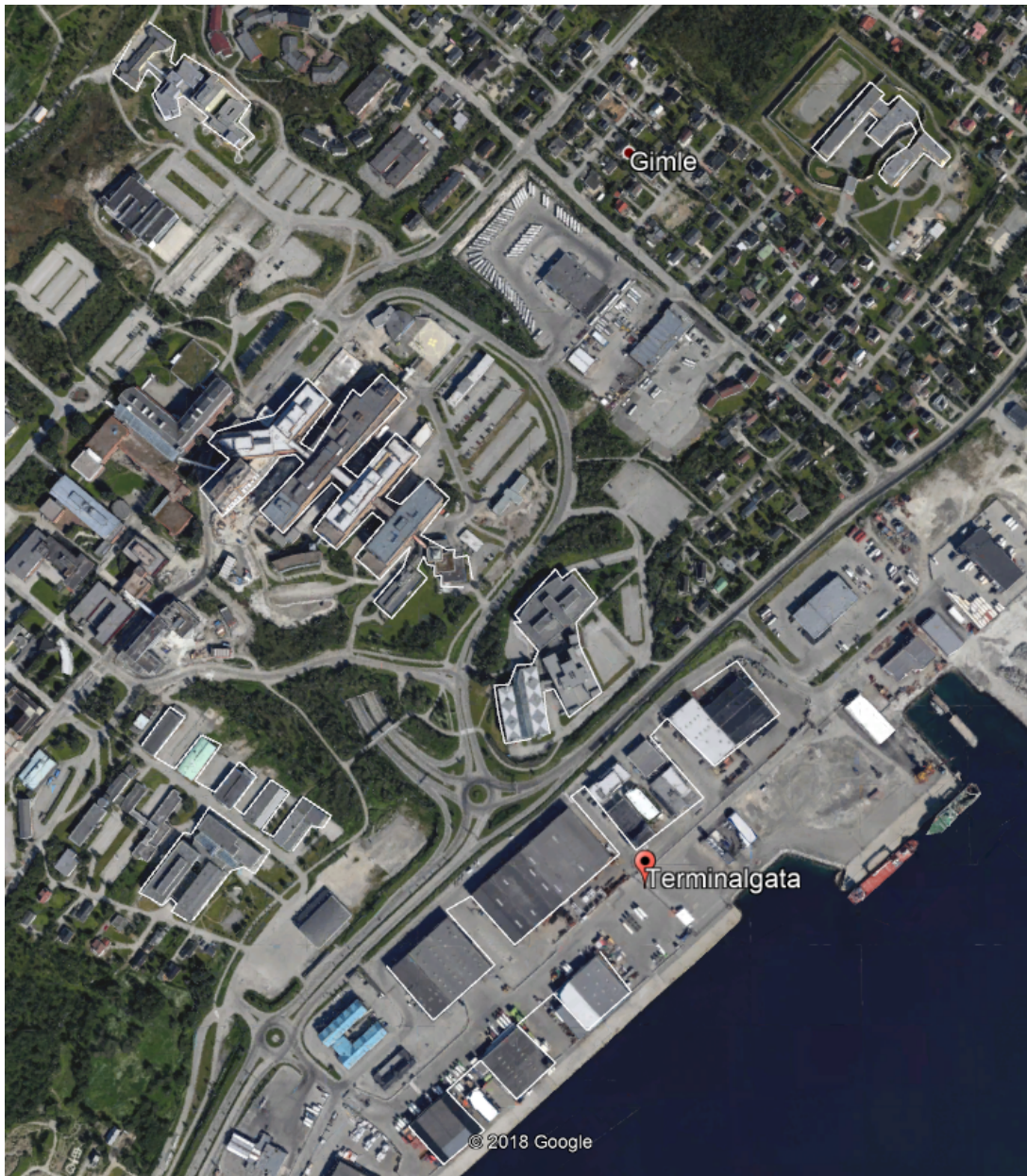


Figure 22 Path demonstrating coordinates of the buildings near Port of Tromsø, Breivika.

The buildings of concern are storage facilities at the port, a high school, an office building, two buildings at the hospital and a prison -the largest buildings in the terrain. Based on the circle shape for the terrain, some of the buildings might be cut or outside of the domain. The buildings are collected the same way as the terrain, and thereafter converted in TCX Converter and recalculated to meters in Matlab. The buildings are scripted to set the centre of the circle, subtracting against the first coordinates. In figure 23 is the script which is depending of the previous script and its location.


```

lat = data_lat_long(:,1);
lon = data_lat_long(:,2);

dczone = utmzone(mean(lat,'omitnan'),mean(lon,'omitnan'));

utmstruct = defaultm('utm');
utmstruct.zone = dczone;
utmstruct.geoid = wgs84Ellipsoid;
utmstruct = defaultm(utmstruct);

[data_x,data_y] = mfwdtran(utmstruct,data_lat_long(:,1),data_lat_long(:,2));

data_x_2 = data_x - data_x(1,1);
data_y_2 = data_y - data_y(1,1);

data = [lat,lon,data_x_2,data_y_2];

```

Figure 23 Script for coordinating the buildings in meters, referencing to the location.

The outcome of the script containing the references of the buildings are converted the same was at the terrain coordinates and saved in a txt-format. In this file is also the point for the emission source, the location of the ship. Due to the created domain, some of the buildings are outside of the domain. Fulfilled script for both Matlab-scripts are available in Appendix B.

3.4.2 Finalizing the model in ANSYS® Workbench

“ANSYS is the global leader in engineering simulation. We help the world’s most innovative companies deliver radically better products to their customers. By offering the best and broadest portfolio of engineering simulation software, we help them solve the most complex design challenges and engineer products limited only by imagination.” (ANSYS, 2018)

Designing in ANSYS is an attempt to imitate the terrain and the emission sources. It includes the geographical points for the added geometry for the buildings and the estimated plume outlet for the emissions. The mesh is analysed to increase the accuracy, and the set-up determines the wanted conditions.

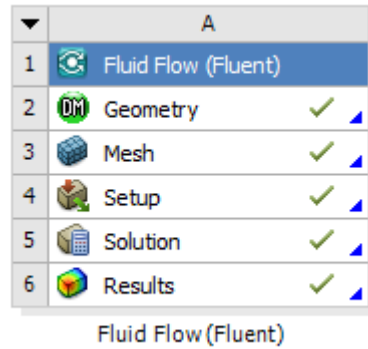


Figure 24 Menu in ANSYS® Workbench.

Above in figure 24 are the different steps for a simulation in ANSYS® workbench, these steps would be further explained in the sub-chapters below.

3.4.2.1 Geometry

The model is set together of the model file made in Solidworks and the coordinate file for the buildings. The analyse system Fluid Flow (Fluent) is used, and the function Design Modeller is opened. The terrain-file made in SolidWorks is imported as an external geometry file.

When the terrain is visible, the function point is indicated and the file with the coordinates of the buildings are imported. The points are now being visible on the terrain. The buildings who are inside the domain for the cylinder is taken into account. To create the buildings, lines are drawn between the different points for the different buildings, generated and thereafter extruded to the wanted height, approximately the height the building has in reality.

Each building has it's on sketch, this to ensure that each building has its own characteristic height.

The source of the pollution is constructed as a pipe. The model has no shape as a ship, because the vessels design for this thesis would only be of esthetical value. The pipe is designed as a tall cylinder. The first model had with a diameter of 10 meters and a height of 50 meters.

After a test run of the model, the pipe was changed, so the second model has three smaller pipes with a height of 30 meters and a diameter of 5 meters each. These three pipes have a

height of 30 meters, and the distance between each pipe is 20 meters.

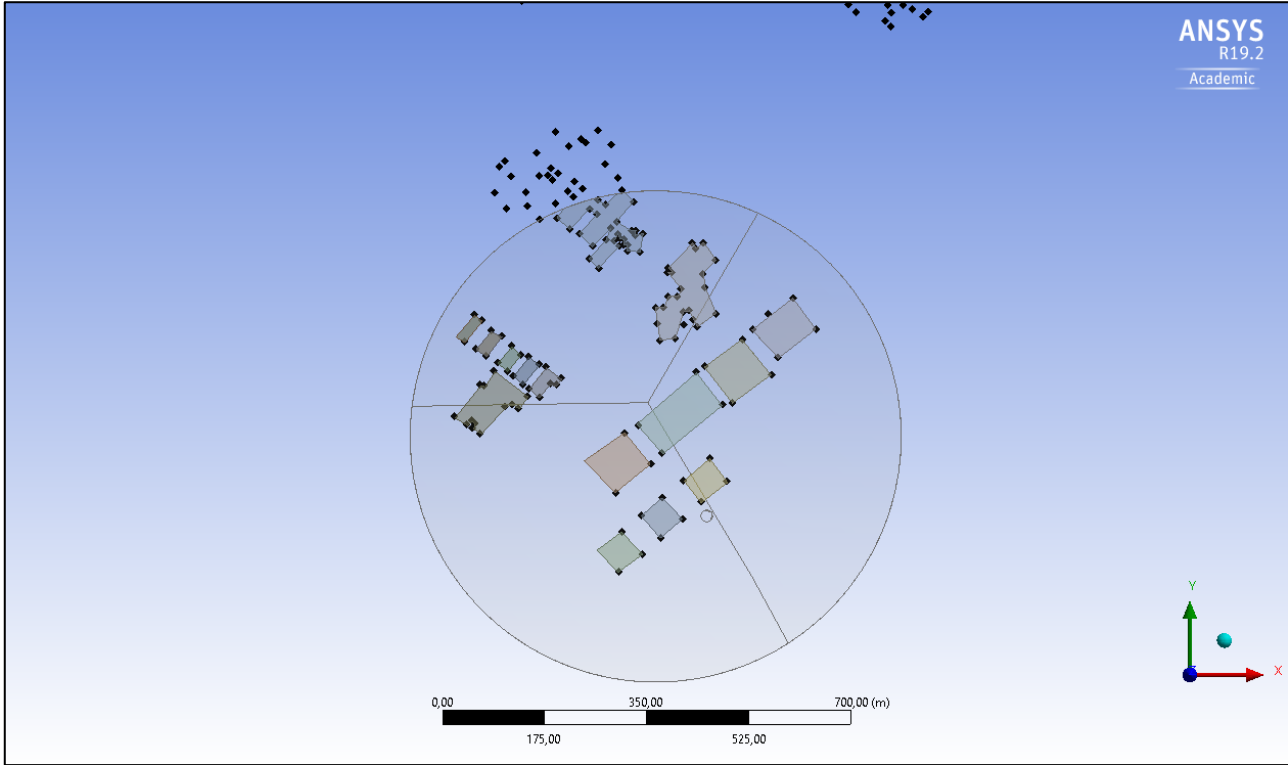


Figure 25 Geometry added to terrain constructed out of geometric points.

Further, the height is adjusted. A lower height would make a larger impact to the surroundings. Due to the geometric of the pipe, the design with three pipes are more realistic than one large. It is more realistic that a vessel has more exhaust pipes than one. This is illustrated in figure 26 and 27. The geometric points for one building in figure 25 is outside of the domain, and the building is not considered further in the work in this thesis. One building is only partly in the domain, and the part inside the domain is considered.

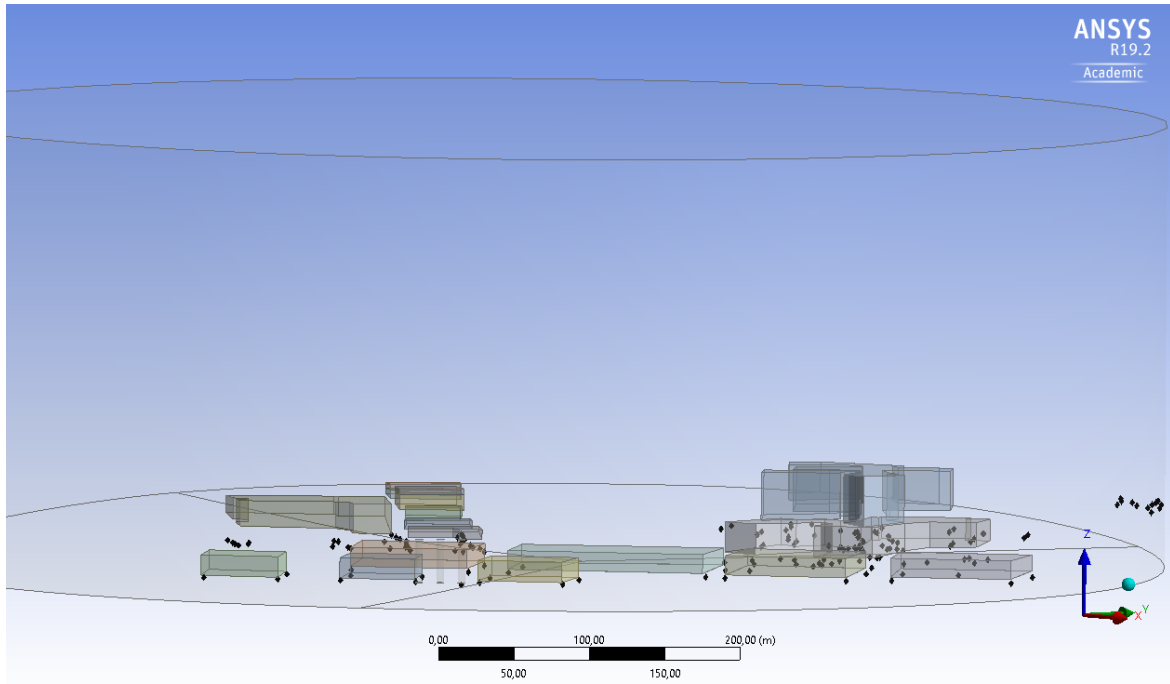


Figure 26 Each building has its own actual height.

To simplify further solution settings, the model has named selections. The terrain is zero_slip, the pipe on the vessel is plume_outlet and the open-air terrain is air_velocity. Zero slip is a function which makes the construction and the terrain firm.

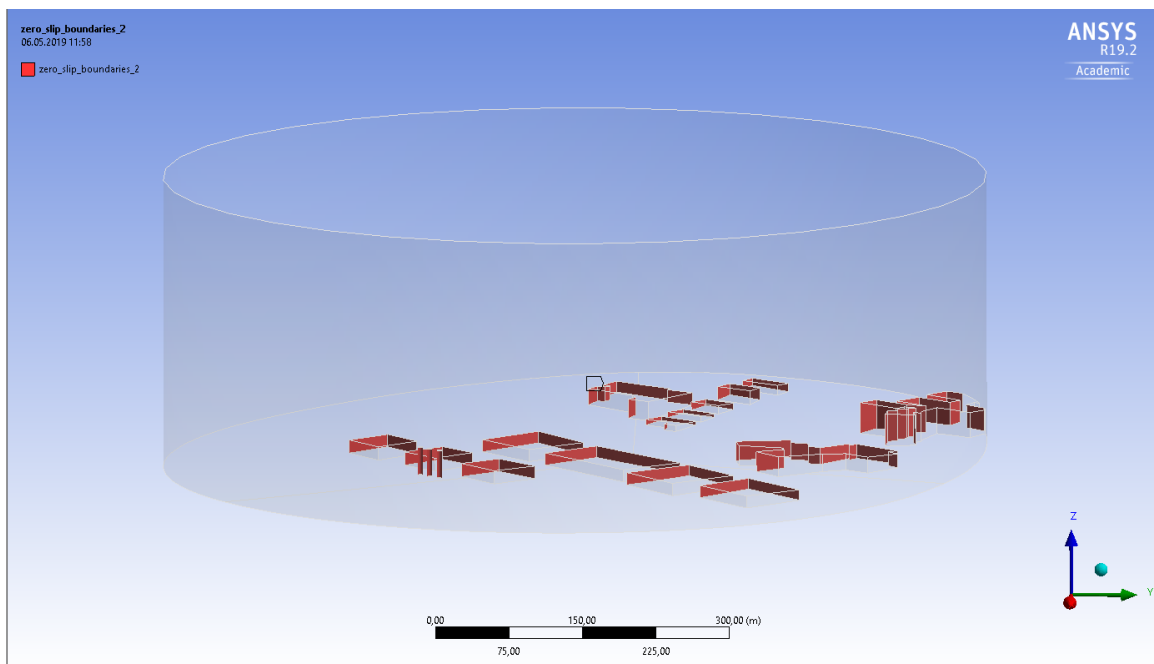


Figure 27 Zero slip boundaries -all the sides of the buildings, including the terrain..

3.4.2.2 Mesh setting analysis

Mesh is a process where the model is divided into several elements, which gives a wider spread of the loads of the component. The higher number of cells, the higher number to collect data from. Despite the possibility to add as many cells as possible, the calculations will get fulfilled at a point. Therefore, mesh setting is tested to find the optimal number of cells to provide as accurate result as possible.

The mesh is set to 25, which indicates an accuracy of the emissions about +/- 25 meters for the surroundings. The nearest area is set to 5, accuracy +/- 5 meters close to vessel to ensure stability of the simulation. The final largest model consists of 1498654 elements, or approximately 1.5 million elements. The medium and small model will have a reduced number of elements, this because of the reduction in height of the pipe resulting a lower number of elements.

Mesh sensitivity analysis was performed to optimize the CFD model. The sensitivity analyses were performed as a test and failure process where the accuracy and number of elements were changed.

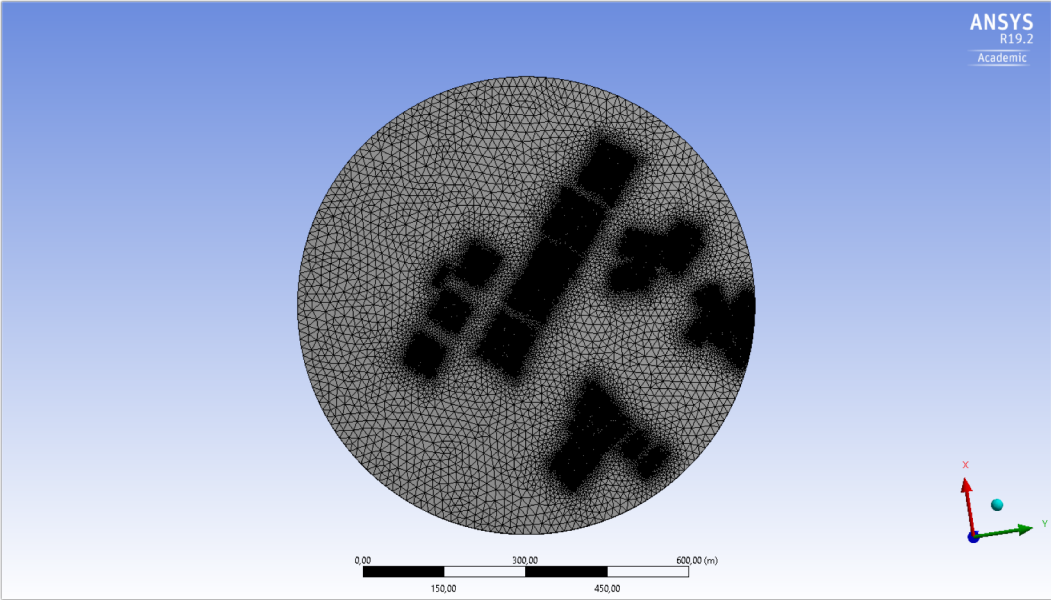


Figure 28 Mesh seen from bottom.

With finer mesh the result will converge to a more accurate solution. Adding a higher number of mesh also increases the number of cells and this would require more from the computer during the simulations. If the number of mesh is too high and the computer cannot handle the amount of the mesh, it may crash.

With the process of testing of the mesh size done, by approximately 1,5 million elements the solutions were convergent and accurate, -considering the capacity of the computer and the size of the domain.

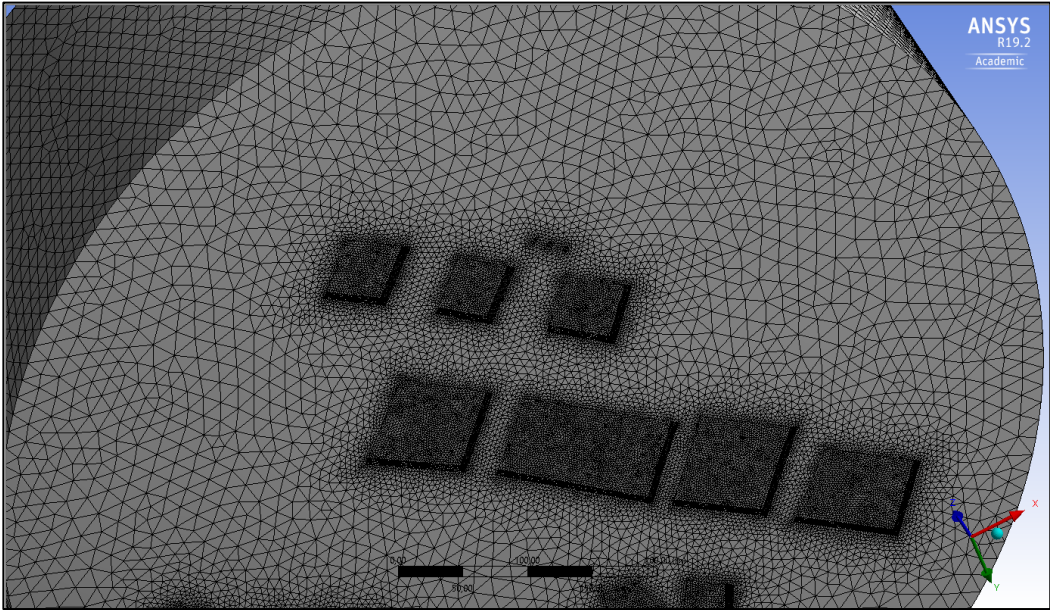


Figure 29 Mesh concentrated around buildings in the terrain.

3.4.2.3 Setup and solution

The settings for the simulations in both setup and solution. In the solution-section the boundary conditions and cell zone conditions are added.

Table 3 Settings for simulations in ANSYS®

Category	Name	Setting
General	transient time	
	z	`-9,81m/s ²
Models	volume of fluid	multiphase
	number of eulerian phases	`2
	implicit	
	implicit body force	
Viscous	k-epsilon	
	realizable	
	standard wall functions	
Materials	select in fluid database	air and CO ₂
Cell zone conditions	operating conditions	
	operating density	`1,225kg/m ³
Boundary conditions	wind outlet	`5 m/s constant
	plume outlet	`25 m/s constant
	phase	`2
	volume fraction	`1
	wind inlet phase	`1
	wind outlet phase	mixture
	plume inlet	phase 2
	wind inlet	phase 1
	wind outlet	mixture
Create	solution data export	
	CFD-post compatible	
	frequency	`20 (time steps)
	quantities	volume fraction phase 1 volume fraction phase 2
Materials	Setting up physics	`phase 1 = air `phase 2 = CO ₂
Run calculations	time step size	`0,0005
	max interactions	`50
	number of time steps	`1000

The phases in boundary conditions consists of two phases. Phase one is air, and phase 2 is CO₂. In the outlet phase are both phases mixed – seen as the plume in the simulation result. The number of time steps is in seconds, which in real time represents 16,6 minutes of polluting.

3.4.2.4 Results

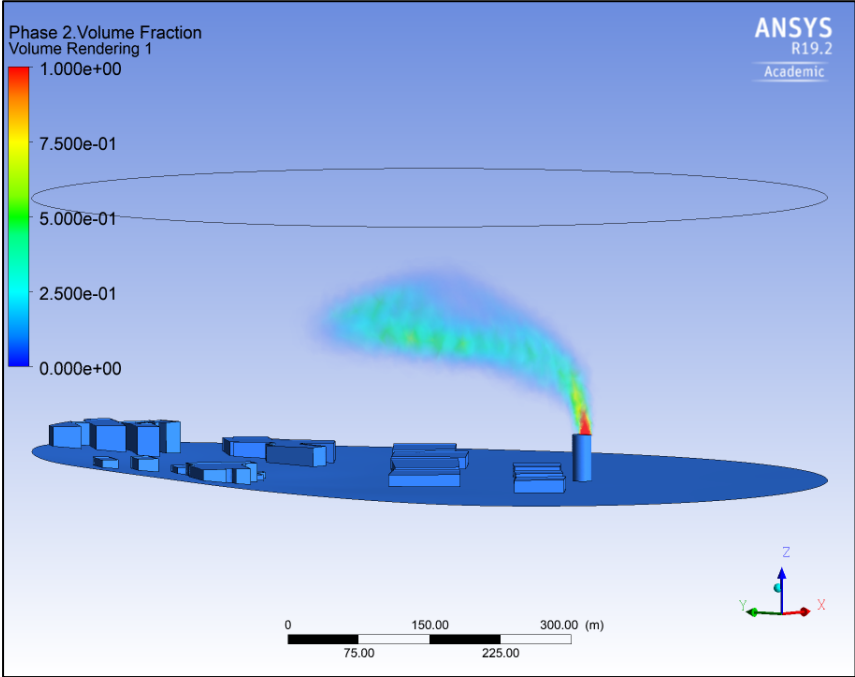


Figure 30 Solution with one large pipe as source.

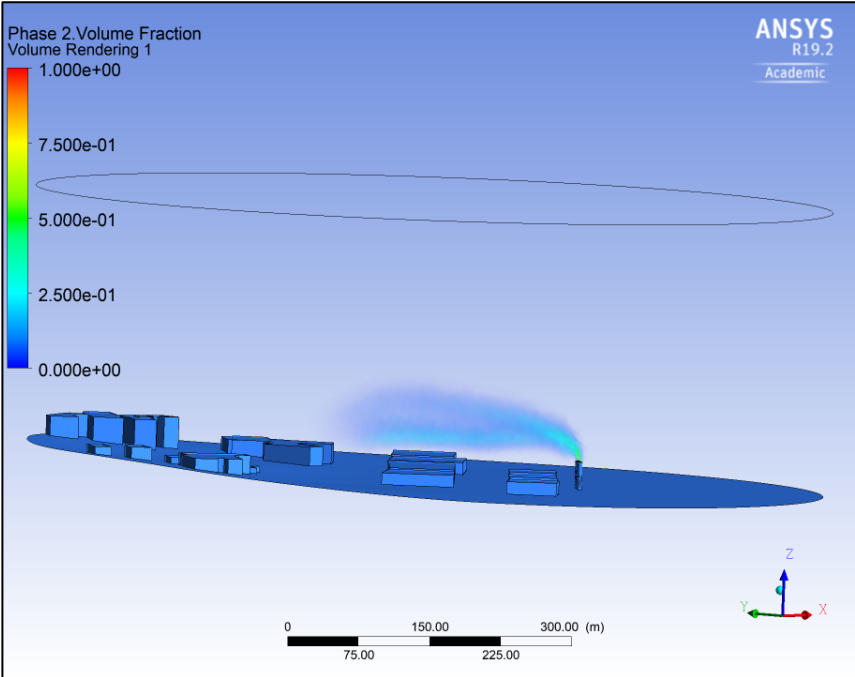


Figure 31 Solution with three pipes as source, reduced height and diameter.

Comparing the two results, it is easy to see that the first simulation result with a large pipe seems over scaled and seems more likely to be a power-plant-situation. The second model is more realistic to represent a vessel at port. It is also more visible in figure 30 and 31 that a

lower height of the pipes give a larger impact, another thing is also that the flow spreads and reaches the atmospheric pressure faster with a higher pipe.

For continued simulations the model with three pipes will be used. There will also be simulations where the height of the pipe is decreased to exemplify vessels with different heights.

3.4.2.5 Residual plot

When the simulation runs in ANSYS®, a graph of the residual plot attending as the simulation is running. The graph as illustrates following:

- Continuity - black
- X-velocity – red
- Y-velocity – green
- Z-velocity – blue
- k – turquoise
- Epsilon – purple
- Vf-Phase 2 – yellow

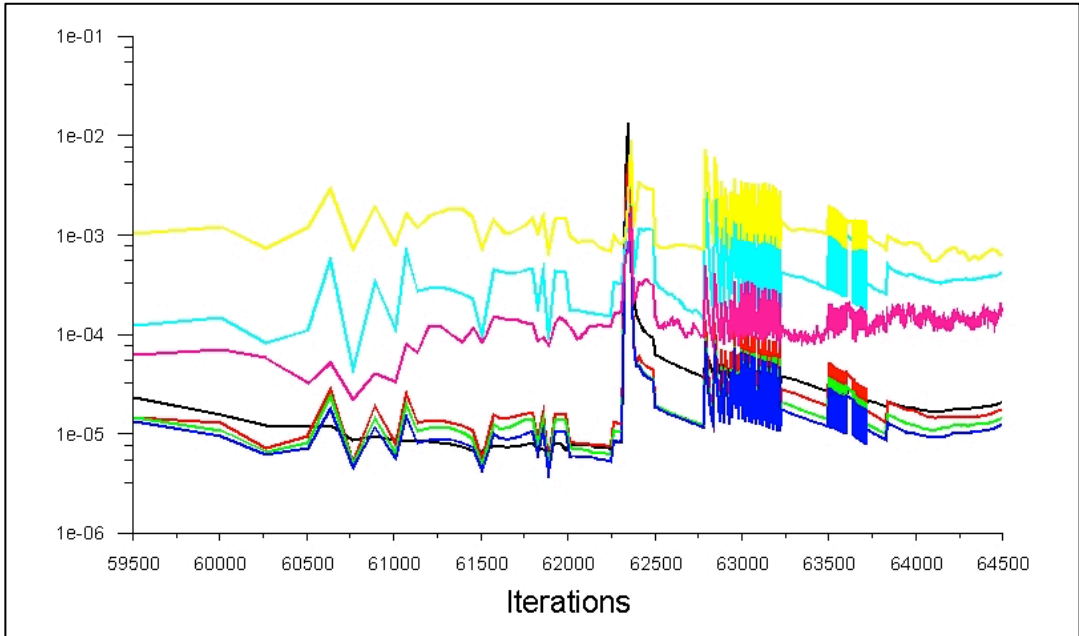


Figure 32 Iterations for several simulations.

Of interest is the Vf-Phase 2 value, which is the volume fraction phase for the pollution. The yellow line in the graph illustrates how the CO₂ is in the model and is creating the emission – the plume. When the graph is steady, the simulation is stable and realistic. Figure 32 includes several simulations, so the “jumps” in the interactions indicates a new simulation is started, which also illustrates the transient time. The linear movement of the Vf-phase 2 indicates a stable and reliable simulation.

3.4.3 Challenges related to the modelling

The idea of designing a terrain for the simulation was initially evaluated to be easy, but no one knew how to put the different parts together. The different steps to finalise the model as described above in chapter 3.4.3 took more than three months. When the scope of the model was larger than the student license would allow for, an academic research license was applied for. The research licence has unlimited of options when it comes to elements and possibilities to run simulations.

It took several rounds and attempts to make a terrain for the simulation. The work coordinates are converted and reopened in a txt-format, so ANSYS could process the data.

The model fit in the terrain coordinates to the mesh setting analysis to perform the optimal simulation. After testing with various mesh and number of elements, pipe height, wind strength and wind directions the model was fulfilled. The three first months when figuring out how to perform the modelling was almost a strain. When the model seemed to be fine one day, it crashed the day after, and when the coordinates seemed to be correct, they had to be re-converted and in another format. The challenges where lined up during the design-period.

4 Results and discussion

In total 56 simulations were performed. Each sequence took about 4-8 hours, depending on how the simulation where set up, -with fresh data or by use of data from earlier simulations as support. The following cases were modelled:

Case A – Chimneys height 30 m

Case B – Chimneys height 20m

Case C – Chimneys height 10 m

Case D – Chimneys height 5m

Table 4 Overview of model and wind strength.

Model	Simulated wind strength (value v)
Case A	1 m/s 3,3 m/s 15 m/s
Case B	3,3 m/s 15 m/s
Case C	3,3 m/s 15 m/s
Case D	3,3 m/s 15 m/s

During the simulations of case A, the wind strength of 1 m/s was so close to zero that it was evaluated to have no impact on the final results. The wind strength of 1m/s isn't included in case B, case C and case D. The simulations of most interest are presented in the subchapters.

All simulation results illustrating the pollution are available in Appendix A. Together with the results will a table be presented, including the wind strength and the wind directions for each case. The documentation of each simulation consists of two pictures, one from above and one from the side. By observing the simulations from above it is possible to see the hidings of pollution behind buildings.

4.1 Case A

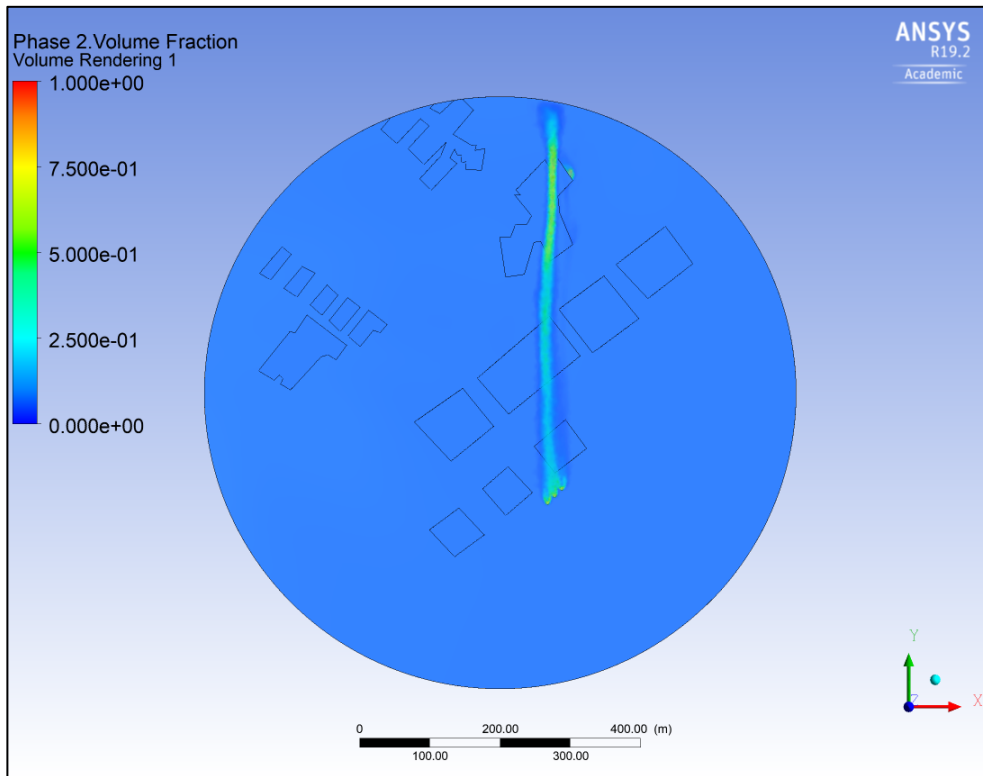


Figure 33 Wind strength 15 m/s illustrated from above.

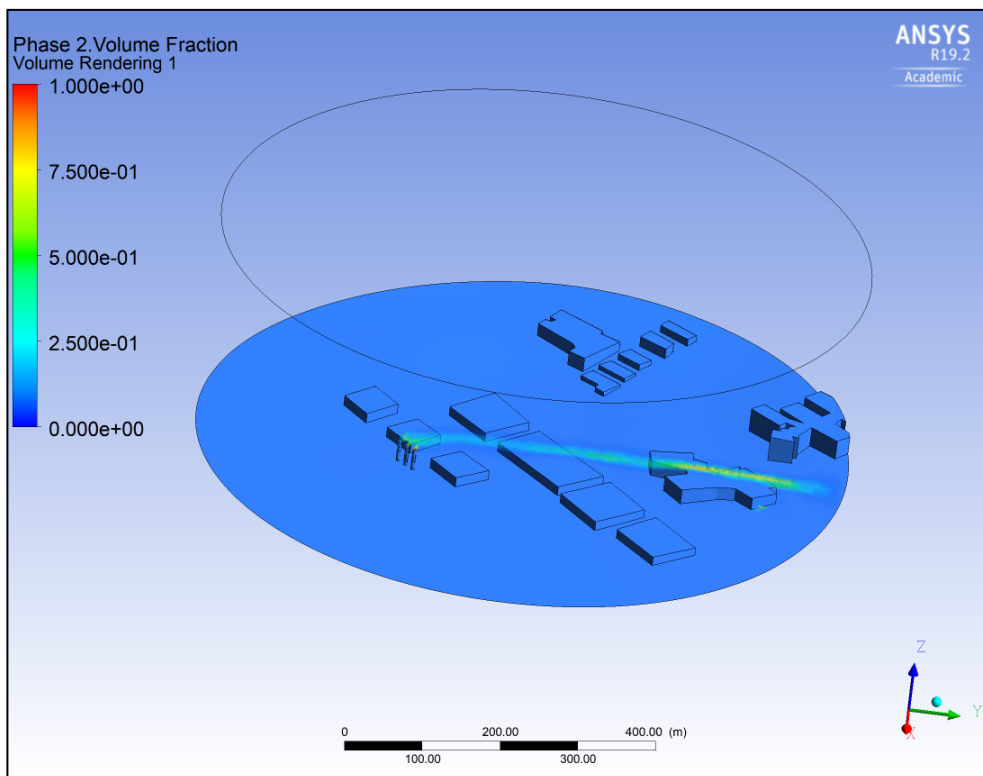


Figure 34 Wind strength 15 m/s seen from the side.

Both in figure 33 and 34 it is possible to catch a glimpse of an accumulation of pollution at the building located in the wind direction. During the simulation the wind strength of 15 m/s is the only one which occur to reach at one of the buildings.

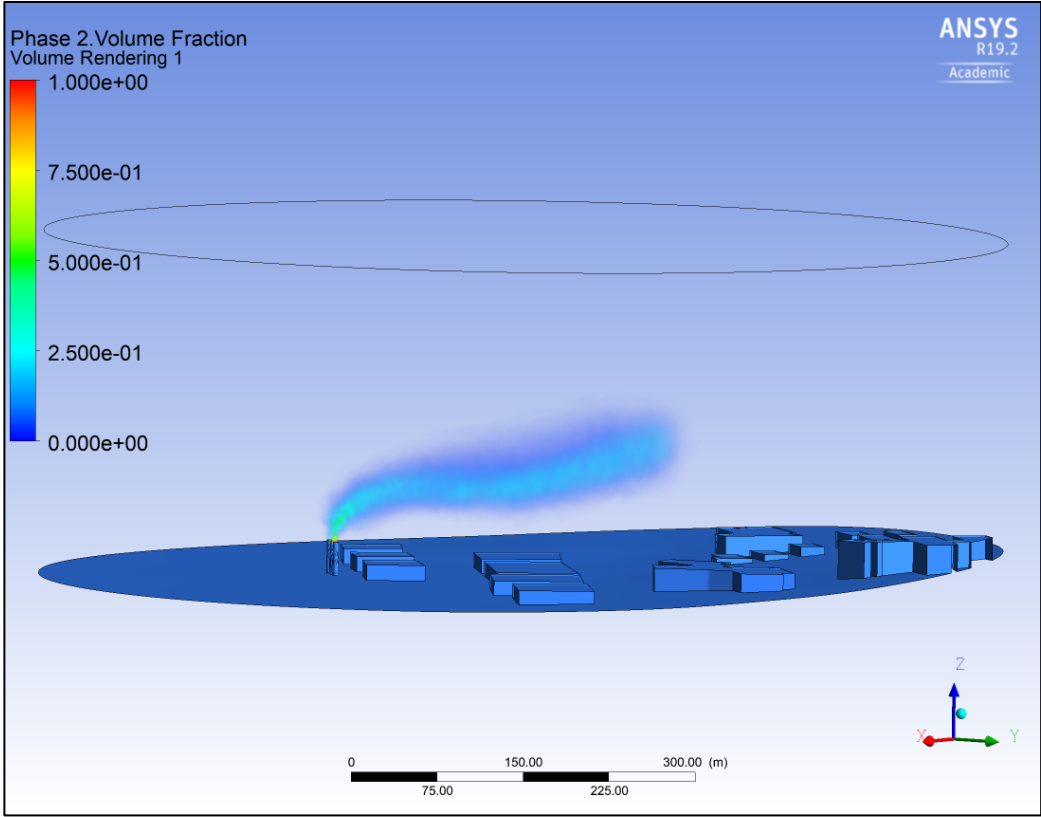


Figure 35 Wind strength 5 m/s seen from the side.

For this model, the simulations with a lower wind strength lower than 5 m/s disperses above the terrain. As illustrated in figure 35, the pollution goes beyond the terrain. Because of the height of the plume, in a real situation, it could reach the buildings outside of the domain or go above the island of Tromsø.

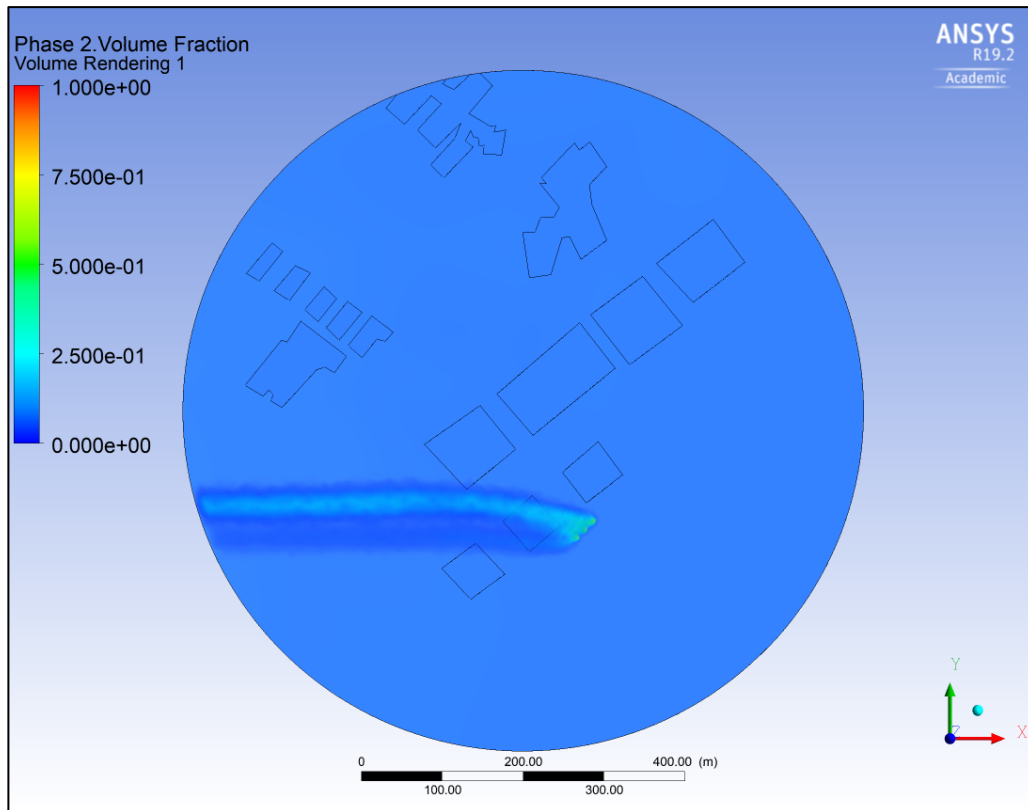


Figure 36 Wind strength 5 m/s seen from above.

With high wind strength the emission drops faster and will influence closer to the terrain. Low wind strength would make the emission rise above the heights in the terrain and even right up.

This could be the result of the emissions for vessels with a height of 30 meters or higher. The emission from a tall vessel might have no effect or give significant pollution in the terrain nearby.

Figure 37 illustrates how the pollution disperse with low wind strength. The swirling of the pollution is maintained when the strength of the outlet of the pollution decreases. This type of effect can also occur between buildings or when pollution gets trapped for instance in a corner of a building.

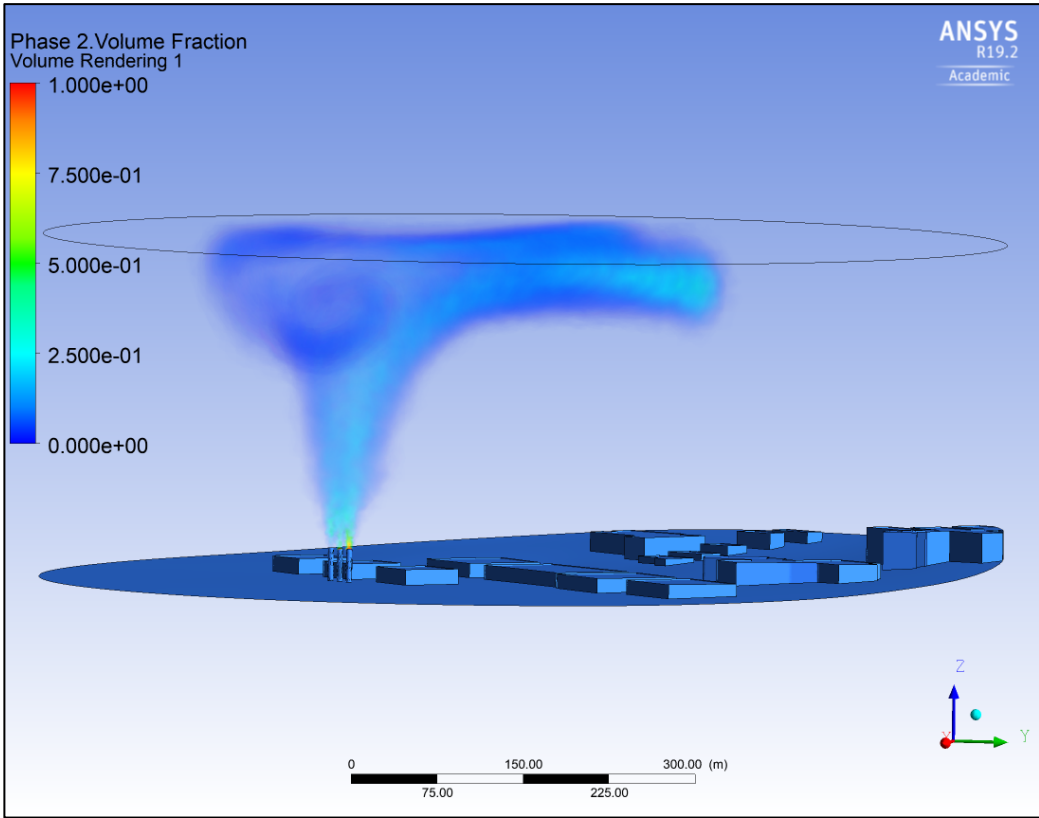


Figure 37 Wind strength 1 m/s, emission goes up.

4.2 Case B

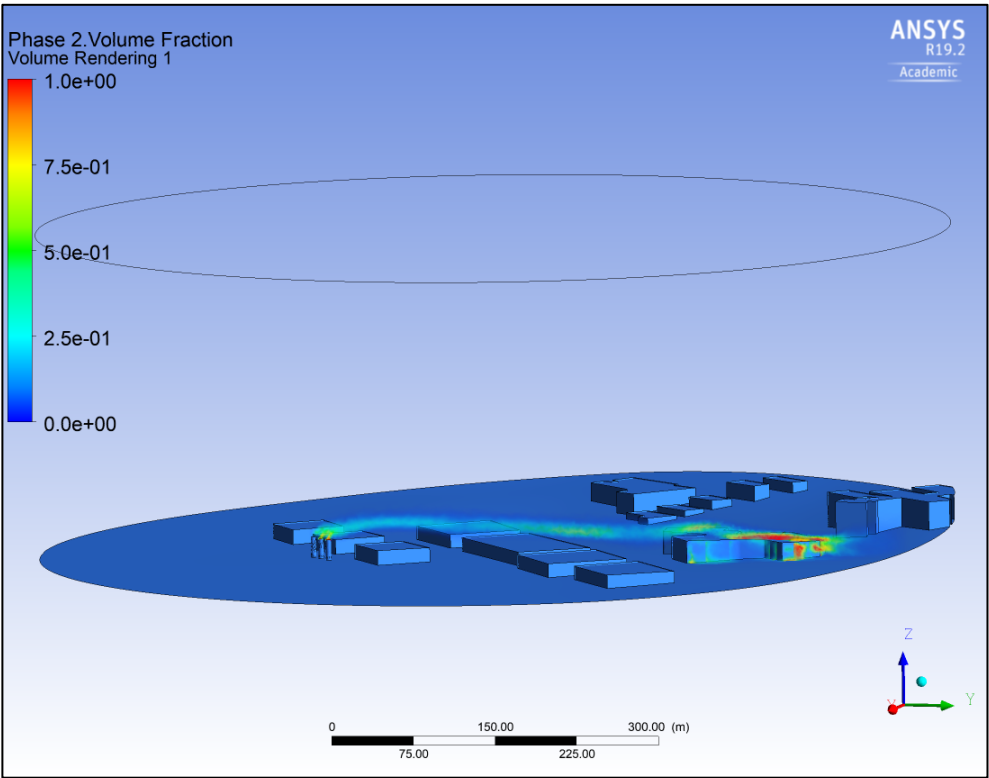


Figure 38 Wind strength 15 m/s seen from the side.

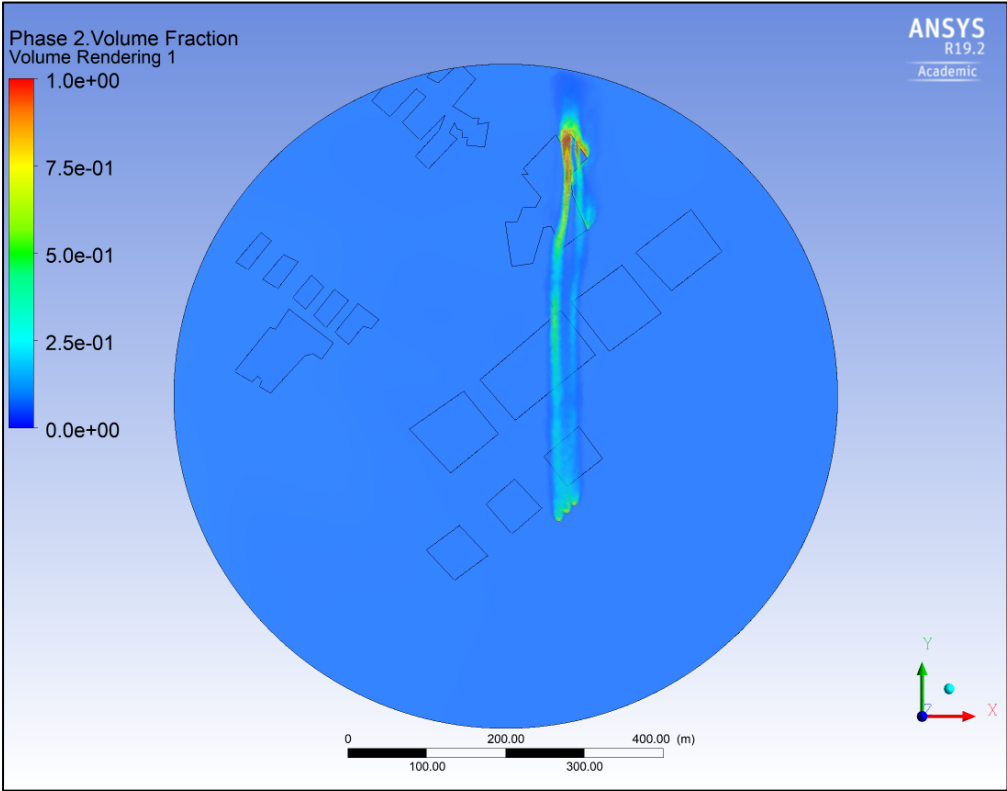


Figure 39 Wind strength 15 m/s seen from above.

By decreasing the pipes to 20 meters the emissions reach the buildings more and the emission is collected in “pockets” -this is the vortex-effect.

“In reference to the windward side of the building, air pushes against the walls of the structure with high pressure. Air which then flows around these sides of a building forms vortex's as the airflow reaches the ground and sweeps into windward corners. Essentially, the presence of urban structures causes these abrupt changes in wind direction (Sam, 2012).”

The vortex-effect for wind is creates corridors of air on the lee-side of the geometry, and the air wold be held there and be circulated down against the terrain. If a landscape has more geometry -for instance streets or canyons, the capture of air wold be the kept in corridors. This is often felt while walking in streets with tall buildings around, where there is wind from the side that you think is isolating for the wind, but in fact the wind is kept between the buildings.

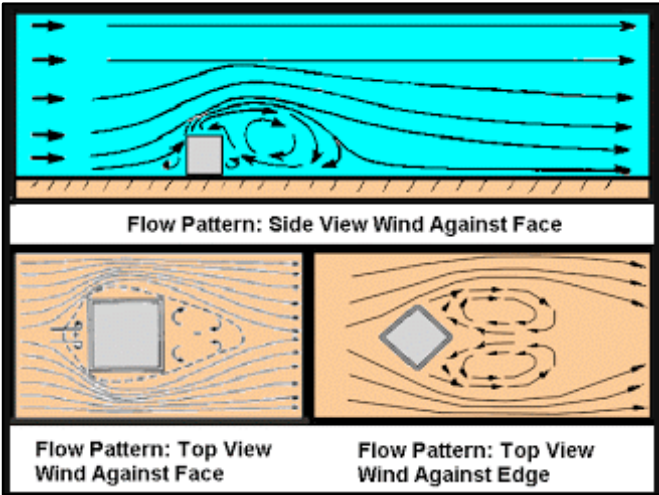


Figure 40 Illustration of the vortex-effect (Sam, 2012).

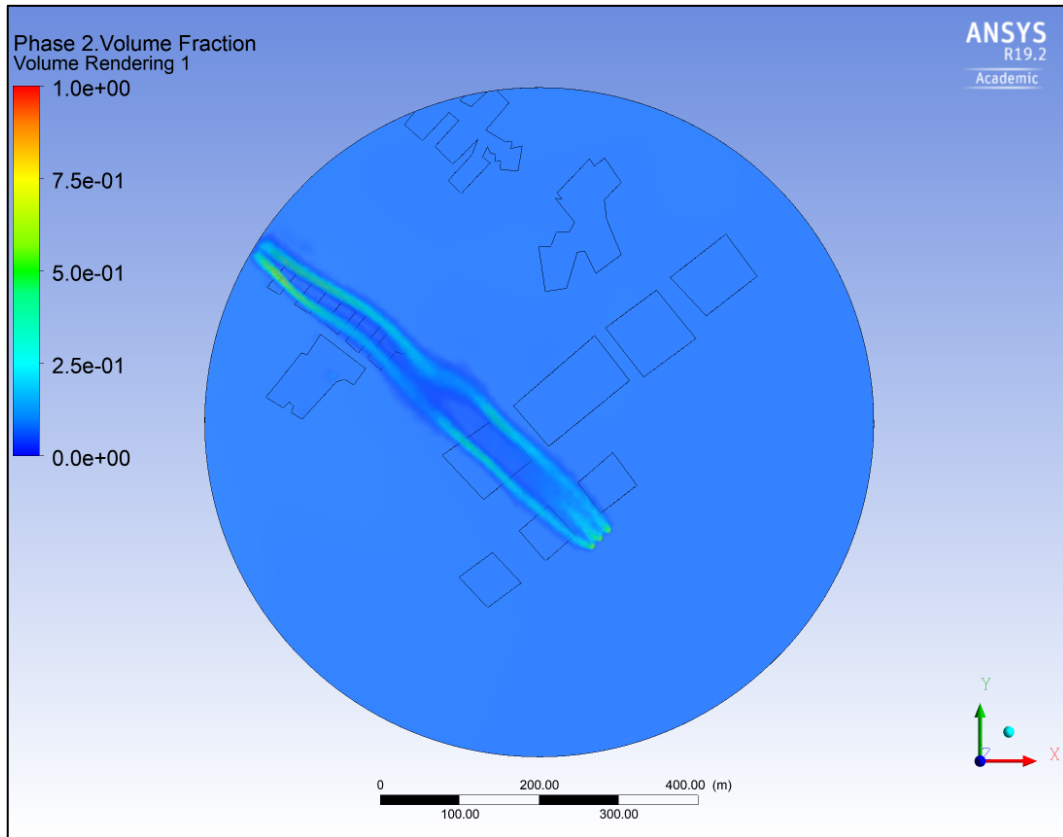


Figure 41 Wind strength 4,25 m/s seen from above.

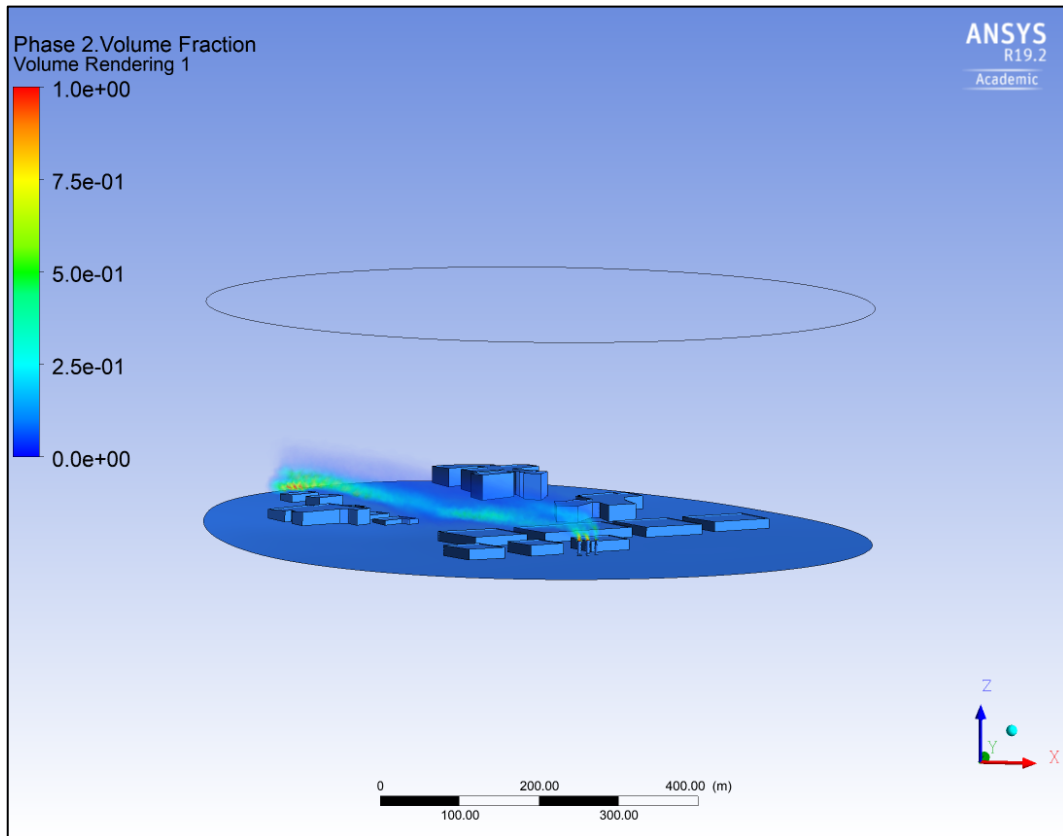


Figure 42 Wind strength 4,25 m/s seen from the side.

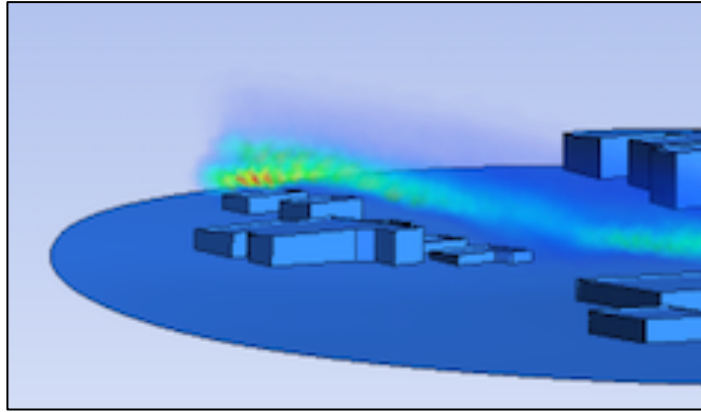


Figure 43 Wind strength 4,25 m/s zoomed in.

For the situation in figure 41, 42 and 43 there is also a vortex occurring behind a building, with a wind strength of 4,25 m/s. This is a high-school building. The movement of the emission is of interest. The flow goes down before its “bouncing” up again. Despite the wall function for the domain, it is likely that the emission gets trapped behind the building and creates a polluted zone. Referring to the time step and time step size the outcome of the emissions represents 16,6 minutes in real time.

4.3 Case C

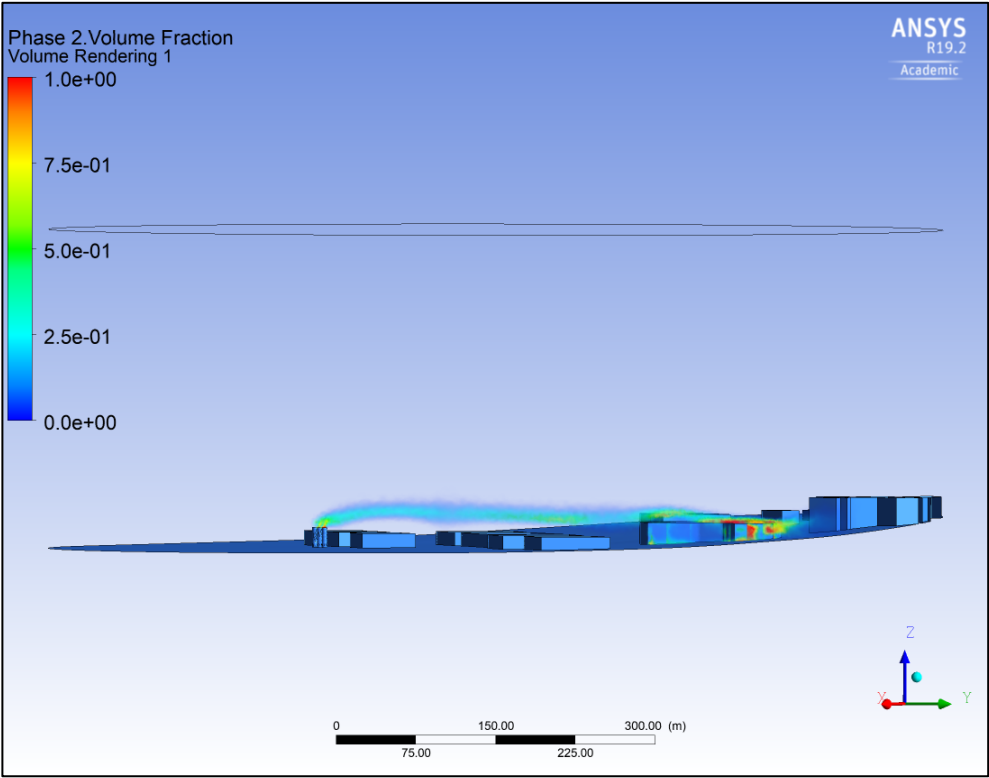


Figure 44 Wind strength 15 m/s seen from the side.

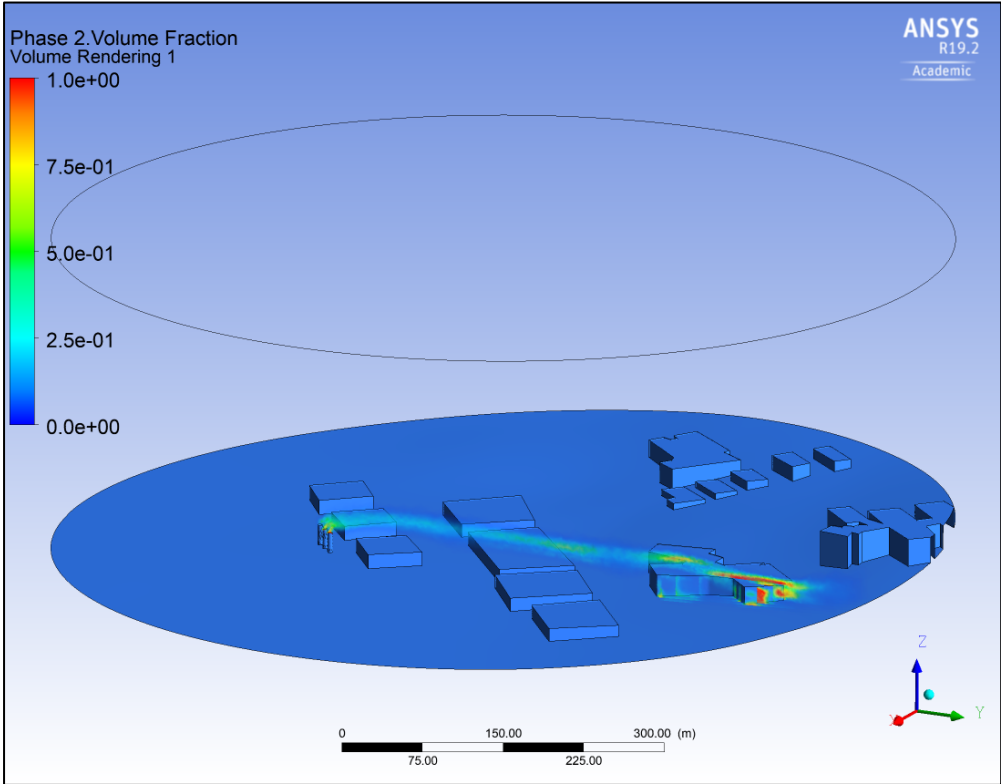


Figure 45 Wind strength 15 m/s seen from above.

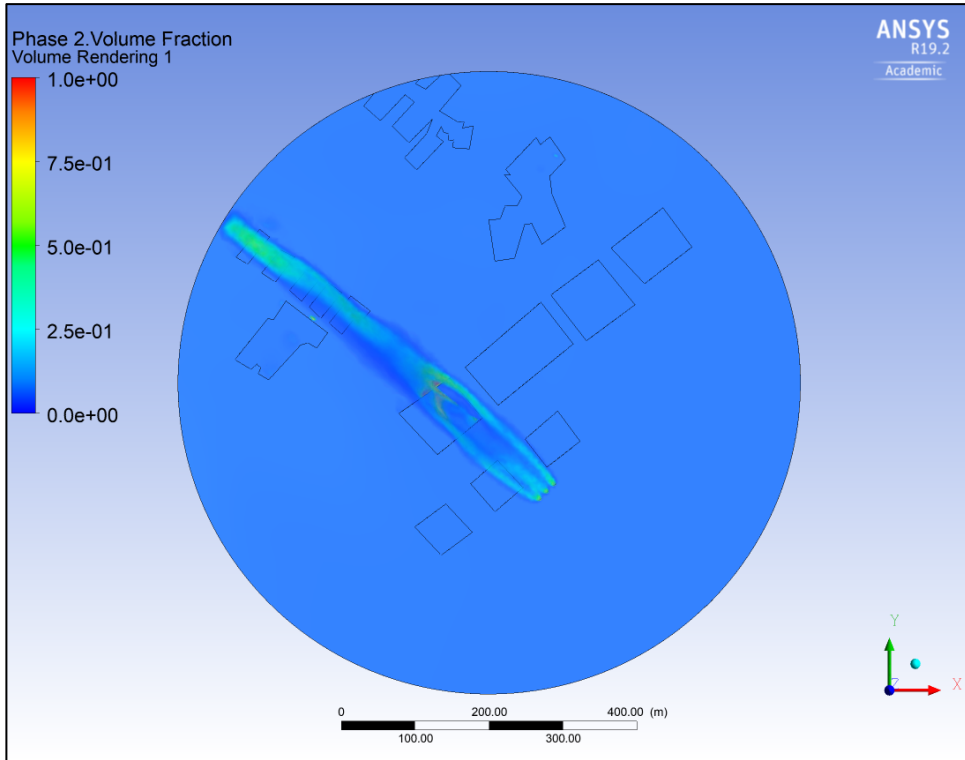


Figure 46 Wind strength 4.25 m/s seen from above.

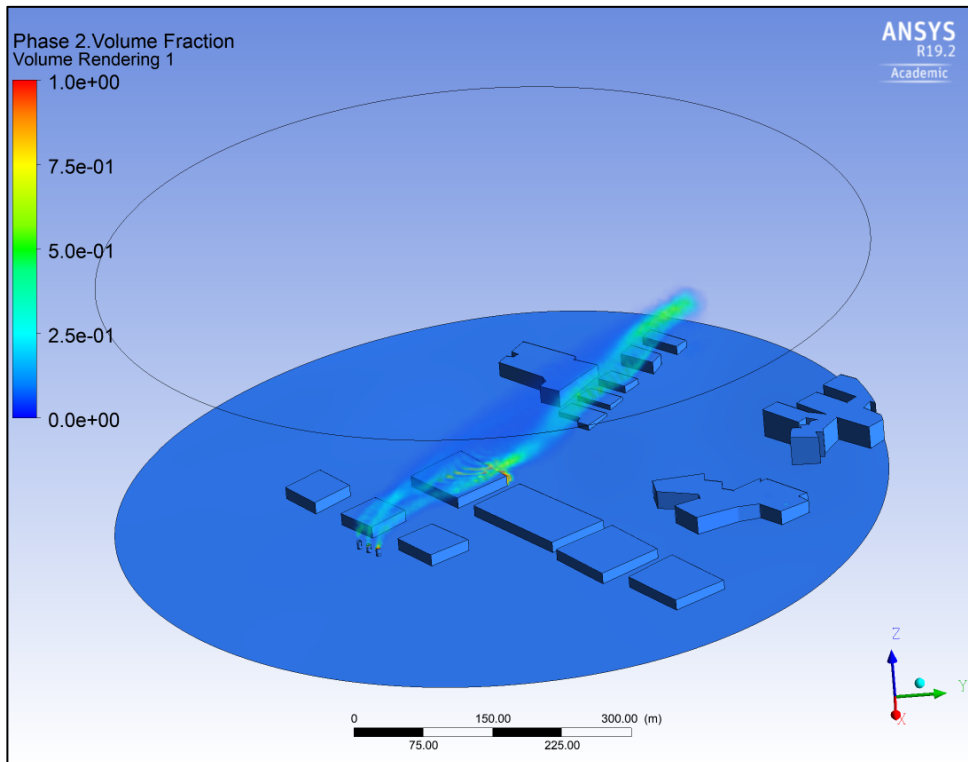


Figure 47 Wind strength 4,25 m/s seen from the side.

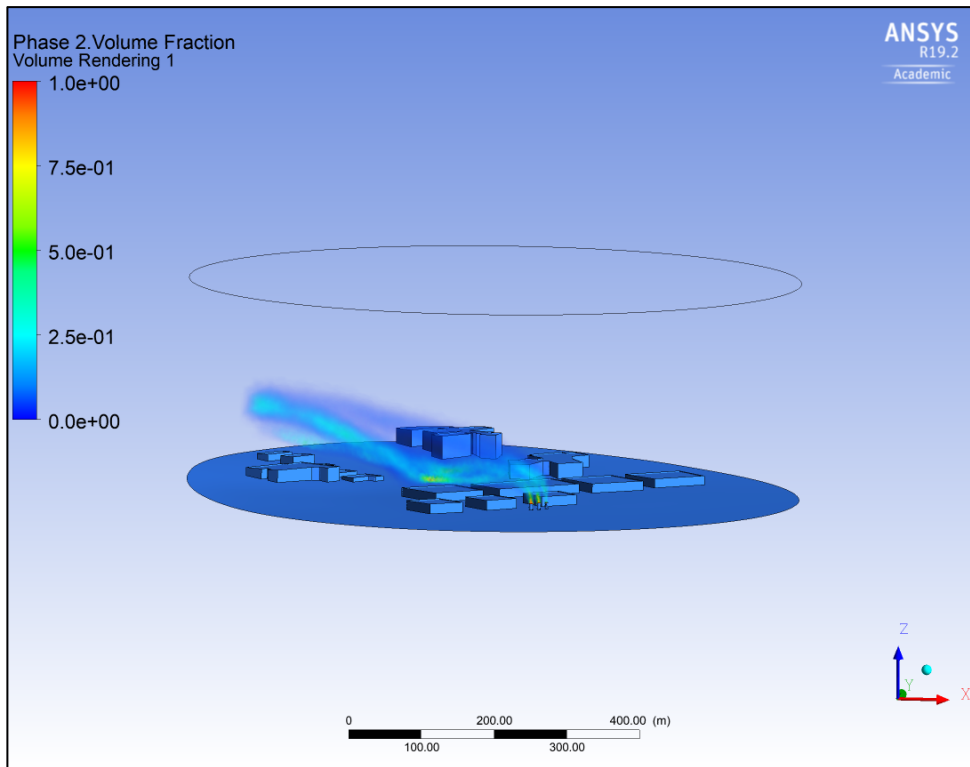


Figure 48 Wind strength 2,8 m/s seen from the side.

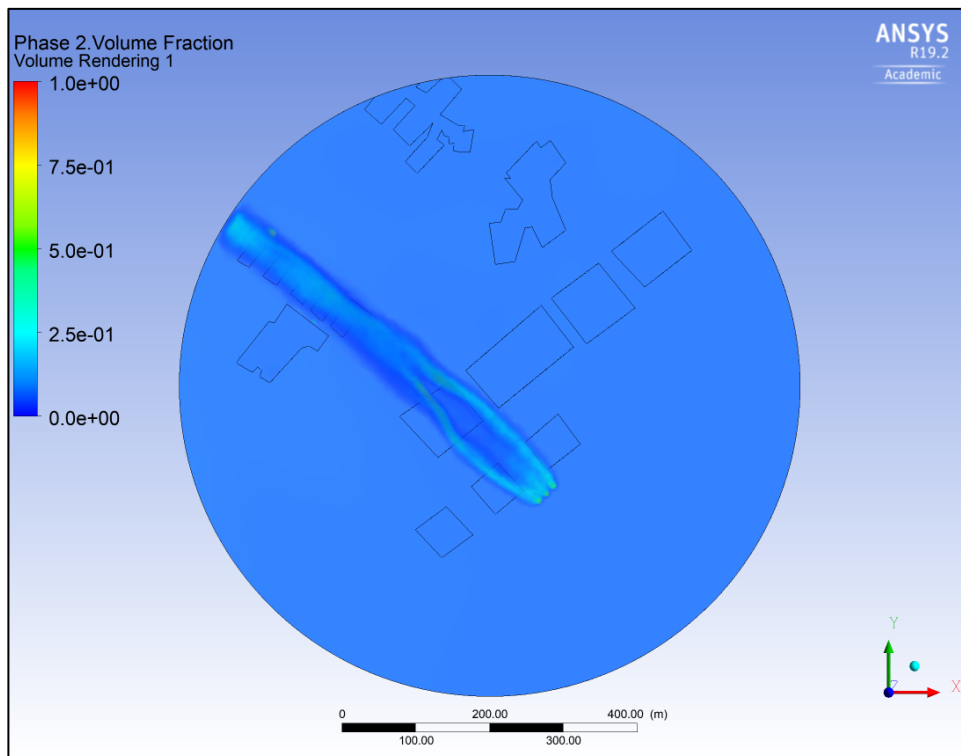


Figure 49 Wind strength 2.8 seen from above.

The presence of the emissions increase as the height of the pipe is decreased. The models continuing the wind strength and wind directions which included small volume of pollution increase the volume due to the reduction in height. Of interest is the emission illustrated in figure 48 and 49 where the emission “bounces” to the terrain before it moved further and dissolves to air.

From previous, one of the main roads are located where the emission is bouncing, and this could contribute to decrease the air quality in the area. Looking at figure 48 and comparing it to figure 22, the area is a junction for both traffic and inhabitants on a daily basis.

4.4 Case D

The height of the provoked model is set to 5 meters. With a decrease of 25 meters from the first large model the effect is highly increased. Despite low wind strength, the influence of the emission is high as seen in figure 52, 53 and 54.

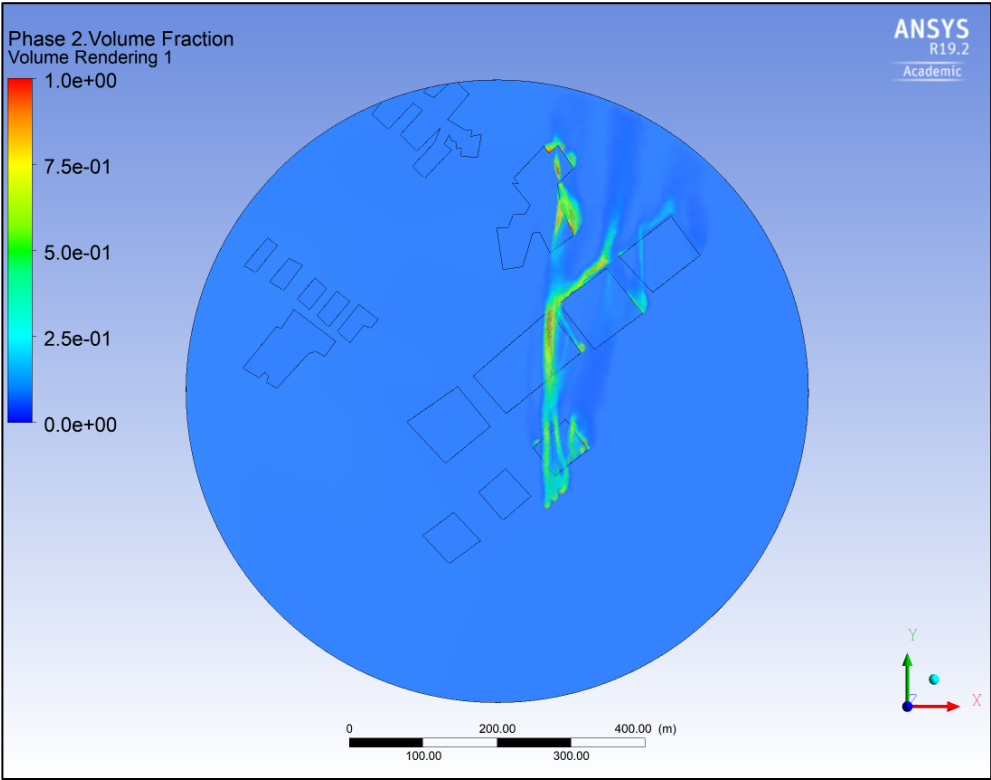


Figure 50 Wind strength 15 m/s with large impact.

The wind strength of 15 m/s strikes the buildings closest to port as well as the buildings further away. The buildings closest to port is storage buildings for goods and a workplace for several people. This location is also a loading and unloading point for vessels, so it is seen as an industrial location. The largest vessels visiting Tromsø arrives at Breivika.

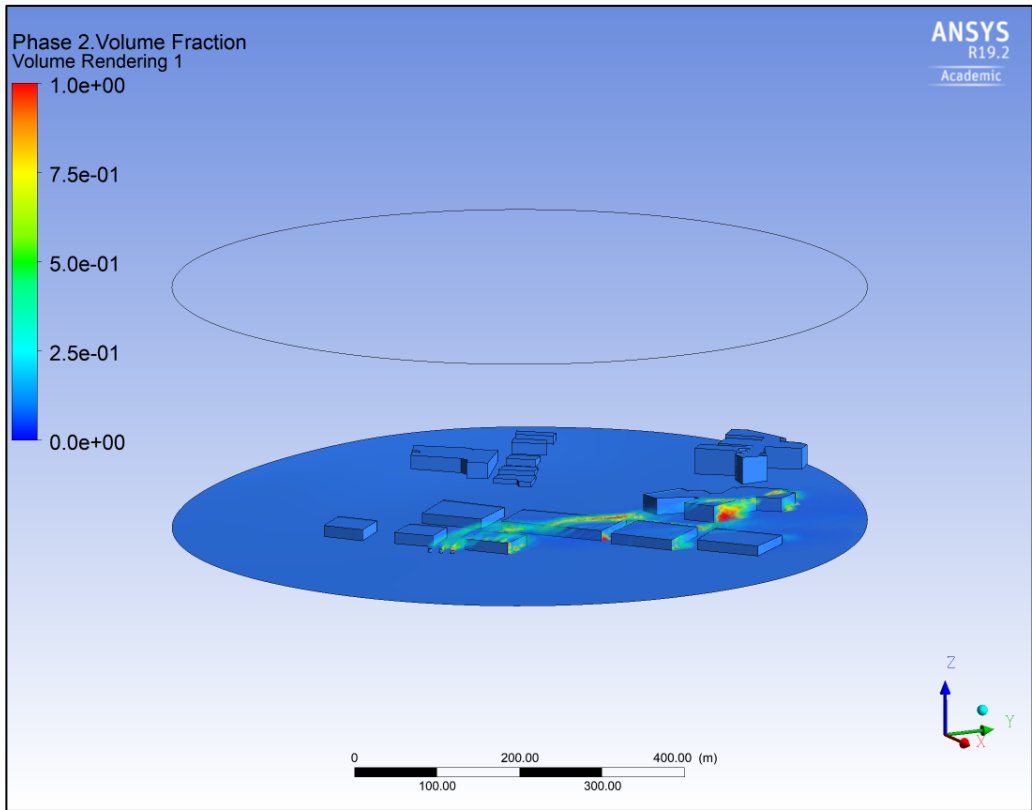


Figure 51 Wind strength 15 m/s with large impact seen from the side.

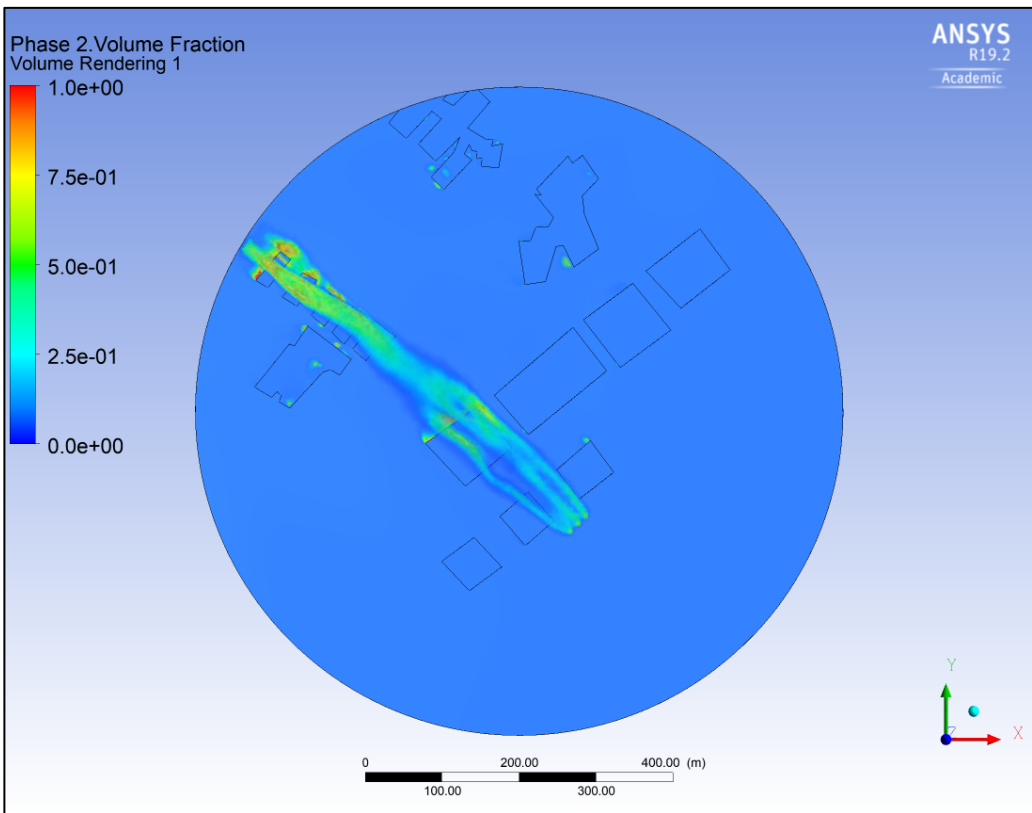


Figure 52 Wind strength below 5 m/s making an unexpected impact.

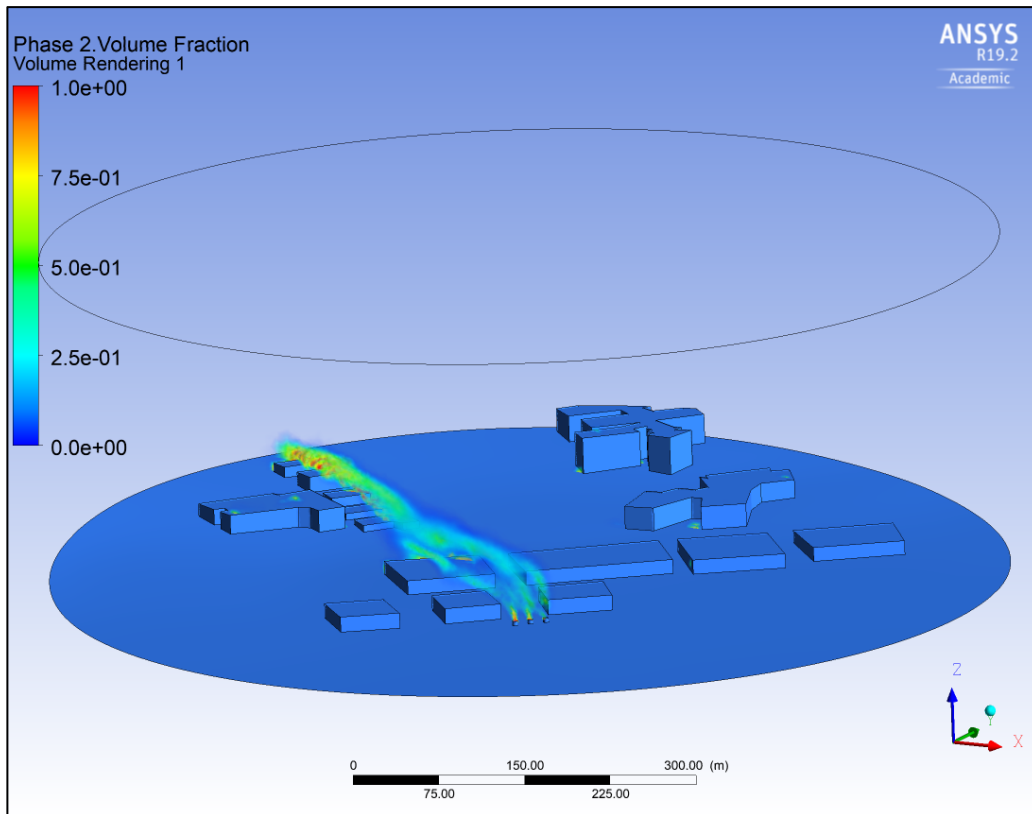


Figure 53 Wind strength below 5 m/s making a remarkable impact.

The results from the simulation with a wind strength below 5 meters per second was unexpectedly high. The collection of CO₂s behind the buildings occurs as a function of the vortex effect. Might this be a result when several of small vessels are at port?

The emission does also create pockets of pollution at other buildings as well, these seen as yellow and red dots in the figures.

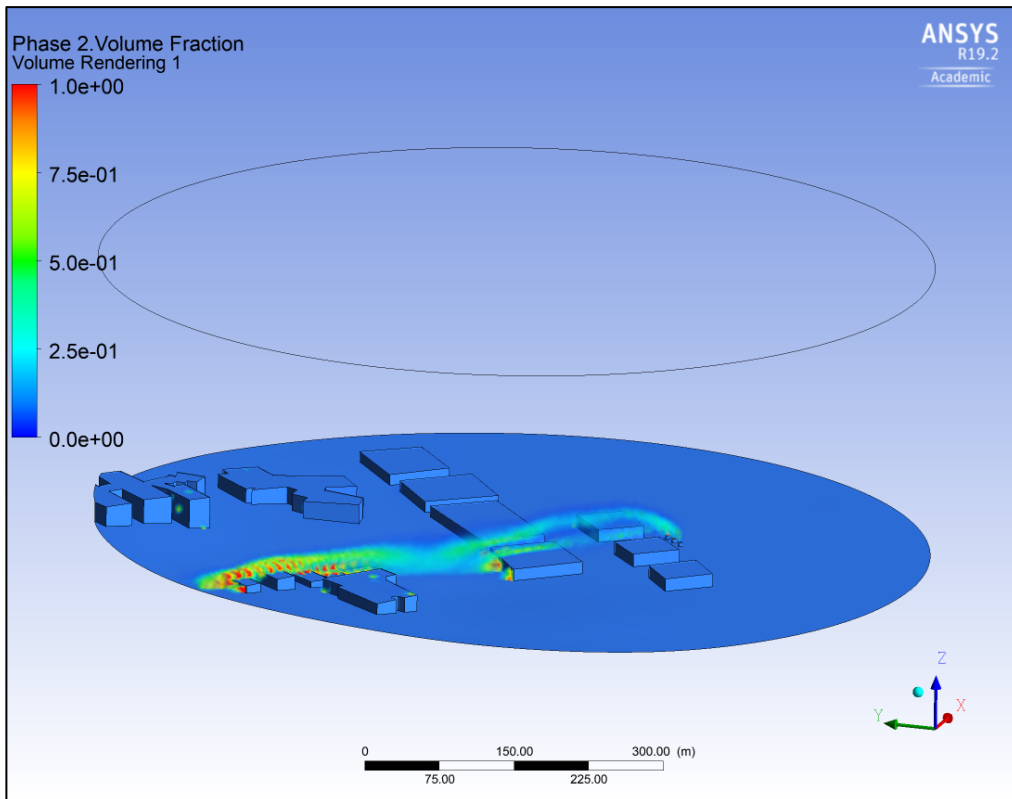


Figure 54 Wind strength below 5 m/s seen from behind

4.5 Air quality

The area for the simulations is a highly trafficked area, including car traffic, people walking /bi-cycling and with ship freight traffic. The area houses industrial business, housing site, a high school and the university. A lot of humans stay in the area, both daytime and night-time.

4.5.1 Air quality per day, any risk?

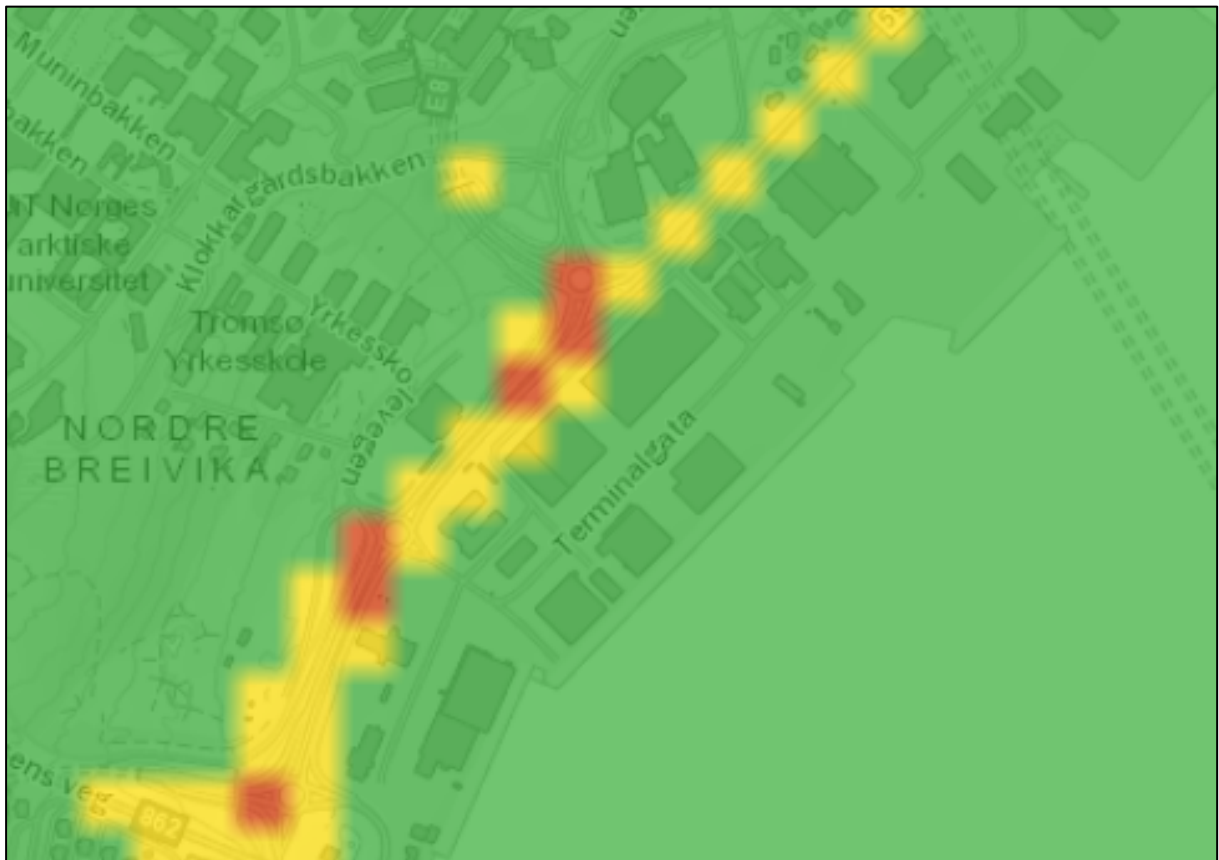


Figure 55 Map from luftkvalitet.miljostatus.no illustrating pollution for the area representing the simulations, 24th of April 2019 (Luftkvalitet i Norge, 2019).

Figure 55 above illustrates the pollution in Breivika as moderate to high (yellow to red), based on data delivered from the Norwegian Environment Agency in collaboration with the Norwegian Public Roads Administration, The Norwegian Meteorological Institute, Norwegian Institute of Public Health and The Norwegian Directorate of Health (Norwegian

Environment Agency, 2018)(29.05.2019). The total of pollutants measured consists of O₃, NO₂, PM₁₀ and PM_{2.5}.

During April and May, the air quality is affected by the sand and tires with studs remaining from the period with icy roads. This remains as dust, which affects the measured air quality, especially the PM rate. Especially during clean-up, the dust gets swarmed up in the air and dust is a harm to people with respiratory diseases as for instance asthma.

Figure 55 indicates the air pollution for the valid day as moderate to high. Activity in the area is recommended by the Norwegian Environment agency, but for inhabitants with respiratory diseases should or sensitive airways reduce the activity level outside for periods with moderate to high pollution.

4.5.2 How can emissions to air be reduced from vessels at port?

The emissions to air are possible to reduce. The substance is to reduce the emissions to air and the heavy oil fraction. It is up to the ship-owner to decide the type of method. New vessels comply with the regulations to reduction of heavy fuel oil, and existing vessels could be rebuilt to satisfy the regulations. It is to the ship-owner to appoint the reduction-method to be used. Some choose one method, some the other.

Scrubber:

Scrubber technology is an option to high-cost low Sulphur fuel as MGO (Marine Gas Oil) as well as LNG (Liquid Natural Gas) and HDME 50.

Scrubbing of fuel is a technique (Latarche, 2017) where the SO_x passing through water stream. When the fuel reacts to the water the sulphuric acid is removed from the exhaust gas which goes out of the system. The water is clean, it can be discharged to the sea. Ship-owners are standing in a cross road for which fuel to use to reduce the emissions to air. Scrubbers is one option for HFO fuel, rebuild and change to MGO or a low Sulphur content fuel.

There are two types of scrubbers; open loop and closed loop. These are both used combined nowadays. The efficiency of the scrubbing is around 98%, so the oil containing 3.5% Sulphur

will have no problem to reach the maximum 0,1% as set in ECA for 2015. New technological scrubbing is done by with use of pellets made of hydrated lime to remove Sulphur.

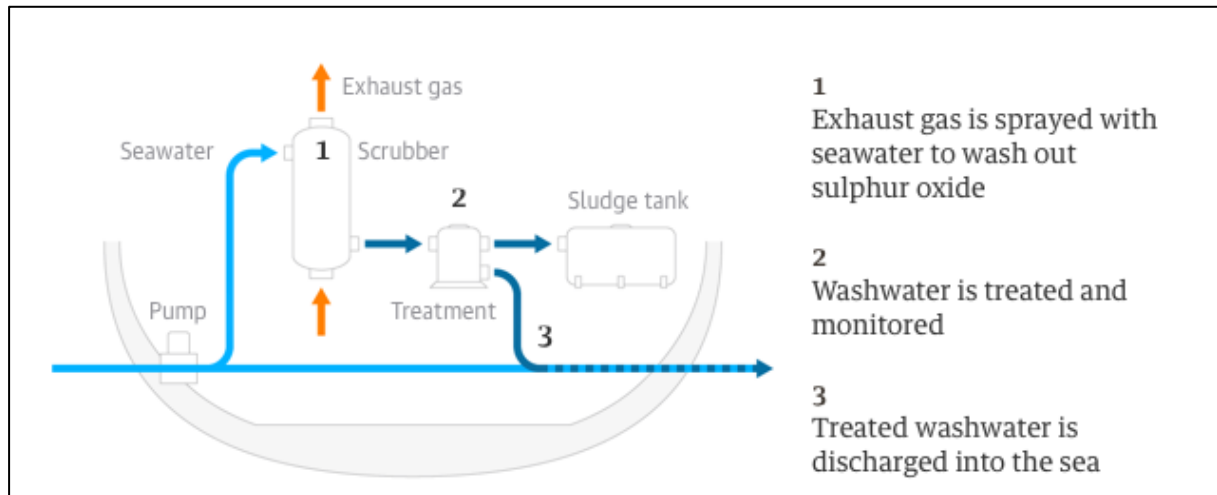


Figure 56 Open scrubber system (Laville, 2018).

A retrofit of the engine for a scrubber system could cost up to 5 million dollars, depending on size of the vessel and producer. Scrubbers are installed to new vessels, but majority in retrofits. For the ship-owner scrubbers could be a cost to reduce the emissions to air for the vessel and in the end a cost versus benefit -difficulty. The scrubber might reduce the emissions up to 30% (Comer, Olmer, Xiaoli, Biswajoy, & Rutherford, 2017).

4.5.2.1 HDME 50 Fuel and LNG

ExxonMobil is one of the fuel companies which have developed a new category of fuels named HDME 50 was launched in 2014 (ExxonMobil, 2018). HDME 50 is a low Sulphur fuel oil by engineers in the marine industry (Akhilesh, 2015).

The fuel is a compliant for the ECA areas and is claimed to have better features as marine gas oil. It is more lubricating than the other fuels, which means less tear of parts and increases the engine efficiency, which is positive in the economic way for maintainability of the engine and total cost for the ship-owner, -The fuel doesn't require a cooling system, due to the lubrication efficiency and has a higher flash point at 70 degrees Celsius (ExxonMobil, 2018) than MGO

with 60-75 degrees Celsius. This is argued to provide a safer operation in the boilers and have a better energy content compared to MGO.

Besides the efficiency for the fuel it is a suggested fuel for the ECA-zones since it complies with the emission regulations in MARPOL Annex VI. HDME 50 have a content of 0,10 % Sulphur. HDME 50 is available in large ports as Amsterdam, Rotterdam and Antwerp.

Nowadays, there is also an increase in existing and new built vessels to be able to run on alternative sources of energy. For instance, the newest vessels from Hurtigruten in Norway able to run on Liquid Natural Gas -LNG. Ship owners sees it as rewarding to operate on LNG because of the emission targets (Newman, 2019).

Børre Gundersen, R&D manager for ABB's marine activities in Norway, states that "*hybrid propulsion systems significantly reduce both fuel consumption and emissions*". Gundersen's colleague Sindre Sæter said: "*Hybridization of 230 offshore supply vessels operating in Norwegian waters could reduce CO₂ emissions by 400,000 tonnes*" (Newman, 2019). Hybrid vessels can operate on LNG or hydrogen, use fuel cells or batteries to provide energy to an electric engine. Per January 2019 there are about 120 LNG-powered vessels (Newman, 2019).

4.5.2.2 Hybrid propulsion system

When operating with hybrid propulsion system are vessels equipped with batteries to store electric energy for use combined to a diesel engine. When installing batteries in vessels the need for large batteries, mechanical drives which generate and create electricity needed. Also, the batteries need a stabilized temperature to run optimal.

The conclusion (Geertsma, Negenborn, Visser, & Hopman, 2017) that hybrid architectures can reduce and consumption fuel and emissions up to 10% - 35%. This would improve comfort -minimal vibrations and smell, manoeuvrability and maintainability -cost to engines and mechanical loading. In figure 57 is a typical hybrid set-up for an engine:

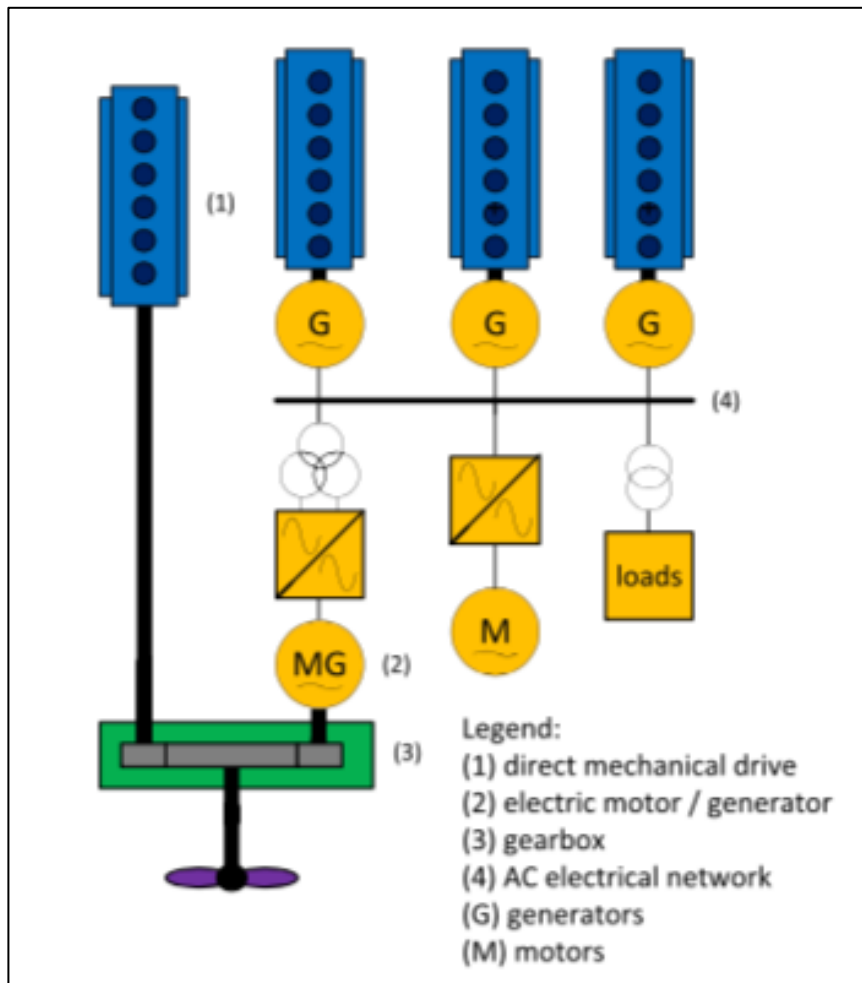


Figure 57 Example set-up for hybrid propulsion system

The hybrid system has a mechanical drive (mark 1) that provides propulsion with high strength efficiency in combination to an electric motor (mark 2) coupled to the gearbox (mark 3) or directly to the propeller. The system could be used as generator for other electrical equipment on the vessel, for example be a part of the electrical network. When the mechanical part of the machine is running, the batteries are loading through the energy send to the generators and provides the batteries with energy.

Use of hybrid propulsion systems makes it possible to switch between mechanical propulsion on fuels containing pollutants and the batteries which have been charged by the mechanical propulsion – so the vessel can run on eco-friendly propulsion for a given time so there is availability to switch from mechanical to electric drive mode.

If both the mechanical and electric drive mode is on the vessel can top strength and without increasing the emissions to air.

The Norwegian company Hurtigruten has ordered two new vessels with hybrid propulsion systems. These vessels are estimated to be in route during spring 2019 (Bergens Tidene, 2017) and their location for transport and tourisms will be in the Antarctic Ocean and the Arctic Ocean – especially they have an interest in the Northwest Passage.

4.5.2.3 ECA zones, an Arctic tractate and “sniffers”

By extending the Emission Control Area to be higher than the Baltic Sea and 62 degrees north it will force vessels to use eco-friendly fuel or to install scrubbers to clean the fuel. If the ECA could be asset as a claim for the Norwegian coastline, Norway would go ahead as a good example. As an example; the East coast and the West coast of the American coastline and parts of the Canadian coast is ECA (Norwegians Shipowners Association, 2014).

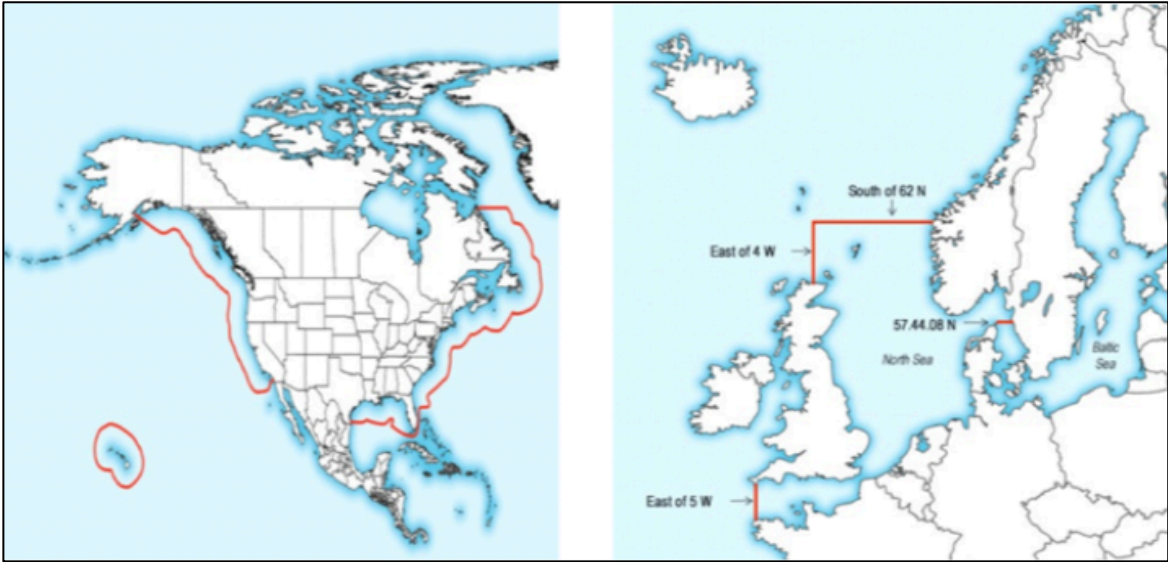


Figure 58 Current ECA-zones (Norwegians Shipowners Association, 2014).

The Antarctic Tractate for IMO’s MARPOL Annex 1 Regulations for the prevention of pollution by oil (IMO, 2011) sets regulations for use of use and transport of fuel. The regulation affects all traffic at sea area south of 60 degrees, except vessels for search-and-rescue operations. Further, if the regulation would be set the opposite way to concern the Arctic, it would affect ship-owners to coerce the use of eco-friendly fuel.

To solve the emissions from vessels at sea the Norwegian Maritime Authority ordered three new drones from the company Norse Asset Solution -NAS (Norwegian Maritime Authority,

2019). The drones from NAS have several of functions for search and rescue-operations including measuring emissions released to air offshore. The drones are equipped with sensors which are flown into the exhaust from the vessels outdistance of 50 meters away from the vessel. When the drone is in the exhaust, it continuously reports the emission and returns to base after the sampling is completed. For doing these samplings, the Norwegian Maritime Authority is collaborating with the coastguard, the Norwegian Coastal Administration and the Norwegian Radiation and Nuclear Safety Authority.

4.5.2.4 Onshore power

Due to the introduction, only 10% of the vessels at Breivika can connect to onshore power. High-voltage onshore power supply requires large capacity of electricity. Port of Oslo in collaboration with Color Line where the first in Norway to build a high-voltage power supply at port (Port of Oslo, 2012). Adding high-voltage power to a cruise vessel makes it possible to shut down the engines on board and still be operative at port. The investment cost for this system was set to 60 million NOK in 2012.

Due to the different frequencies of the high-voltage for vessels, frequency converters have a major role to convert the power to fit the vessel. European vessels mostly operate on 50 Hz, though US, Canada, large countries in South America and Asia are operating on 60 Hz.

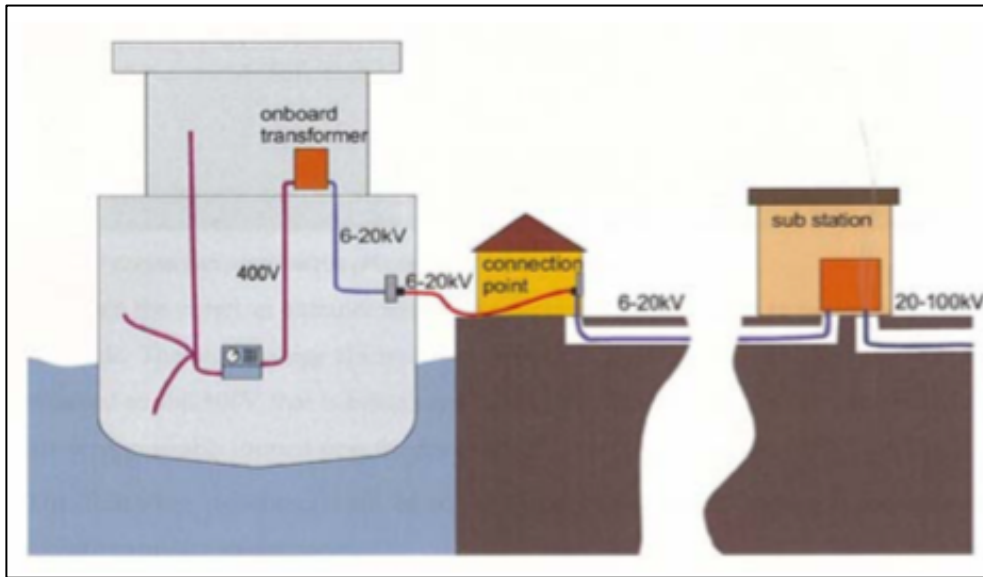


Figure 59 General design of a high-voltage shore connection system (Port of Oslo, 2012).

The ISO/IEC/IEEE 80005-1:2012 regulation sets the general requirements for high-voltage shore connection (ISO, 2012): “*IEC/ISO/IEEE 80005-1:2012(E) describes high voltage shore connection (HVSC) systems, on board the ship and on shore, to supply the ship with electrical power from shore. This standard is applicable to the design, installation and testing of HVSC systems and addresses:*

- *HV shore distribution systems;*
- *shore-to-ship connection and interface equipment;*
- *transformers/reactors;*
- *semiconductor/rotating convertors;*
- *ship distribution systems; and*
- *control, monitoring, interlocking and power management systems.*

It does not apply to the electrical power supply during docking periods, e.g. dry docking and other out of service maintenance and repair.”

4.5.3 IMO's adopted mandatory measures to reduce GHG emissions from shipping

IMO is continually working to reduce the emissions from international shipping (IMO, 2019). With the Energy Efficiency Design Index (EEDI) mandatory for new ships, and the Ship Energy Efficiency Management Plan (SEEMP) IMO have adopted mandatory measures to reduce emissions. Further, IMO is the only organization to adopt energy-efficiency measures applying to all countries. The EEDI is mandatory for all new vessels, and the SEEMP is a requirement for all vessels.

The initial IMO GHG strategy envisages a reduction in carbon intensity of international shipping – a reduction of CO₂ per transport work. The total annual GHG emission from international shipping should be reduced by 40% in 2030 and by at least 50% in 2050 compared to the emissions in 2008.

The strategy includes the vision: “*IMO remains committed to reducing GHG emissions from international shipping and, as a matter of urgency, aims to phase them out as soon as possible in this century*” (IMO, 2019).

Following levels of ambitions follows the vision (IMO, 2019):

- 1) Carbon intensity of the ship to decline through implementation of further phases of the energy efficiency design index (EEDI) for new ships.
- 2) Carbon intensity of international shipping to decline.
- 3) GHG emissions from international shipping to peak and decline.

4.6 Results from OpenFOAM

OpenFOAM is a simulation software specialised in CFD simulations. The file containing the pipes with a height of 30 meters was sent to Dr. Asier Zubiaga and his team at ZHAW - Zürcher Hochschule für Angewandte Wissenschaften at department ICP- Institute of Computational Physics to be simulated in OpenFOAM. In this subchapter will the simulations from Dr. Asier Zubiaga and his team be presented and compared against the self-made simulations as a quality check.

The pipes in these simulations are 30 meters high. Three cases were simulated with following wind strength:

- Case 1 $v = (-3.54, 3.54)$
- Case 2 $v = (15.0, 0.0)$
- Case 3 $v = (-5.4, 25.0)$

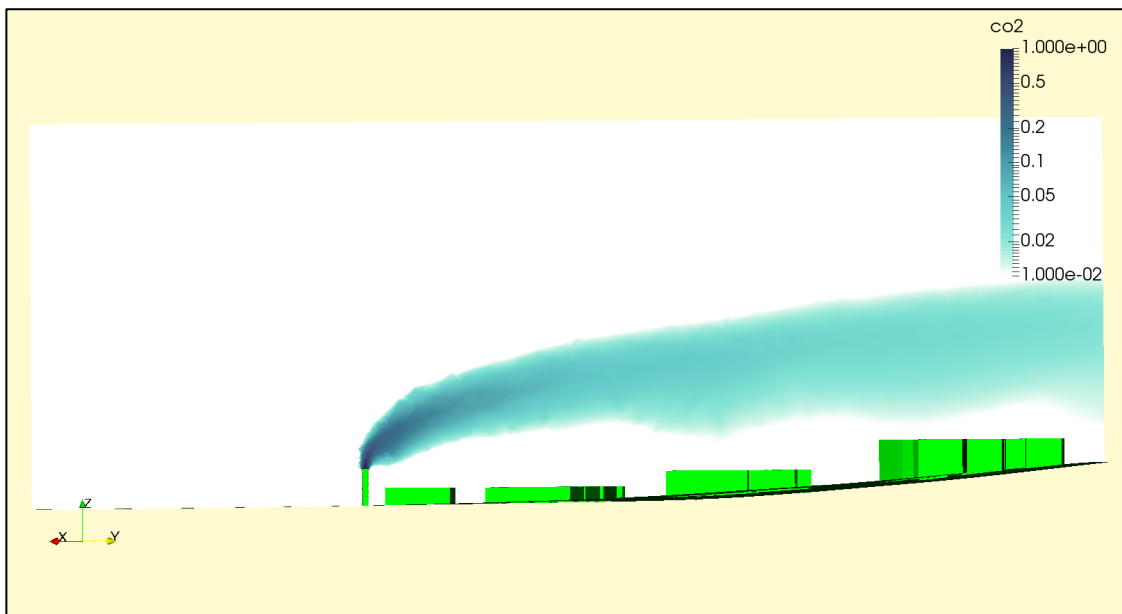


Figure 60 Result case 1 from OpenFOAM wind strength

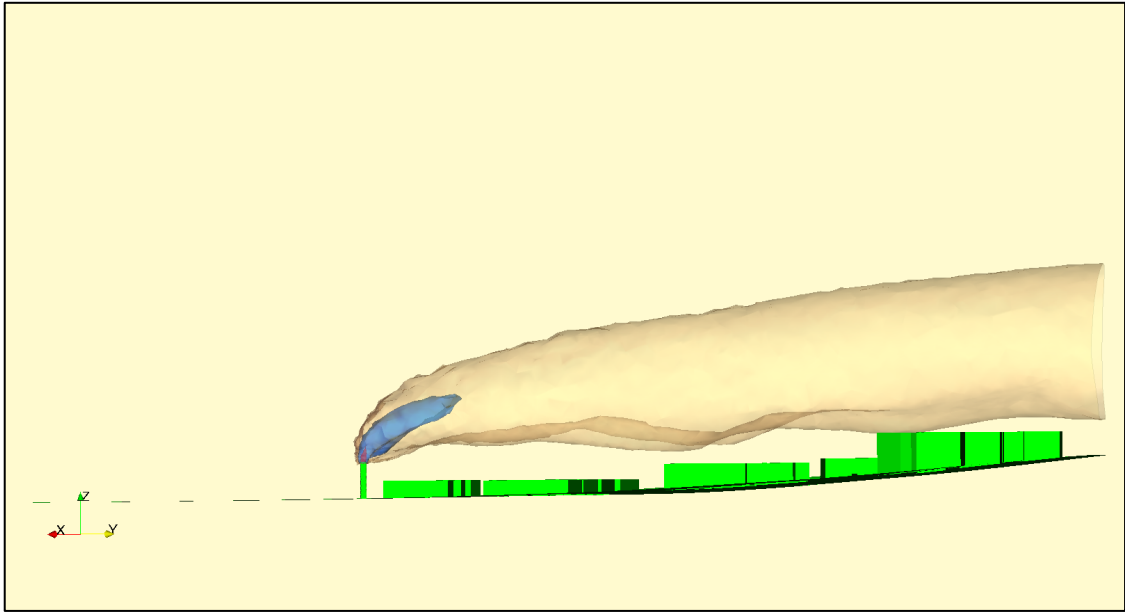


Figure 61 Result case 1 from OpenFOAM wind strength

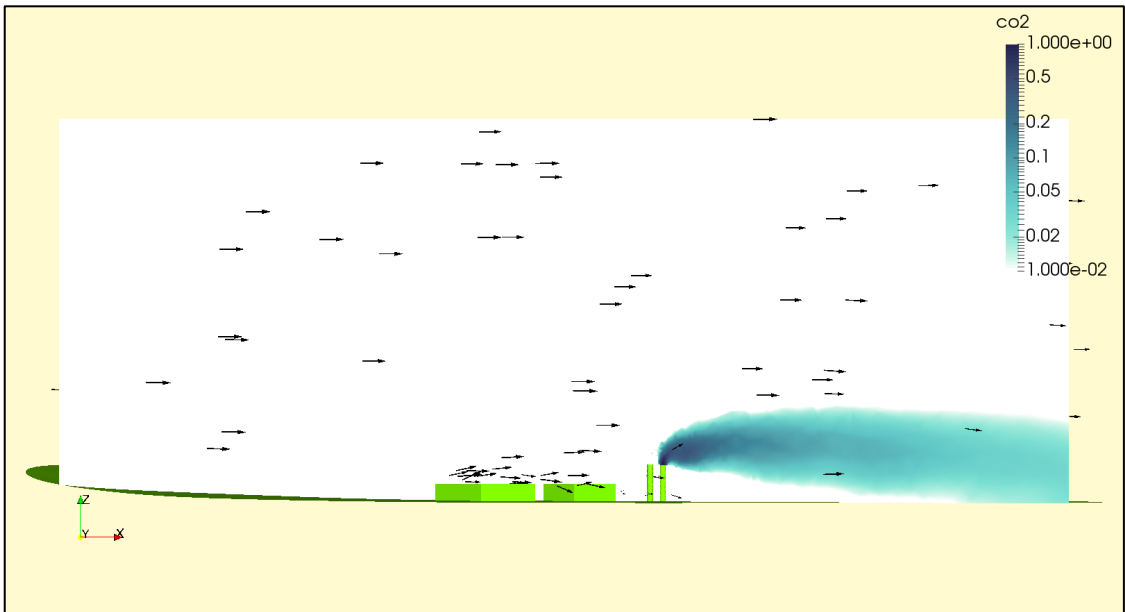


Figure 62 Result case 2 from OpenFOAM wind strength

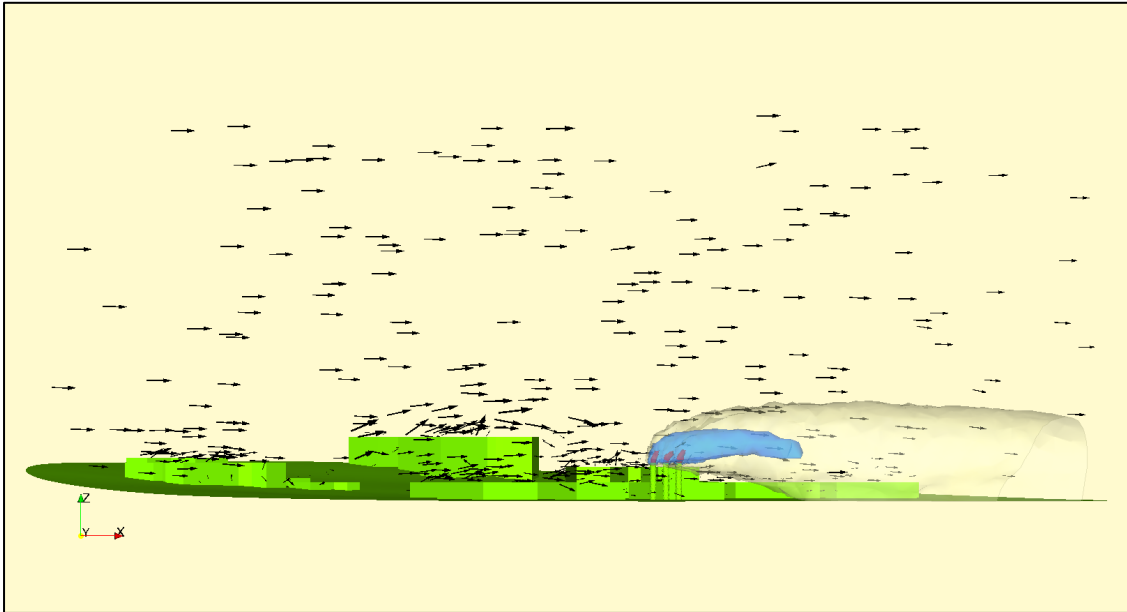


Figure 63 Result case 2 from OpenFOAM wind strength

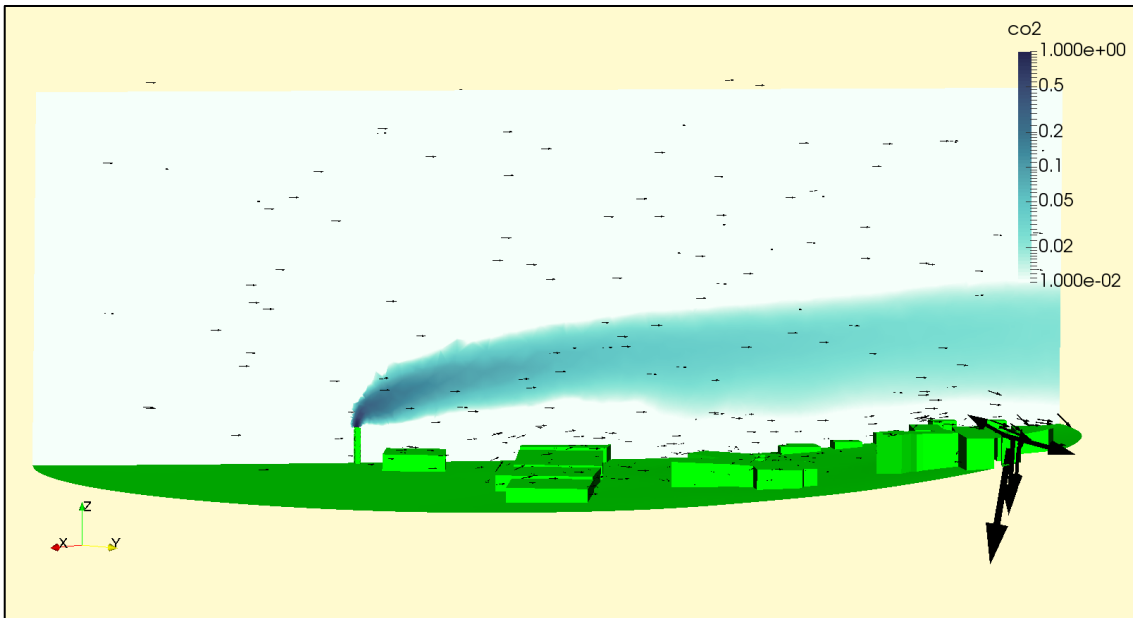


Figure 64 Result case 3 from OpenFOAM wind strength

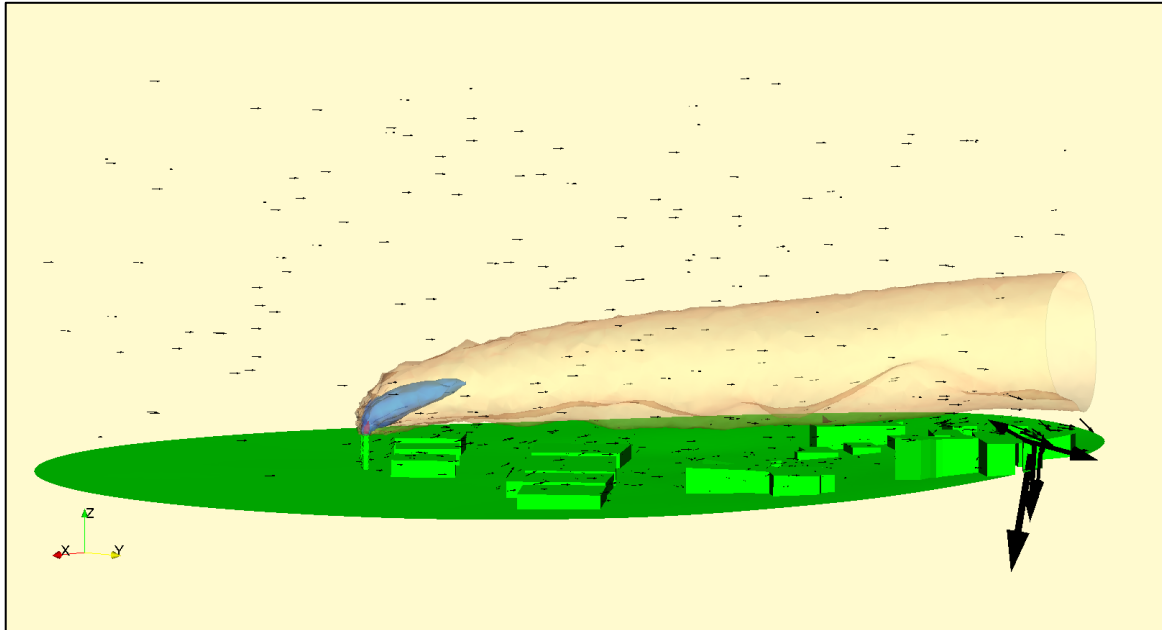


Figure 65 Result case 3 from OpenFOAM wind strength

The results simulated in OpenFOAM is qualitatively showing the same as visible in ANSYS®. The same outcome despite different wind conditions, the plume goes over the buildings. The results show more diffusion than the results from ANSYS®, this might be because of the difference between the software's.

4.7 Bow-tie

Threats	Preventive Barriers	Unwanted occurrence	Restrictive Barriers	Consequence
Old vessels				Smog
	Regulations		Onshore power	
Heavy Fuel Oil	Eco-friendly Fuel		Implementing an Arctic tractate	Climate: Increasing temperature
	Scrubbers	Emissions to air from vessels at port of Breivika	Fuel restrictions	
Dry weather	Economy to rebuild engines		Restrictions for being outside	Allergic reactions/ asthma
			Reduction in strength	
Several large vessels at port				Diseases: airways and cardio

Figure 66 Bow-tie for emissions to air vessels at Port of Breivika

To summarize the unwanted occurrence of emissions released to air from vessels at Port of Breivika a bow-tie used. The bow-tie illustrates the threats of the unwanted occurrence together with the preventive and restrictive barriers and the consequence if the occurrence happens. Barriers are supposed to stop or reduce the consequences (Rausand & Utne, 2011). The bow-tie is a good tool to view the possible threats and their possible affects.

The preventive barriers are supposed to reduce the likelihood of the unwanted occurrence, and the restrictive barriers are supposed to mitigate the consequences. The barriers are a safety functions which can be technical, operational or organizational. Installing of scrubber system is a technical function, reduction of strength is an operational function and the regulations are an organizational function for the unwanted occurrence. Presenting the barriers in a bow-tie is a suitable systemizing tool for the threats and its consequences.

4.8 Research questions

- Is it possible to make a realistic model to use in ANSYS®?

The two-phase model considers wind strength and wind direction, so the results from the simulations indicates a potential outcome if the weather conditions are optimal. Referring to the literature review in chapter 2, CFD simulations are executed to estimate emissions to air. The article in subchapter 2.2 has results illustrating the dispersion of the emission in the same way as ANSYS®. This result is illustrated in figure 6. The highest content of CO₂ is coloured red and the smallest amount is coloured red. It is also easy to see the flow of the emission.

The terrain for the developed model is recognizable according to the figures illustrating the terrain. If figure 22 and figure 30 is set beside each other they are close to identical. If the weather conditions are acting in benefit of the model, the situation in the simulation could be a realistic estimate for the emission. Due to the error margin of 5 meters from the converter program all the coordinates have the same error margin which makes it equal to the model.

- Does the flow of CO₂ impact the environment near Port of Breivika?

From the CFD results in chapter 4.1, 4.2, 4.3, and 4.4 we learn that onshore wind and high wind strength could have effect. Optimal wind direction and weather condition could CO₂ make an impact to the environment near Port of Breivika. The flow of CO₂ near buildings increases when the pipe height decreases. Half of the emissions flows against the sea and would disperse before it reaches land at the other side of the sound.

Of concern is also the simulations not represented in the chapters above. They are either evaporating directly to air or towards the ocean. Despite the simulations are considering CO₂ released to air, the combination of other pollutants as NO_x, SO_x, VOC and methane released to air together with the CO₂. These pollutants might affect the ocean and the surroundings without being visible for the eye.

When vessels are laying at port for several of hours, the affect from the emissions would be continuing if they stay at port. Observations of cruise vessels the past years witnesses that the vessels are arriving at night and leaving at evening the next day. When the cruise vessels aren't at port the space is used for fishing and cargo vessels.

The model with lower pipes than the initial model of 30 meters might furnish simulations for smaller vessels than cruise vessels. It might also be the outcome of several smaller vessels at port at once.

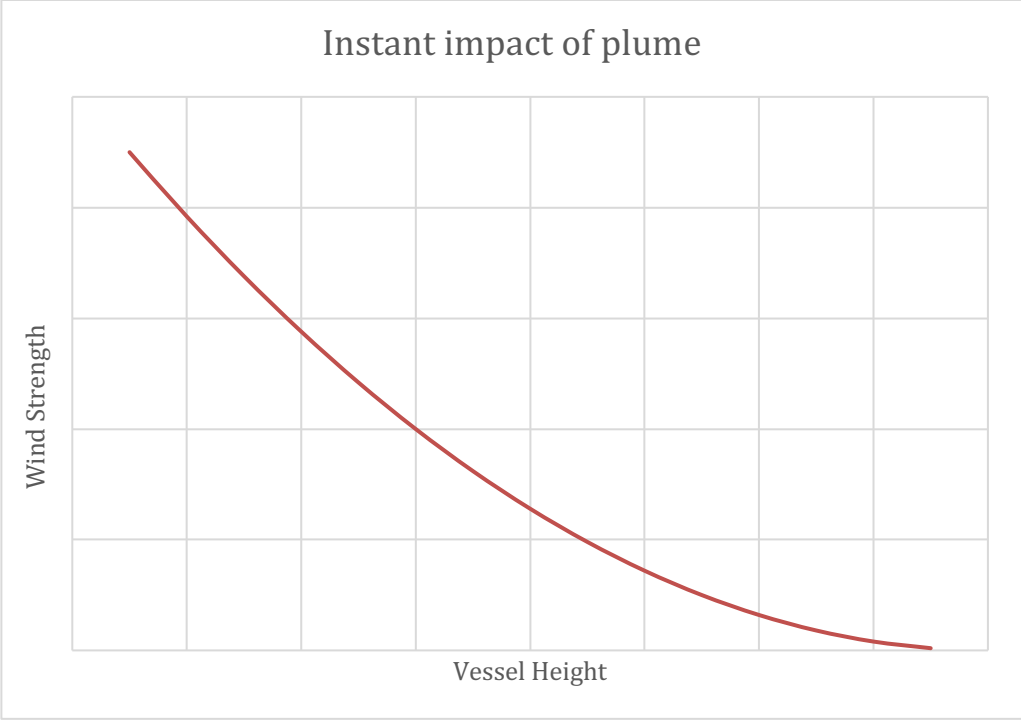


Figure 67 Impact of plume in addition to wind strength and vessel height.

-What is the impact of wind direction/strength and vessel height towards the pollutant transport?

As observed from CFD simulations in chapter 4.1, 4.2, 4.3 and 4.4 the impacts with onshore wind illustrates the largest impacts.

High wind strength effects within all heights of the pipes. Low wind strength affects when the height of the pipe is low. The lower the pipe is, the less wind strength is required to have a result of CO₂ pockets at the local environment. Onshore wind, from east to west, wind from south-east and wind against north affects the emission

The height of the pipe performs a major role. Decreasing the height increases the effect of the emission. This indicates that lower vessels make a larger impact than higher vessels to the nearby buildings. However, tall vessels might affect the constructions and the terrain outside the domain, within high buildings higher up in the terrain.

5 Conclusion and recommendation

The presented simulations are an estimate of a possible outcome if the weather conditions are optimal due to wind strength and wind direction. High wind strength and tall vessels could make impact on the surroundings, and by decreasing the height of the vessel the impact could increase. Cruise vessels with a height of 30 meters or more are likely to act on the environment higher up in the terrain outside of the domain for the simulations.

Following conclusion can be drawn from the above given study:

CFD simulations:

- CFD has been used to study pollutant transport in the urban environments. Referring to the literature review in chapter 2 it is a well-used method. CFD visualizes the flow of the emission, -a result easy to understand.
- The CFD model required detailed geographical information. This can be obtained from freely available sources such as Google Earth. The obtained information had to be set by freehand. Having geographical knowledge of the area is an advantage, hence the result of the simulation due to the actual air quality daily.
- Two-phase model can be ran using ANSYS® Fluent or another software capable of solving CFD. This thesis had a preface study to get familiar with the software. In chapter 3.2 is the preface study presented. It is possible to add phases. Adding phases requires more time within the calculations, as well as storage and efficiency of the computer.
- Mesh sensitivity analysis optimizes the simulation. When the number of elements is convergent, the simulation could be more accurate according to the geographical information. Mesh sensitivity analysis plays a major role to the results of the simulation.

- Comparing ANSYS® vs OpenFOAM are two different software's simulating the same file. The settings in OpenFOAM is as close to identical as the settings for ANSYS®.

Modelling CO₂ plume transport

- CFD is a reasonable tool to study the plume transport. Referring to the literature review in chapter 2 and the performed simulations for this thesis. The modelling of CO₂ results an estimation based on the sets the conditions for the simulation.
- The results from the test study appeal to the full-scale model. The vortex effect is recognizable at both models, adding several buildings adds more potential to increase the attendance of the effect.

Impact of wind strength/direction and vessels height

- From full-scale simulations, it was found that higher wind strengths result in lower plume dispersion, however the plume stays closer to the terrain. This brings in the concentrated amount of pollutants closer to the public areas.
- Another found was that lower vessels height results in plumes higher above in the air, not effecting the public areas and effect reverses when the vessels heights are lower. Therefore, it can be assumed that higher vessels are better for public health in terms of instant release of pollutants for the geographical area near Port of Breivika.

Flow of pollution:

- High wind strength and onshore wind make the flow of pollution against the terrain. For the wind strengths affecting the most, the vortex-effect is creating pockets of pollution at the lee side of the buildings.
- Low wind strength will the pollution disperse to air. For some outcomes, the flow of the pollution will drop against the terrain and thereafter disperse.
- When the pollution is flowing between buildings in the terrain, pockets of pollution appears. Because of the wind strength and its direction. In both Case C and case D low height of the potential vessel illustrates the effect.
- High wind strength in combination with a low vessel might increase the impact to the surroundings nearby.

Results from OpenFOAM:

- The results from OpenFOAM indicates that the model has been successful within the scientific content. The modelled file was able to be opened in both ANSYS® and OpenFOAM.
- OpenFOAM illustrates more diffusion in the results, which might be caused because of the difference between the software's.
- The results from OpenFOAM is a good quality check for the simulations in ANSYS®.

Recommendations for the future work are:

1. Supporting the CFD results with real-time data. The Norwegian Institute for Air Research can be engaged to this.
2. Running more complex CFD cases with enlarged domain. Adding phases to the domain would increase the trustworthiness of the simulation.
3. Real-time measurements via drones. Measure the pollution directly from cruise vessels at port of Breivika.
4. Stronger checks at the port, include Port of Tromsø in the work.
5. Availability of shore power supply, study about the amount of power supply needed to host onshore power to cruise vessels.
6. Study of other pollutants as NO_x, SO_x, VOC. How far do they reach compared to CO₂?

6 Bibliography

Akhilesh, B. (2015, June 22). *linkedin.com*. Retrieved from HDME 50, A low sulphur fuel oil: <https://www.linkedin.com/pulse/hdme-50-low-sulphur-fuel-oil-akhilesh-bs/>

ANSYS. (2018, October 23). *ansys.com*. Retrieved from about ansys: <https://www.ansys.com/about-ansys>

ANSYS, I. (2009, January 23). *afs.enea.it*. Retrieved from 1.2 Continuity and Momentum Equations: <http://www.afs.enea.it/project/neptunius/docs/fluent/html/th/node11.htm>

Barentswatch. (2015, oktober 1). *barentswatch.no*. Retrieved from Barentswatch: <https://www.barentswatch.no/artikler/Hva-er-Arktis/>

Bergens Tidene. (2017, desember 5). *Nå kan du bli med på ekspedisjon i Nordvestpassasjen som turist*. Retrieved from bt.no: https://www.bt.no/reise/Na-kan-du-bli-med-pa-ekspedisjon-i-Nordvestpassasjen_-som-turist-Prislapp-fra-96000_-10869b.html

Comer, B., Olmer, O., Xiaoli, M., Biswajoy, R., & Rutherford, D. (2017). *Black Carbon Emissions And Fuel Use In Global Shipping*. Washington DC: The International Concil on Clean Transportation.

DNV GL. (2019, February 1). *dnvgl.com*. Retrieved from Green Coastal Shipping Program: <https://www.dnvgl.com/maritime/green-coastal-shipping-programme/index.html>

Enova. (2018, June 28). *Over 50 nye millioner til landstrøm*. Retrieved from presse.enova.no: <http://presse.enova.no/pressreleases/over-50-nye-millioener-til-landstroem-2551693>

ExxonMobil. (2018, April 12). Retrieved from product description HDME 50: <https://www.mobil.com/English-US/Commercial-Fuel/pds/GLXXExxonMobil-Premium-HDME-50?p=1>

Geertsma, R., Negenborn, R., Visser, K., & Hopman, J. (2017). *Design and control of hybrid powe and propulsopn systems for smart ships: A rewiev of developments*. Netherland: University of Technology, The Netherlands.

- Halasz, P. (2019). *Factors Affecting Arctic Weather and Climate*. Retrieved from National Snow and Ice Data Center: https://nsidc.org/cryosphere/arctic-meteorology/factors_affecting_climate_weather.html
- IMO. (2005, May 19). *lovdata.no*. Retrieved from Protocol on adoption of annex VI to the International convention for the prevention of pollution from ships, 1973/78 on regulations for the prevention of air pollution from ships: <https://lovdata.no/dokument/TRAKTATEN/traktat/1997-09-26-1?q=MARPOL%20annex%20vi>
- IMO. (2011). *lovdata.no*. Retrieved from MARPOL vedlegg 1 Hindring av oljeforurensning: <https://lovdata.no/static/SF/sf-20120530-0488-01-02.pdf?timestamp=1442303188000?t=1555632000030>
- IMO. (2019, May). *imo.org*. Retrieved from Reducing greenhouse gas emissions from ships: <http://www.imo.org/en/MediaCentre/HotTopics/Pages/Reducing-greenhouse-gas-emissions-from-ships.aspx>
- ISO. (2012, July). *iso.org*. Retrieved from ISO/IEC/IEEE 80005-1:2012: <https://www.iso.org/standard/53588.html>
- Khawaja, H. A. (2012). *Addition of Euler Extensions in CFD Code*. University of Cambridge: Hassan Abbas Khawaja.
- Khawaja, H. A. (2012). *CFD-DEM simulations of two phase flow in fluid beds*. University of Cambridge: University of Cambridge .
- Lange, R., & Johansen, E. (2018, December 7). *itromso.no*. Retrieved from Flere cruisepassasjerer har gjestet Tromsø i 2018 enn det finnes innbyggere i Stavanger: <https://www.itromso.no/nyheter/2018/12/07/Flere-cruisepassasjerer-har-gjestet-Troms%C3%B8-i-2018-enn-det-finnes-innbyggere-i-Stavanger-18028399.ece>
- Latarche, M. (2017, October 3). *ShipInsight*. Retrieved from How do scrubbers on ships really work: <https://shipinsight.com/scrubbers-ships-work/>
- Laville, S. (2018, October 29). *Thousands of ships could dump pollutants at sea to avoid dirty fuel ban*. Retrieved from The Guardian:

<https://www.theguardian.com/environment/2018/oct/29/thousands-of-ships-could-dump-pollutants-at-sea-to-avoid-dirty-fuel-ban>

Luftkvalitet i Norge. (2019, April 22). *luftkvalitet.miljostatus.no*. Retrieved from Luftkvalitet i Norge: <https://luftkvalitet.miljostatus.no/kart/69.7363/18.59931/14/aqi>

Newman, N. (2019, January 17). *Engineering and Technology*. Retrieved from Hybrid ships take to the high seas: <https://eandt.theiet.org/content/articles/2019/01/hybrid-ships-take-to-the-high-seas/>

Norwegian Environment Agency. (2018, December). *luftkvalitet.miljøstatus.no*. Retrieved from Helsesråd og forurensningsklasser: <https://luftkvalitet.miljostatus.no/artikkel/613>

Norwegian Maritime Authority. (2019, March 19). *sdir.no*. Retrieved from Sniffer svovelsynderne - før de legger til kai: <https://www.sdir.no/aktuelt/nyheter/sniffer-svovelsynderne--for-de-legger-til-kai/?fbclid=IwAR2-FcKEcFKuU0zEpOrN7wJEo0oZrXHZf1DEiyyZFs7S0ls8vywmi-IbsvU>

Norwegian Meteorological Institute. (2019, January 14). *Weather staticstics for Tromsø observation*. Retrieved from yr.no: https://www.yr.no/place/Norway/Troms/Tromsø/Tromsø_observation_site/statistics.html#t6

Norwegians Shipowners Association. (2014). *rederi.no*. Retrieved from Ren luft: <https://rederi.no/om-oss/fagomrader/internasjonalt-samarbeid-og-klima/miljo/strategi/ren-luft/>

Palacios, R. (2006, August 17). *mathworks.com*. Retrieved from deg2utm: <https://www.mathworks.com/matlabcentral/fileexchange/10915-deg2utm>

Port of Oslo. (2012). *oslohavn.no*. Retrieved from Fact about the onshore power supply at Port of Oslo: https://www.oslohavn.no/filestore/Brosjyrer_og_rapporter/Kortversjonlandstrmengelsk2013.pdf

Rafaelsen, R., Hansen, K., Borch, A., Nielsen, M., Røymo, K., Edvardsen, R., . . . Joachimsen, E. (2019, February 4). *Begrensede muligheter for cruiseanløp på*

Vestlandet kan gi en ny, stor mulighet for Nord-Norge. Retrieved from itromso.no:
<https://www.itromso.no/meninger/2019/02/01/Begrensede-muligheter-for-cruiseanl%C3%B8p-p%C3%A5-Vestlandet-kan-gi-en-ny-stor-mulighet-for-Nord-Norge-18387550.ece>

Rausand, M., & Utne, I. (2011). Risikoanalyse -teori og metoder. In M. Rausand, & I. B. Utne, *Risikoanalyse - teori og metoder* (p. 389). Trondheim: Tapir Akademisk Forlag .

Sam. (2012, March 31). *leonardthegeographerunit.blogspot.com*. Retrieved from A2 Geography U3: Contemporary Geography Issues:
<http://leonardthegeographerunit3.blogspot.com/2012/03/uhis-urban-heat-islands-winds.html>

Sætrum, T. (2018, November 22). (S. K. Madsen, Interviewer) 9008, Tromsø, Norway.

Sharcnet. (2019, May 8). *sharcnet.ca*. Retrieved from 4.1.3 The k-epsilon model:
https://www.sharcnet.ca/Software/Ansys/16.2.3/en-us/help/cfx_mod/i1345899.html

Toja-Silva, F., Chen, J., Hachinger, S., & Hase, F. (2017). *CFD simulation on CO2 dispersion from urban thermal power plant: Analysis of turbulent Schmidt number and comparison with Gaussian plume model*. Journal of Wind Engineering & Industrial Aerodynamics: Science Direct .

APPENDIX A – RESULTS SIMULATIONS

Figure list:

- Figure 1 Case 1,0 picture 15
- Figure 2 Case 1,0 picture 25
- Figure 3 Case 1,1 picture 16
- Figure 4 Case 1,1 picture 26
- Figure 5 Case 1,2 picture 17
- Figure 6 Case 1,2 picture 27
- Figure 7 Case 2,0 picture 18
- Figure 8 Case 2,0 picture 28
- Figure 9 Case 2,1 picture 19
- Figure 10 Case 2,1 picture 29
- Figure 11 Case 2,2 picture 110
- Figure 12 Case 2,2 picture 210
- Figure 13 Case 3,0 picture 111
- Figure 14 Case 3,0 picture 211
- Figure 15 Case 3,1 picture 112
- Figure 16 Case 3,1 picture 212
- Figure 17 Case 3,2 picture 113
- Figure 18 Case 3,2 picture 213
- Figure 19 Case 4,0 picture 114
- Figure 20 Case 4,0 picture 214
- Figure 21 Case 4,1 picture 115
- Figure 22 Case 4,1 picture 215
- Figure 23 Case 4,2 picture 116
- Figure 24 Case 4,2 picture 216
- Figure 25 Case 5,0 picture 117
- Figure 26 Case 5,0 picture 217
- Figure 27 Case 5,1 picture 118
- Figure 28 Case 5,2 picture 218
- Figure 29 Case 6,0 picture 119
- Figure 30 Case 6,0 picture 219
- Figure 31 Case 6,1 picture 120
- Figure 32 Cas 6,1 picture 220
- Figure 33 Case 6,2 picture 121
- Figure 34 Case 6,2 picture 221
- Figure 35 Case 7,0 picture 122
- Figure 36 Case 7,0 picture 222
- Figure 37 Case 7,2 picture 123
- Figure 38 Case 7,2 picture 223
- Figure 39 Case 8,0 picture 124
- Figure 40 Case 8,0 picture 224
- Figure 41 Case 8,2 picture 125

Figure 42 Case 8,2 picture 2	25
Figure 43 Case 9,0 picture 1	28
Figure 44 Case 9,0 picture 1	28
Figure 45 Case 9,1 picture 1	29
Figure 46 Case 9,1 picture 2	29
Figure 47 Case 10,0 picture 1	30
Figure 48 Case 10,0 picture 2	30
Figure 49 Case 10,1 picture 1	31
Figure 50 Case 10,1 picture 2	31
Figure 51 Case 11,0 picture 1	32
Figure 52 Case 11,0 picture 2	32
Figure 53 Case 11,1 picture 1	33
Figure 54 Case 11,1 picture 2	33
Figure 55 Case 12,0 picture 1	34
Figure 56 Case 12,0 picture 2	34
Figure 57 Case 12,1 picture 1	35
Figure 58 Case 12,1 picture 2	35
Figure 59 Case 13,0 picture 1	36
Figure 60 Case 13,0 picture 2	36
Figure 61 Case 13,1 picture 1	37
Figure 62 Case 13,1 picture 2	37
Figure 63 Case 14,0 picture 1	38
Figure 64 Case 14,0 picture 2	38
Figure 65 Case 14,1 picture 1	39
Figure 66 Case 14,1 picture 2	39
Figure 67 Case 15,0 picture 1	40
Figure 68 Case 15,0 picture 2	40
Figure 69 Case 15,1 picture 1	41
Figure 70 Case 15,1 picture 2	41
Figure 71 Case 16,0 figure 1	42
Figure 72 Case 16,0 figure 2	42
Figure 73 Case 16,1 figure 1	43
Figure 74 Case 16,1 picture 2	43
Figure 75 Case 10,7 picture 1	45
Figure 76 Case 17,0 picture 2	45
Figure 77 Case 17,0 picture 3	46
Figure 78 Case 17,1 picture 1	47
Figure 79 Case 17,1 picture 2	47
Figure 80 Case 1,0 picture 1	48
Figure 81 Case 18,0 picture 2	48
Figure 82 Case 18,1 picture 1	49
Figure 83 Case 18,1 picture 2	49
Figure 84 Case 19,0 figure 1	50
Figure 85 Case 19,0 figure 2	50
Figure 86 Case 19,1 figure 1	51
Figure 87 Case 19,1 figure 2	51
Figure 88 Case 20 picture 1	52

Figure 89 Case 20 picture 2	52
Figure 90 Case 20,1 picture 1	53
Figure 91 Case 20,1 picture 2	53
Figure 92 Case 21,0 picture 1	54
Figure 93 Case 21,0 picture 2	54
Figure 94 Case 21,1 picture 1	55
Figure 95 Case 21,1 picture 2	55
Figure 96 Case 22,0 picture 1	56
Figure 97 Case 22,0 picture 2	56
Figure 98 Case 22,1 picture 1	57
Figure 99 Case 22,1 picture 2	57
Figure 100 Case 23,0 picture 1	58
Figure 101 Case 23,0 figure 2	58
Figure 102 Case 23,1 figure 1	59
Figure 103 Case 24,0 picture 1	60
Figure 104 Case 24,0 picture 2	60
Figure 105 Case 24,0 picture 3	61
Figure 106 Case 24,1 picture 1	62
Figure 107 Case 24,1 picture 2	62
Figure 108 Case 25,0 picture 1	63
Figure 109 Case 25,0 picture 2	63
Figure 110 Case 26,0 picture 1	64
Figure 111 Case 26,0 picture 2	64
Figure 112 Case 26,0 picture 3	65

30 meters

Case	V _x	V _y	Calculated value	Date for simulation	File name	Status
1,0	0	15 m/s		12.mar.19	FFF_case_1_0	ok
1,1	0	3,3 m/s		13.mar.19	FFF_case_1_1	ok
1,2	0	1 m/s		13.mar.19	FFF_case_1_2	ok
2,0	15sin45 m/s	15sin45 m/s	12,7	13.mar.19	FFF_case_2_0	ok
2,1	3,3sin45 m/s	3,3sin45 m/s	2,8	14.mar.19	FFF_case_2_1	ok
2,2	1sin45 m/s	1sin45 m/s	0,85	14.mar.19	FFF_case_2_2	ok
3,0	5 m/s	0		18.mar.19	FFF_case_3_0	ok
3,1	3,3 m/s	0		18.mar.19	FFF_case_3_1	ok
3,2	1 m/s	0		18.mar.19	FFF_case_3_2	ok
4,0	5sin45 m/s	^-5sin45 m/s	^-4.25	19.mar.19	FFF_case_4_0	ok
4,1	3,3sin45 m/s	^-3,3sin45 m/s	^-2,8	19.mar.19	FFF_case_4_1	ok
4,2	1sin45 m/s	^-1sin45 m/s	^-0,85	20.mar.19	FFF_case_4_2	ok
5,0	0,0	^-5 m/s		20.mar.19	FFF_case_5_0	ok
5,1	0,0	^-3,3 m/s		20.mar.19	FFF_case_5_1	ok
5,2	0,0	^-1 m/s		21.mar.19	FFF_case_5_2	ok
6,0	^-5sin45 m/s	^-5sin45 m/s	^-4,25	21.mar.19	FFF_case_6_0	ok
6,1	^-3,3sin45 m/s	^-3,3sin45 m/s	^-2,8	22.mar.19	FFF_case_6_1	ok
6,2	^-1sin45 m/s	^-1sin45 m/s	^-0,85	22.mar.19	FFF_case_6_2	ok
7,0	^-5 m/s	0		22.mar.19	FFF_case_7_0	ok
7,1	^-3,3 m/s	0		22.mar.19	FFF_case_7_1	ok
7,2	^-1 m/s	0		22.mar.19	FFF_case_7_2	ok
8,0	^-5 m/s	5sin45 m/s	^4.25	22.mar.19	FFF_case_8_0	ok
8,1	^-3,3 m/s	3,3sin45 m/s	^2,8	23.mar.19	FFF_case_8_1	ok
8,2	^-1 m/s	1sin45 m/s	^0,85	23.mar.19	FFF_case_8_2	ok

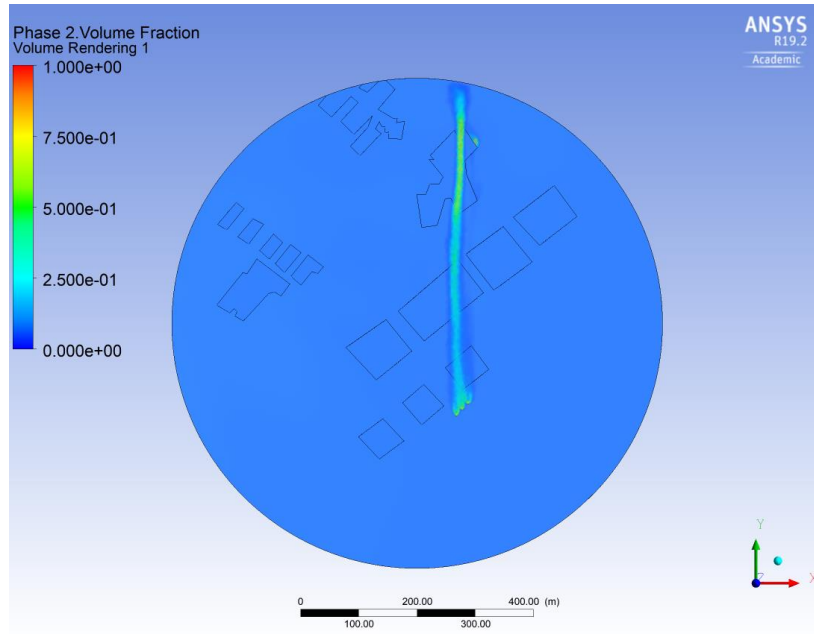


Figure 1 Case 1,0 picture 1

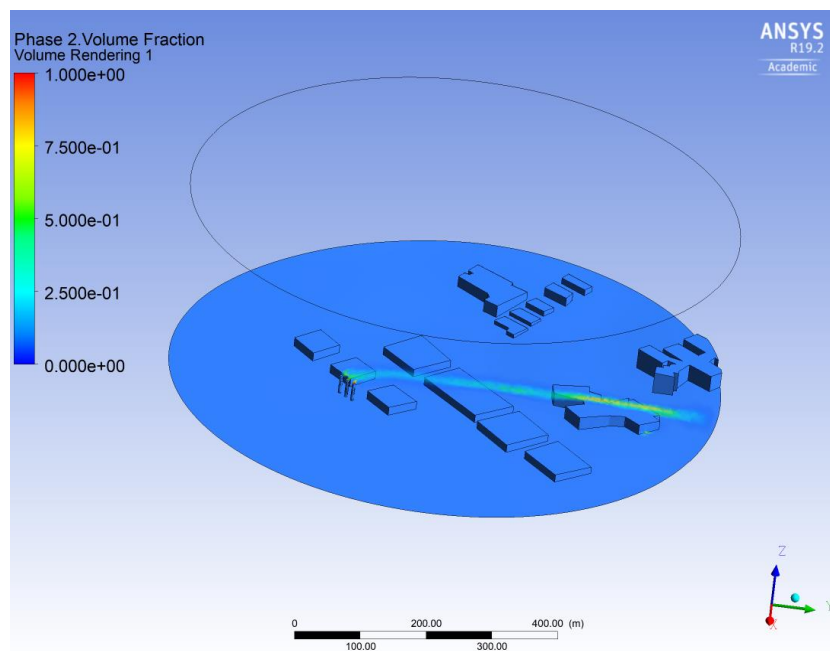


Figure 2 Case 1,0 picture 2

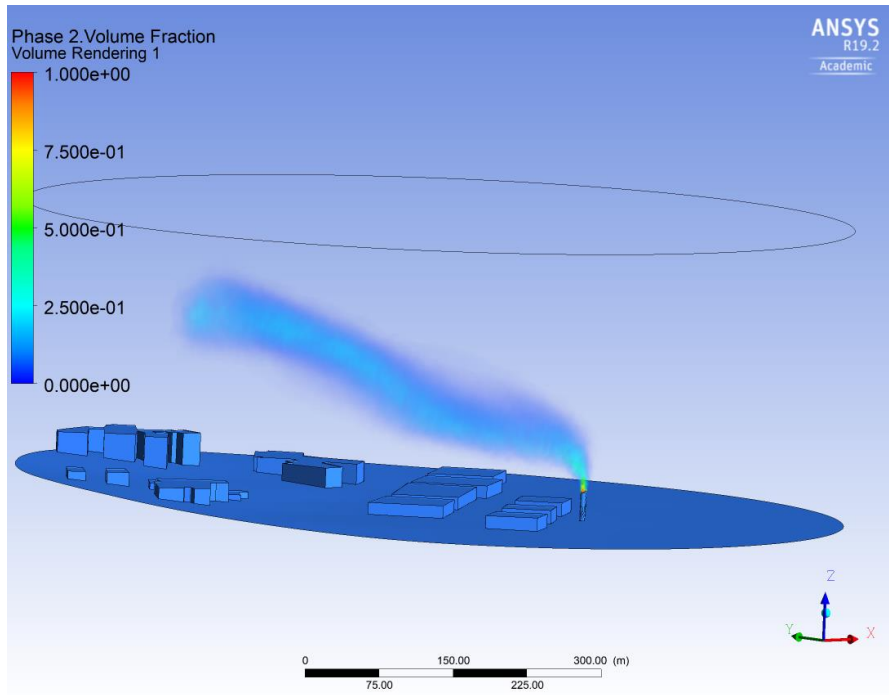


Figure 3 Case 1,1 picture 1

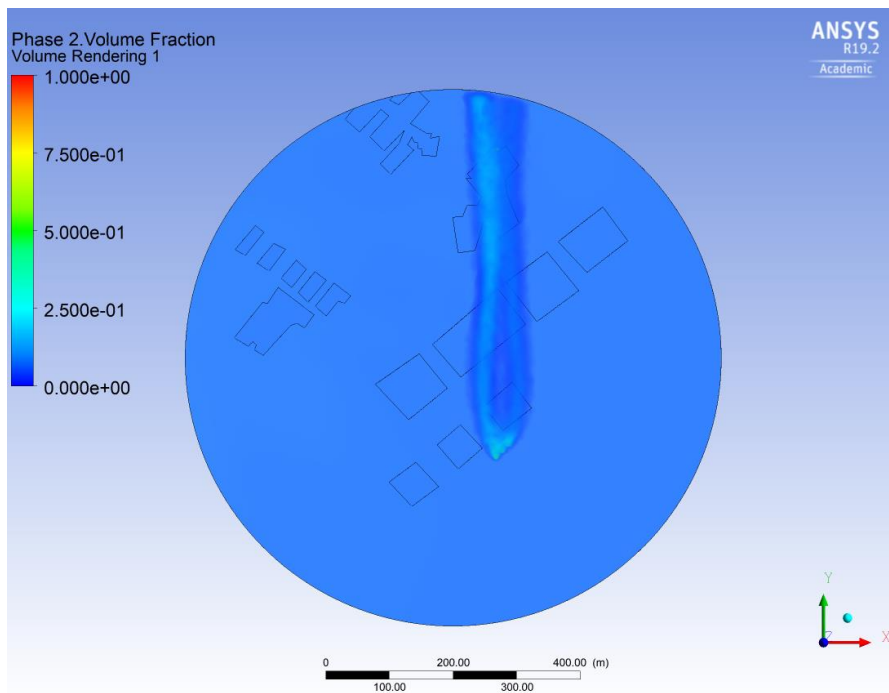


Figure 4 Case 1,1 picture 2

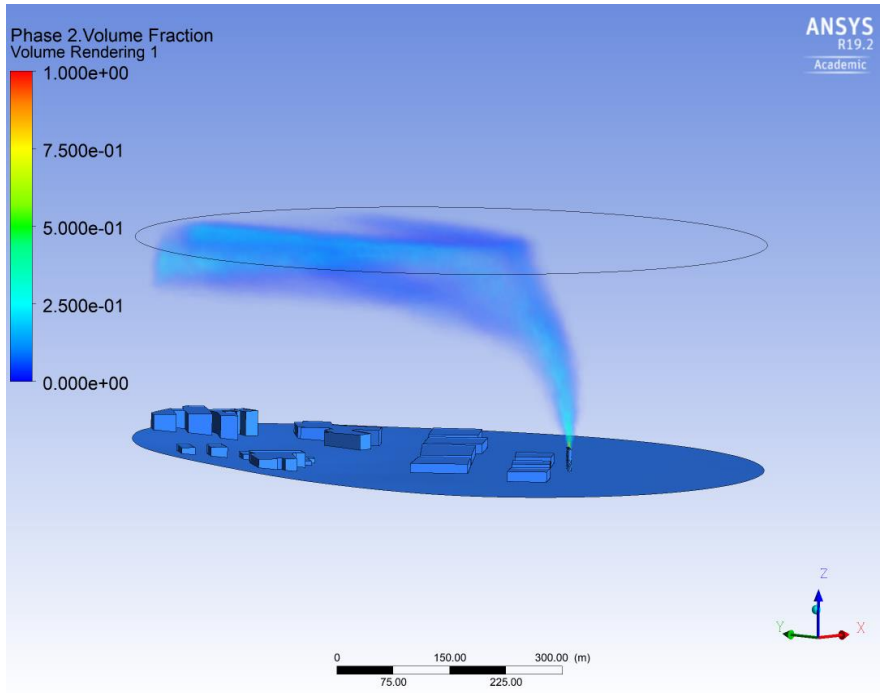


Figure 5 Case 1,2 picture 1

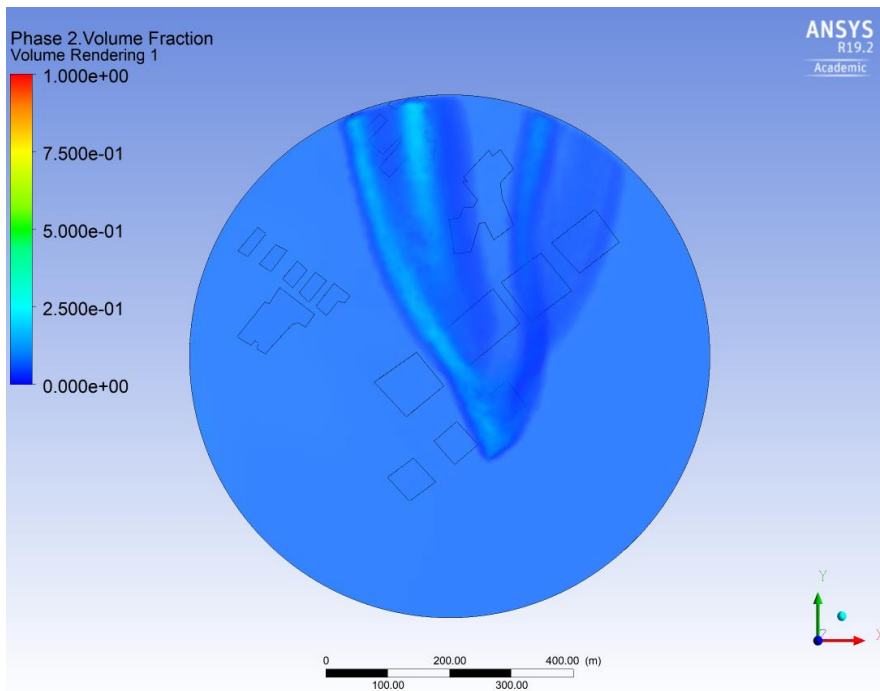


Figure 6 Case 1,2 picture 2

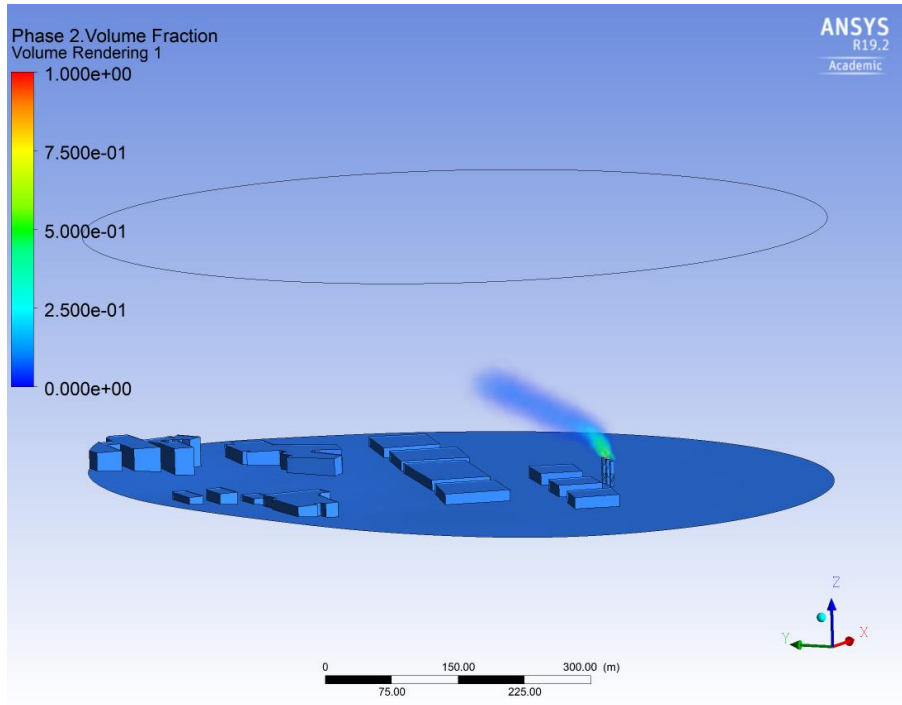


Figure 7 Case 2,0 picture 1

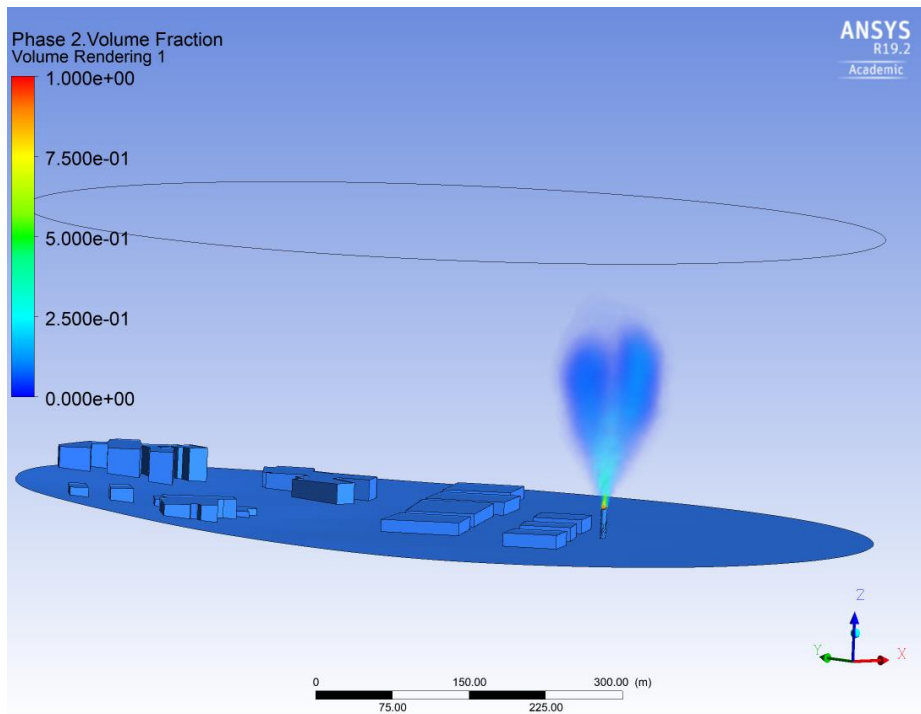


Figure 8 Case 2,0 picture 2

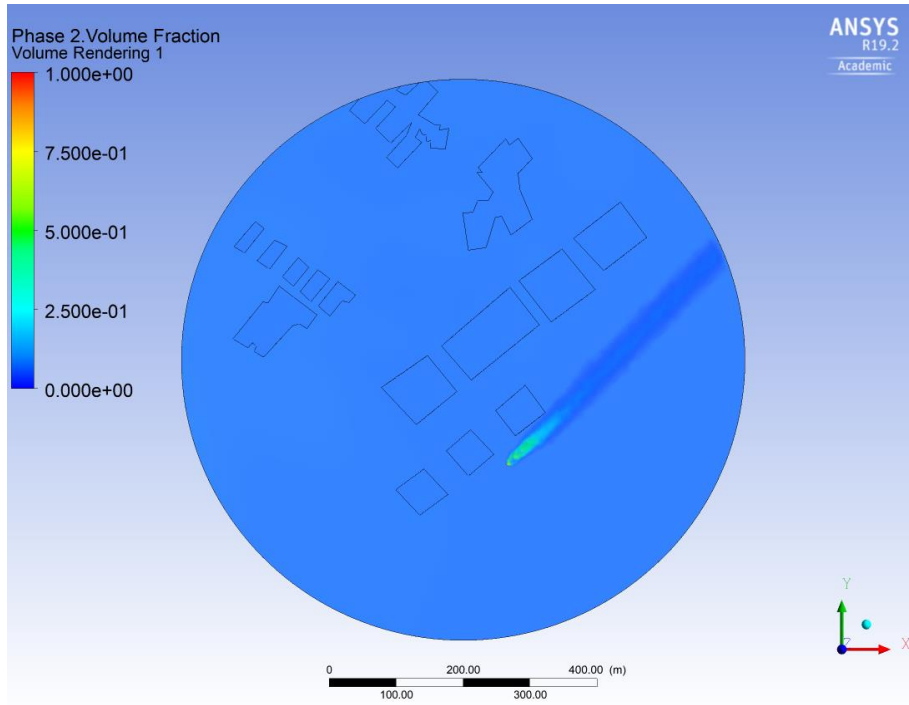


Figure 9 Case 2,1 picture 1

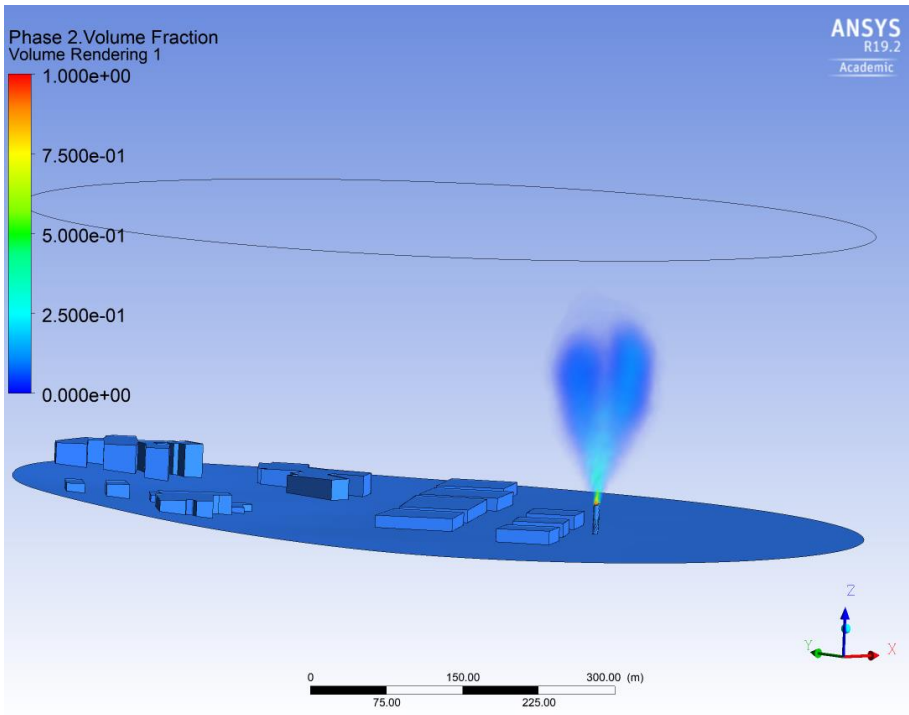


Figure 10 Case 2,1 picture 2

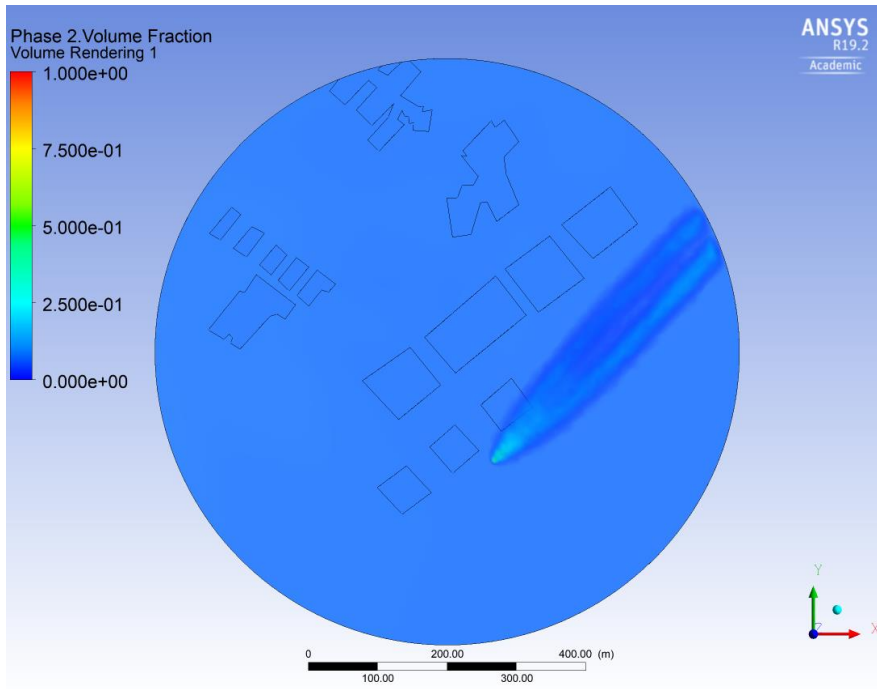


Figure 11 Case 2,2 picture 1

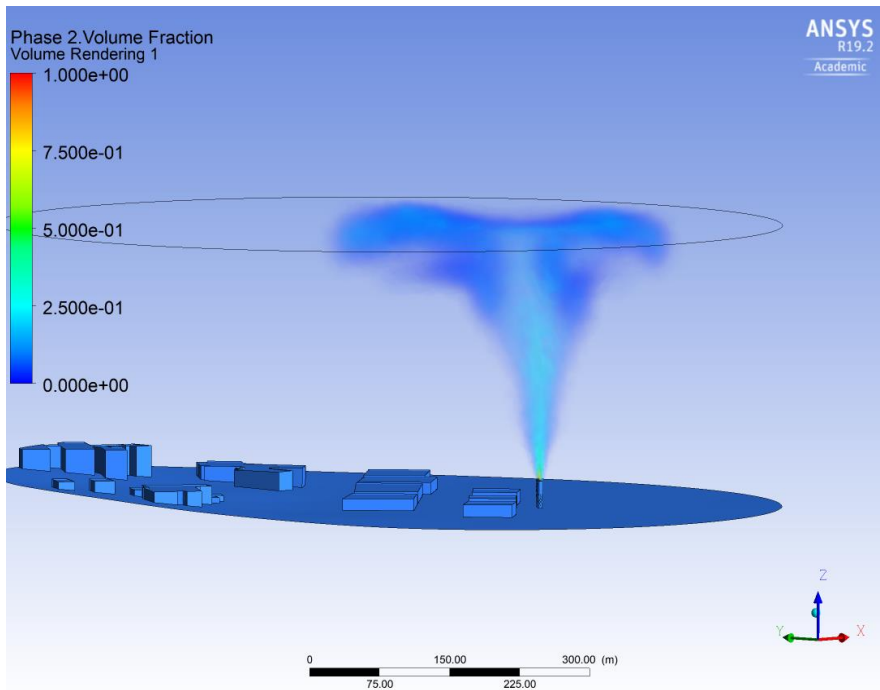


Figure 12 Case 2,2 picture 2

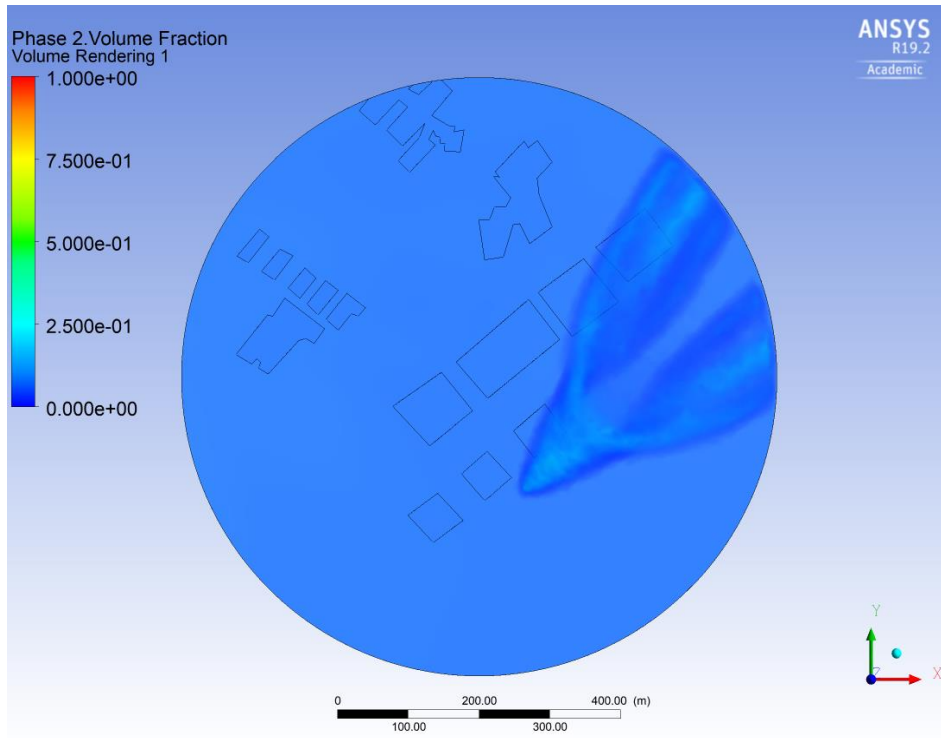


Figure 13 Case 3,0 picture 1

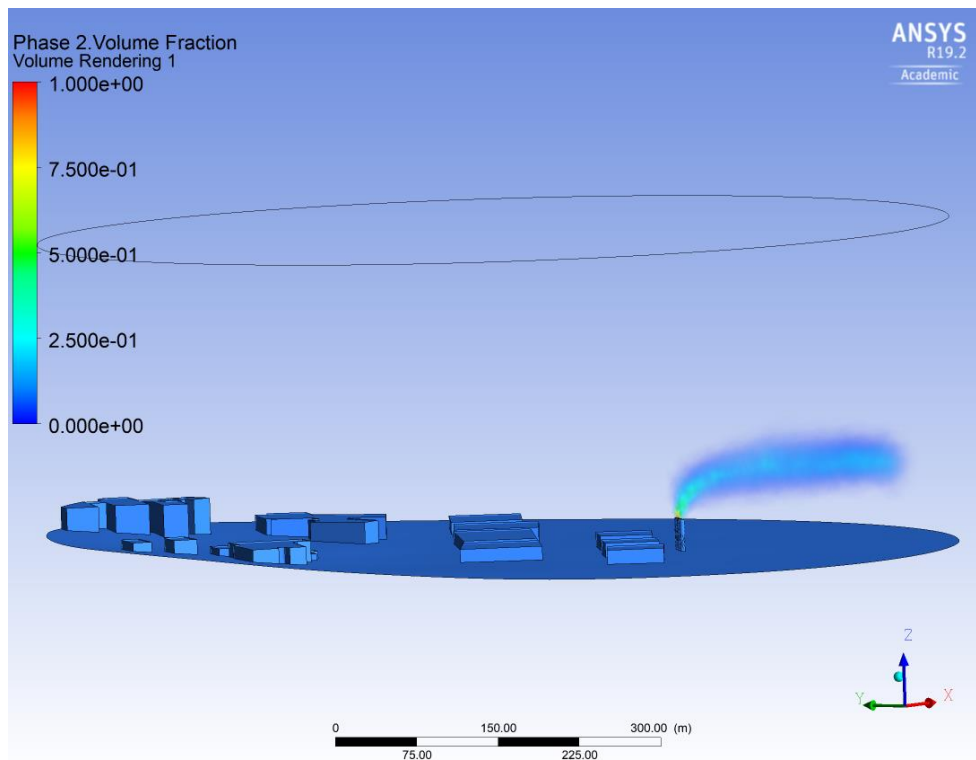


Figure 14 Case 3,0 picture 2

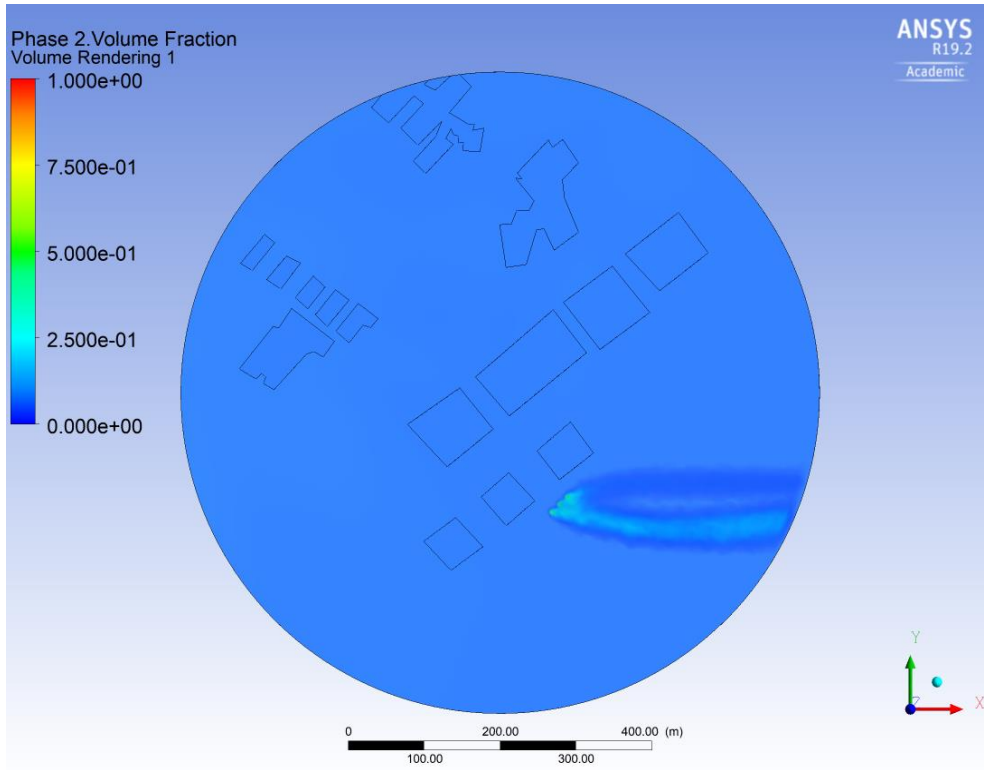


Figure 15 Case 3,1 picture 1

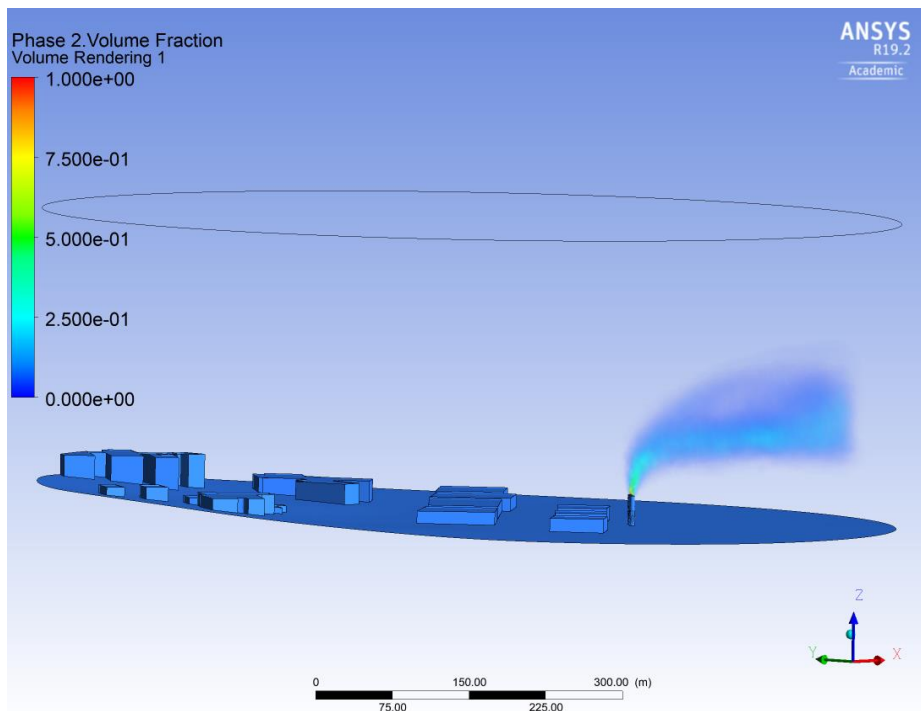


Figure 16 Case 3,1 picture 2

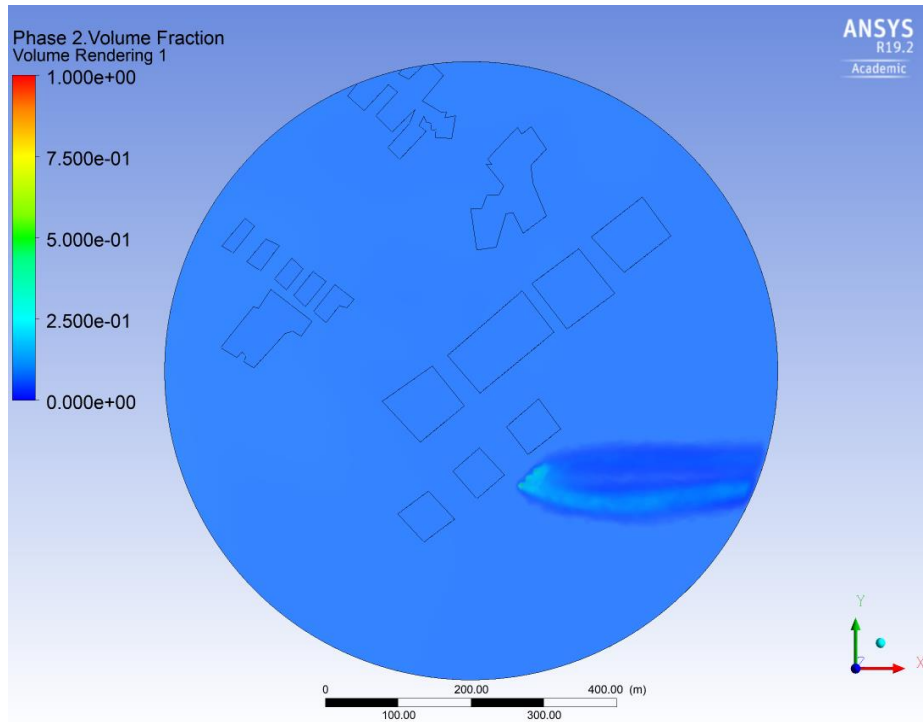


Figure 17 Case 3,2 picture 1

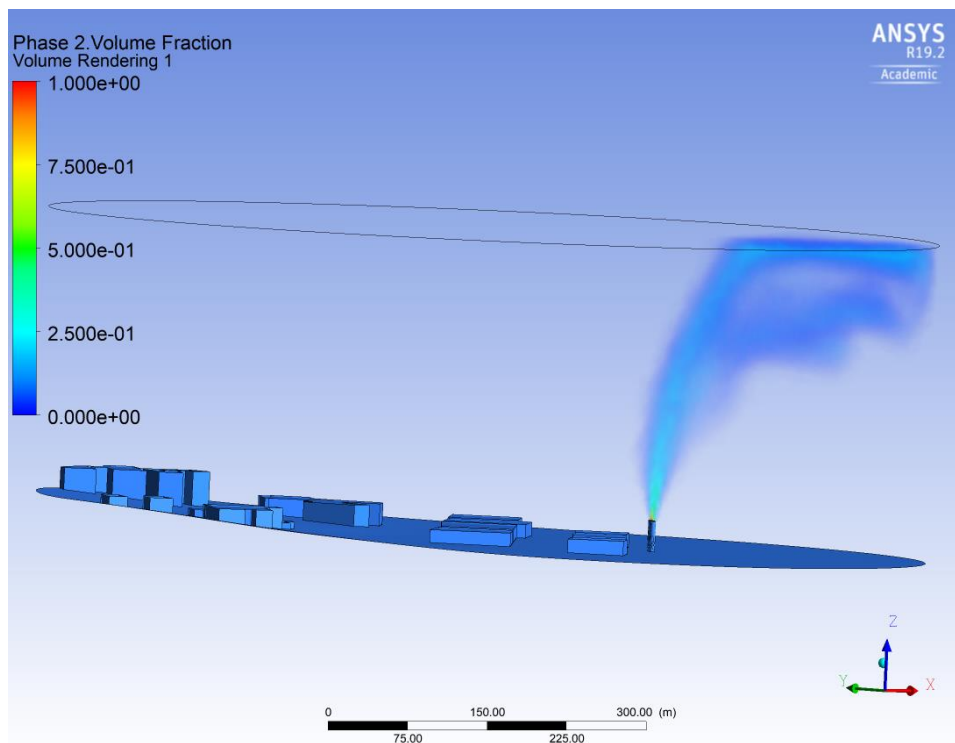


Figure 18 Case 3,2 picture 2

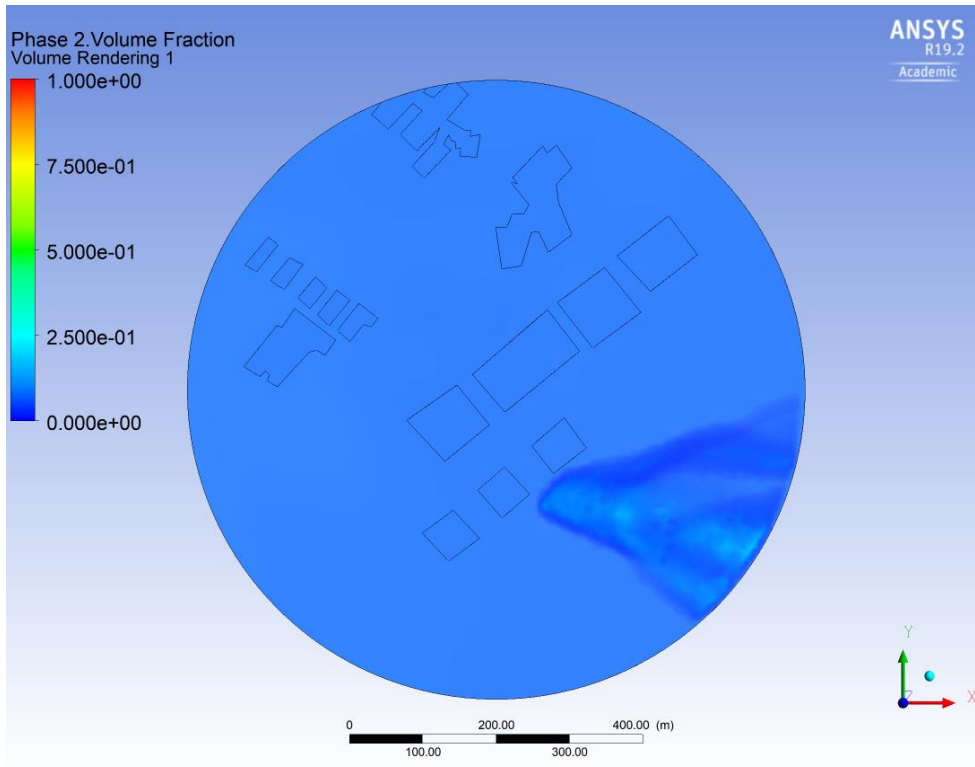


Figure 19 Case 4,0 picture 1

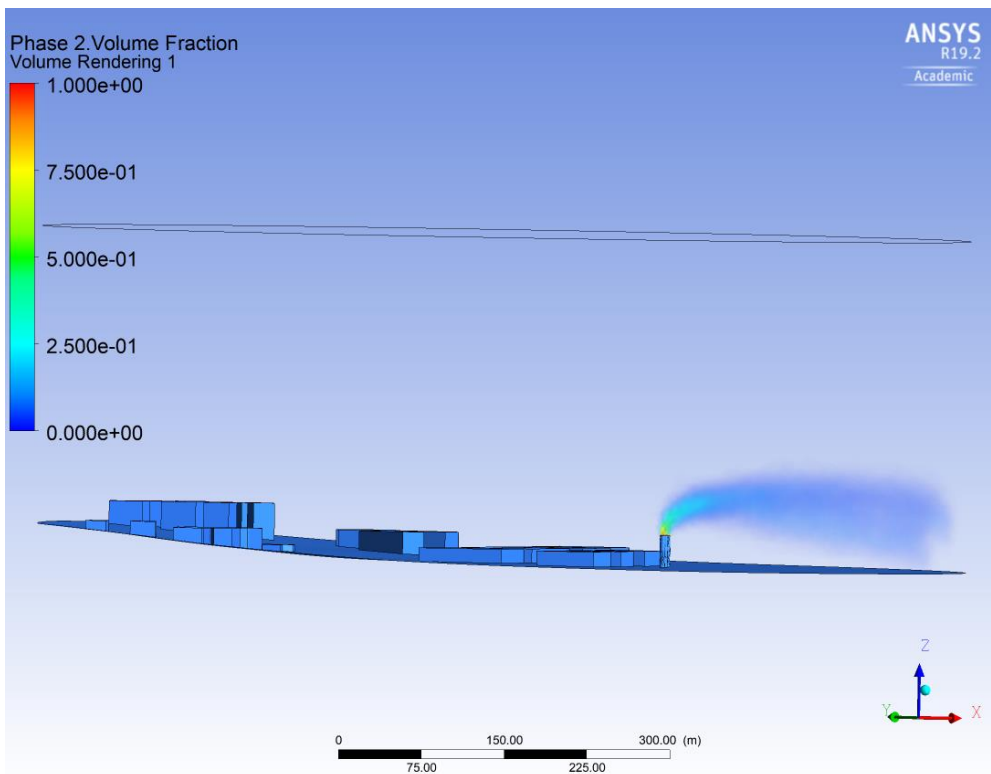


Figure 20 Case 4,0 picture 2

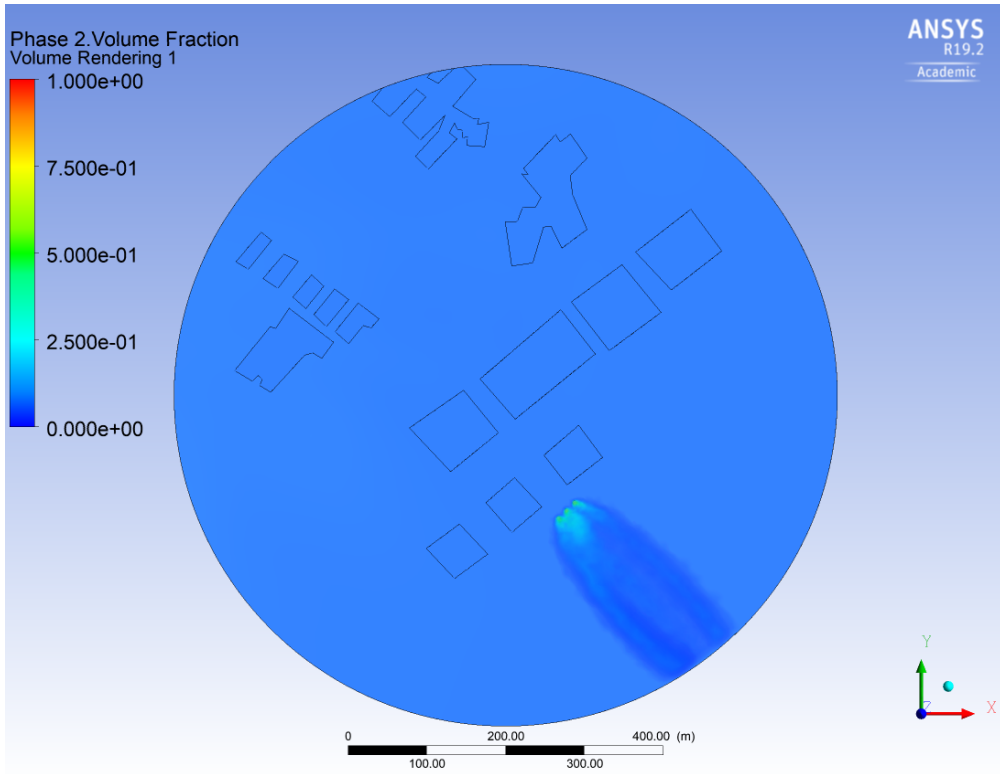


Figure 21 Case 4,1 picture 1

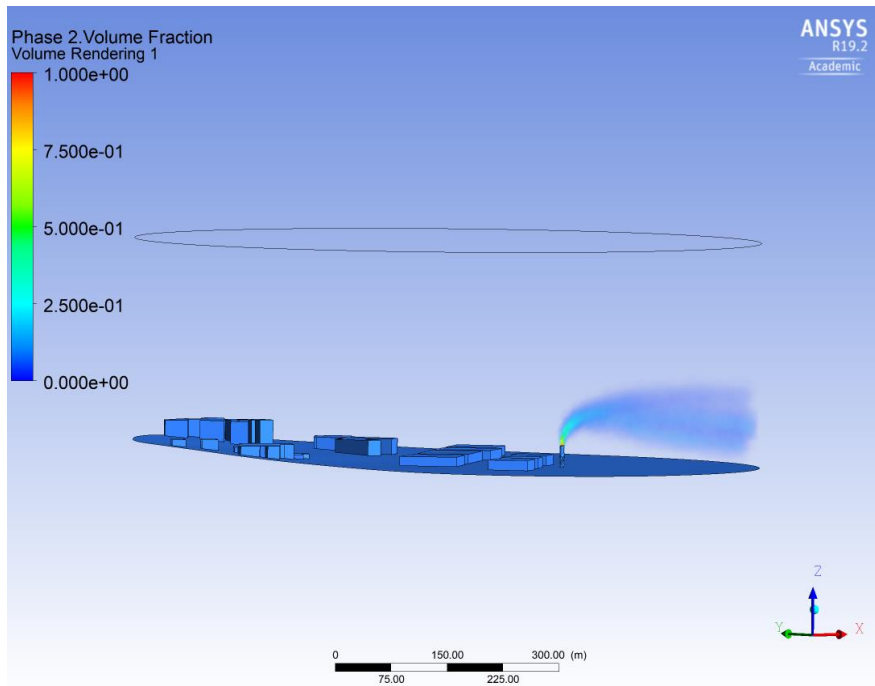


Figure 22 Case 4,1 picture 2

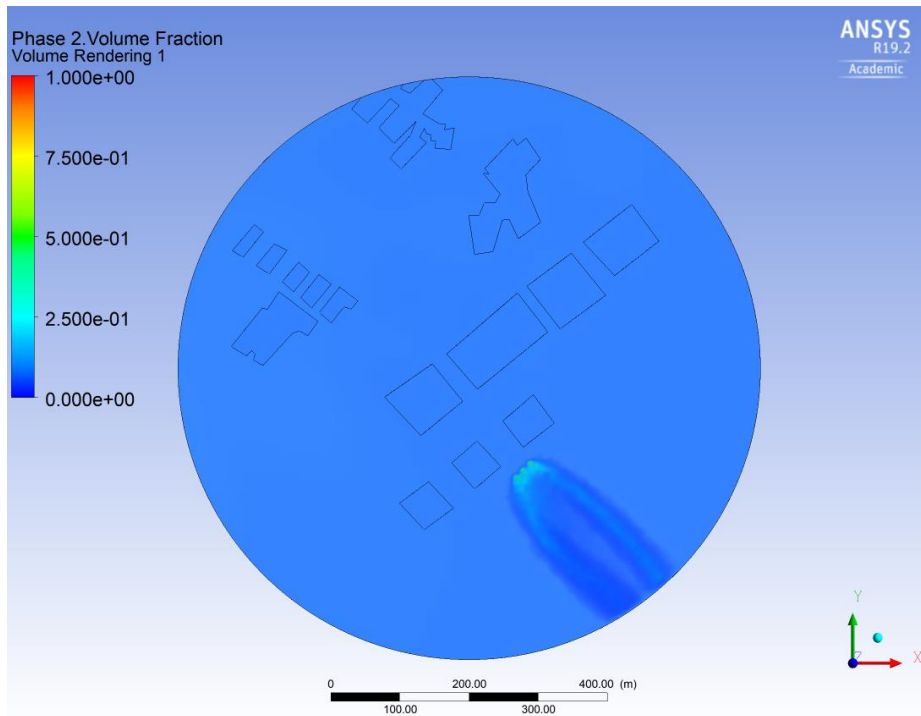


Figure 23 Case 4,2 picture 1

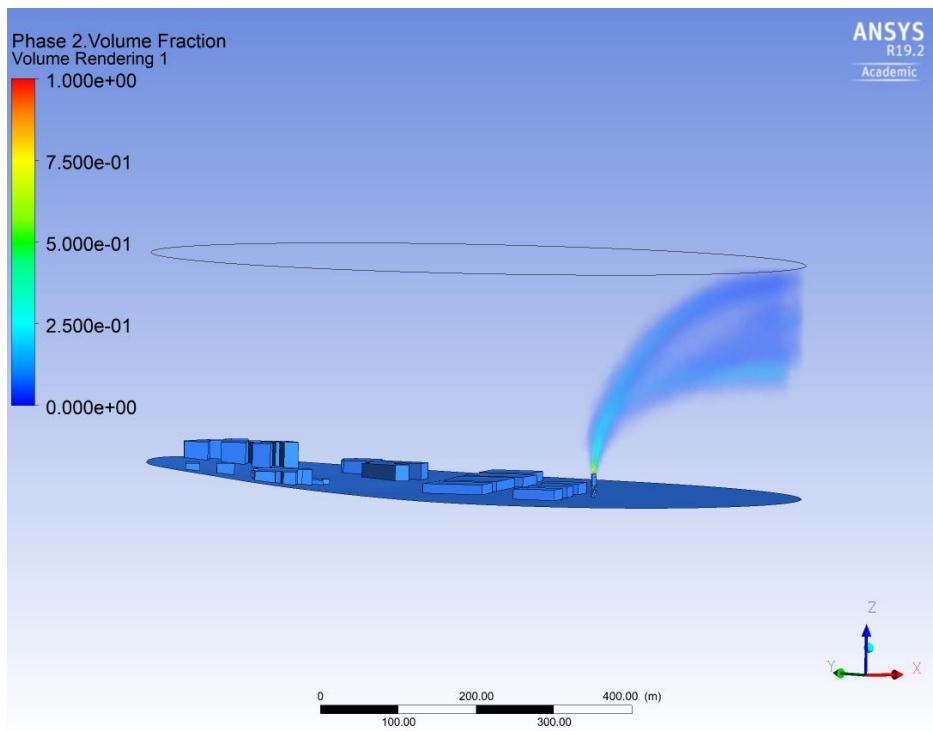


Figure 24 Case 4,2 picture 2

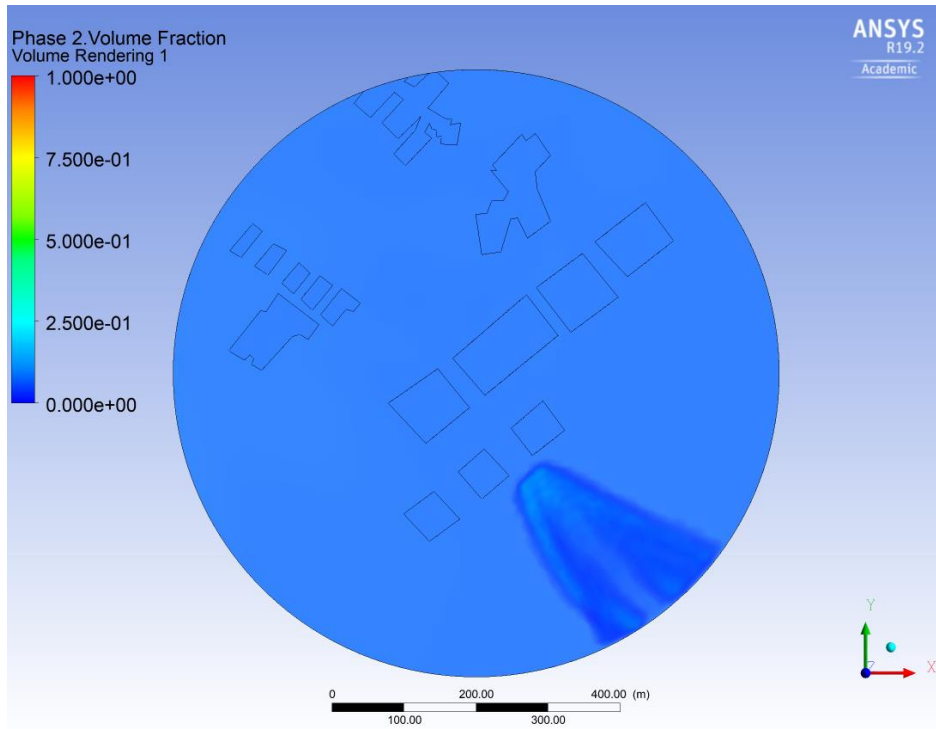


Figure 25 Case 5,0 picture 1

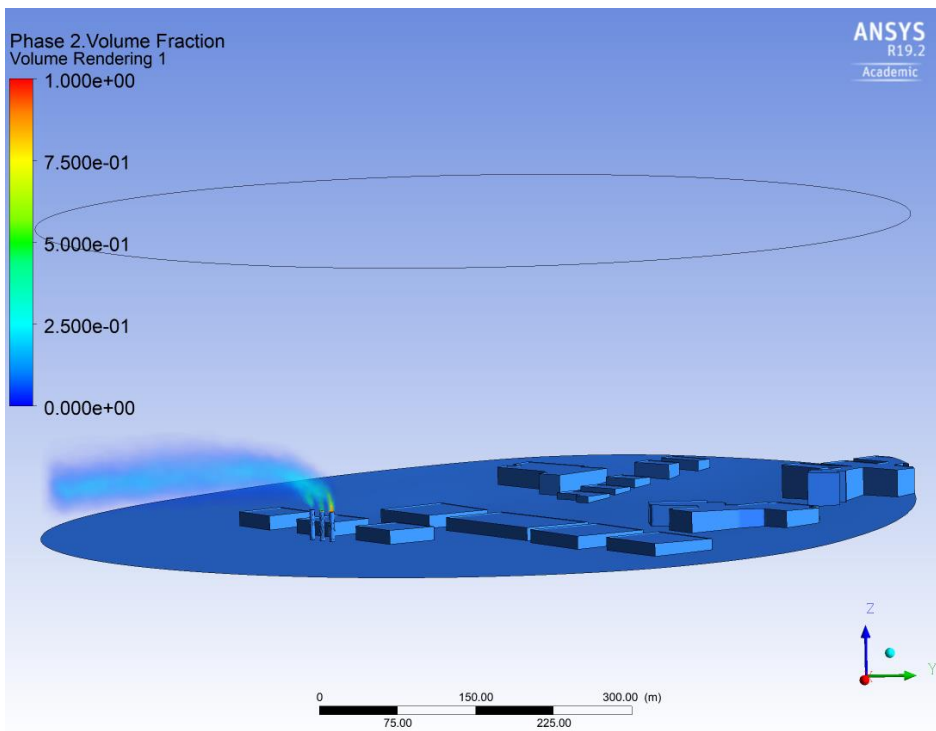


Figure 26 Case 5,0 picture 2

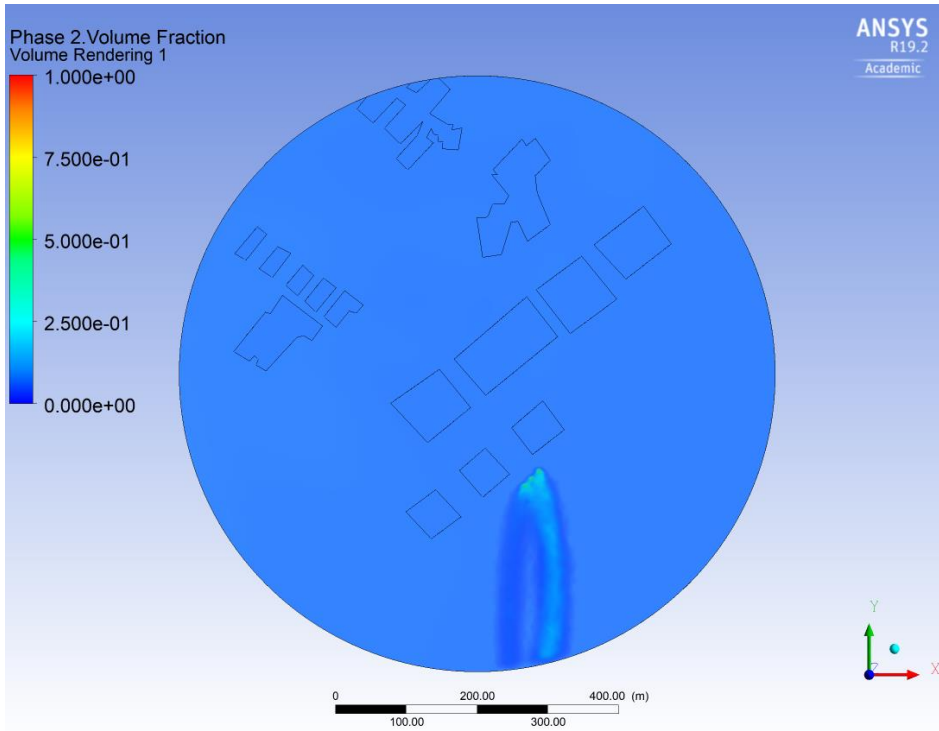


Figure 27 Case 5,1 picture 1

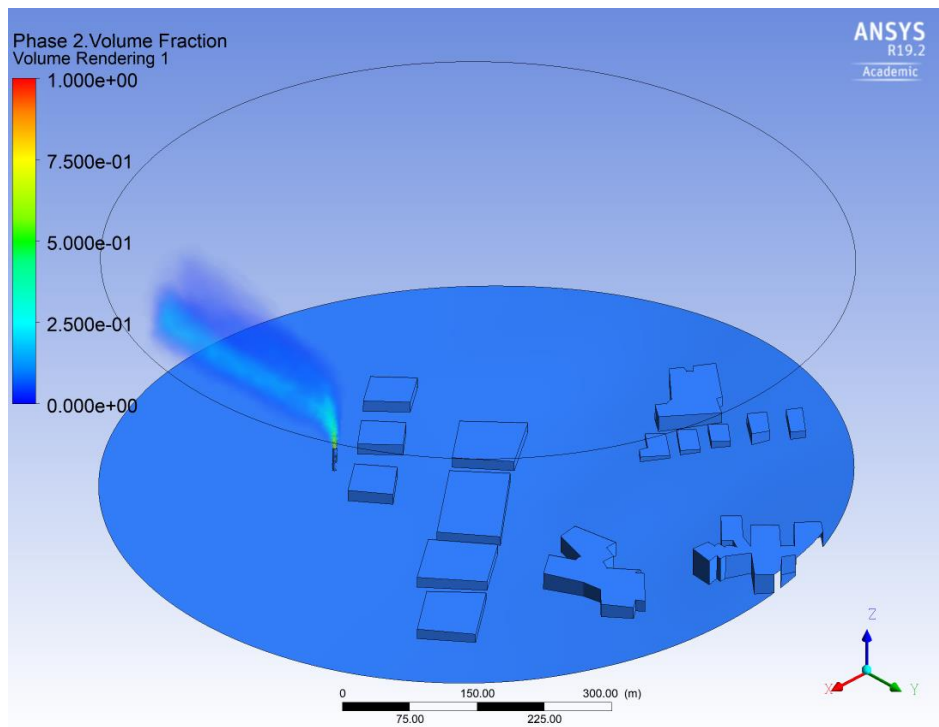


Figure 28 Case 5,2 picture 2

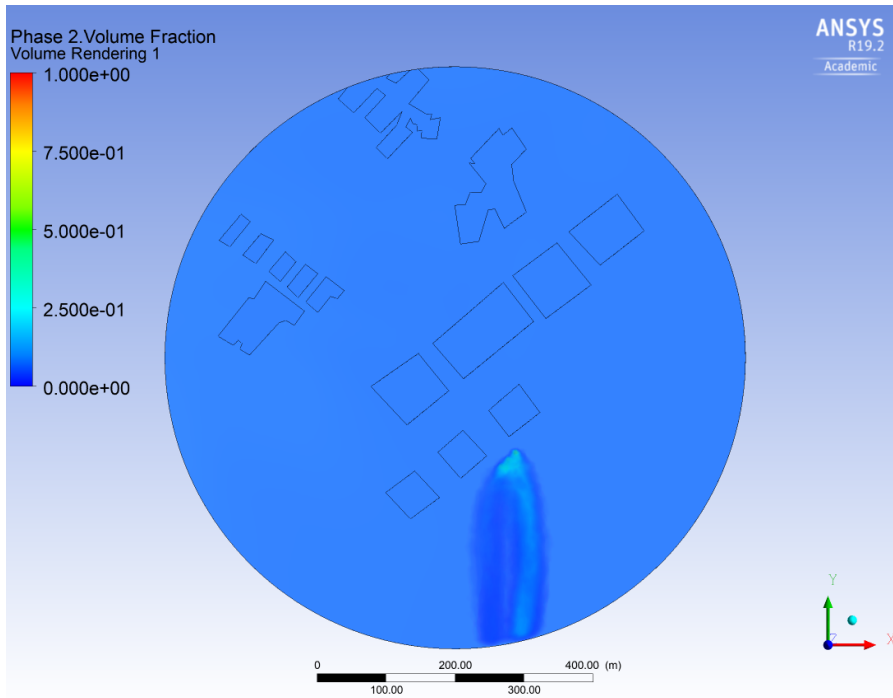


Figure 29 Case 6,0 picture 1

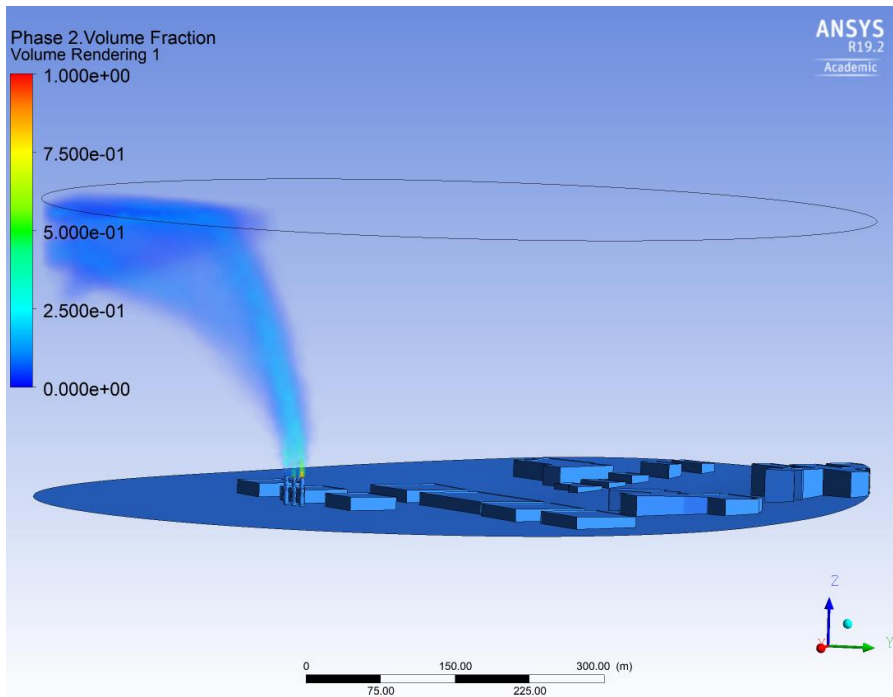


Figure 30 Case 6,0 picture 2

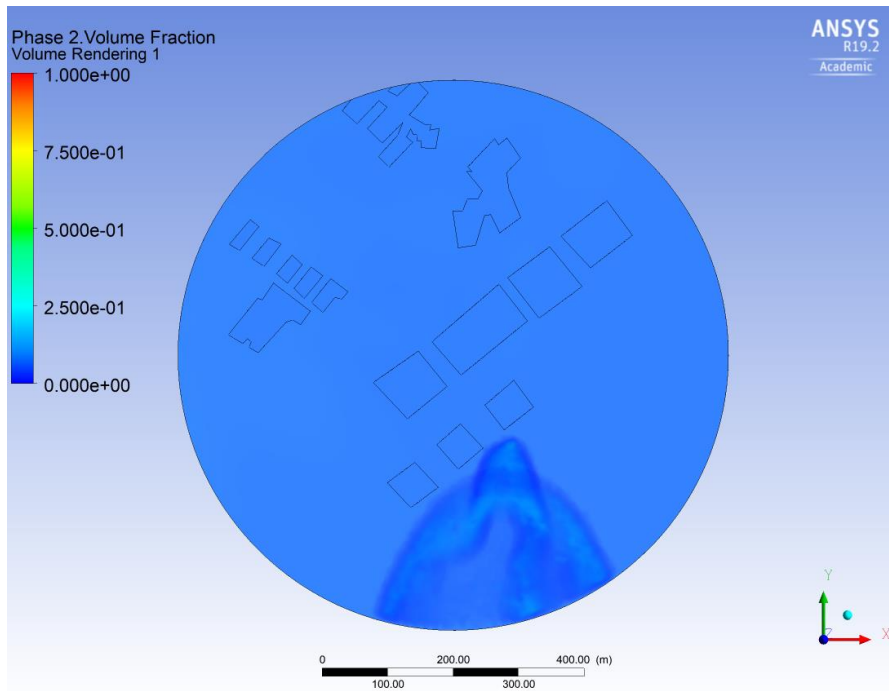


Figure 31 Case 6,1 picture 1

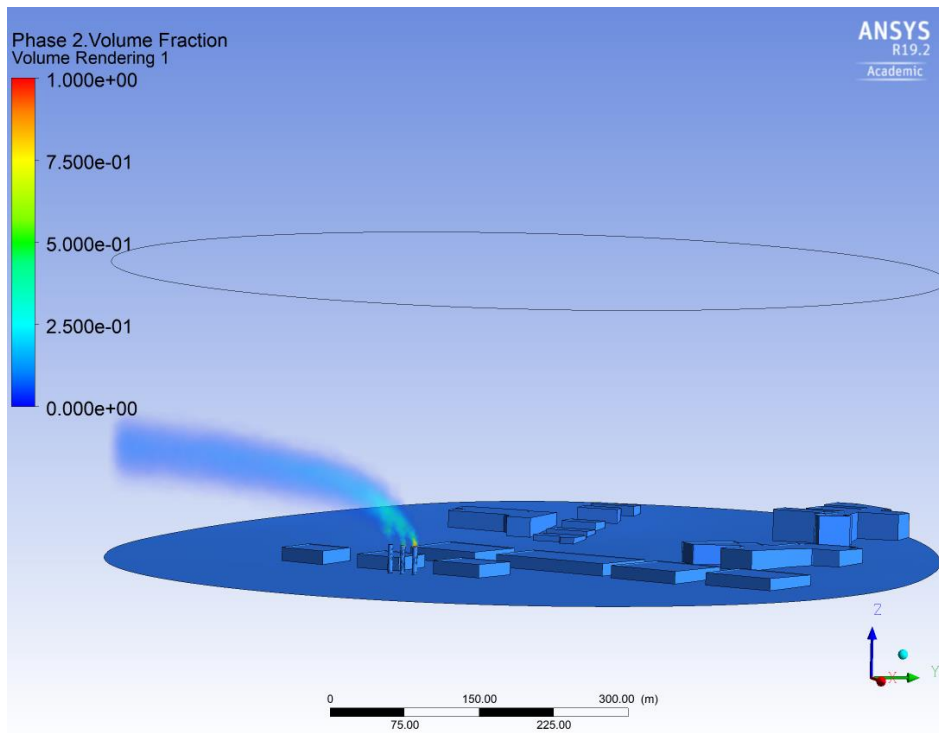


Figure 32 Cas 6,1 picture 2

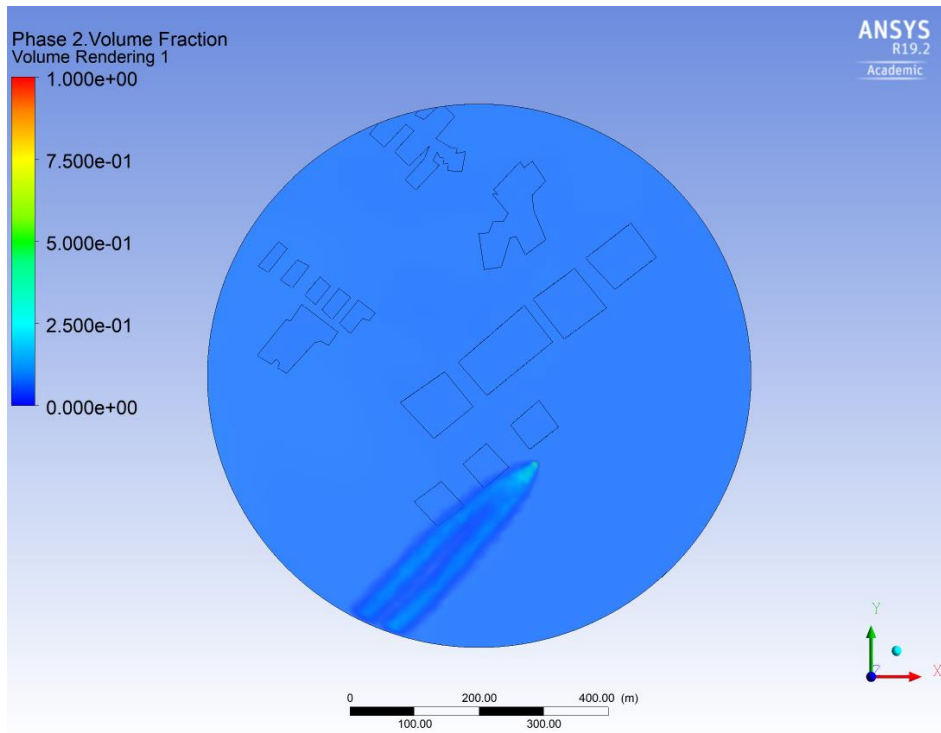


Figure 33 Case 6,2 picture 1

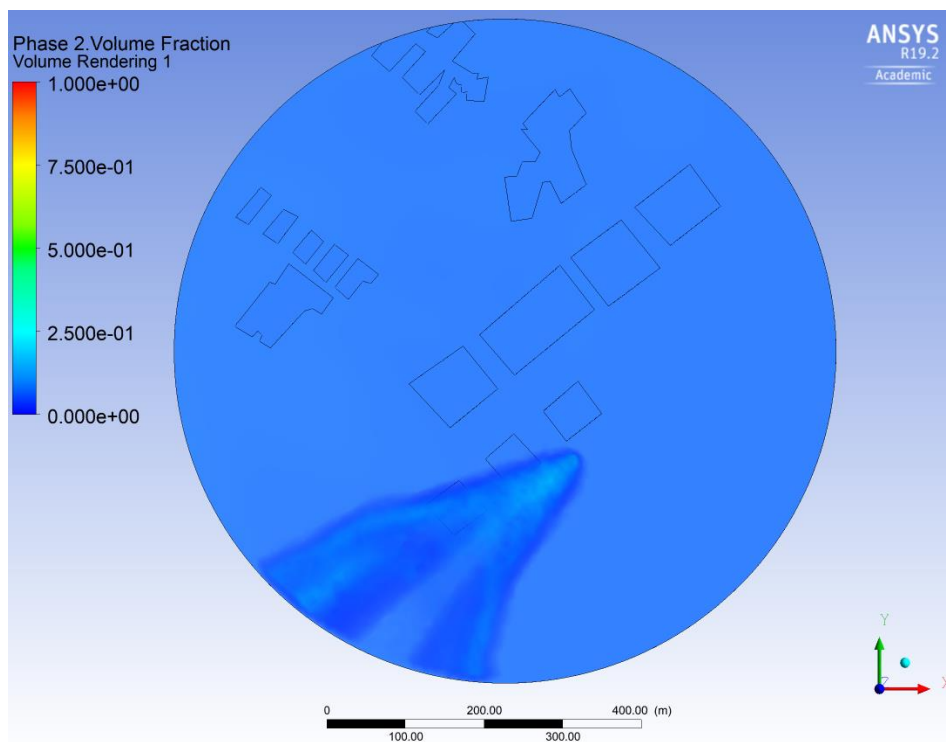


Figure 34 Case 6,2 picture 2

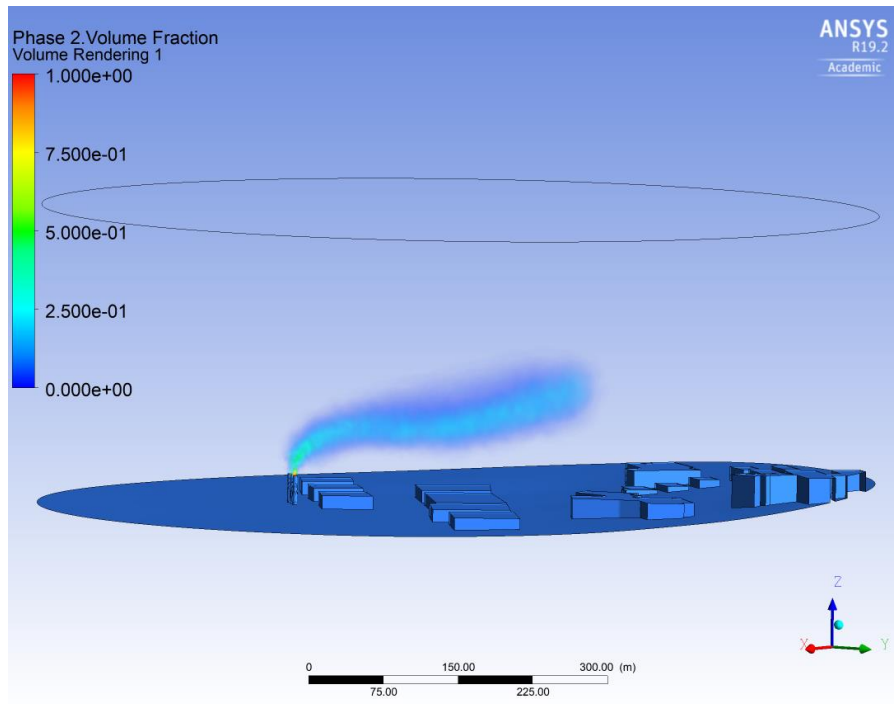


Figure 35 Case 7,0 picture 1

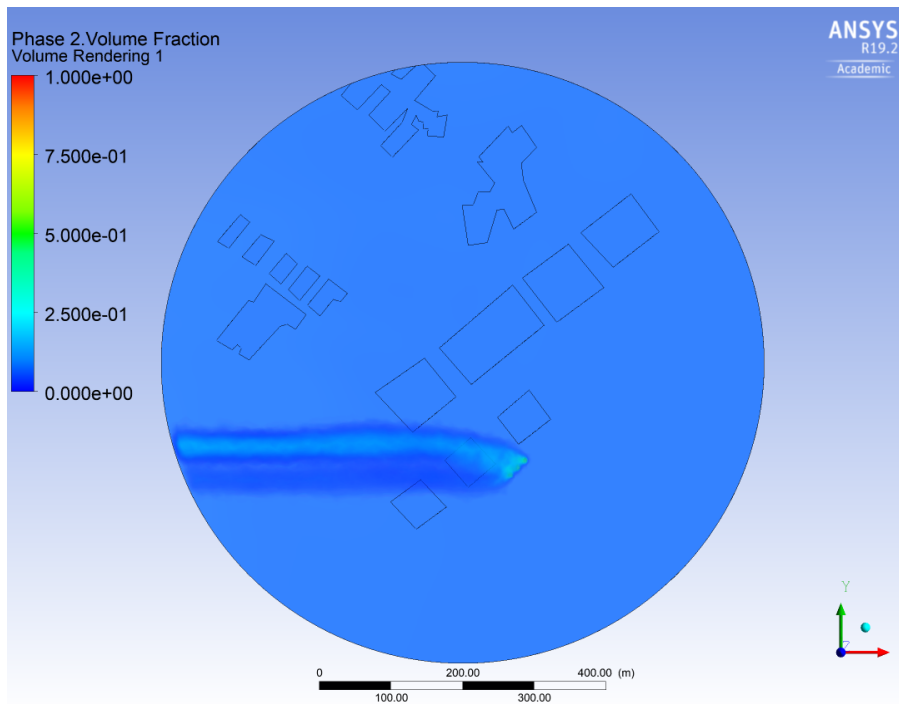


Figure 36 Case 7,0 picture 2

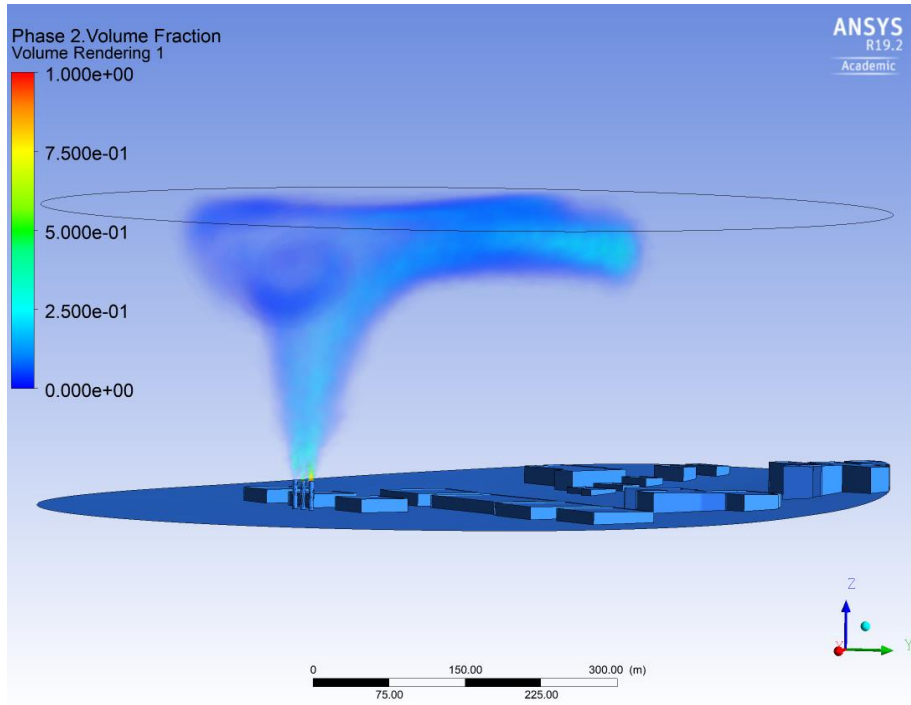


Figure 37 Case 7,2 picture 1

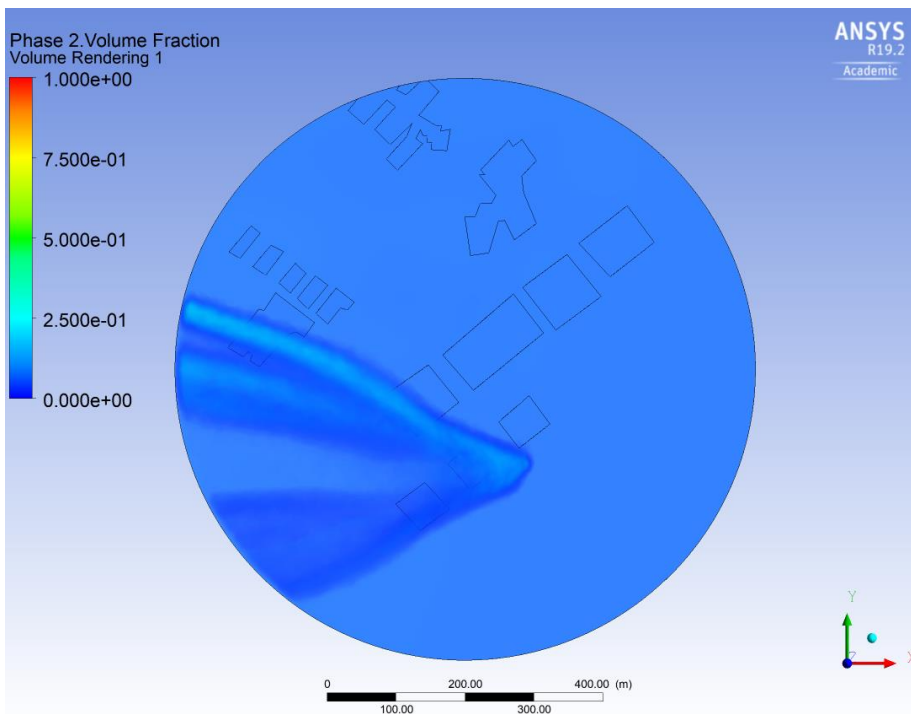


Figure 38 Case 7,2 picture 2

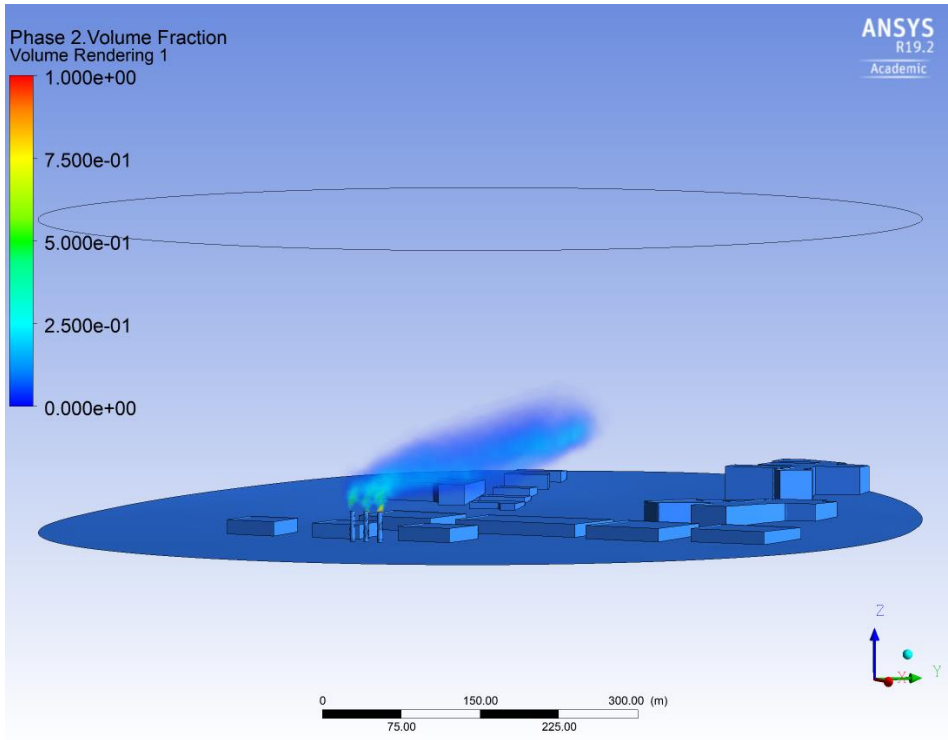


Figure 39 Case 8,0 picture 1

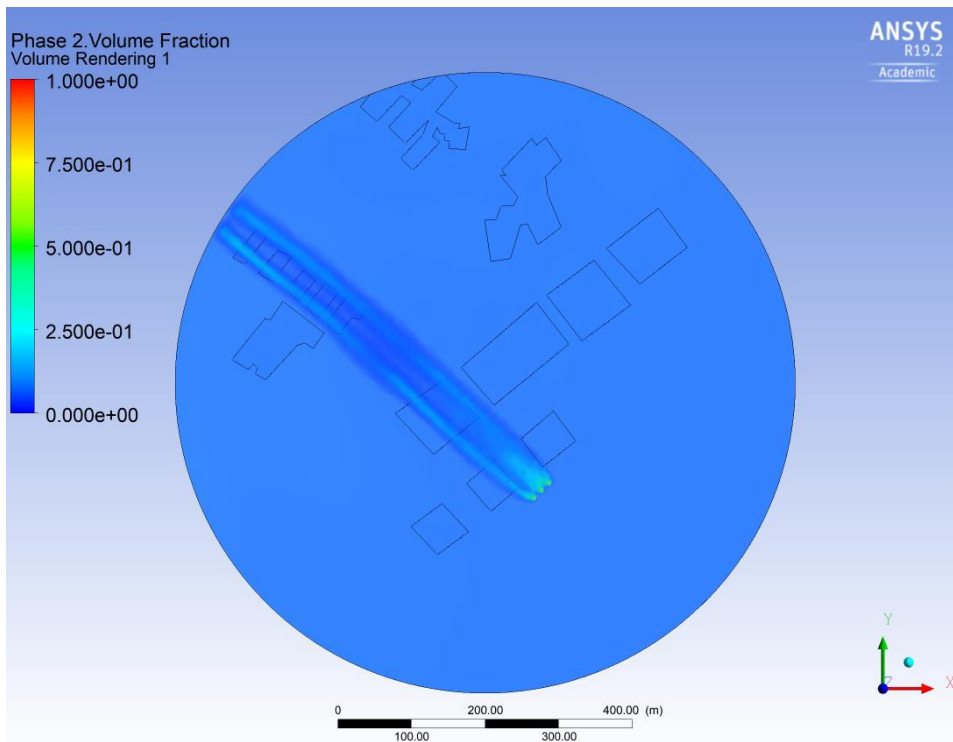


Figure 40 Case 8,0 picture 2

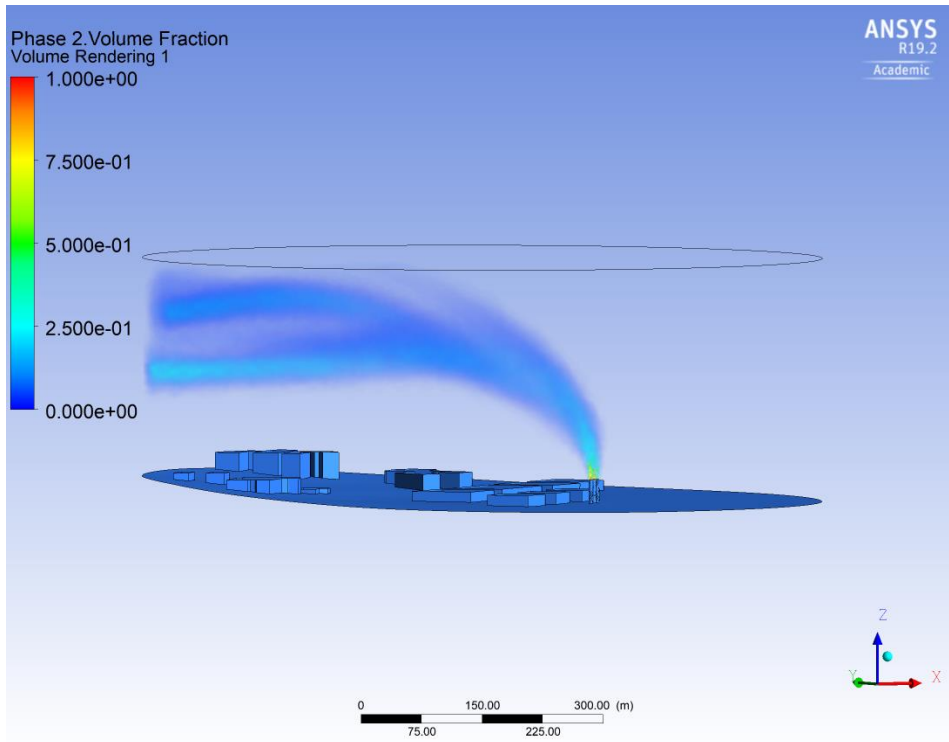


Figure 41 Case 8,2 picture 1

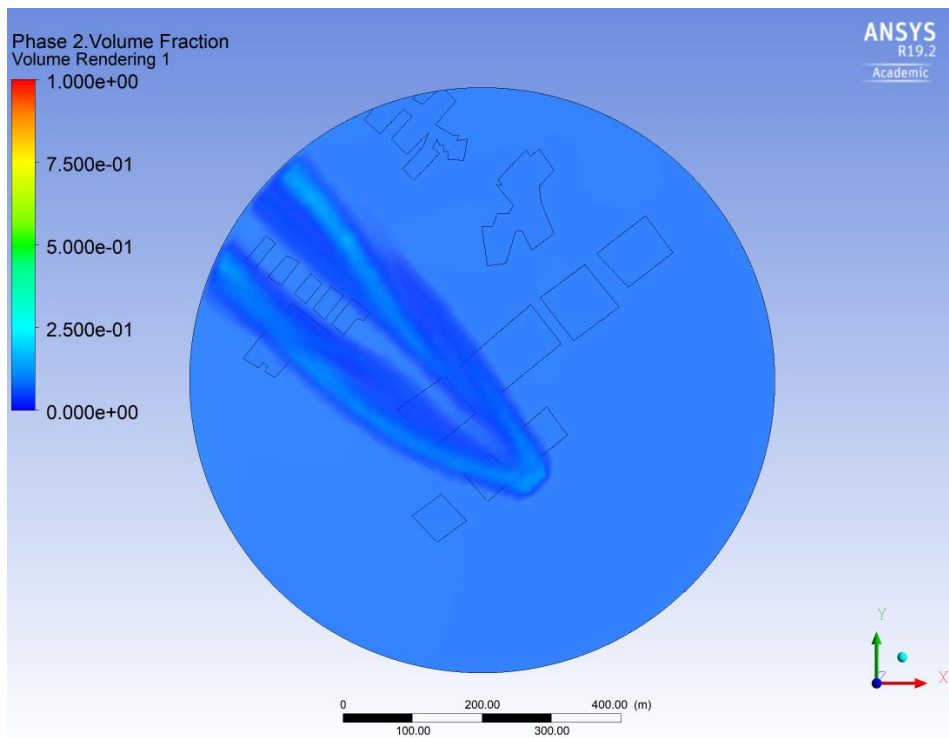


Figure 42 Case 8,2 picture 2

20 meter

Case	Vx	Vy	Calculated value	Date of simulation	File name	Status
9,0	0,0	15		30.mar.19	FFF_case_9_0	ok
9,1	0,0	3,3		31.mar.19	FFF_case_9_1	ok
10,0	15sin45 m/s	15sin45 m/s	12,7	01.apr.19	FFF_case_10_0_1	ok
10,1	3,3sin45 m/s	3,3sin45 m/s	2,8	01.apr.19	FFF_case_10_1_1	ok
11,0	5 m/s	0		02.04.2019	FFF_case_11_0	ok
11,1	3,3 m/s	0		03.04.2019	FFF_case_11_0_1	ok
12,0	5sin45 m/s	$\sqrt{5}$ sin45 m/s	$\sqrt{4.25}$	03.04.2019	FFF_case_12_0	ok
12,1	3,3sin45 m/s	$\sqrt{3.3}$ sin45 m/s	$\sqrt{2.8}$	04.04.2019	FFF_case_12_1	ok
13,0	0,0	$\sqrt{5}$ m/s		04.04.2019	FFF_case_13_0_1	ok
13,1	0,0	$\sqrt{3.3}$ m/s		04.04.2019	FFF_case_13_1_0	ok
14,0	$\sqrt{5}$ sin45 m/s	$\sqrt{5}$ sin45 m/s	$\sqrt{4.25}$	04.04.2019	FFF_case_14_0_1	ok
14,1	$\sqrt{3.3}$ sin45 m/s	$\sqrt{3.3}$ sin45 m/s	$\sqrt{2.8}$	10.04.2019	FFF_case_14_1_0	
15,0	$\sqrt{5}$ m/s	0		23.04.2019	FFF_case_15_0_1	ok
15,1	$\sqrt{3.3}$ m/s	0		23.04.2019	FFF_case_15_1_1	ok
16,0	$\sqrt{5}$ m/s	5sin45 m/s	$\sqrt{4.25}$	24.04.2019	FFF_case_16_0_1	ok
16,1	$\sqrt{3.3}$ m/s	3,3sin45 m/s	$\sqrt{2.8}$	24.04.2019	FFF_case_16_1_1	ok

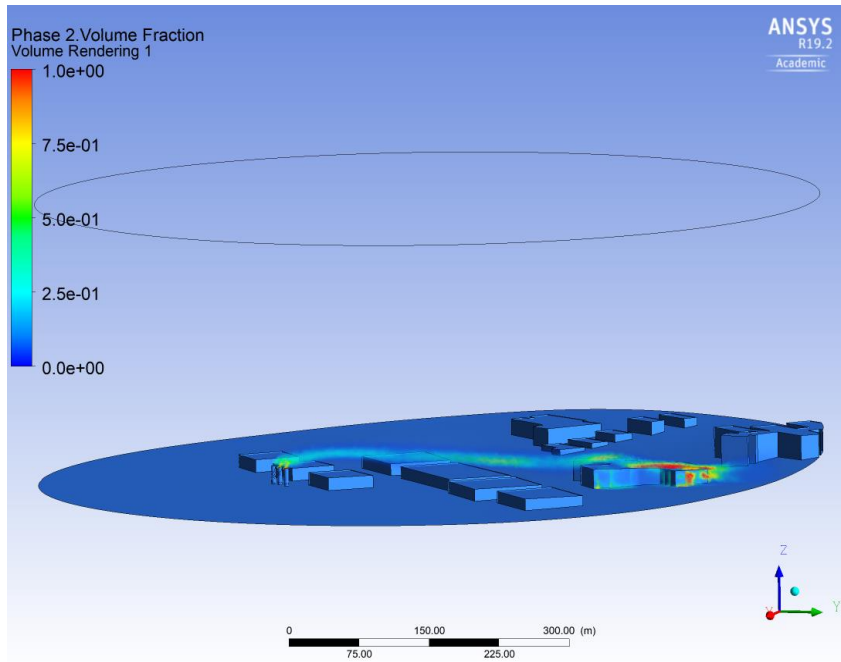


Figure 43 Case 9,0 picture 1

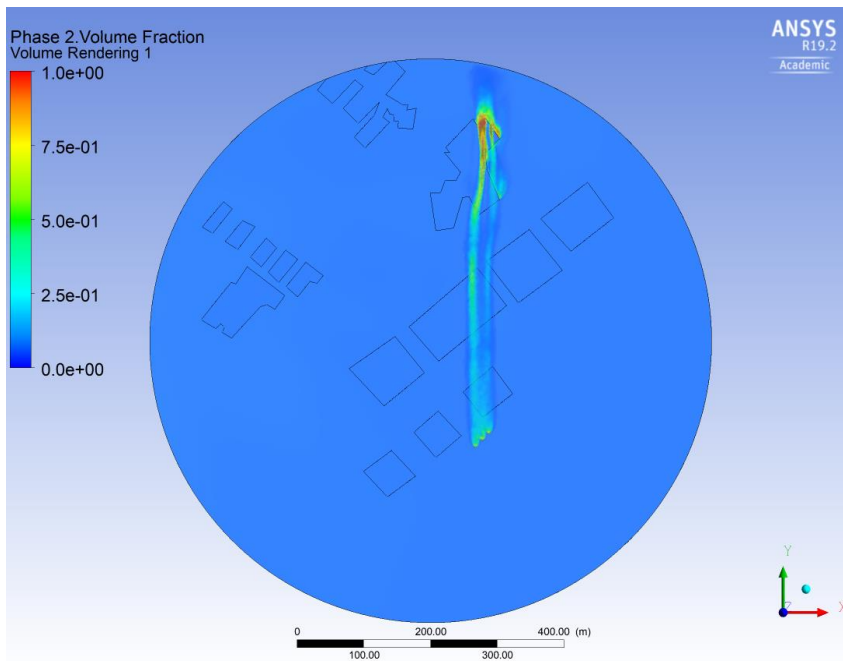


Figure 44 Case 9,0 picture 1

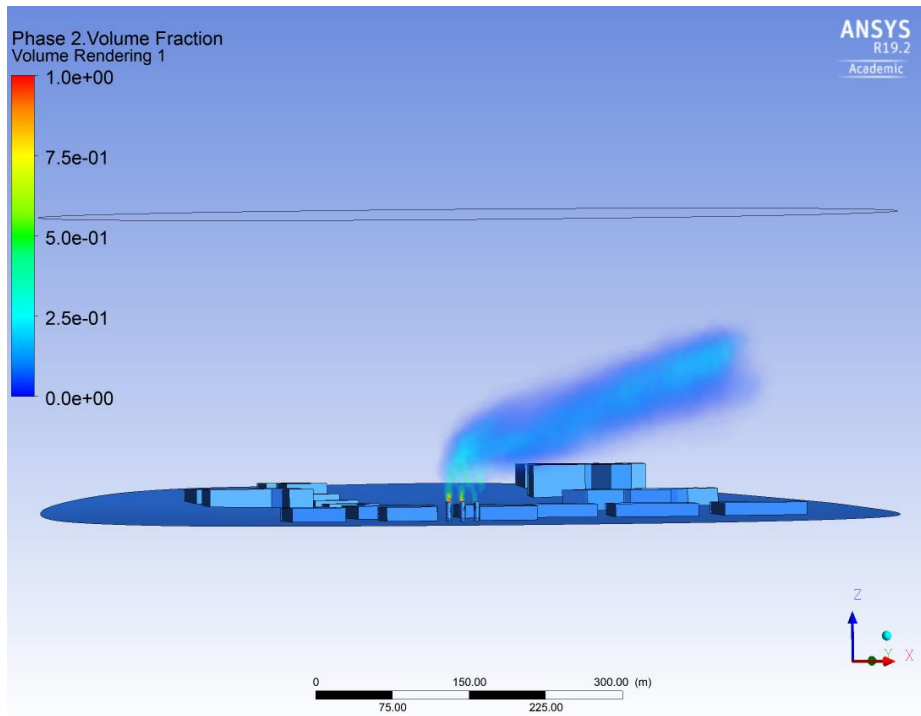


Figure 45 Case 9,1 picture 1

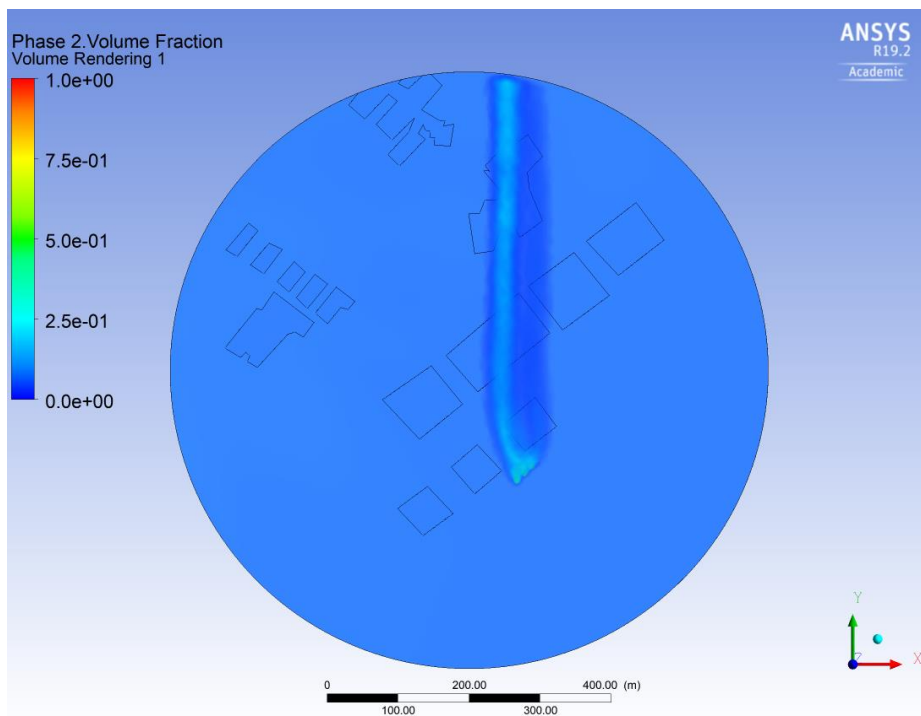


Figure 46 Case 9,1 picture 2

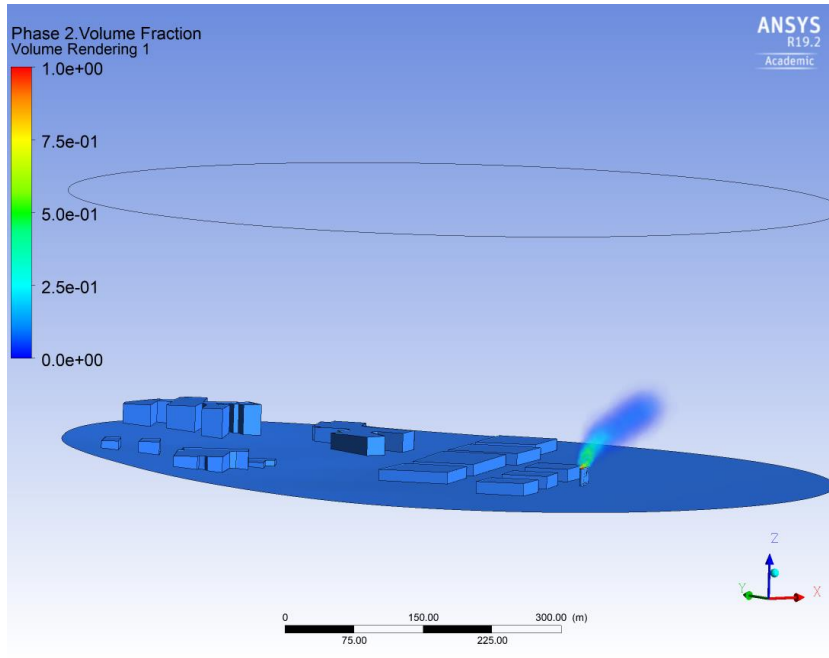


Figure 47 Case 10,0 picture 1

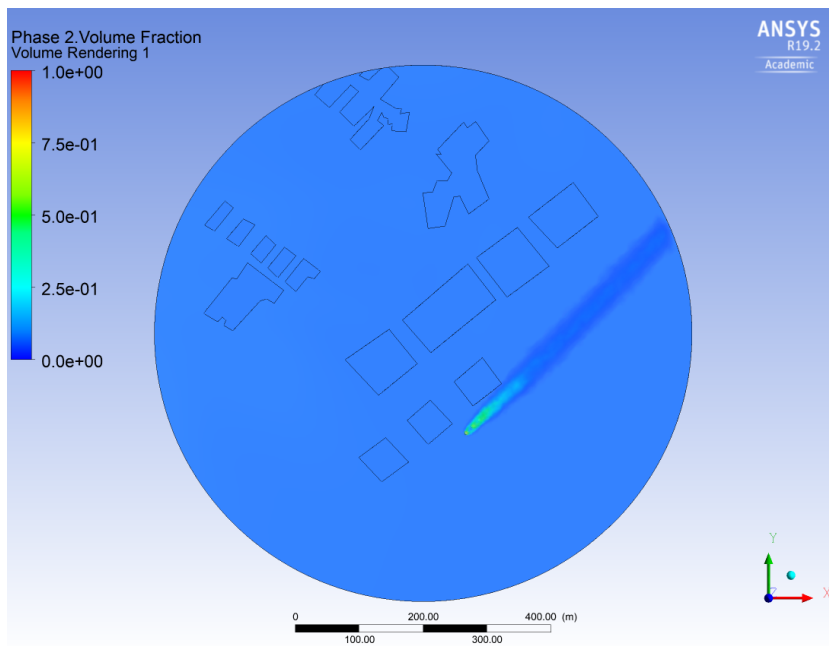


Figure 48 Case 10,0 picture 2

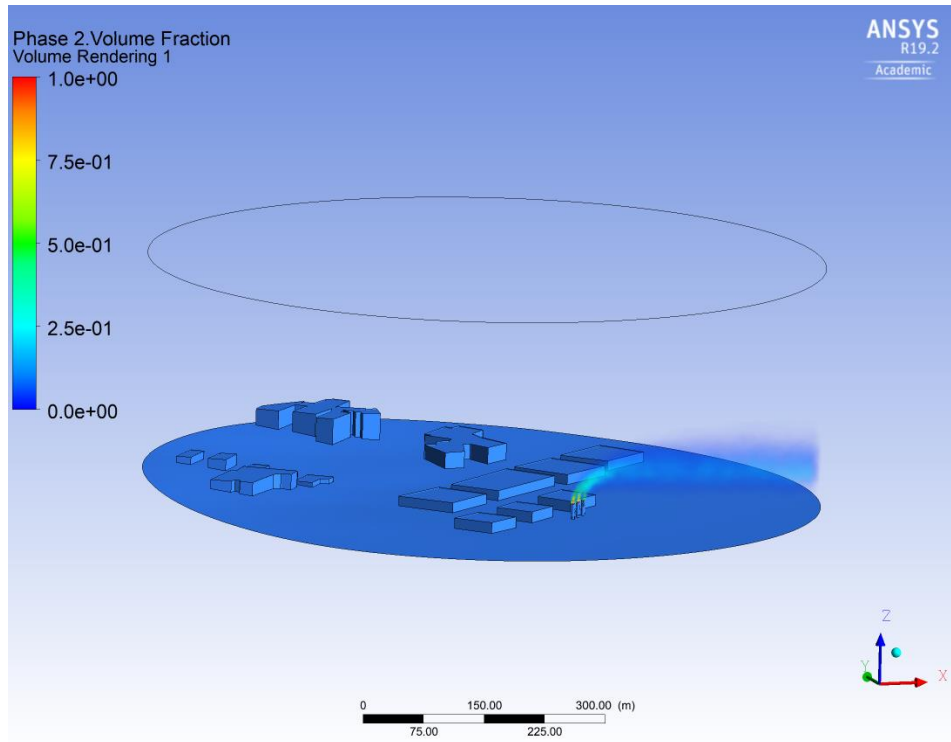


Figure 49 Case 10,1 picture 1

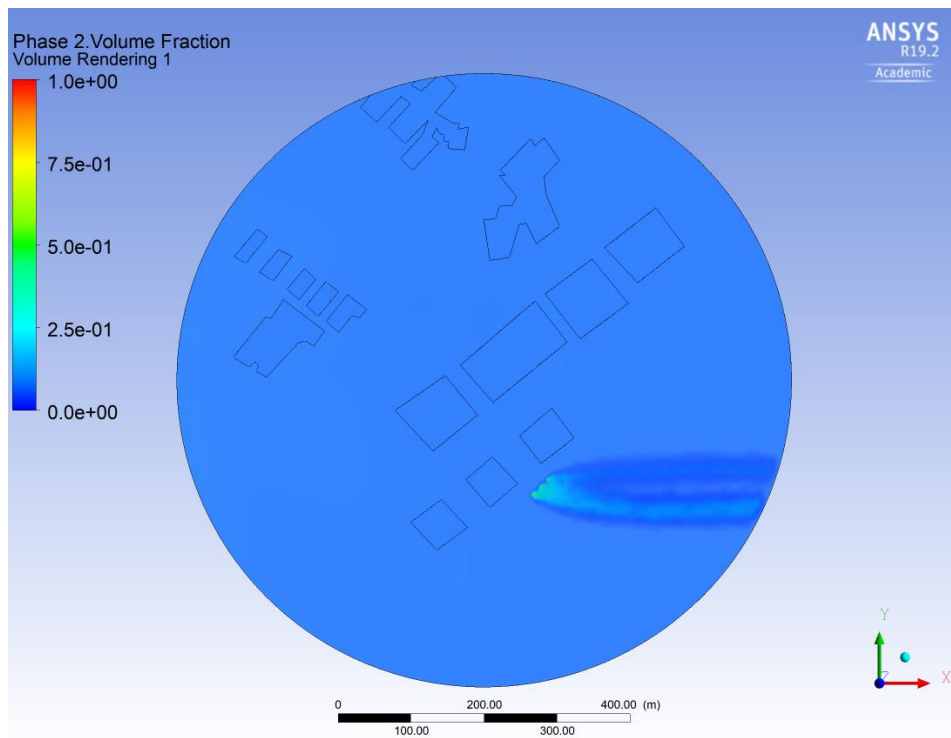


Figure 50 Case 10,1 picture 2

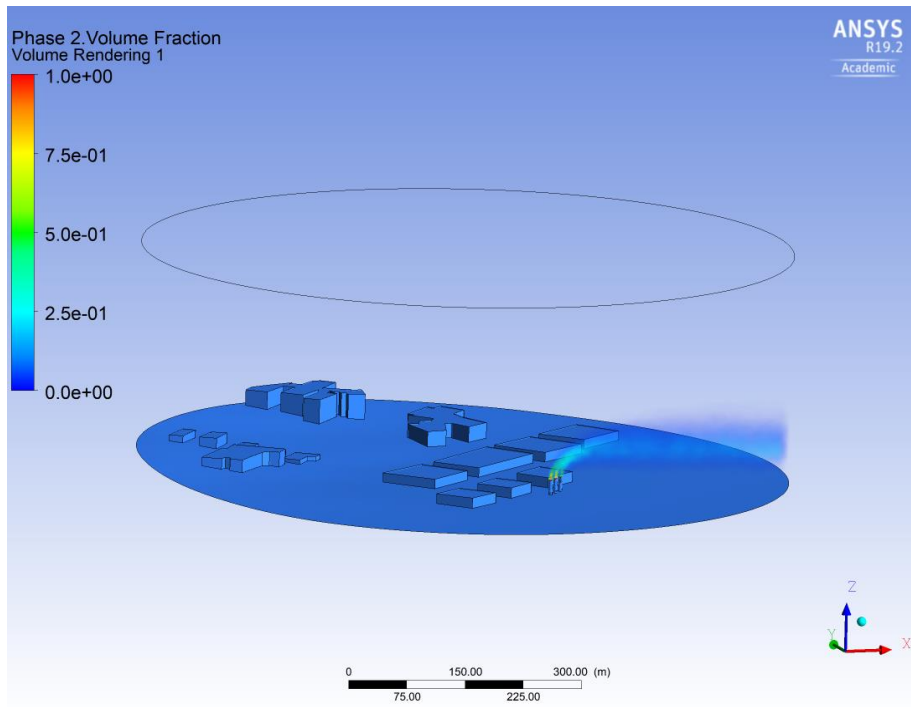


Figure 51 Case 11,0 picture 1

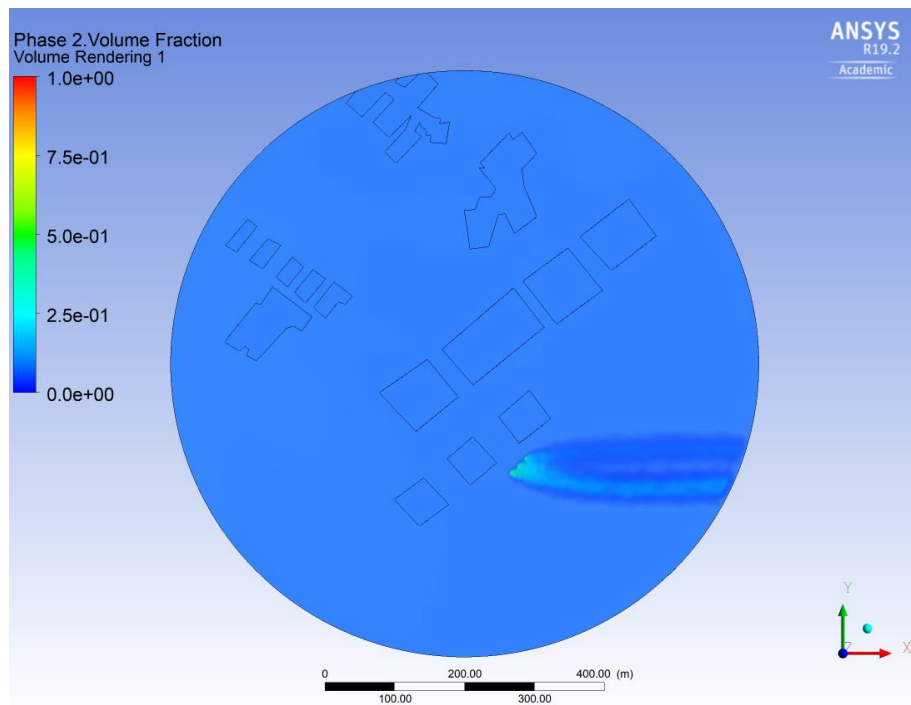


Figure 52 Case 11,0 picture 2

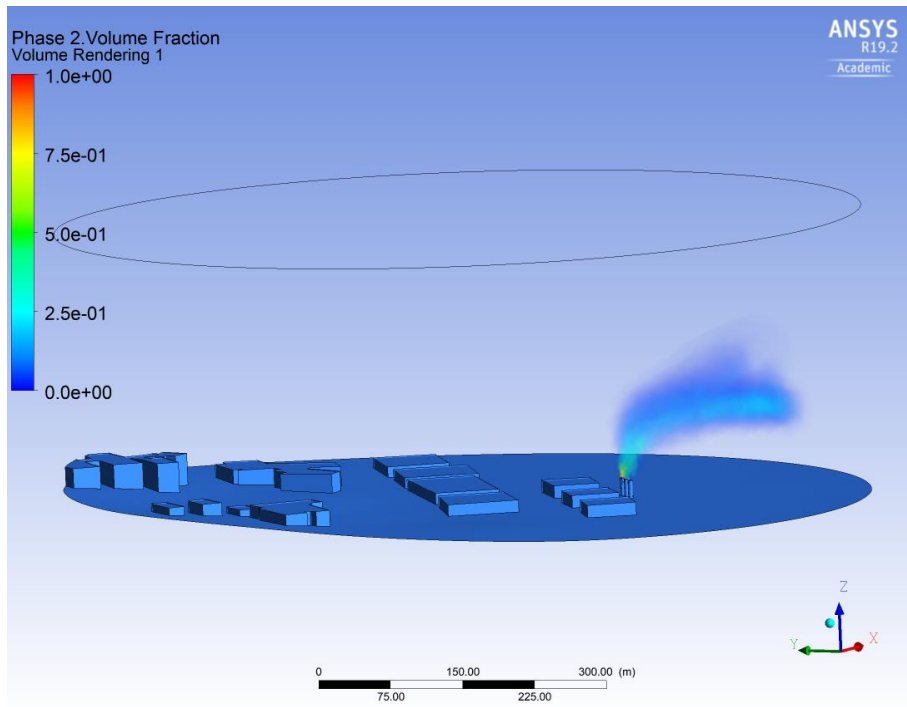


Figure 53 Case 11,1 picture 1

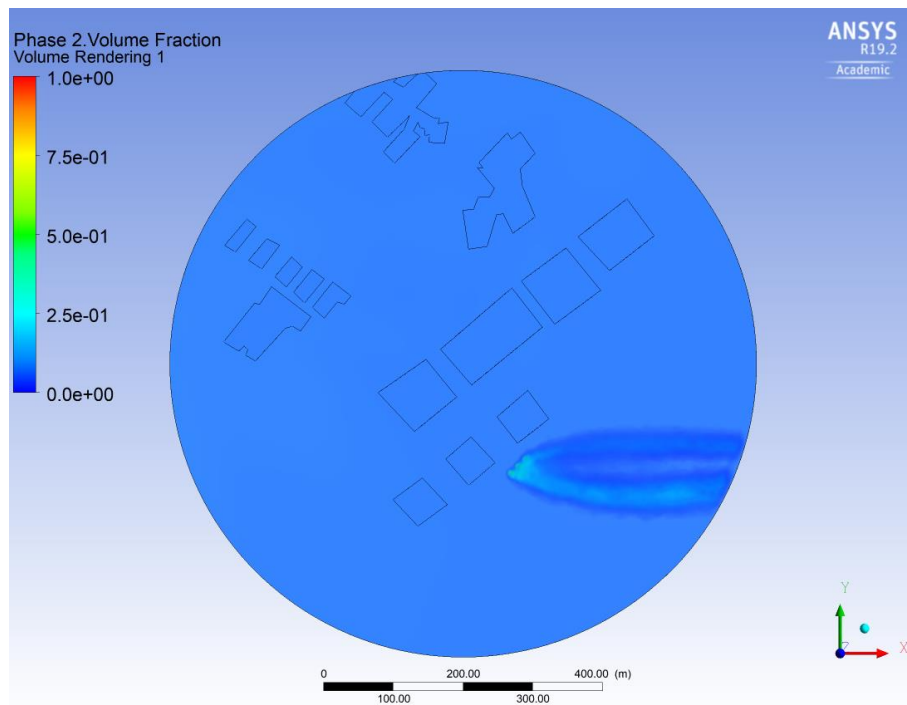


Figure 54 Case 11,1 picture 2

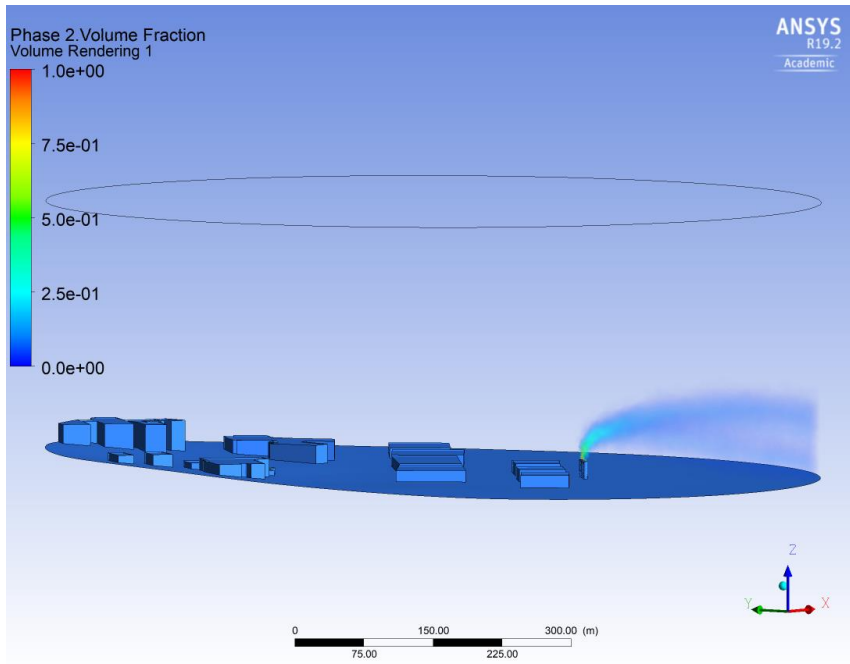


Figure 55 Case 12,0 picture 1

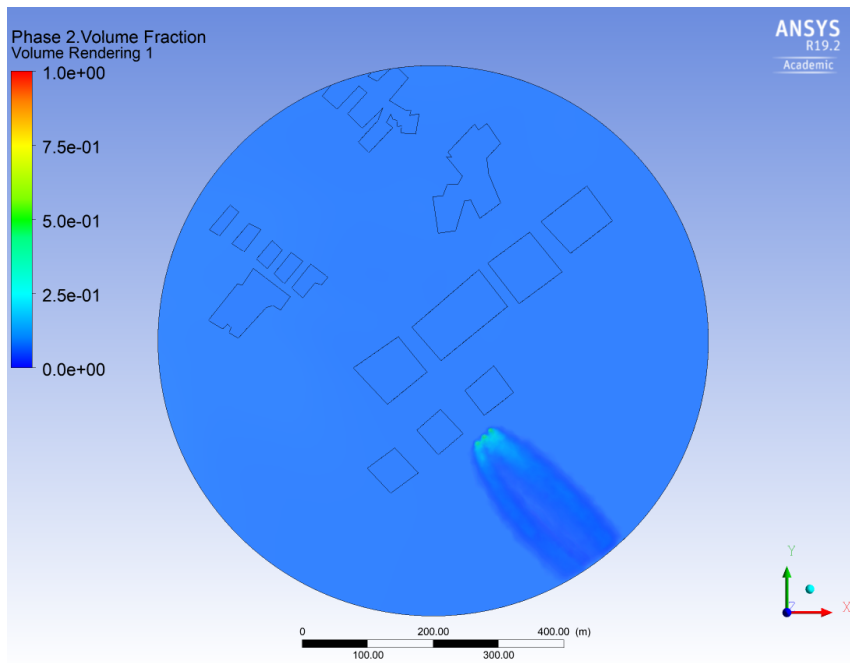


Figure 56 Case 12,0 picture 2

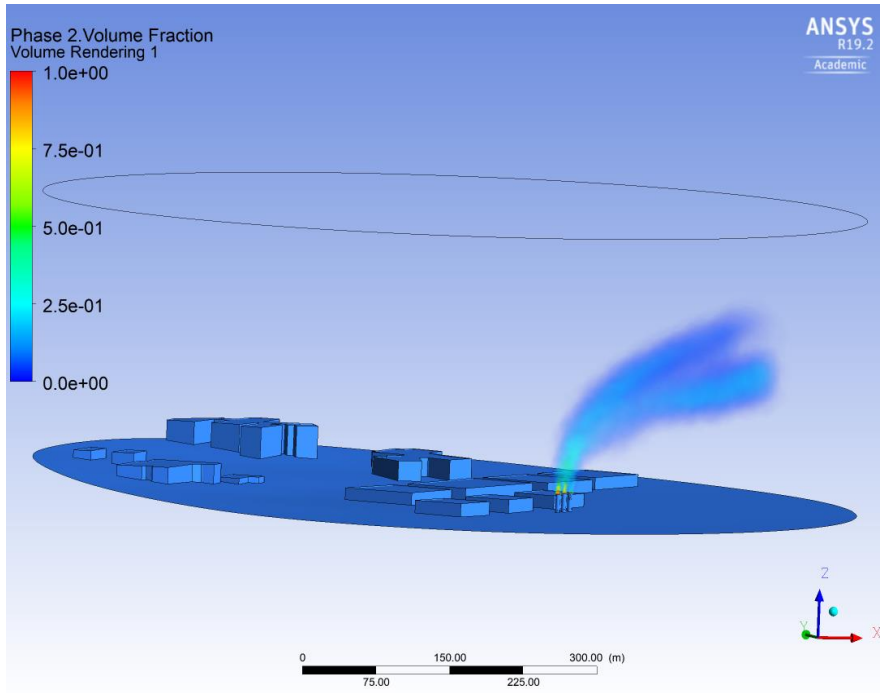


Figure 57 Case 12,1 picture 1

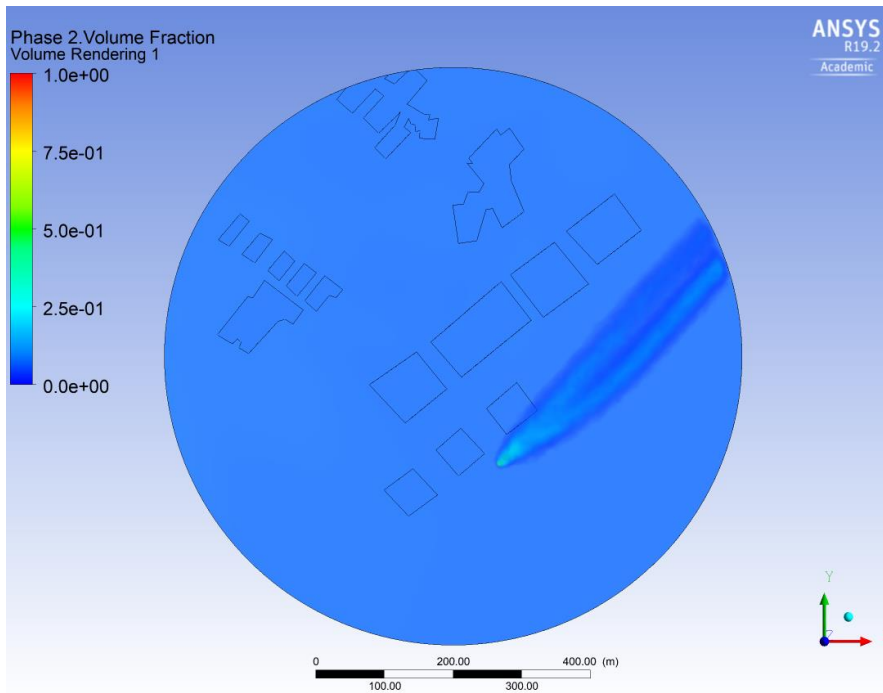


Figure 58 Case 12,1 picture 2

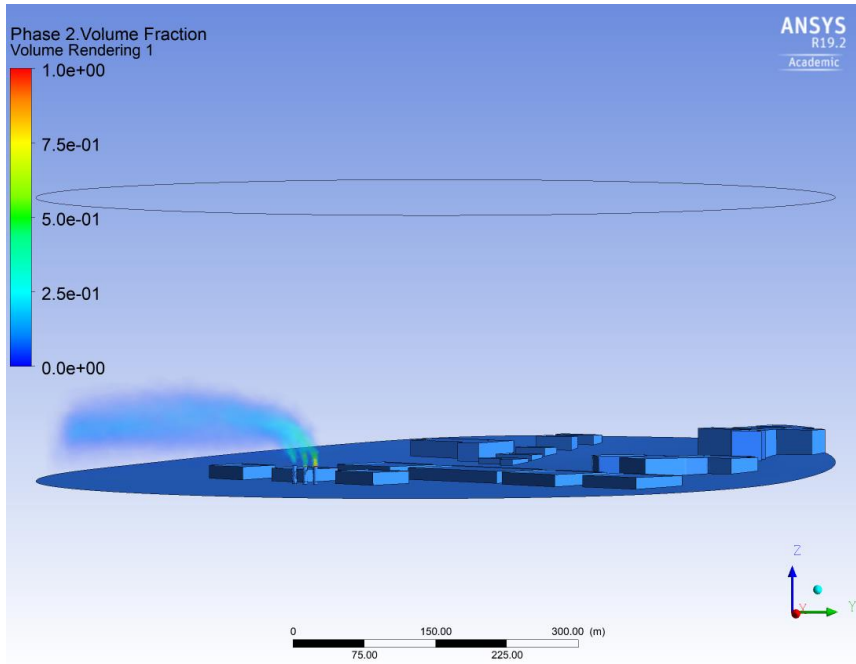


Figure 59 Case 13,0 picture 1

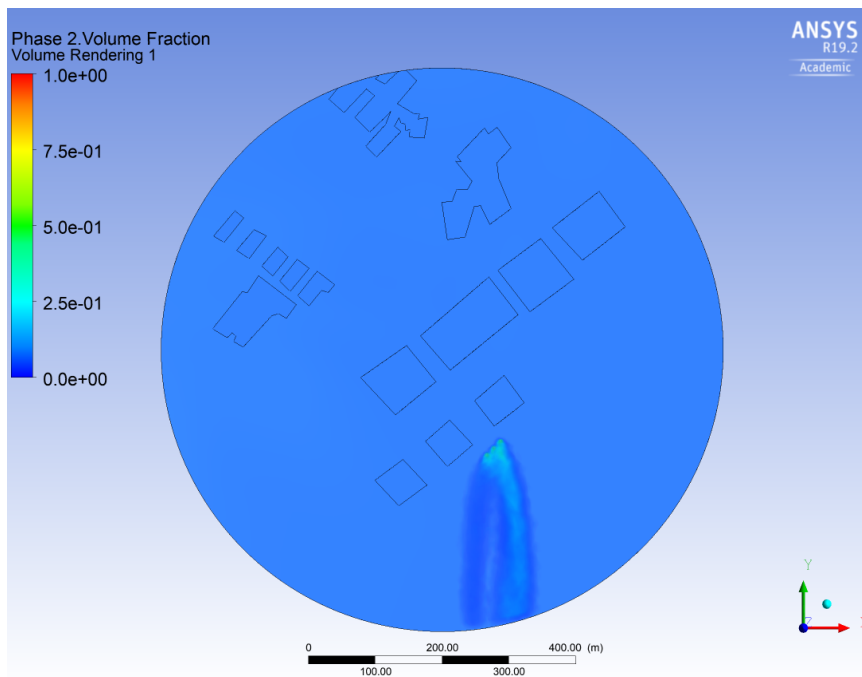


Figure 60 Case 13,0 picture 2

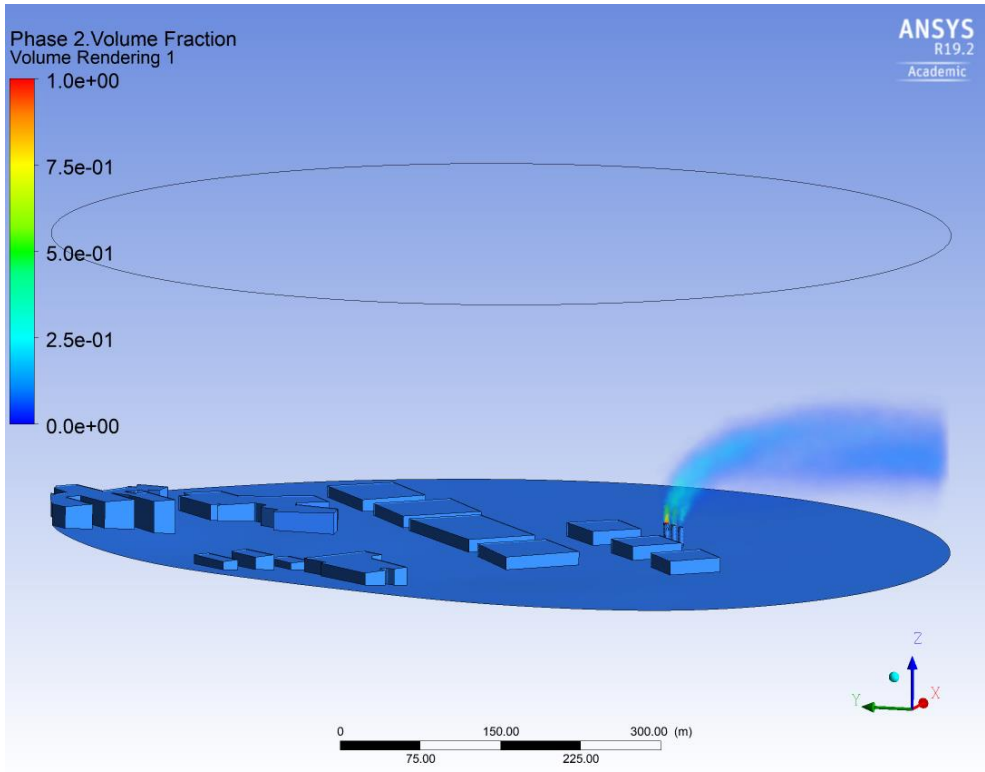


Figure 61 Case 13,1 picture 1

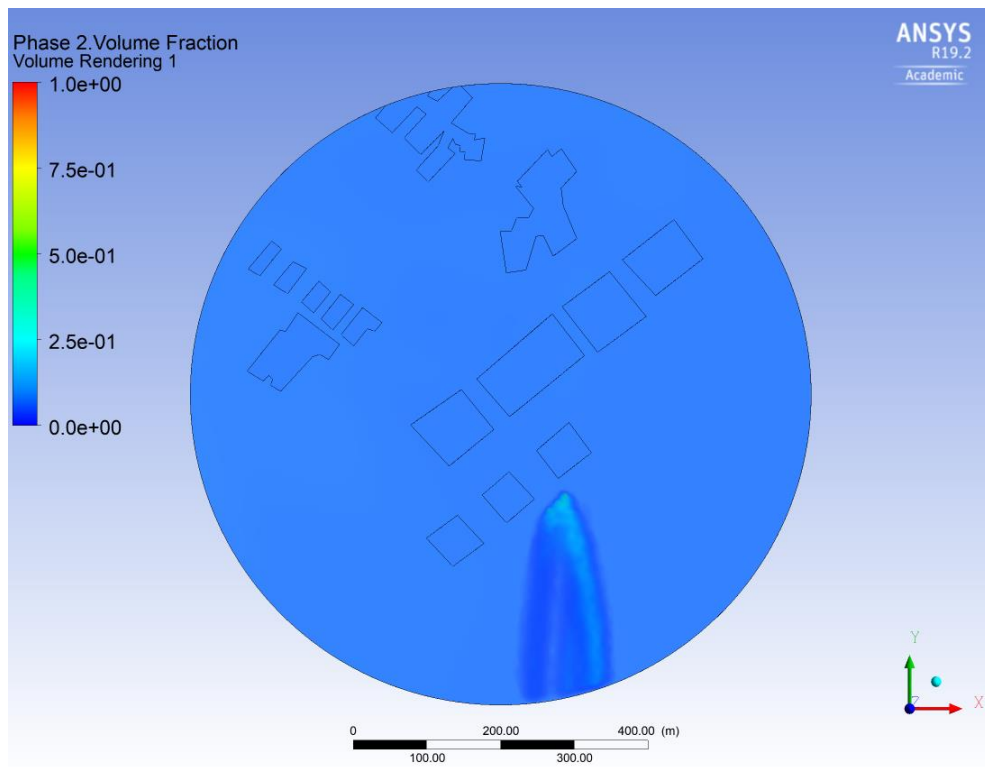


Figure 62 Case 13,1 picture 2

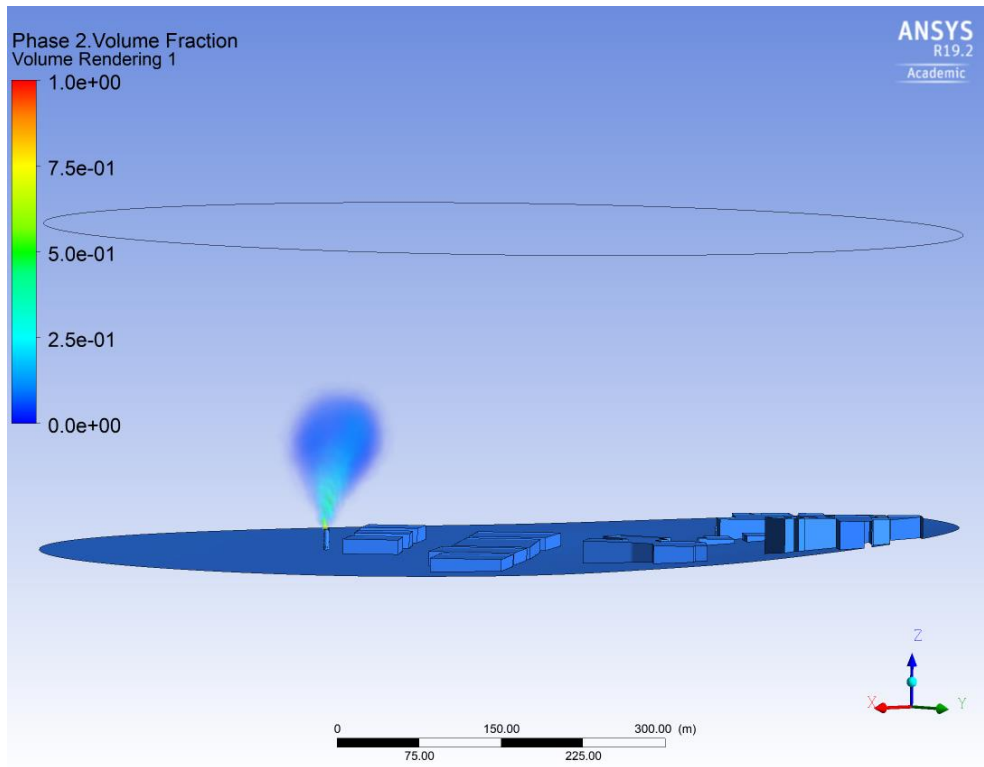


Figure 63 Case 14,0 picture 1

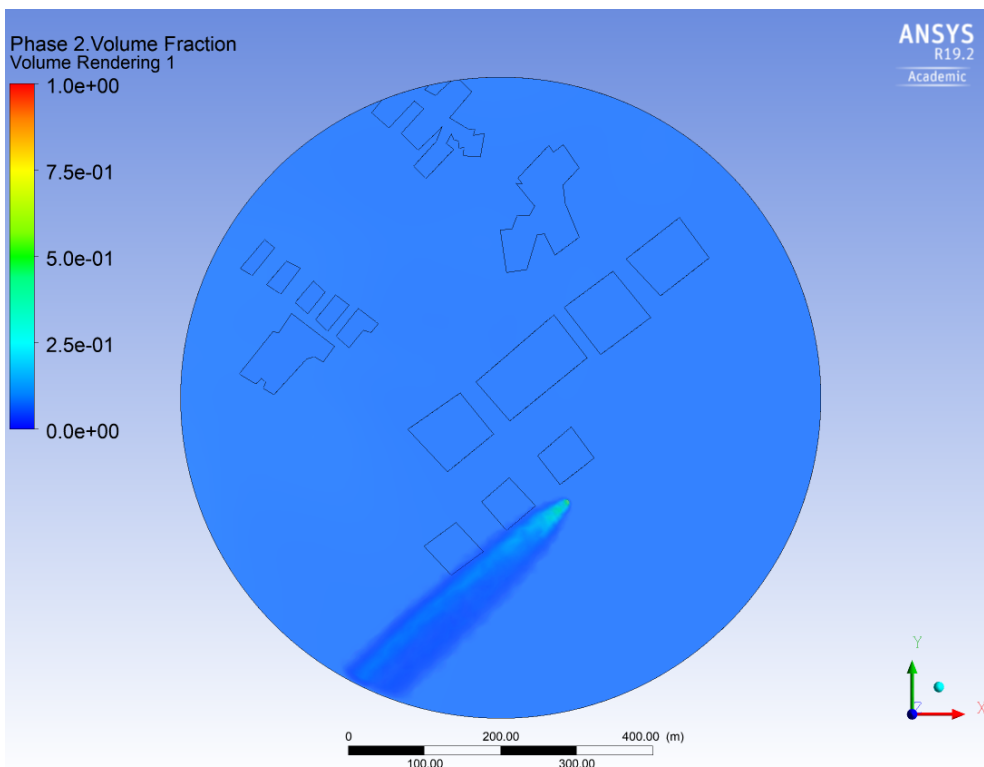


Figure 64 Case 14,0 picture 2

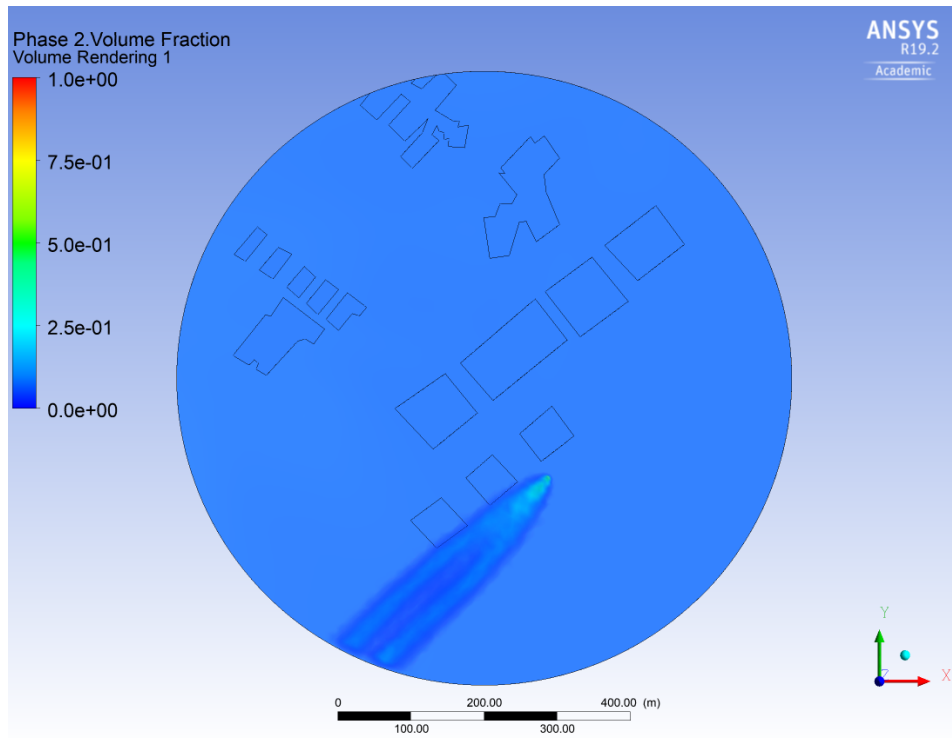


Figure 65 Case 14,1 picture 1

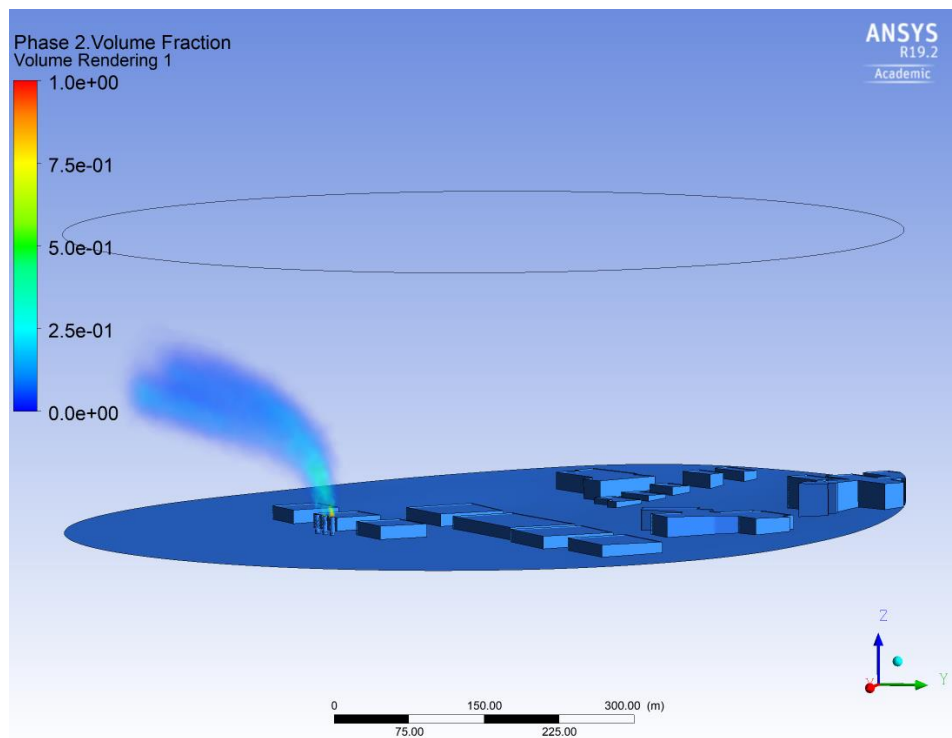


Figure 66 Case 14,1 picture 2

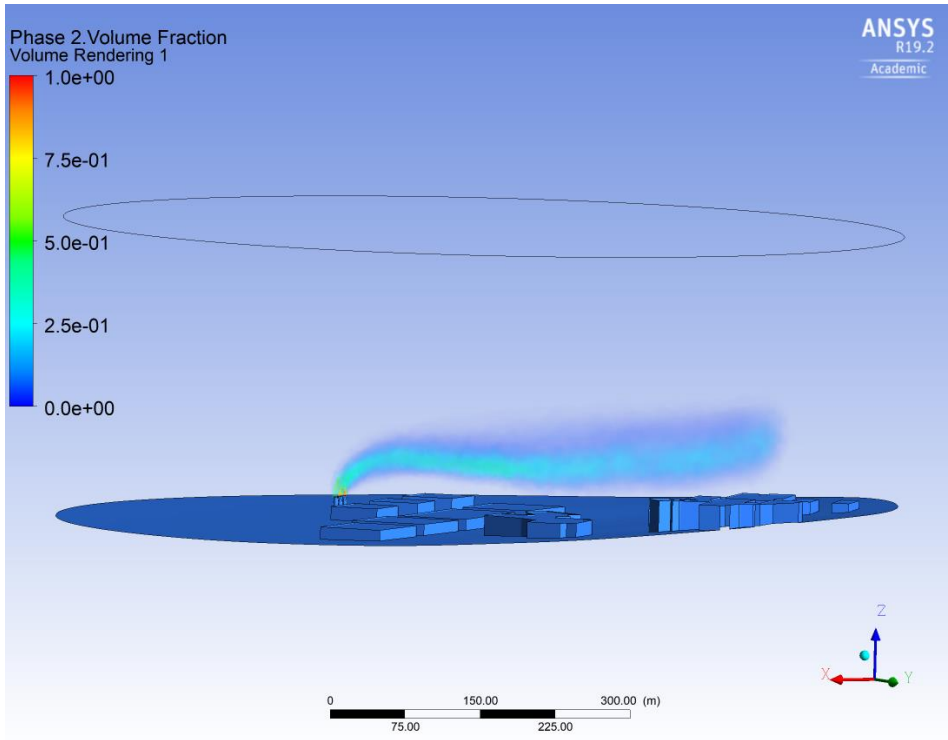


Figure 67 Case 15,0 picture 1

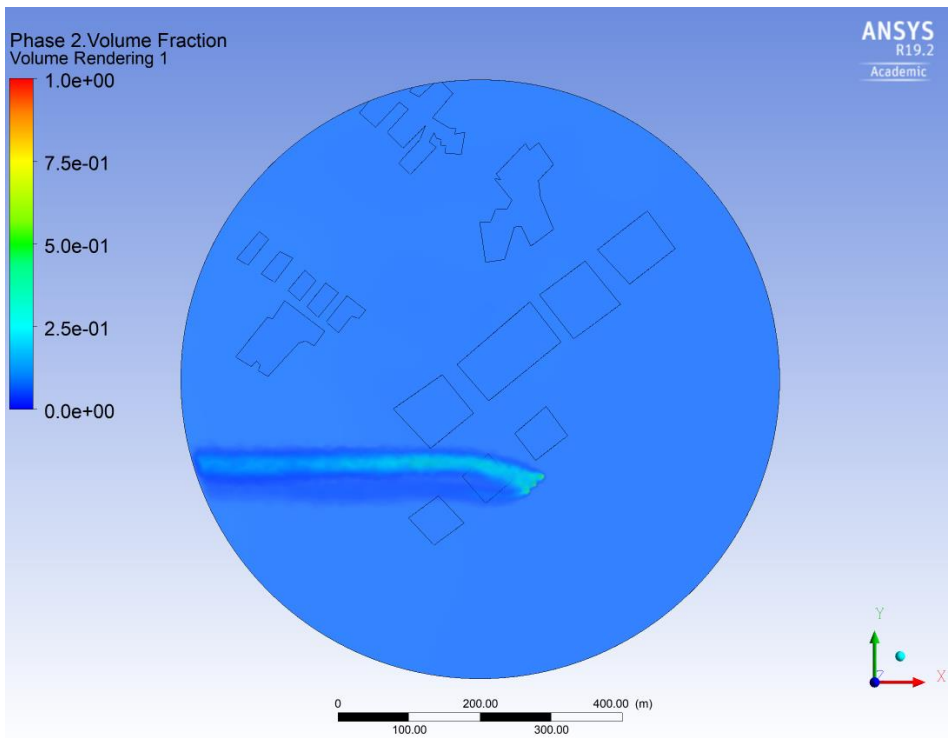


Figure 68 Case 15,0 picture 2

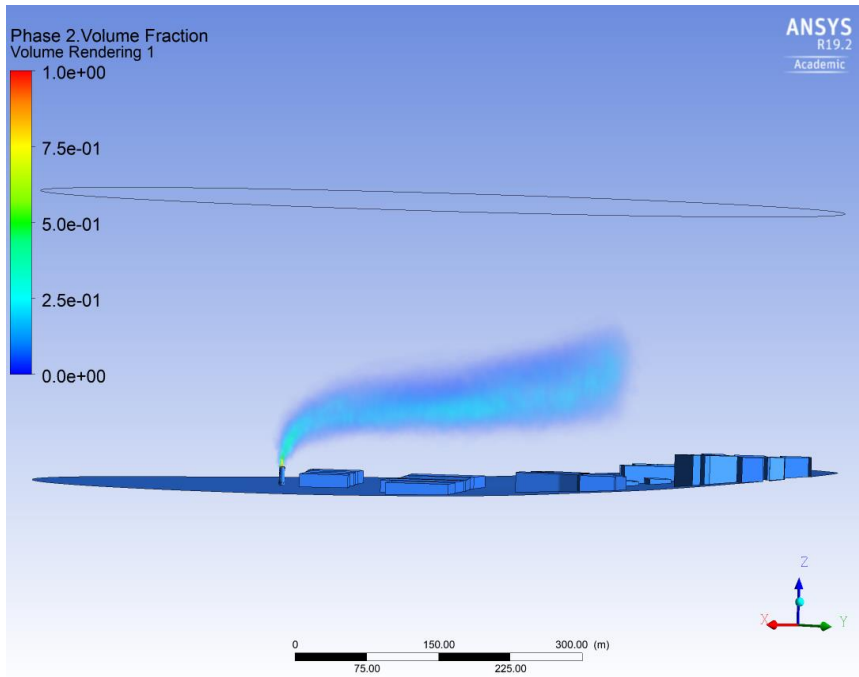


Figure 69 Case 15,1 picture 1

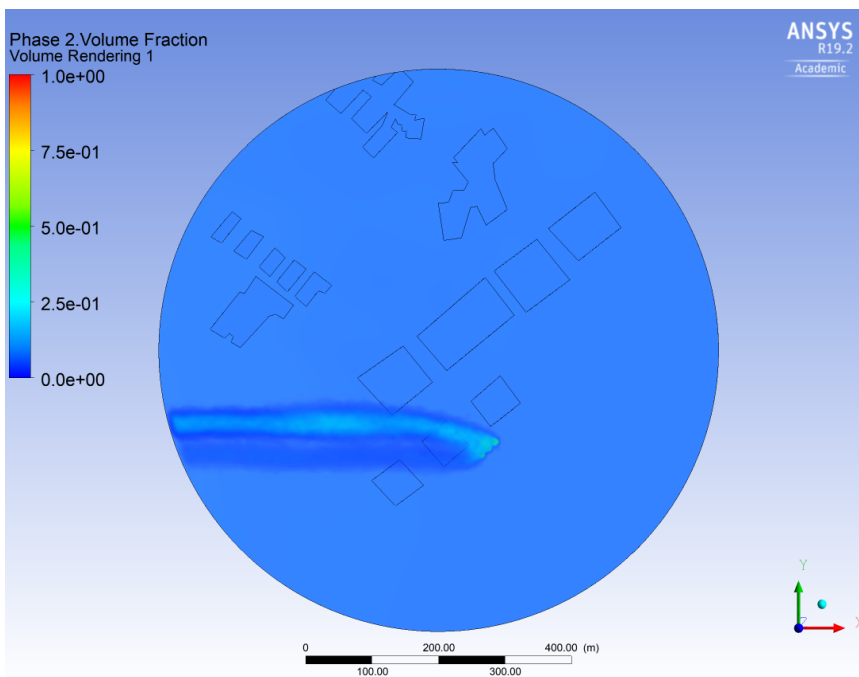


Figure 70 Case 15,1 picture 2

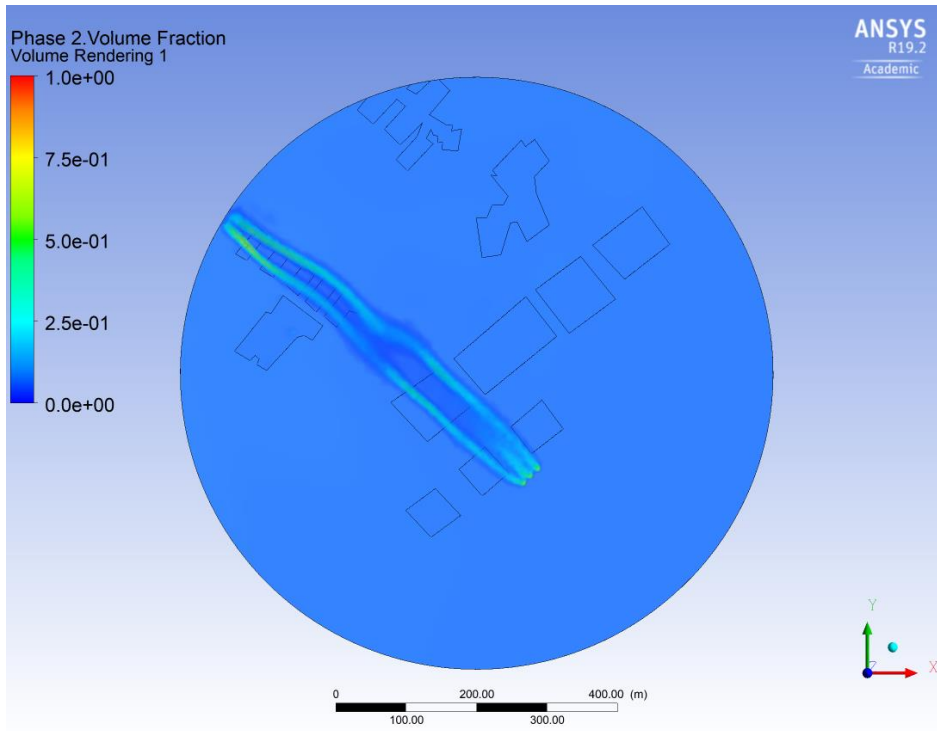


Figure 71 Case 16,0 figure 1

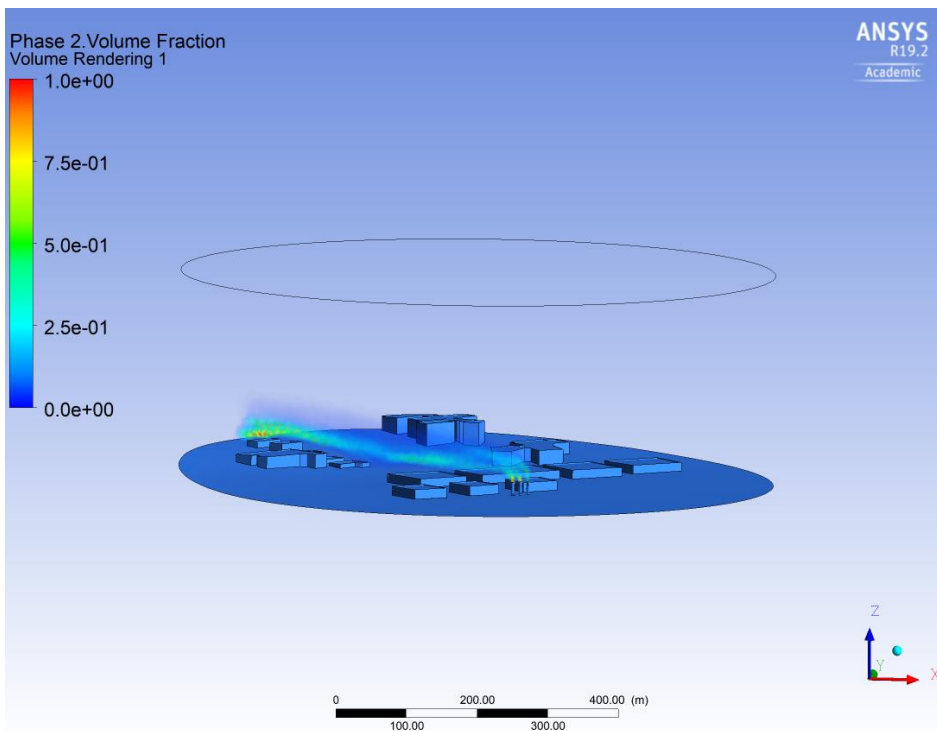


Figure 72 Case 16,0 figure 2

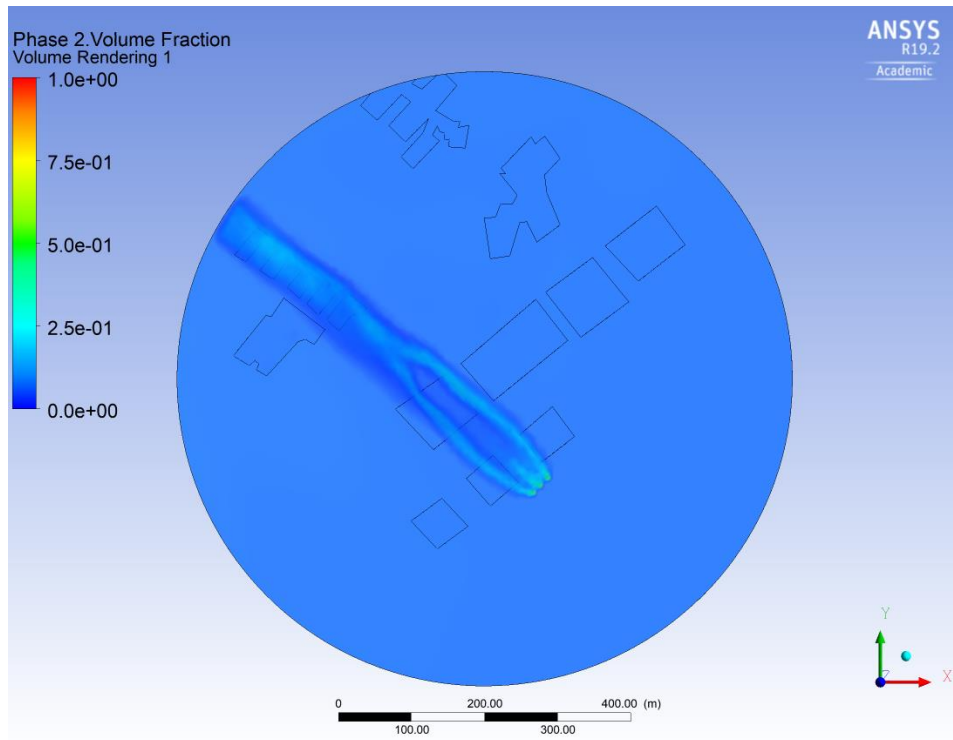


Figure 73 Case 16,1 picture 1

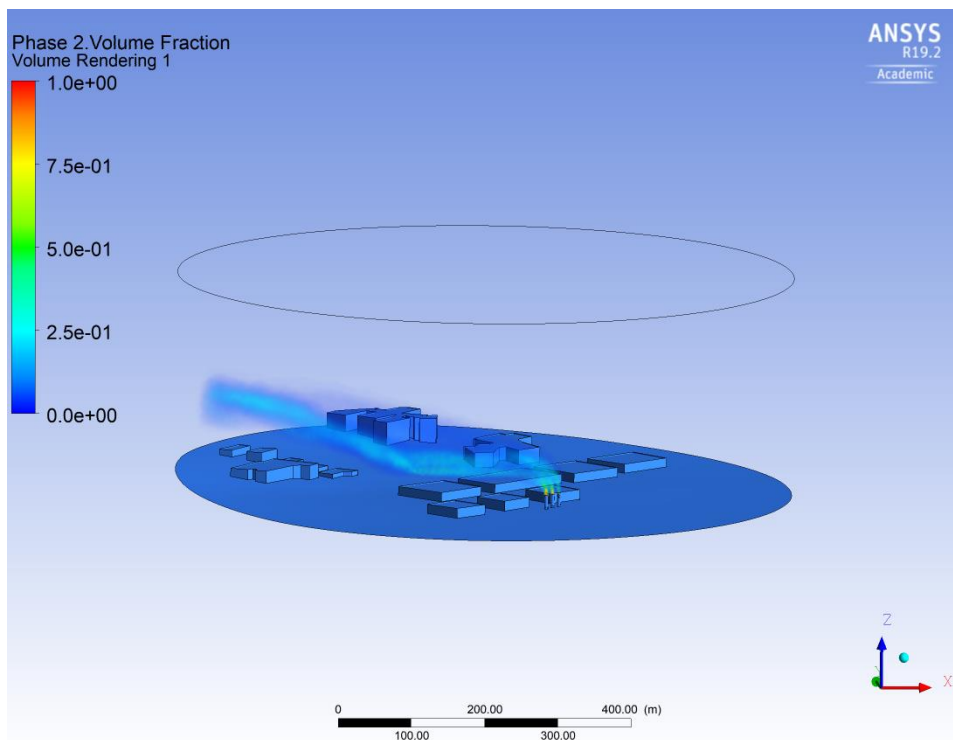


Figure 74 Case 16,1 picture 2

10 meters

Case	Vx	Vy	Calculated value	Date of simulation	File name	Status
17,0	0,0	15		25.04.2019	FFF_case_17_0_1	ok
17,1	0,0	3,3		25.04.2019	FFF_case_17_1_0	ok
18,0	15sin45 m/s	15sin45 m/s	12,7	26.04.2019	FFF_case_18_0_1	ok
18,1	3,3sin45 m/s	3,3sin45 m/s	2,8	26.04.2019	FFF_case_18_1_0	ok
19,0	5 m/s	0		01.05.2019	FFF_case_19_0_1	ok
19,1	3,3 m/s	0		01.05.2019	FFF_case_19_1_0	ok
20,0	5sin45 m/s	$\sqrt{5}$ sin45 m/s	$\sqrt{4.25}$	30.04.2019	FFF_case_21_0_1	ok
20,1	3,3sin45 m/s	$\sqrt{3.3}$ sin45 m/s	$\sqrt{2.8}$	30.04.2019	FFF_case_20_1_0	ok
21,0	0,0	$\sqrt{5}$ m/s		29.04.2019	FFF_case_21_0_1	ok
21,1	0,0	$\sqrt{3.3}$ m/s		29.04.2019	FFF_case_21_1_0	ok
22,0	$\sqrt{5}$ sin45 m/s	$\sqrt{5}$ sin45 m/s	$\sqrt{4.25}$	29.04.2019	FFF_case_22_0_1	ok
22,1	$\sqrt{3.3}$ sin45 m/s	$\sqrt{3.3}$ sin45 m/s	$\sqrt{2.8}$	28.04.2019	FFF_case_22_1_0	ok
23,0	$\sqrt{5}$ m/s	0		28.04.2019	FFF_case_23_0_1	ok
23,1	$\sqrt{3.3}$ m/s	0		27.04.2019	FFF_case_23_1_0	ok
24,0	$\sqrt{5}$ m/s	5sin45 m/s	$\sqrt{4.25}$	27.04.2019	FFF_case_24_0_1	ok
24,1	$\sqrt{3.3}$ m/s	3,3sin45 m/s	$\sqrt{2.8}$	26.04.2019	FFF_case_24_1_0	ok

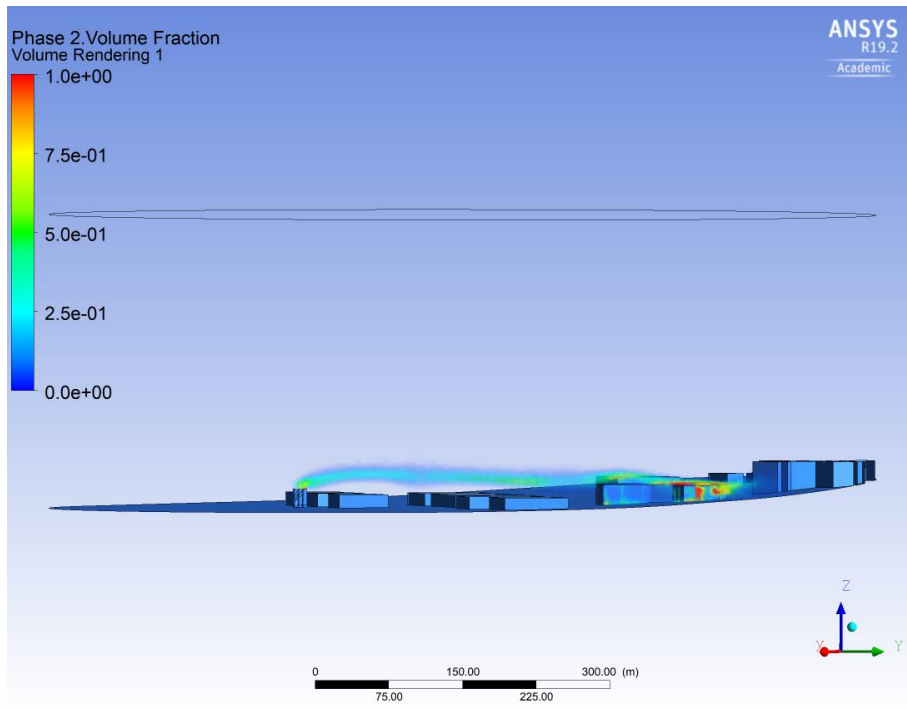


Figure 75 Case 10,7 picture 1

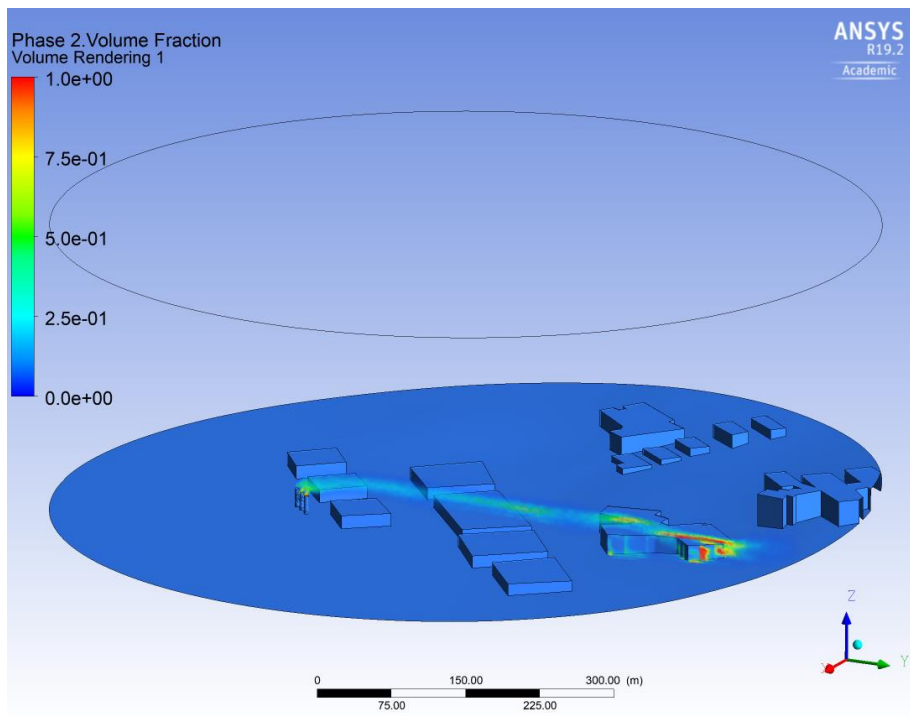


Figure 76 Case 17,0 picture 2

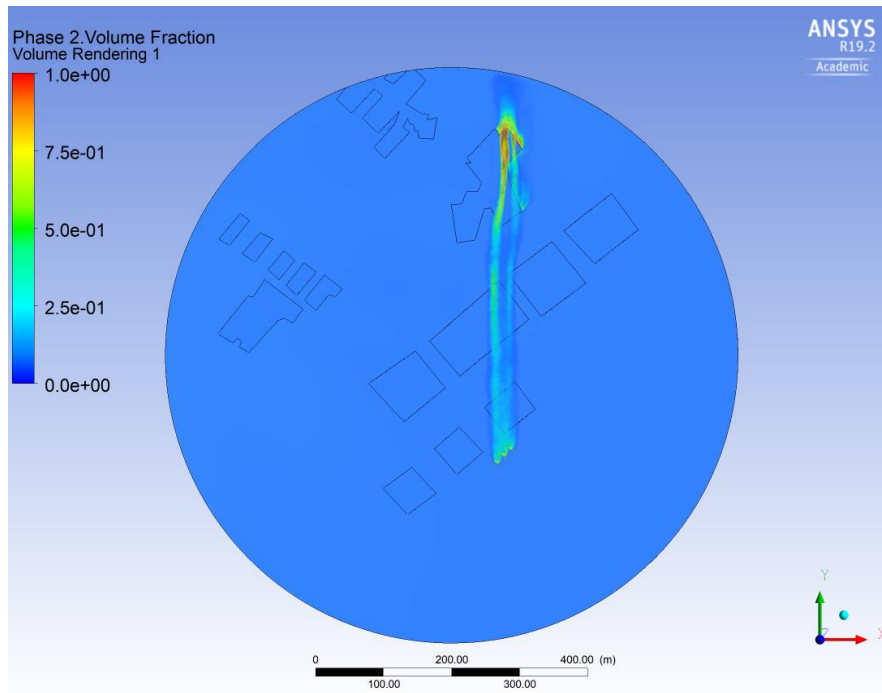


Figure 77 Case 17,0 picture 3

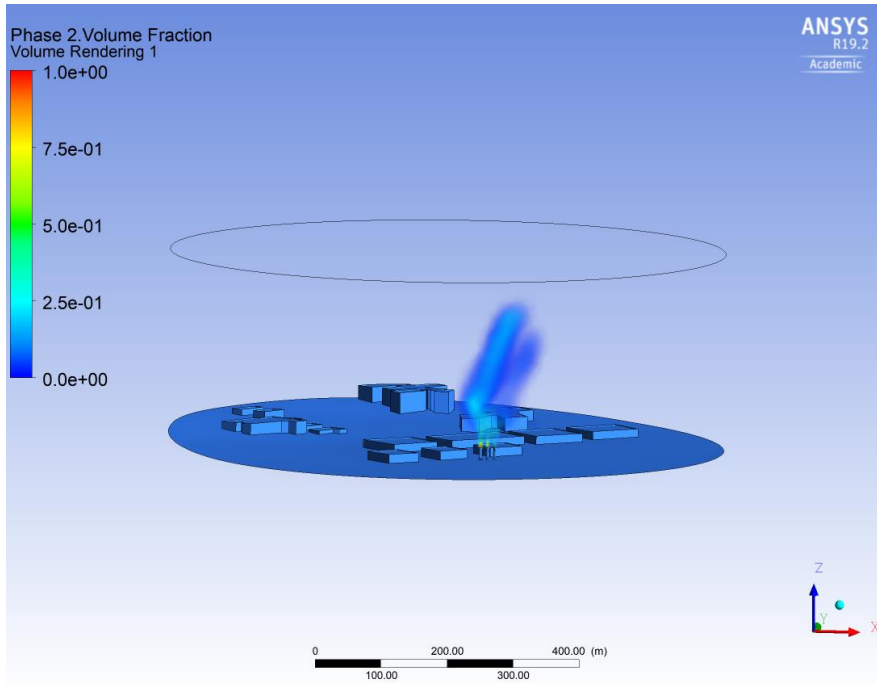


Figure 78 Case 17,1 picture 1

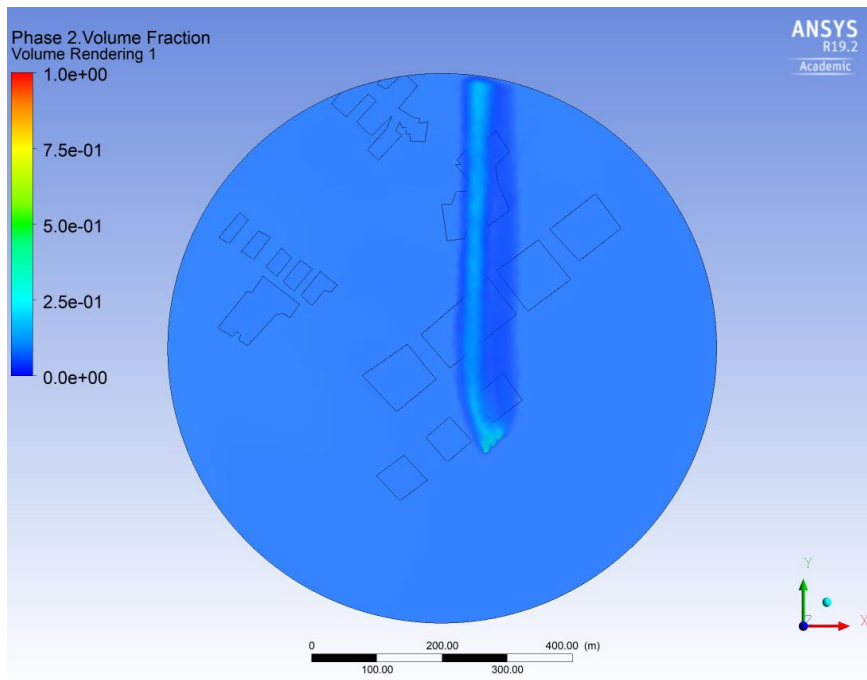


Figure 79 Case 17,1 picture 2

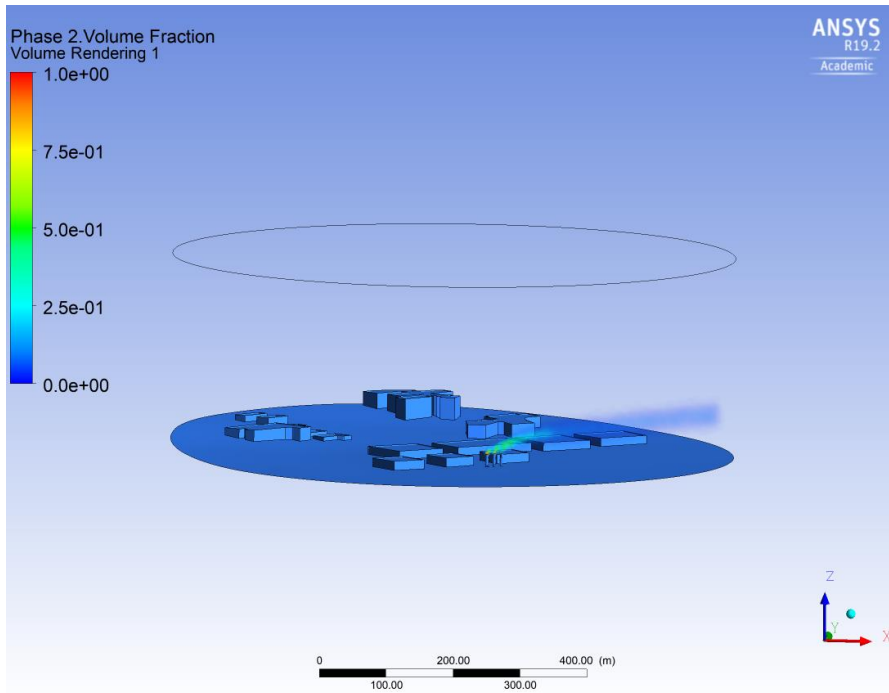


Figure 80 Case 1,0 picture 1

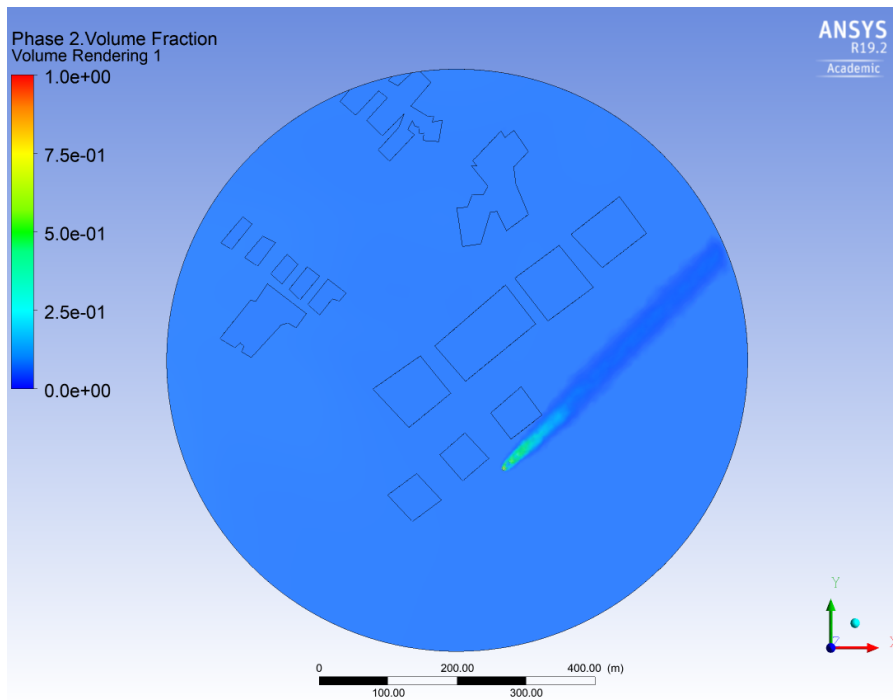


Figure 81 Case 18,0 picture 2

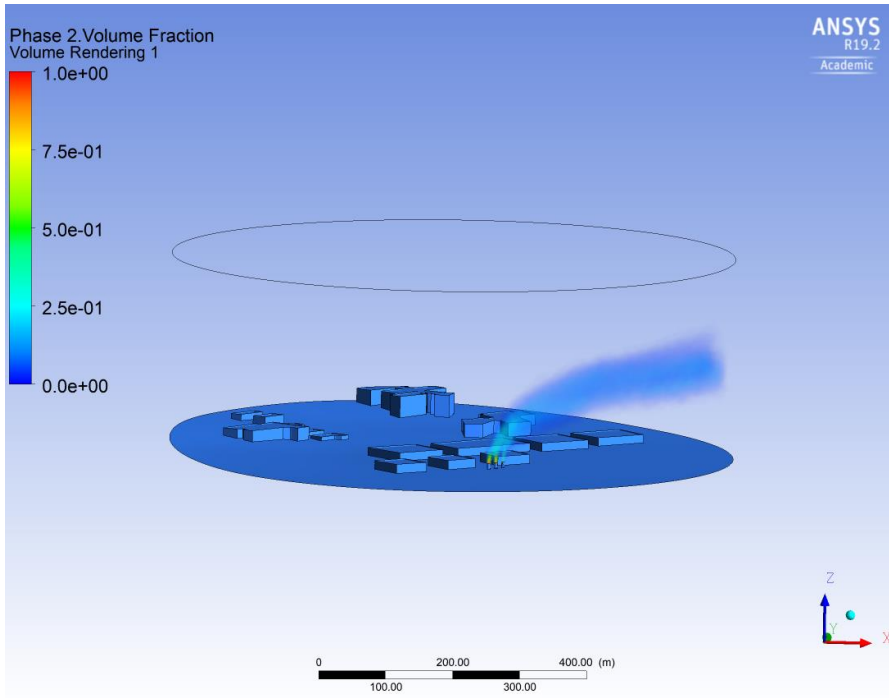


Figure 82 Case 18,1 picture 1

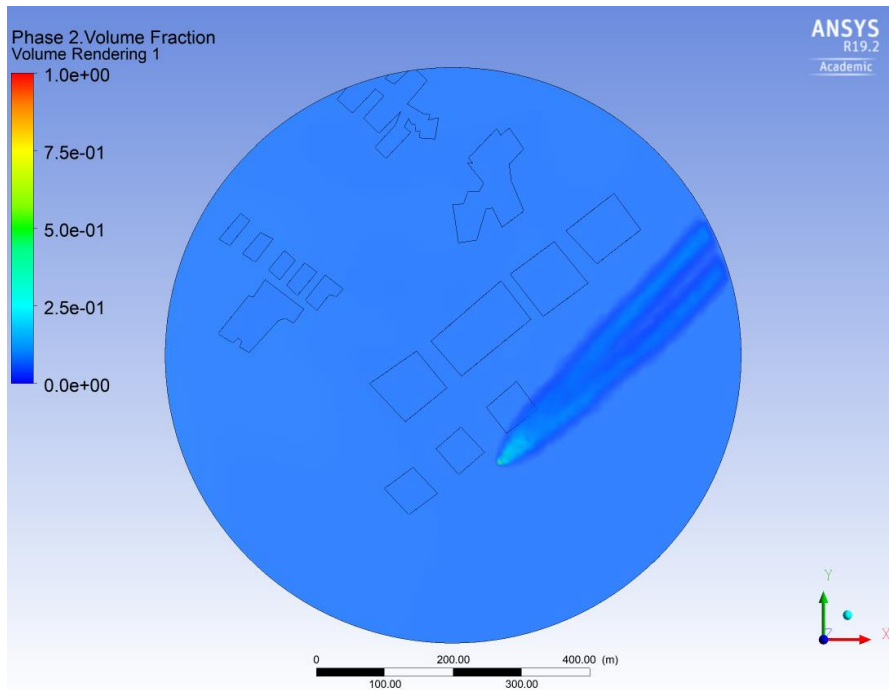


Figure 83 Case 18,1 picture 2

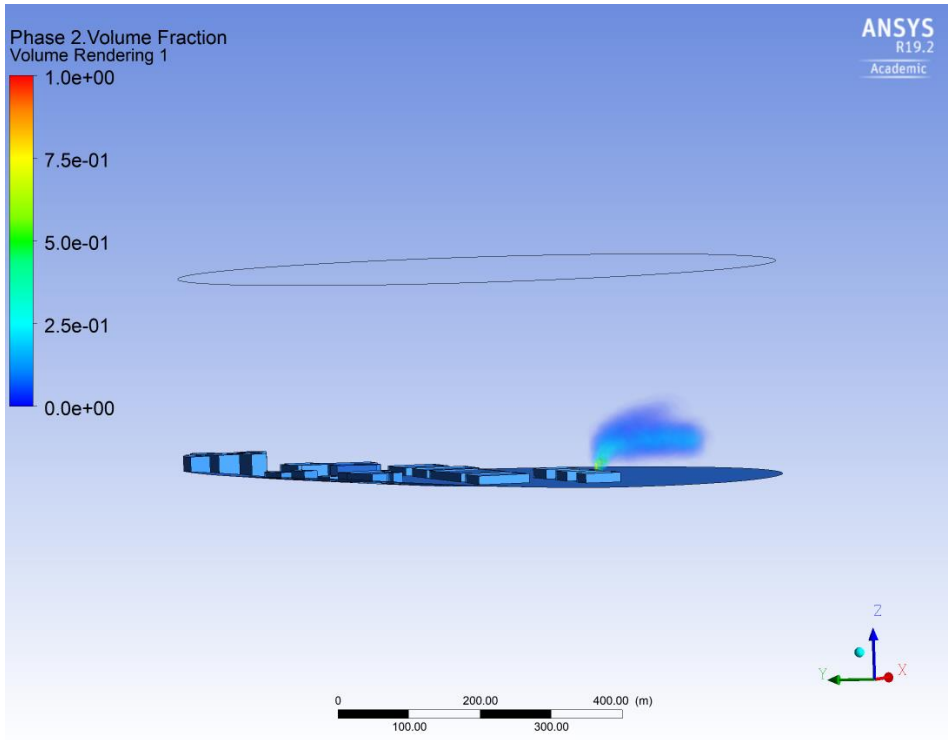


Figure 84 Case 19,0 figure 1

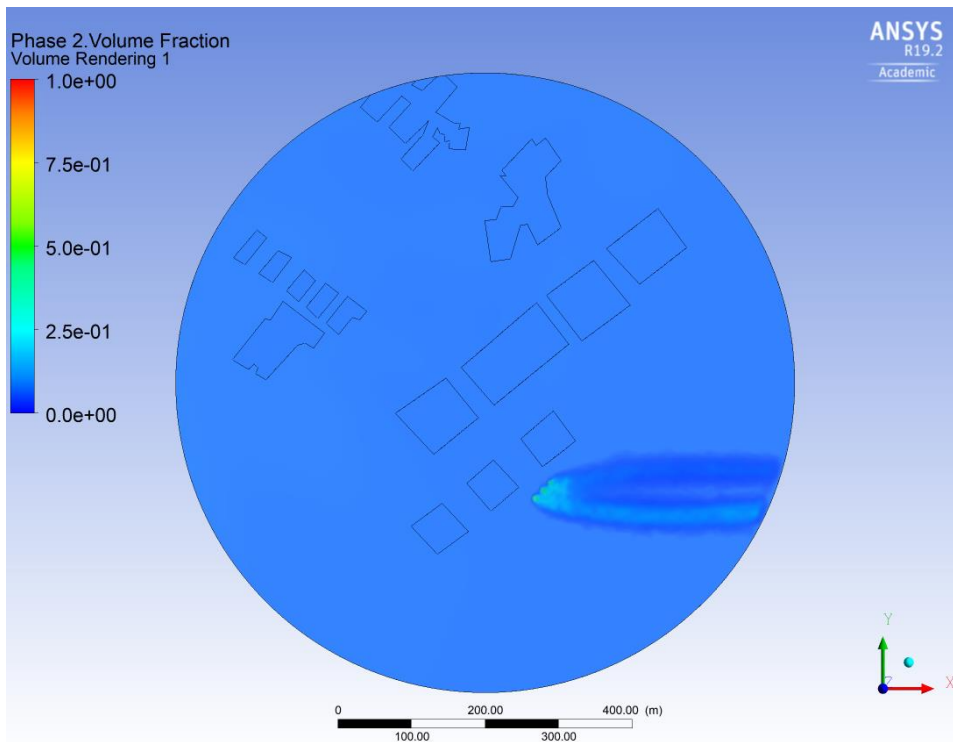


Figure 85 Case 19,0 figure 2

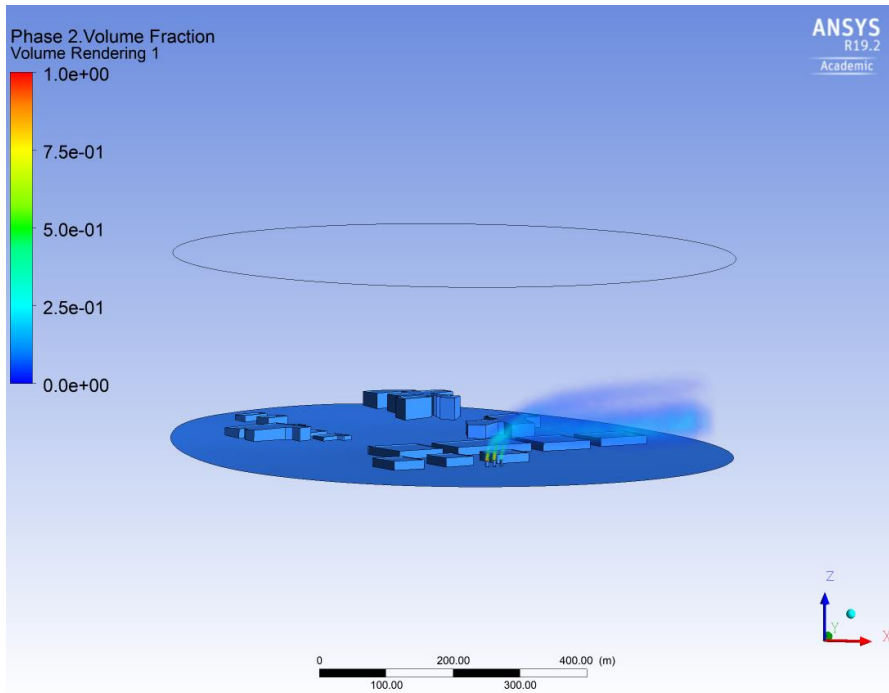


Figure 86 Case 19,1 figure 1

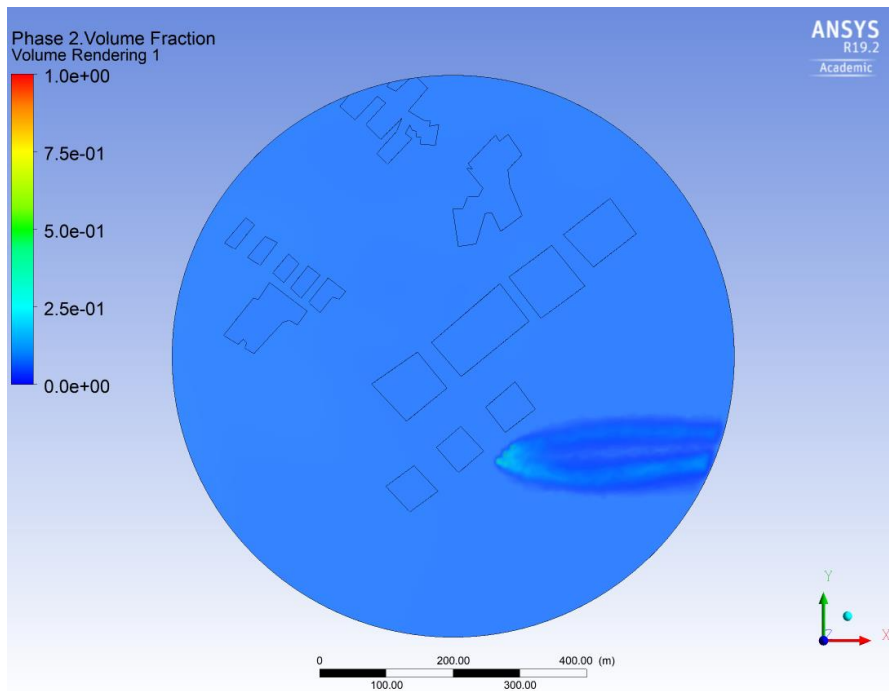


Figure 87 Case 19,1 figure 2

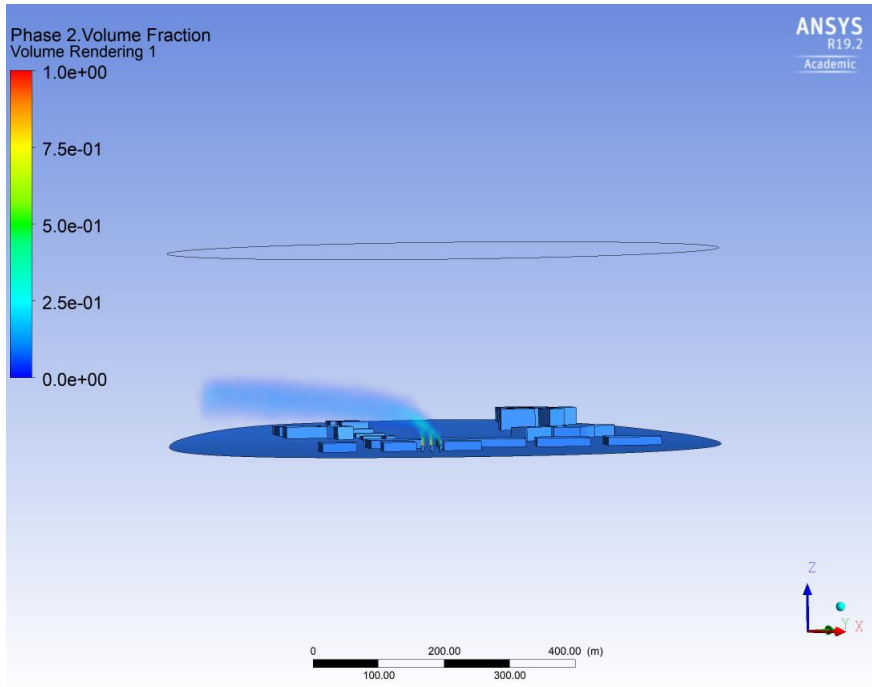


Figure 88 Case 20 picture 1

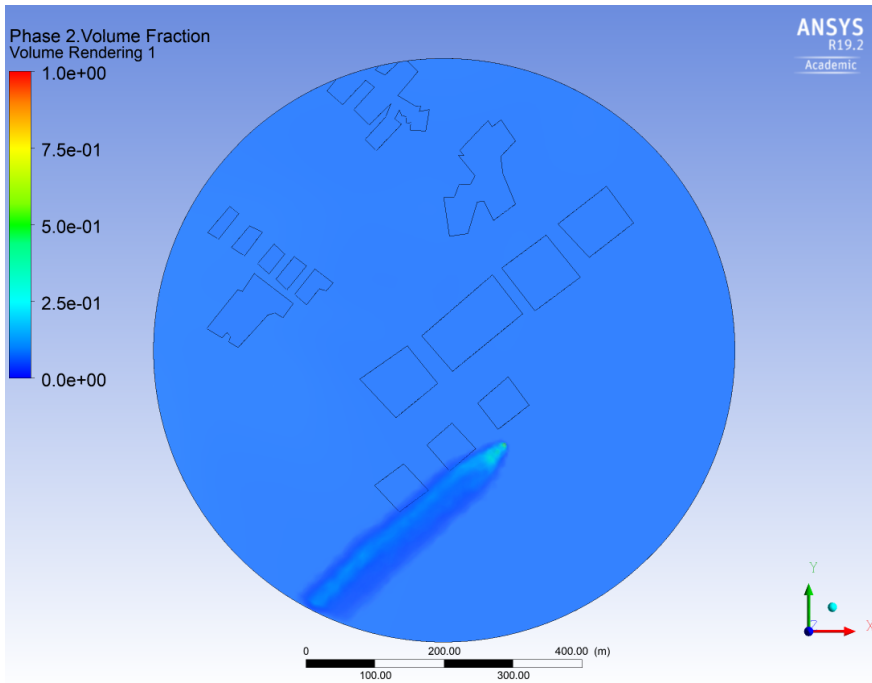


Figure 89 Case 20 picture 2

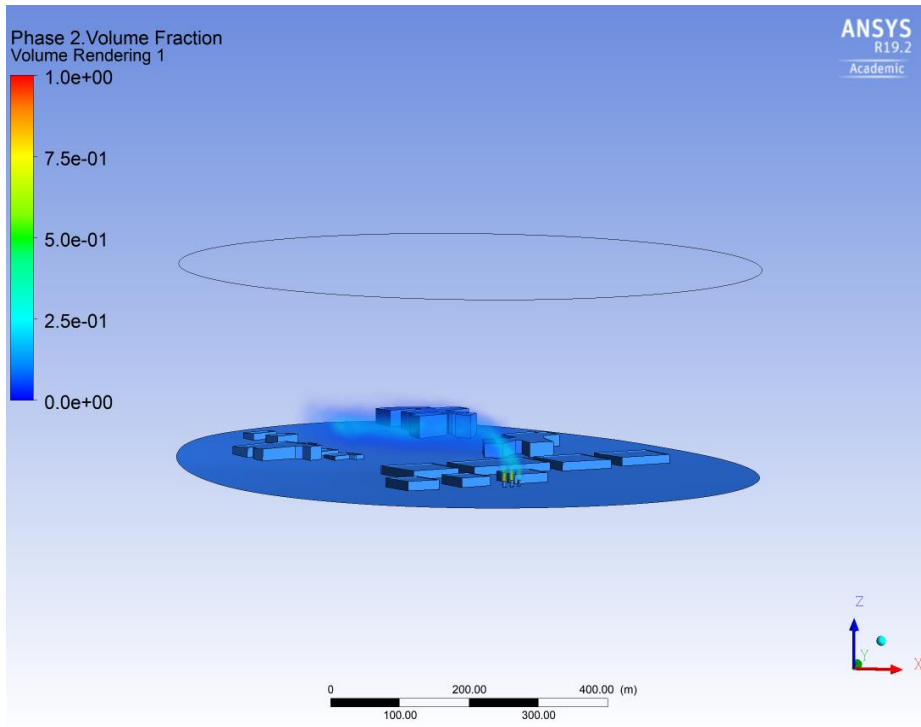


Figure 90 Case 20,1 picture 1

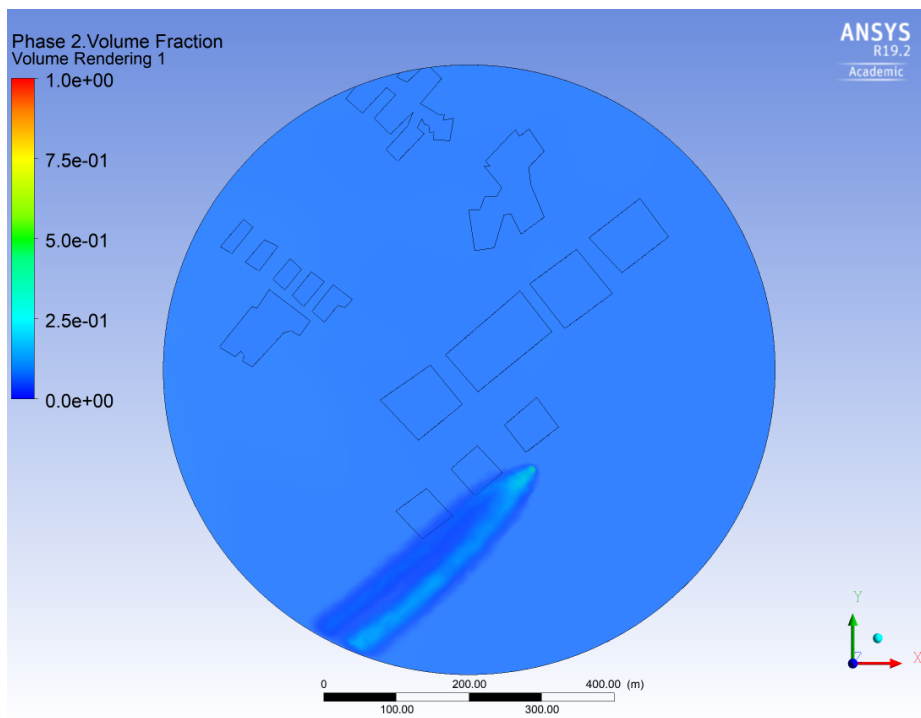


Figure 91 Case 20,1 picture 2

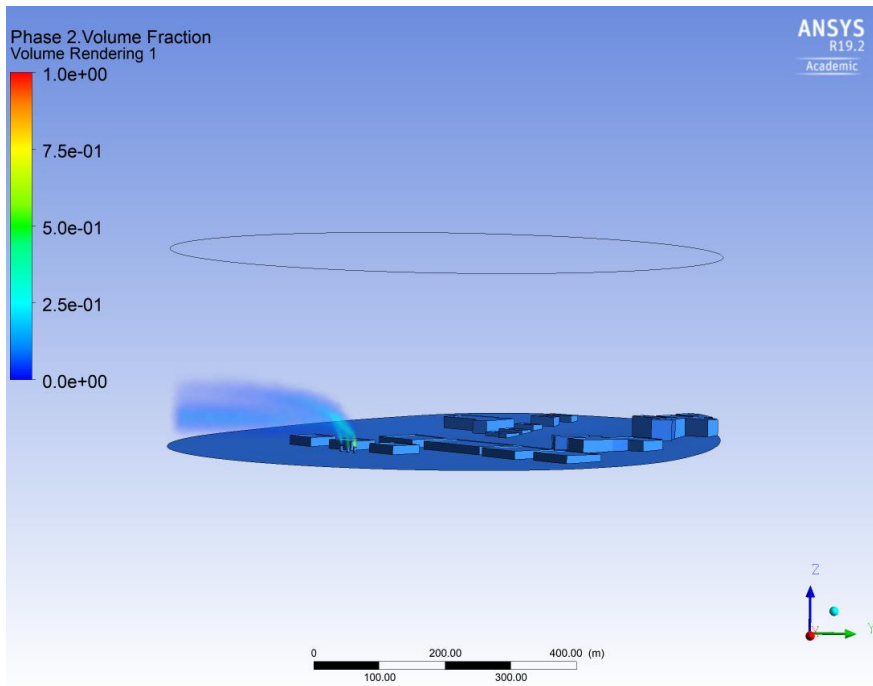


Figure 92 Case 21,0 picture 1

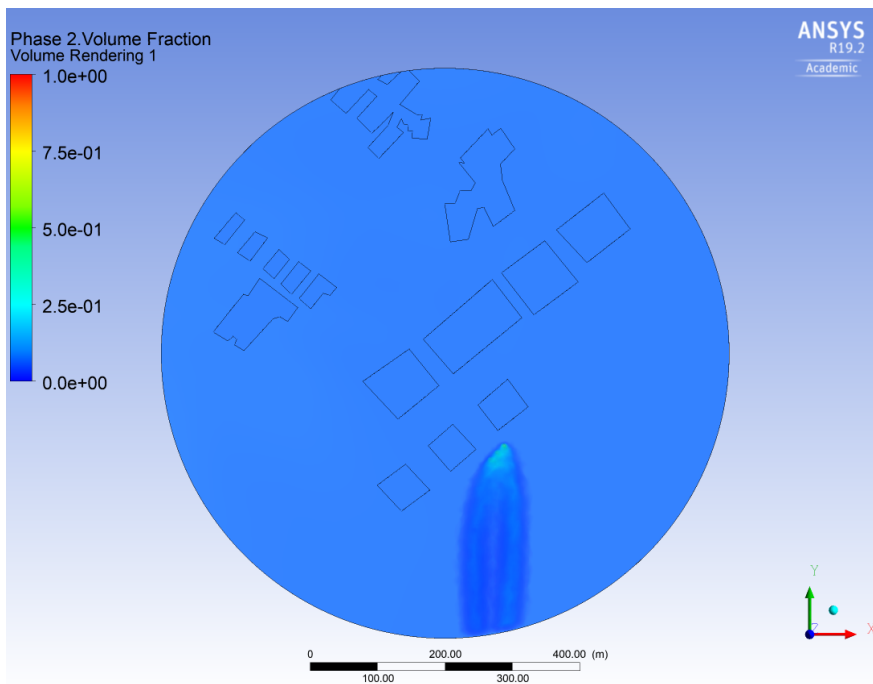


Figure 93 Case 21,0 picture 2

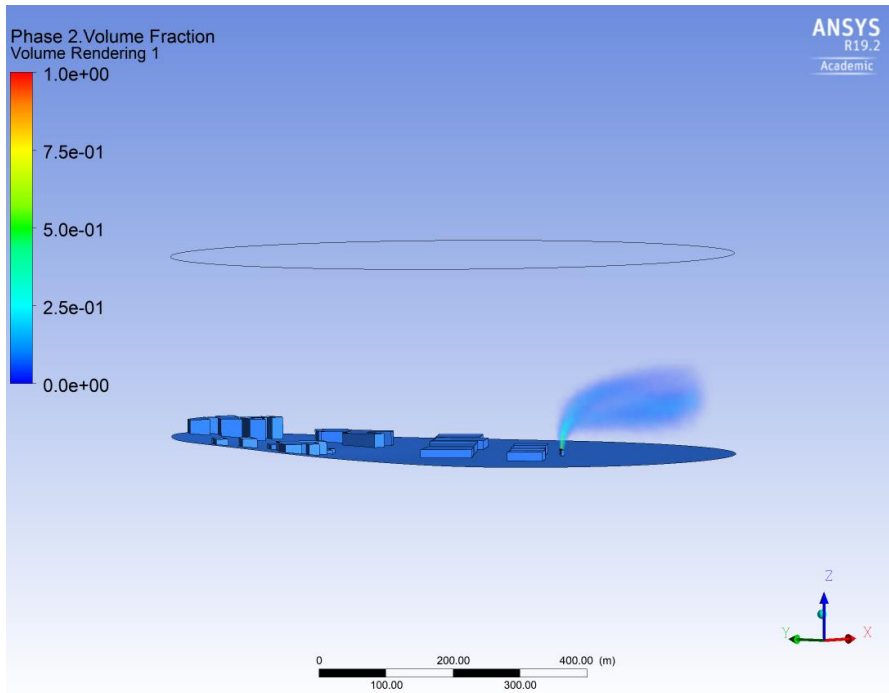


Figure 94 Case 21,1 picture 1

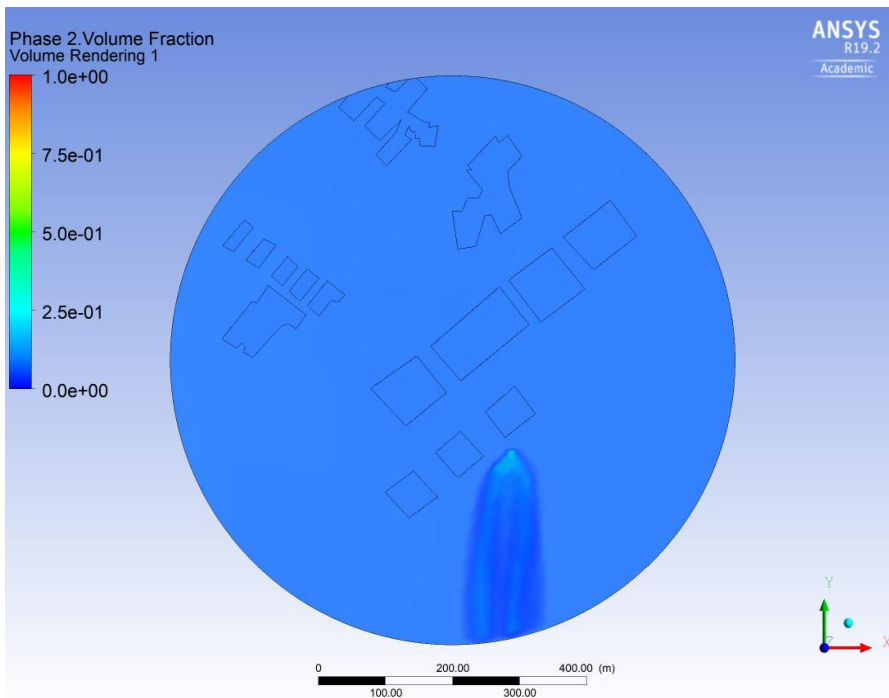


Figure 95 Case 21,1 picture 2

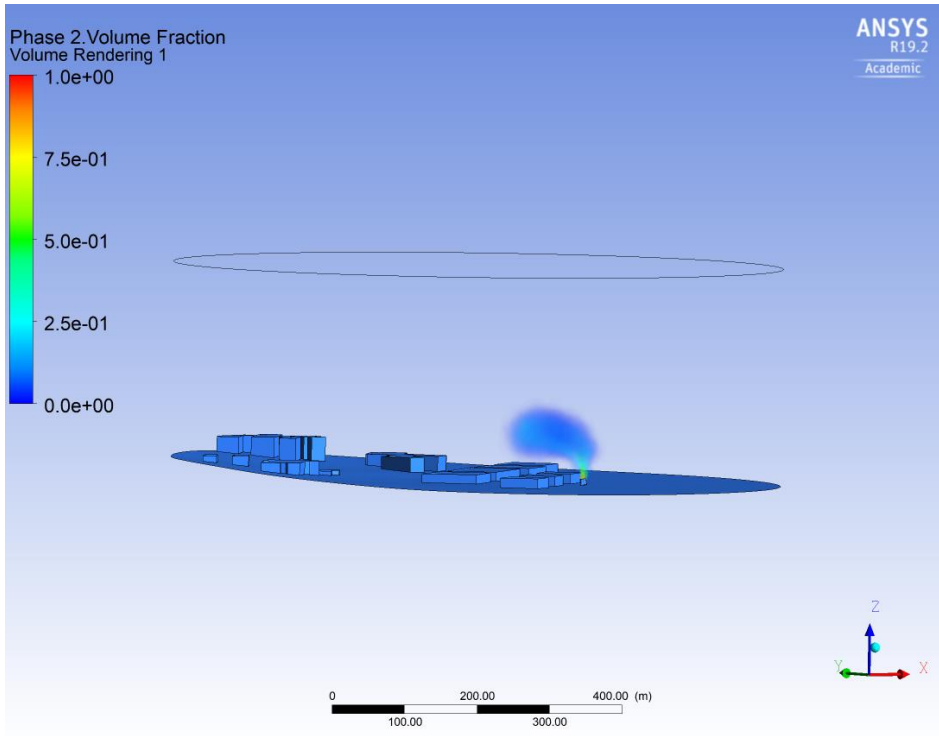


Figure 96 Case 22,0 picture 1

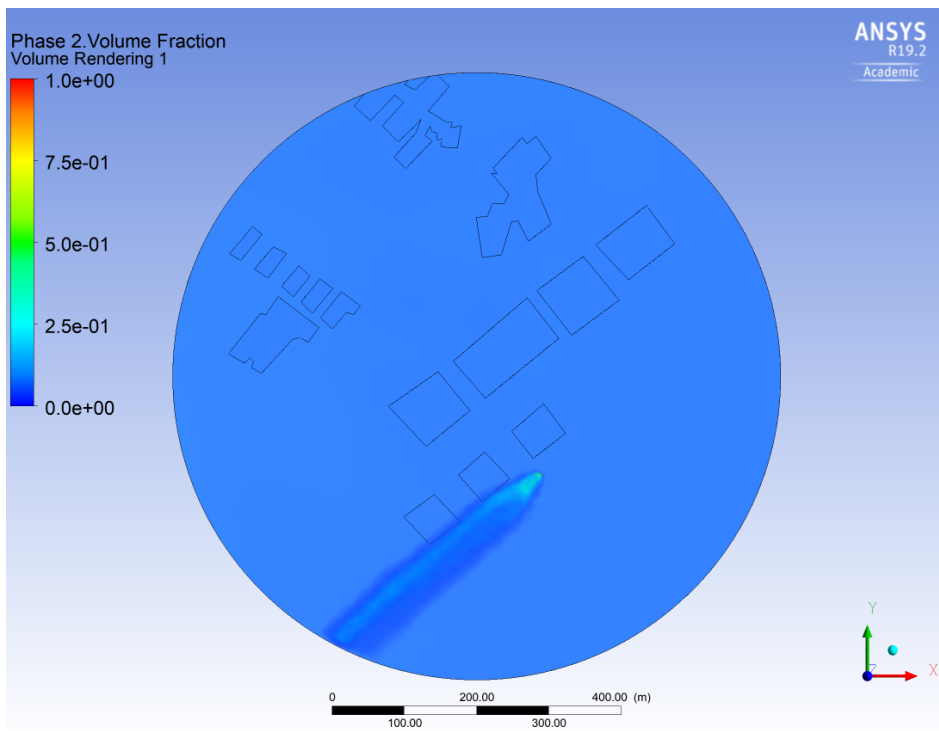


Figure 97 Case 22,0 picture 2

switch

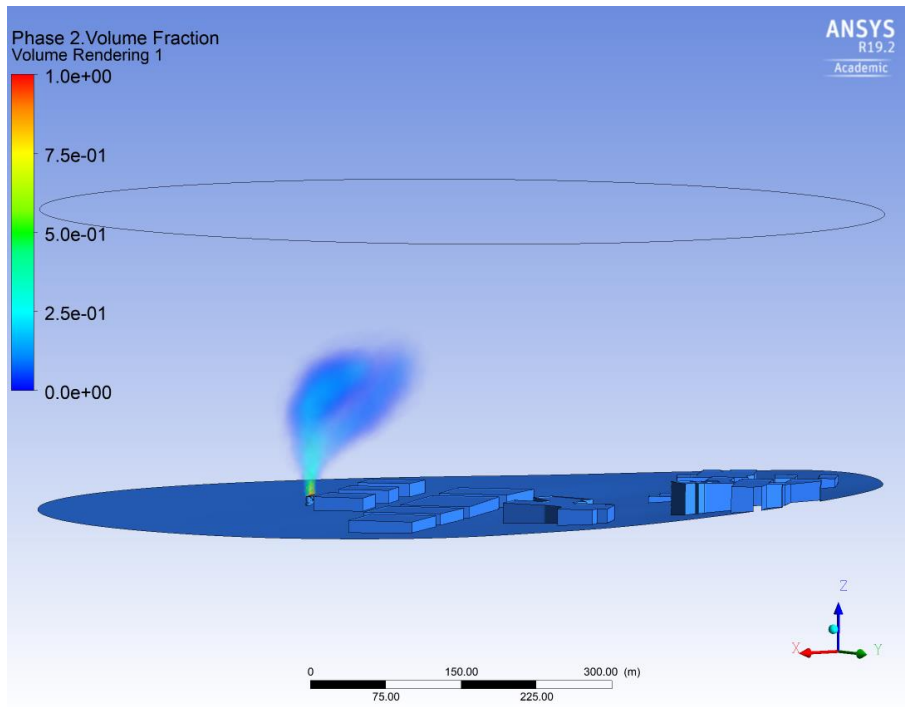


Figure 98 Case 22,1 picture 1

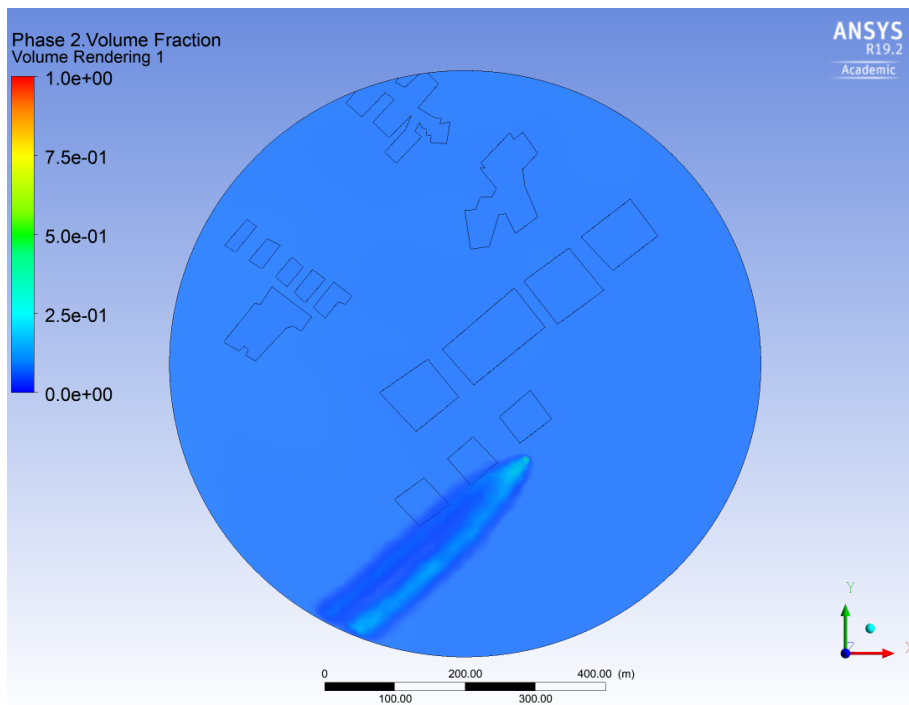


Figure 99 Case 22,1 picture 2

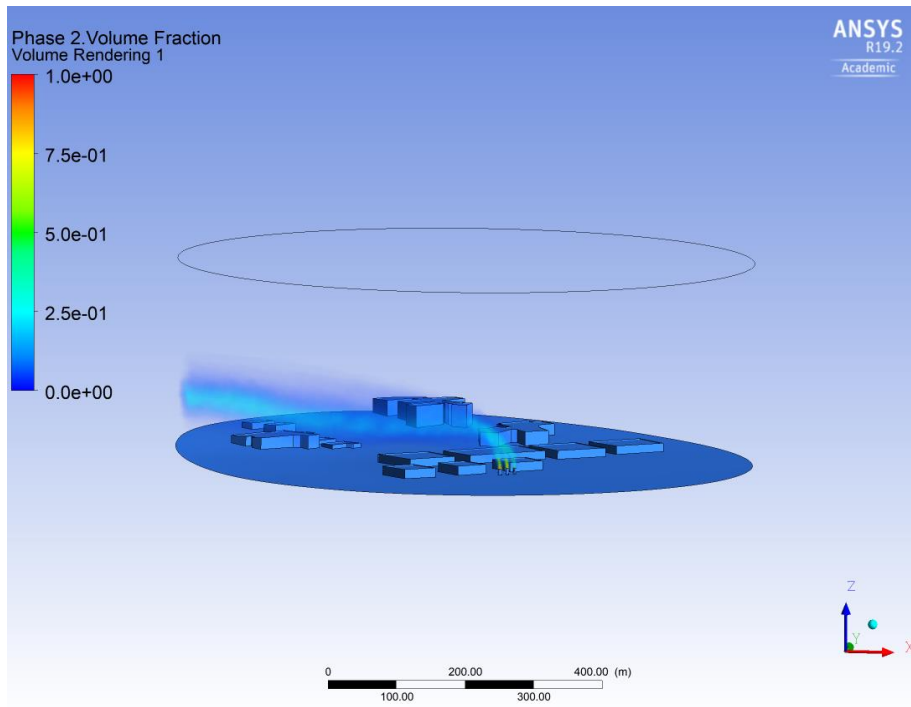


Figure 100 Case 23,0 picture 1

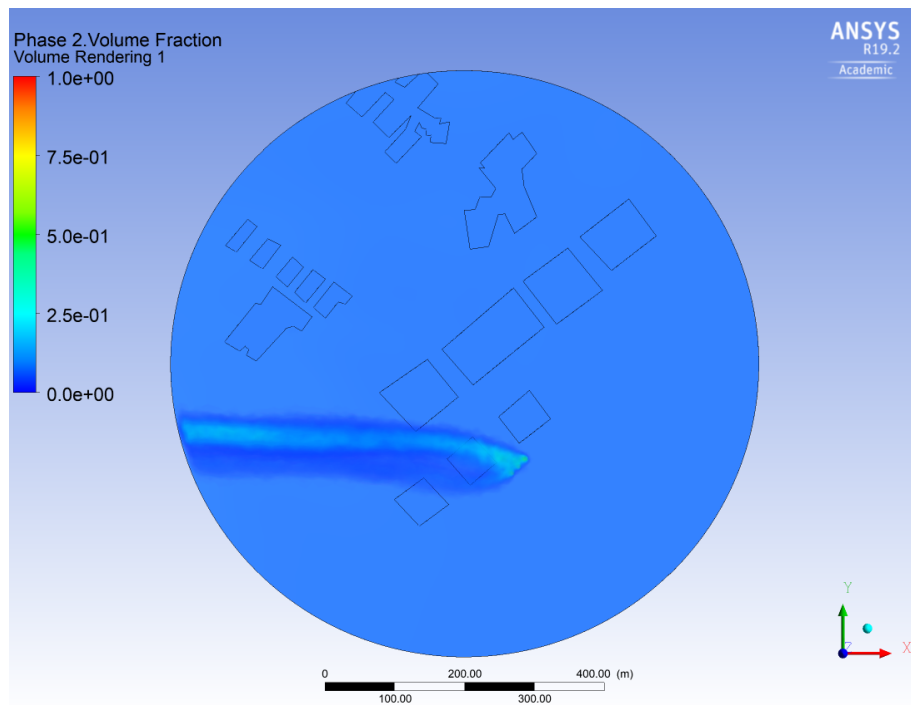


Figure 101 Case 23,0 figure 2

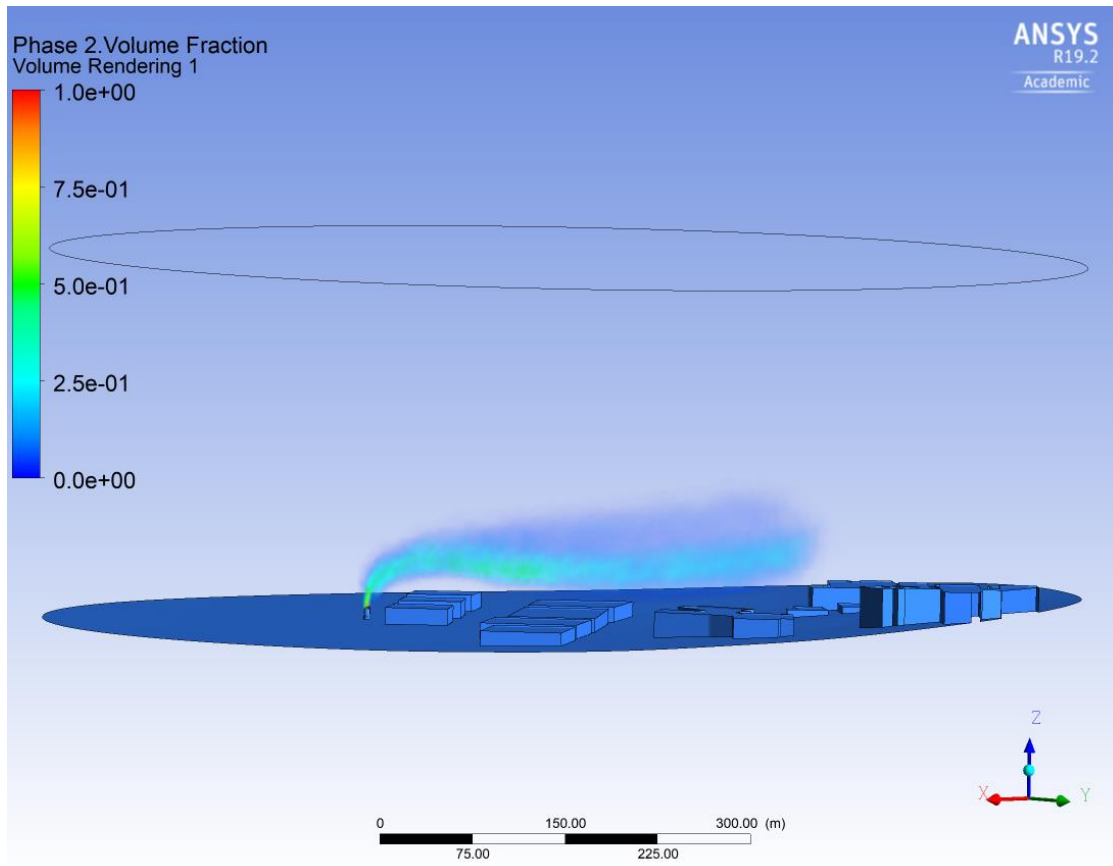


Figure 102 Case 23,1 figure 1

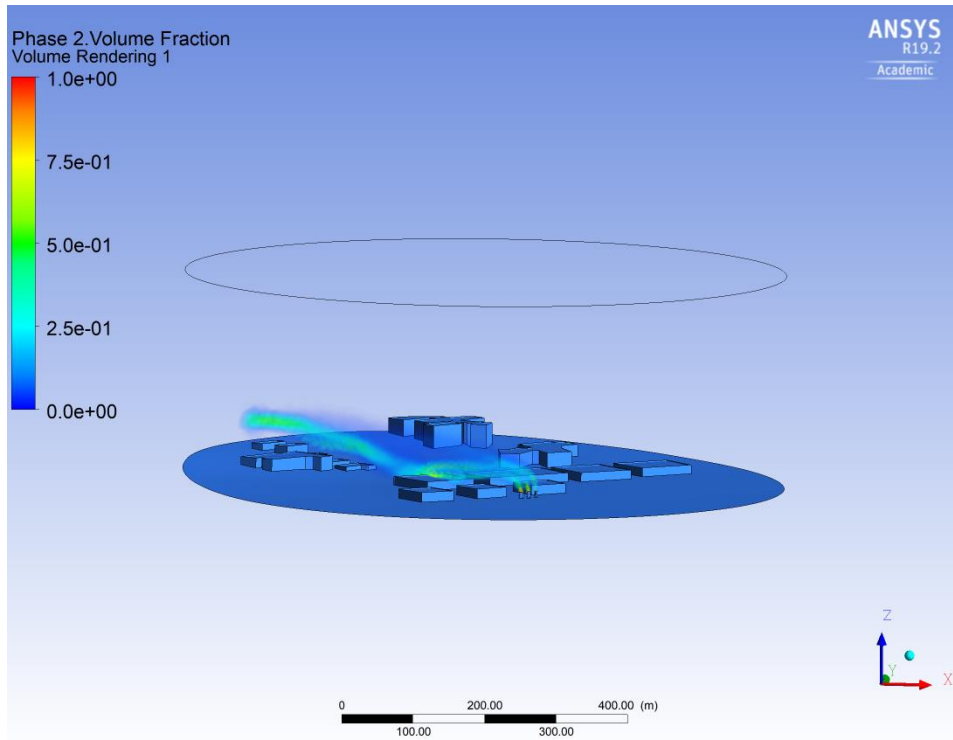


Figure 103 Case 24,0 picture 1

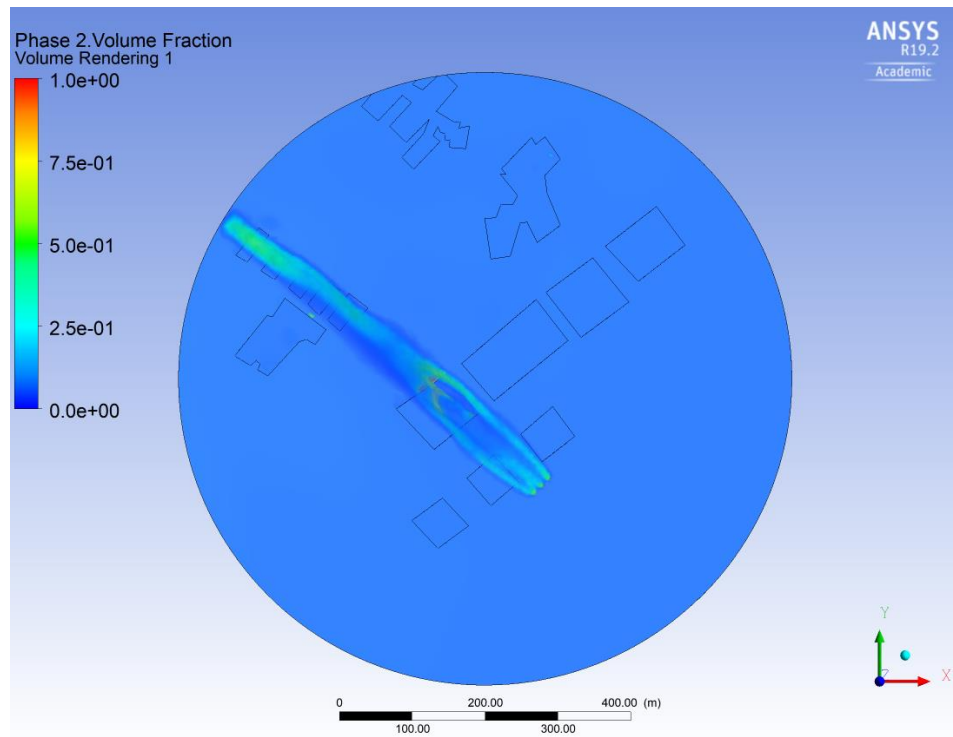


Figure 104 Case 24,0 picture 2

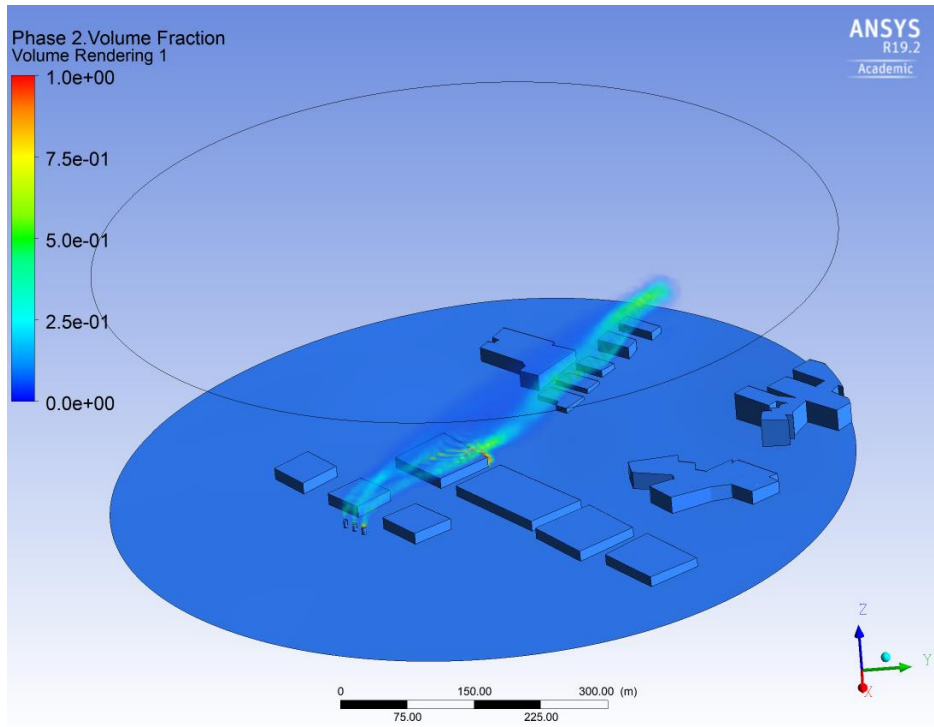


Figure 105 Case 24,0 picture 3

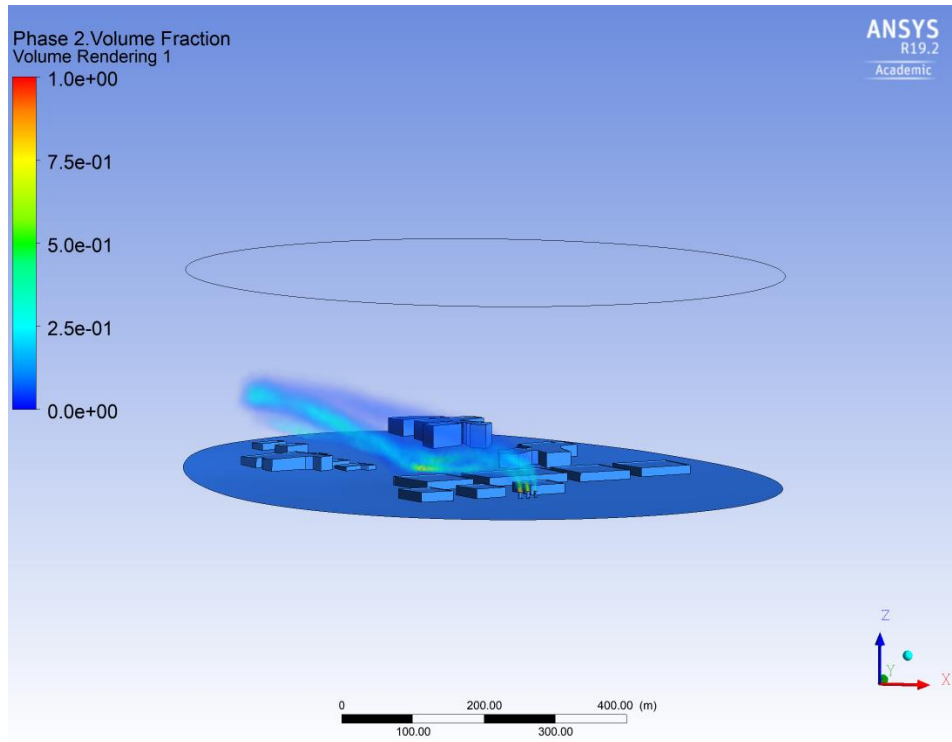


Figure 106 Case 24,1 picture 1

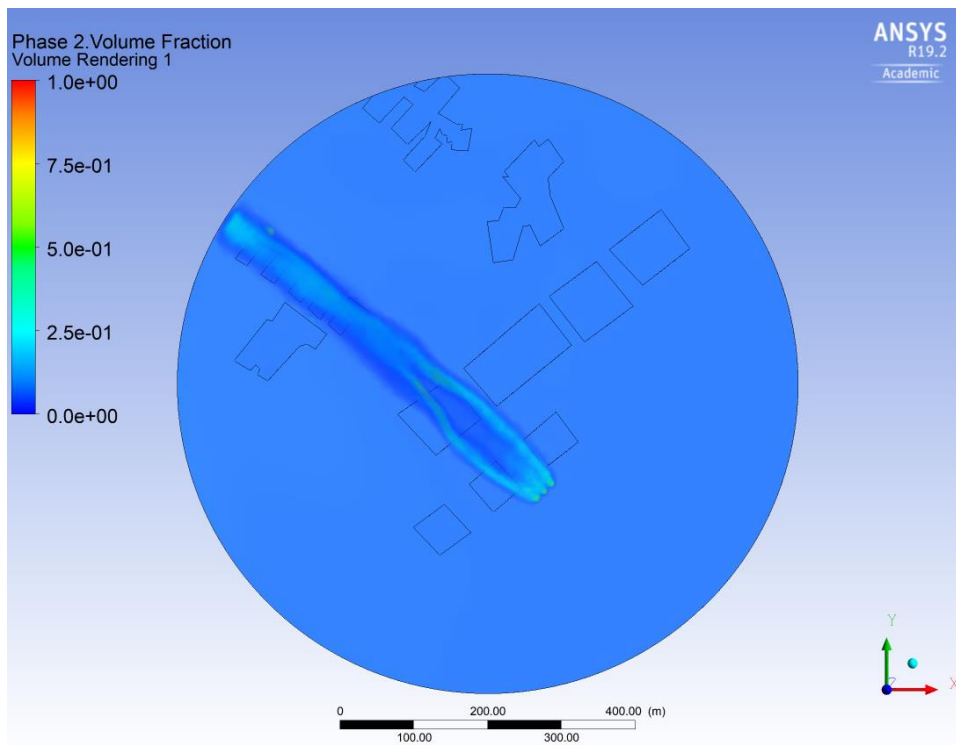


Figure 107 Case 24,1 picture 2

5 meters

Case	Vx	Vy	Calculated value	Date for simulation	File name	Status
25.0	0,0	15m/s		07.05.2019	FFF_case_25_0_1	ok
26.0	-5,0	4,25		14.05.2019	FFF_case_26_0_1	ok

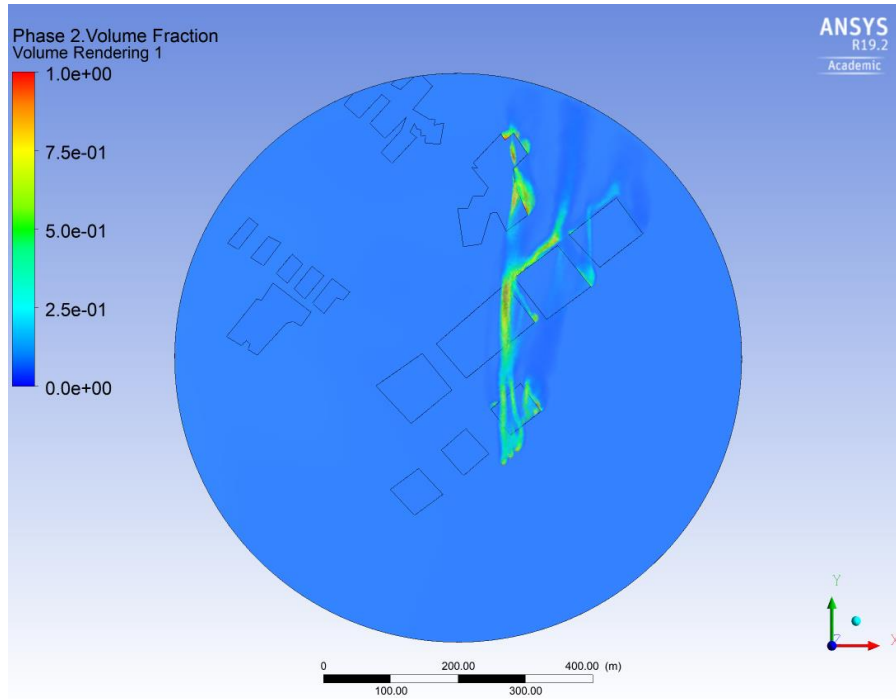


Figure 108 Case 25,0 picture 1

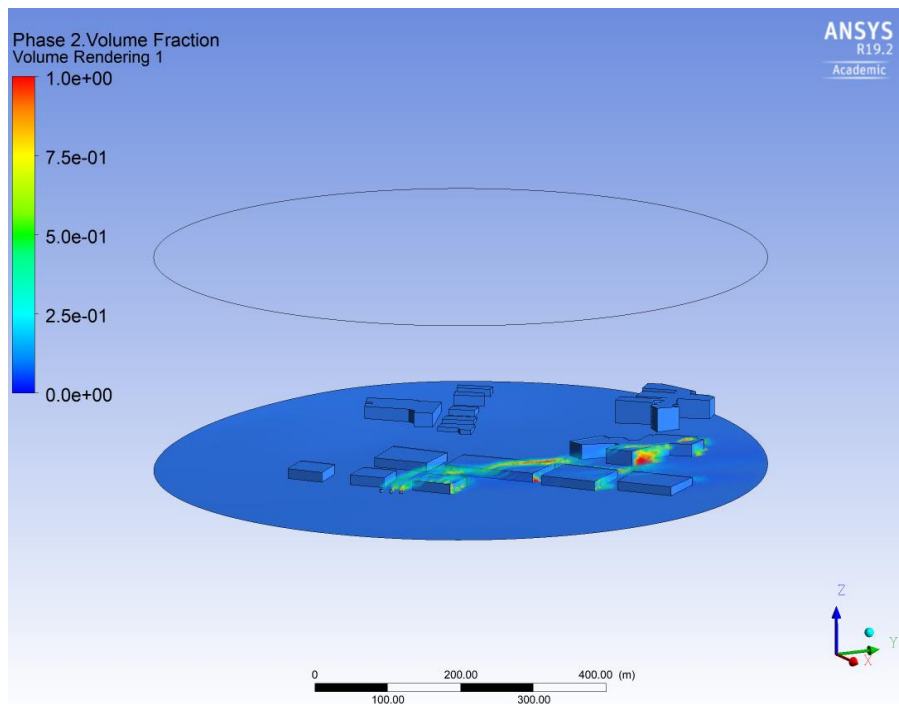


Figure 109 Case 25,0 picture 2

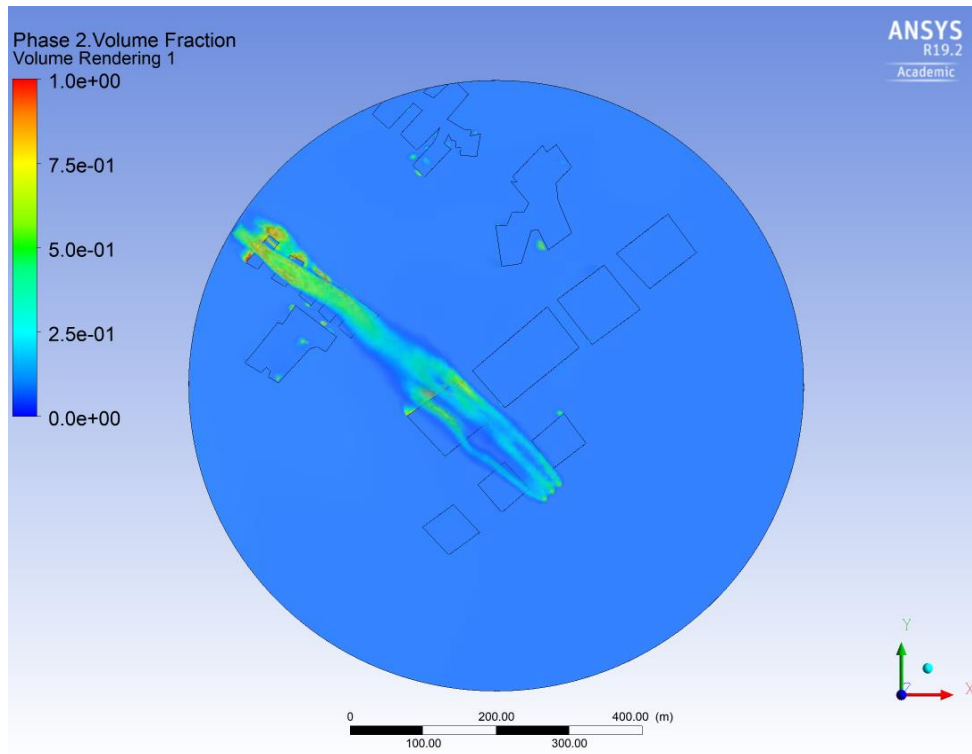


Figure 110 Case 26,0 picture 1

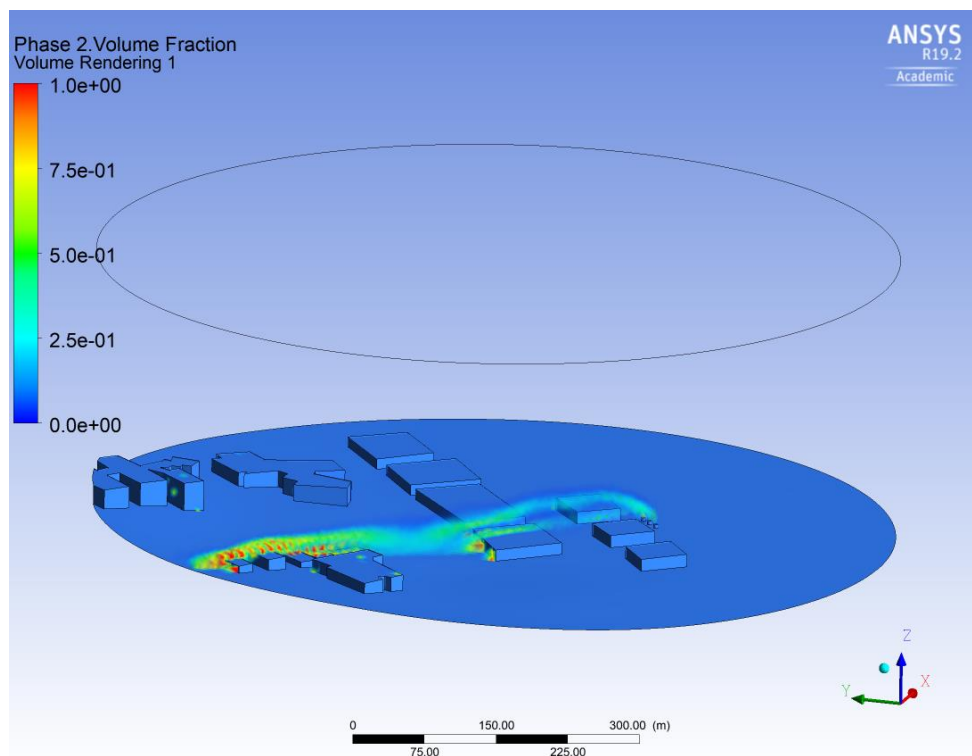


Figure 111 Case 26,0 picture 2

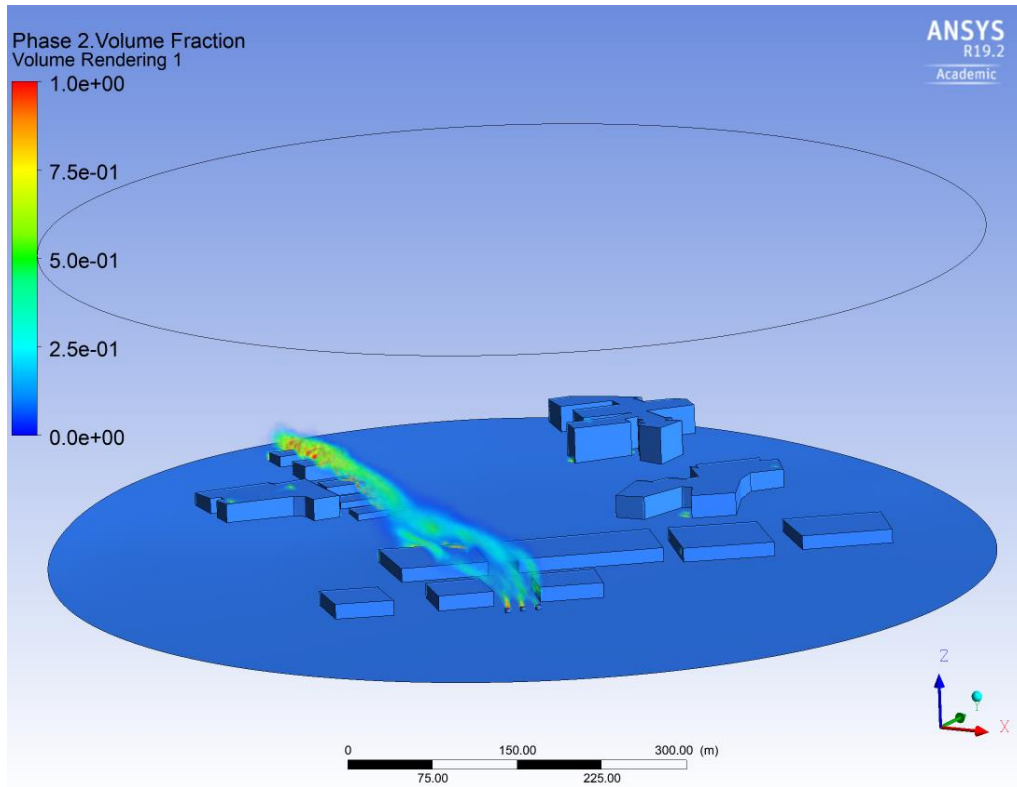


Figure 112 Case 26,0 picture 3

APPENDIX B – MATLAB SCRIPT

Script 1: Terrain

```
clear all
close all

data_lat_long = [69.684068  18.986887
69.682314  18.980882
69.681377  18.975759
69.680258  18.972709
69.678666  18.971785
69.675872  18.973057
69.674431  18.974479
69.675663  18.975839
69.677999  18.976535
69.67955   18.976102
69.680847  18.981477
69.681498  18.987779
69.68264   18.989721
69.683793  18.991284
69.683747  18.995595
69.682357  18.99432
69.680796  18.991792
69.679825  18.987475
69.678967  18.98147
69.67743   18.977559
69.675105  18.977983
69.674266  18.978657
69.675768  18.981015
69.677153  18.983093
69.678031  18.985114
69.678655  18.98826
69.67965   18.991686
69.680723  18.995899
69.681341  18.997955
69.681581  19.00045
69.680549  19.00277
69.679474  19.00097
69.678556  18.998157
69.677873  18.994951
69.676681  18.991688
69.675900  18.985951
69.674438  18.982246
69.674337  18.986345
69.675763  18.991069
69.676291  18.995288
69.677169  18.999619
69.678283  19.001869
69.680138  19.005077
69.683841  18.990557
69.676564  18.99765
69.682258  18.977996
69.674806  18.988651
69.679951  18.972121
69.673849  18.983477];

lat = data_lat_long_alt(:,1);
lon = data_lat_long_alt(:,2);
alt = data_lat_long_alt(:,3);
```

```
dczone =
utmzone(mean(lat, 'omitnan'), mean(lon, 'omitnan'), mean(alt, 'omitnan'));

utmstruct = defaultm('utm');
utmstruct.zone = dczone;
utmstruct.geoid = wgs84Ellipsoid;
utmstruct = defaultm(utmstruct);

[data_x, data_y] =
mfwdtran(utmstruct, data_lat_long_alt(:, 1), data_lat_long_alt(:, 2), data_lat_l
ong_alt(:, 3));

data_x_2 = data_x - data_x(1, 1);
data_y_2 = data_y - data_y(1, 1);
data_z_2 = data_z - data_z(1, 1);
```

Script 2: Buildings

```
clear all
close all

data_lat_long = [69.680711 18.987550
69.680903 18.987496
69.680927 18.987747
69.680798 18.987940
69.680681 18.988121
69.680896 18.988942
69.681297 18.988399
69.681503 18.988299
69.681714 18.988840
69.681976 18.988271
69.681889 18.987944
69.681970 18.987787
69.681574 18.986764
69.681506 18.986929
69.681506 18.986730
69.681252 18.987356
69.681141 18.987205
69.681133 18.986806
69.680962 18.986617
69.680956 18.986255
69.680713 18.986353
69.680454 18.986515
69.680493 18.987177

69.676882 18.985032
69.677166 18.986032
69.677498 18.985104
69.677754 18.985934
69.677424 18.986820
69.677730 18.987779
69.678048 18.986832
69.678315 18.987724
69.678002 18.988553
69.678330 18.989645
69.678672 18.988878

69.678090 18.984761
69.678558 18.986279
69.679021 18.985070
69.679141 18.985688
69.678726 18.986769
69.679504 18.989372
69.679995 18.988165
69.680083 18.988511
69.679534 18.989786
69.679984 18.991478
69.680515 18.990147
69.680672 18.990575
69.680257 18.991751
69.680709 18.993391
69.681172 18.992330
69.680914 18.991237
```

69.685670	18.997192
69.685552	18.997657
69.685641	18.997882
69.685873	18.997175
69.686037	18.997011
69.686183	18.996562
69.686095	18.996281
69.686151	18.996071
69.686191	18.996186
69.686300	18.995831
69.685707	18.994327
69.685587	18.994693
69.686023	18.995793
69.685960	18.995998
69.685839	18.995700
69.685720	18.996103
69.685907	18.996560
69.685942	18.996860
69.685847	18.996993
69.685723	18.996767
69.685607	18.996264
69.685475	18.996017
69.685391	18.996239

69.686555	18.978248
69.686372	18.978125
69.686344	18.978260
69.686445	18.978456
69.686248	18.979434
69.686012	18.980145
69.685854	18.979848
69.685716	18.980242
69.685596	18.979887
69.685840	18.978929
69.685889	18.979077
69.686081	18.978442
69.686051	18.978296
69.685909	18.978383
69.685863	18.978016
69.686071	18.977688
69.686192	18.977897
69.686299	18.977580
69.686090	18.977326
69.686255	18.976718
69.686538	18.977155

69.682082	18.985595
69.682059	18.985249
69.682126	18.985271
69.682125	18.985086
69.682254	18.984423
69.682572	18.985138
69.682745	18.984600
69.682513	18.983919
69.682576	18.983559
69.682935	18.984409
69.683134	18.983803

69.682744	18.982866
69.682848	18.982484
69.683442	18.984066
69.683646	18.983448
69.683452	18.982924
69.683508	18.982722
69.682970	18.981753
69.683039	18.981437
69.683396	18.982194
69.683601	18.981592
69.683278	18.980786
69.683136	18.979383
69.683039	18.979157
69.682893	18.979684
69.682639	18.978964
69.682399	18.979532
69.682664	18.980357
69.682918	18.980940
69.682939	18.981313
69.682863	18.981522
69.682451	18.980450
69.682255	18.981031
69.682506	18.981695
69.682698	18.982220
69.682617	18.982476
69.682283	18.981772
69.682117	18.982351
69.682442	18.983214
69.682362	18.983519
69.682057	18.982793
69.681867	18.983402
69.682155	18.984163
69.681969	18.983980
69.681672	18.983252
69.681531	18.983693
69.681884	18.984579
69.681960	18.984342
69.682069	18.984497
69.681999	18.984581
69.681988	18.984762
69.681899	18.984755
69.681909	18.984929
69.681813	18.984930
69.681807	18.985493

69.680763	18.978261
69.680676	18.978618
69.680339	18.977883
69.680233	18.978383
69.680523	18.979024
69.680443	18.979496
69.680130	18.978857
69.680035	18.979355
69.680296	18.979946
69.680167	18.980363
69.679910	18.979810
69.679840	18.980061
69.680141	18.980726
69.680031	18.981185
69.679707	18.980502

69.679651	18.980795
69.679993	18.981512
69.679830	18.982208
69.679724	18.982006
69.679742	18.981723
69.679528	18.981268

69.679360	18.979754
69.679395	18.980049
69.679335	18.980338
69.679530	18.980711
69.679908	18.979216
69.679675	18.978793
69.679693	18.978609
69.679183	18.977529
69.679065	18.978087
69.679132	18.978288
69.679086	18.978432
69.679016	18.978314
69.678940	18.978683

69.684068	18.986887
69.682314	18.980882
69.681377	18.975759
69.680258	18.972709
69.678666	18.971785
69.675872	18.973057
69.674431	18.974479
69.675663	18.975839
69.677999	18.976535
69.67955	18.976102
69.680847	18.981477
69.681498	18.987779
69.68264	18.989721
69.683793	18.991284
69.683747	18.995595
69.682357	18.99432
69.680796	18.991792
69.679825	18.987475
69.678967	18.98147
69.67743	18.977559
69.675105	18.977983
69.674266	18.978657
69.675768	18.981015
69.677153	18.983093
69.678031	18.985114
69.678655	18.98826
69.67965	18.991686
69.680723	18.995899
69.681341	18.997955
69.681581	19.00045
69.680549	19.00277
69.679474	19.00097
69.678556	18.998157
69.677873	18.994951
69.676681	18.991688
69.675900	18.985951
69.674438	18.982246
69.674337	18.986345

```

69.675763    18.991069
69.676291    18.995288
69.677169    18.999619
69.678283    19.001869
69.680138    19.005077
69.683841    18.990557
69.676564    18.99765
69.682258    18.977996
69.674806    18.988651
69.679951    18.972121
69.673849    18.983477

69.677784    18.988827];

lat = data_lat_long(:,1);
lon = data_lat_long(:,2);

dczone = utmzone(mean(lat, 'omitnan'), mean(lon, 'omitnan'));

utmstruct = defaultm('utm');
utmstruct.zone = dczone;
utmstruct.geoid = wgs84Ellipsoid;
utmstruct = defaultm(utmstruct);

[data_x, data_y] =
mfwdtran(utmstruct, data_lat_long(:,1), data_lat_long(:,2));

data_x_2 = data_x - data_x(1,1);
data_y_2 = data_y - data_y(1,1);

data = [lat, lon, data_x_2, data_y_2];

```